TRANSIENT NEUTRONIC-THERMALHYDRAULIC COUPLING

IN A PT-SCWR

COUPLED NEUTRONIC-THERMALHYDRAULIC TRANSIENT BEHAVIOUR
OF A PRESSURE TUBE TYPE SUPERCRITICAL WATER-COOLED REACTOR

By

DAVID WILLIAM HUMMEL, B.ENG.MGT., M.A.SC.

A Thesis

Submitted to the School of Graduate Studies

in Partial Fulfillment of the Requirements

for the Degree

Doctor of Philosophy

McMaster University

DOCTOR OF PHILOSOPHY (2015)   McMaster University

(Department of Engineering Physics)   Hamilton, Ontario

TITLE: Coupled Neutronic-Thermalhydraulic Transient
                       Behaviour of a Pressure Tube type Supercritical
                       Water-Cooled Reactor

AUTHOR: David William Hummel, B.Eng.Mgt, M.A.Sc.
                       (Engineering Physics, McMaster University)

SUPERVISOR: Professor David Novog

NUMBER OF PAGES: xx, 273

Abstract

The Generation IV International Forum has established several goals for the next generation of nuclear energy systems, which are to be substantial improvements over contemporary designs. In Canada Generation IV research efforts have focused on developing the Pressure Tube type SuperCritical Water-cooled Reactor (PT-SCWR), an evolution of CANada Deuterium Uranium (CANDU) technology. An integral part of the PT-SCWR is the High Efficiency Re-entrant Channel (HERC), wherein coolant first travels downward through a centre flow tube and then upward around the fuel. The large density variation of supercritical fluids, combined with the negative Coolant Void Reactivity (CVR), make the concept similar to a Boiling Water Reactor (BWR). The objective of this study was thus to apply the state-of-the-art in BWR analysis to the PT-SCWR.

Models were created using the DRAGON (neutron transport), DONJON (neutron diffusion/spatial kinetics), and CATHENA (channel thermalhydraulics) computer codes. A procedure for DONJON-CATHENA coupling was developed to enable simulation of coupled transients. The specifications of the HERC necessitated multiple coolant reactivity feedbacks be included in the model, in turn requiring extensions to the DONJON source code. The model created for this work is thus among the first to incorporate multiple coolant feedbacks in core-level coupled spatial kinetics and thermalhydraulics transient analysis, and is uniquely capable of simulating such transients in the PT-SCWR.

This work found that while the total CVR was negative as required, the reactivity effect of coolant void solely around the fuel was positive. As a consequence additional heat delivered from fuel to coolant, which decreases the coolant density, has a positive reactivity effect making BWR-like coupled instabilities impossible. On the other hand, in some postulated transients, such as Loss-Of-Coolant Accidents (LOCAs) or Loss-Of-Flow Accidents (LOFAs), this positive reactivity results in temporary power excursions. A fast-acting shutdown system is potentially necessary to limit damage to the fuel in such transients.

Acknowledgements

Table of Contents

List of Figures

xi

List of Tables

List of Acronyms

AECL	Atomic Energy of Canada Limited
AHWR	Advanced Heavy Water Reactor
ATR	Advanced Thermal Reactor
BOC	Beginning Of Cycle
BWR	Boiling Water Reactor
CANDU	CANada Deuterium Uranium
CATHENA	Canadian Algorithm for THErmalhydraulic Network Analysis
CVR	Coolant Void Reactivity
EOC	End Of Cycle
FTC	Fuel Temperature Coefficient
GDC	General Design Criteria
GENHTP	GENeralized Heat Transfer Package
GFR	Gas-cooled Fast Reactor
GIF	Generation IV International Forum
HEM	Homogeneous Equilibrium Model
HERC	High Efficiency Re-entrant Channel
HPLWR	High Performance Light Water Reactor
IAEA	International Atomic Energy Agency
IQS	Improved Quasi-Static
IST	Industry Standard Toolset
LAPP	Lower Axial Power Peaking

LER	Linear Element Rating
LFR	Lead-cooled Fast Reactor
LOCA	Loss-Of-Coolant Accident
LOFA	Loss-Of-Flow Accident
LWR	Light Water Reactor
MOC	Middle Of Cycle
MOX	Mixed OXide
MSR	Molten Salt Reactor
NEA	Nuclear Energy Agency
NRCan	Natural Resources Canada
NSERC	Natural Science and Engineering Research Council
OECD	Organization for Economic Co-operation and Development
PHTS	Primary Heat Transport System
PHWR	Pressurized Heavy Water Reactor
PIE	Propagation of Input Errors
PT-SCWR	Pressure Tube type SuperCritical Water-cooled Reactor
SCFR-H	SuperCritical Fast Reactor – High temperature
SCLWR-H	SuperCritical Light Water Reactor – High temperature
SCWR	SuperCritical Water-cooled Reactor
SFR	Sodium-cooled Fast Reactor
U.S.NRC	United States Nuclear Regulatory Commission
UVUT	Unequal Velocity Unequal Temperature
VHTR	Very High Temperature Reactor
YSZ	Yttria-Stabilized Zirconia

List of Symbols

The descriptions presented in this thesis cross over multiple disciplines which each have their own established nomenclature. This text will use the typical signs and symbols to remain consistent with literature, but as a consequence some may possess different meanings depending on the context in which they are presented. Each symbol will be introduced when it first appears in the text for greater clarity.

A	Area [m^{-2}]
A	Atomic mass [u]
c_l	Concentration of delayed neutron precursor group l [atoms·cm^{-3}]
c_p	Specific heat capacity [J·kg^{-1}·°C^{-1}]
D	Diffusion constant [cm]
D_h	Hydraulic diameter [m]
e	Specific energy [kJ·kg^{-1}]
E	Neutron energy [eV]
E^*	Excitation energy [eV]
F_{wall}	Wall force [N]
$\vec{g}$	Gravitational acceleration [m·s^{-2}]
h	Specific enthalpy [kJ·kg^{-1}]
h_{fg}	Latent heat of vaporization [kJ·kg^{-1}]
I	Intensity [neutrons·cm^{-2}·s^{-1}]
I^g	Resonance integral in energy group g
J	Neutron current [neutrons·cm^{-2}·s^{-1}]
k	Neutron multiplication constant
k	Thermal conductivity [W·m·°C^{-1}]
k_B	Boltzmann's constant [J·K^{-1}]

K	Minor hydraulic loss constant (form loss)
L	Length [m]
m_n	Neutron rest mass [u]
MR	Moderating ratio
n	Neutron density [neutrons·cm^{-3}]
N	Nuclei density [atoms·cm^{-3}]
N_A	Nuclei per unit area [atoms·cm^{-2}]
N_{pch}	Phase change number
N_{sub}	Subcooling number
N_{TPC}	Trans-pseudocritical number
N_{spc}	Sub-pseudocritical number
Nu	Nusselt number
P	Pressure [Pa]
P_l	Legendre polynomial of degree l
P_w	Wetted perimeter [m]
Pr	Prandtl number
q''	Heat flux [W·m^{-2}]
q'''	Volumetric heat generation [W·m^{-3}]
r	Position (x,y,z) [cm,cm,cm]
Re	Reynolds number
s	Nuclei source [atoms·cm^{-3}·s^{-1}]
S	Neutron source [neutrons·cm^{-3}·s^{-1}]
t	Time [s]
T	Temperature [°C; K]
u	Velocity [m·s^{-1}]
v	Neutron velocity [m·s^{-1}]
Y_{lm}	Spherical harmonic of degree l and order m
Y_x	Relative yield of isotope x

Greek Letters

α	Proportionality constant
β	Delayed neutron fraction
β	Volumetric expansion coefficient [°C^{-1}]
Γ	Generation rate [kg·m^{-3}·s^{-1}]
ϵ	Surface roughness [m]
λ	Decay constant [s^{-1}]
Λ	Mean neutron generation time [s]
μ	Scattering angle [rad]
μ	Viscosity [Pa·s]
ν	Number of neutrons released per fission event
ξ	Neutron lethargy per scattering event
Π_h	Heated perimeter [m]
ρ	Density [kg·m^{-3}]
ρ	Reactivity [mk; 1 mk = 100 pcm]
σ	Normal stress [Pa]
σ	Microscopic cross-section [barn; 1 barn = 10^{-24} cm^{-2}]
Σ	Macroscopic cross-section [cm^{-1}]
τ	Shear stress [Pa]
ϕ	Scalar flux density [neutrons·cm^{-2}·s^{-1}]
Φ	Angular flux density [neutrons·cm^{-2}·s^{-1}]
$\chi(E)$	Energy spectrum of neutrons released from fission
$\vec{\Omega}$	Direction [sr]

Subscripts and Superscripts

a	Absorption interaction
d	Delayed neutron
eff	Effective

f	Fission interaction
g	Energy group
in	Inlet
∞	Infinite lattice
l	Liquid
p	Prompt neutron
pc	Pseudocritical
s	Scattering interaction
t	Total
tr	Transport
v	Vapour

Declaration of Academic Achievement

This study was performed by the author during the years 2010-2015 based on the advice and recommendations of a four-member supervisory committee consisting of Professors David Novog, Adriaan Buijs, John Luxat, and Laurence Leung.

All models described within this thesis were created by the author using open-source computer codes (DRAGON and DONJON), AECL's CATHENA code, and custom scripts and functions written by the author as indicated. Neutron kinetics data was provided by Frederic Salaun based on independent calculations outside of this work.

Considerable effort went towards modification of the DONJON 3.02g FORTRAN source code, which was performed in consultation with Professor Guy Marleau at École Polytechnique de Montréal. The author identified several errors in the feedback module that were corrected by Professor Marleau. Extensions to the feedback module, uniquely necessary for this work, were made by the author.

Chapter 1

Introduction

1.1 Background

Beginning with the first demonstration plants in the early 1950s, nuclear fission reactors have been producing useful energy in the form of electricity for nearly 60 years. The technology behind these first prototypes (Generation I) has progressed through early commercial power generation (Generation II) in the 1960s to today's operating reactors (Generations II and III) and new evolutionary designs currently under construction (Generation III+) [1]. As of 2014, there were 435 operating power reactors and 71 under construction throughout the world [2]. In 2011, nuclear power provided 2,518 TW·h of electricity, accounting for 13% of all global energy consumption and comprising as much as 78% of all electrical generation in developed nations (e.g. France) and as little as 2% in developing nations (e.g. China) [3].

In a critical review of the future prospects of nuclear energy (published in the journal *Energy Economics*), J. F. Ahearne posits that nuclear will likely remain an integral part of the global energy mix in the foreseeable future due to the increasing cost of fossil fuels and their associated greenhouse gas emissions [1]. Ahearne further predicts that demand for nuclear energy will remain relatively flat in the developed nations of Europe and North America, but will grow considerably in developing nations where electricity demand per capita is increasing rapidly [1].

Nevertheless, James A. Lake (former president of the American Nuclear Society) identifies several challenges facing the future of nuclear energy, stating [4]:

- The economics of nuclear power must be competitive with other energy sources. While operating costs of nuclear are typically very low, the high

1

capital costs and long construction, licensing and commissioning times do not compare favourably against natural gas.

- The public must be confident in the safety of nuclear power. While most reactor technology has proven very safe, the reliance on operations and maintenance creates vulnerability in countries with less sophisticated support infrastructures and different safety cultures.

- There must be a management strategy for nuclear waste and the back-end of the fuel cycle. Often these issues are very political, but may be resolved with sufficient will, leadership, and consensus.

- The commercial nuclear fuel cycle must be resistant to the proliferation of nuclear weapons. As nuclear power becomes more widely deployed around the world, the reactor supplier and operator must both be consistent in their resistance to proliferation.

- There must be a sustainable supply of skilled labour and highly qualified personnel to preserve the critical nuclear technology infrastructure. This includes international cooperation in research and development institutions, national laboratories, universities, and industry.

The Generation IV International Forum (GIF) was established to foster international cooperation in developing the next generation of nuclear energy systems that meet these challenges.

1.1.1 The Generation IV Program

GIF initially consisted of nine nations (Argentina, Brazil, Canada, France, Japan, the Republic of Korea, the Republic of South Africa, the United Kingdom, and the Unites States of America), later joined by Switzerland, Russia, and the European Union, that have formally committed research and development resources to designing the next generation of reactors. GIF has defined four goals for Generation IV nuclear energy systems [5]:

1. **Improved sustainability**: focused on nuclear waste management and resource utilization. This includes extending the nuclear fuel supply by recycling current spent fuel and exploring new nuclear fuels, as well as reducing the requirement for long-term nuclear waste repositories (i.e. by reducing the volume of waste and the decay heat burden).

2. **Improved economics**: focused on improving the cost competitiveness and reducing the financial risk of nuclear energy systems. This includes increasing plant and fuel cycle efficiency, design simplifications, and utilizing nuclear energy as a source of process heat for secondary applications.

3. **Improved safety**: focused on improving safety and reliability of plant systems relative to Generation III+ designs, as well as improving accident management, minimizing the consequences of an accident, and reducing the need for off-site response. This includes the use of inherent/passive safety features and enhancing public confidence in the safety of nuclear energy.

4. **Improved proliferation resistance**: focused on controlling and securing nuclear materials and facilities. This includes design features that inherently make repurposing of nuclear materials for weapons more difficult, as well as increasing the physical protection and robustness of facilities themselves.

Furthermore, participation in the Generation IV research and development program by research and academic institutions (i.e. universities) ensures a new supply of skilled and highly qualified personnel for the nuclear industry, meeting Lake's final challenge [6].

GIF identified six reactor technologies that may potentially achieve the goals for Generation IV: the Very High Temperature Reactor (VHTR), the Gas-cooled Fast Reactor (GFR), the Sodium-cooled Fast Reactor (SFR), the Lead-cooled Fast Reactor (LFR), the Molten Salt Reactor (MSR), and the SuperCritical Water-cooled Reactor (SCWR) [5]. The members of GIF, as well as some non-signatory members (e.g. China), would each perform research and development work on at least one of these technologies.

The SCWR is regarded as the most direct extension of well-developed Light Water Reactor (LWR) technology (the most common reactor type currently deployed) and therefore, in the view of some experts, the most easily realizable Generation IV concept [7]. It is in fact the only Generation IV concept that uses water as the primary coolant. Three members of GIF thus formerly agreed to develop the SCWR concept: Canada, Japan, and the European Union (later joined by China). Each would cooperate in three research and development areas:

system integration and assessment (i.e. reactor design), thermalhydraulics and safety, and materials and chemistry [8].

1.1.2　The Supercritical Water-cooled Reactor

As could be inferred from its name, the SCWR's key feature is the use of water beyond the thermodynamic critical point (374 °C at 22.1 MPa) as primary coolant. This offers several advantages over contemporary LWRs [5]:

- The higher temperature results in higher thermodynamic efficiency of the plant (approaching 50%, compared to 30-35% in LWRs). Supercritical water coolant is already deployed in some fossil fuel generation plants for this very reason.
- A lower mass flow per unit thermal power is required than in an LWR, reducing the size requirements of Primary Heat Transport System (PHTS) components and subsequently the size requirements for containment.
- With a direct cycle of supercritical coolant, steam handling components (generators, dryers, separators, etc.) are omitted entirely, reducing the number of major components and eliminating their associated costs.
- Since supercritical water exists in a single thermodynamic phase, the boiling crisis (i.e. departure from nucleate boiling or dry out) that is a major safety concern in LWRs cannot exist.

Each member participating in the Generation IV SCWR project has developed or is developing its own unique SCWR concept. The European Union and Japanese designs are superficially similar in that they are both evolutions of LWR designs [8]. The Canadian SCWR concept has a substantially different pedigree, however. As described by Torgerson, Shalaby, and Pang, the Canadian SCWR concept is an evolution of the CANada Deuterium Uranium (CANDU) reactor [9].

1.1.3　The Canadian SCWR Concept

The CANDU reactor, or more generally the Pressurized Heavy Water Reactor (PHWR), has three key differences from LWRs [9]:

1. Multiple pressure tubes contain the core in lieu of a single large vessel: Each channel in a CANDU reactor (of which there typically over 300) is a ≈6 m long horizontal tube that contains a series of 12+ fuel bundles (equivalent to a single LWR assembly). These tubes provide the pressure

boundary for the PHTS, whereas a LWR uses a single large vessel (with vertical flow) as the primary pressure boundary.

2. Isolation of the PHTS from a low pressure and temperature heavy water moderator: a separate calandria tube (with an annular gas gap) thermally isolates the pressure tubes from the large tank of heavy water (called the calandria) in which they sit, which serves as the neutron moderator. The primary coolant and moderator are thus entirely separate, unlike in an LWR where they are both the same fluid. Heavy water is a much more efficient neutron moderator than light water due to the decreased neutron absorption, but this comes at the expense of a longer neutron slowing-down distance. A CANDU core is thus larger than an LWR of the same power.

3. The capability for online refueling: a fueling machine can connect to the ends of each pressure tube and shift individual fuel bundles in and out of the core while the reactor is operating. An LWR uses a batch refuelling scheme, where the reactor is periodically shut down and every assembly in the core is shuffled or replaced at once. The online refuelling system, together with the much high efficiency heavy water moderator, allows CANDU reactors to use natural (i.e. unenriched) uranium fuel.

The Canadian SCWR concept has, nevertheless, evolved substantially from its CANDU roots. The prohibitive mechanical requirements of a fueling machine that could connect to supercritical coolant channels predicated the switch from online refuelling to batch fuelling with enriched (plutonium-thorium) fuel [10, 11]. The need for a separate calandria tube was eschewed by placing a ceramic insulator inside the pressure boundary as part of the High Efficiency Re-entrant Channel (HERC) concept [12]. The pressure tubes and separate heavy water moderator were maintained, however. The Canadian SCWR concept, henceforth referred to as the Pressure Tube type SuperCritical Water-cooled Reactor (PT-SCWR), is shown in Figure 1.1.

According to Leung, the PT-SCWR concept achieves all of the Generation IV design goals, including [13]:
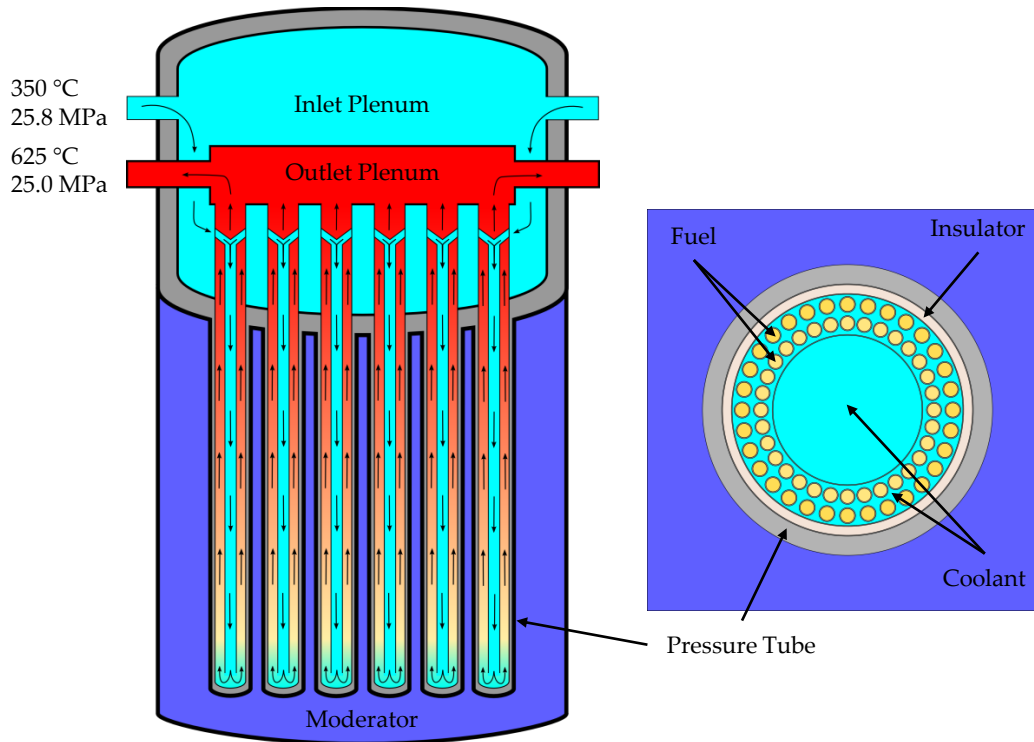
Figure 1.1: Current PT-SCWR conceptual design

- **Improved economics**: like the other SCWR concepts, the use of supercritical water coolant promises plant simplification and higher thermodynamic efficiency, reducing the relative cost per MW of electrical power.

- **Improved safety**: a passive decay heat removal system drastically reduces the core damage frequency relative to Generation III+ reactors. Thorium fuel also has a much higher melting point and thermal conductivity than uranium fuel, which contributes positively to overall plant safety as well.

- **Improved sustainability**: thorium is much more abundant than uranium, and a closed thorium fuel cycle offers extension of existing fissile reserves.

- **Improved proliferation resistance**: any ^{233}U created from ^{232}Th in the PT-SCWR will be contaminated with the highly radioactive ^{232}U, which would require special handling if any fuel was to be diverted to other uses. Further, ^{232}U is extremely difficult to separate from ^{233}U (the process

would need to be similar to isotopic enrichment), which further complicates diversion.

The PT-SCWR is being developed in collaboration between Atomic Energy of Canada Limited (AECL) and Canadian universities through the Natural Science and Engineering Research Council (NSERC) with support from Natural Resources Canada (NRCan) [14].

1.1.4 Impact of Supercritical Fluids on Reactor Design

Being beyond the thermodynamic critical point, supercritical fluids by definition exists in a region where the liquid and gas phases are indistinguishable. Supercritical fluids are thus typically considered to exist in a single thermodynamic phase. Nevertheless, supercritical fluids undergo sudden and large changes to their thermo-physical properties when crossing what is referred to as the *pseudocritical transition*, defined as the local temperature and pressure at which the fluid specific heat capacity is maximized. For a given PHTS operating pressure there is thus a *pseudocritical point*, i.e. a point where the temperature rate of change of thermo-physical properties is very high. Fluids on opposite sides of the pseudocritical point will thus have very different properties, even though the relative change in fluid enthalpy is small. Figure 1.2, adapted from a paper by Licht, Anderson and Corradini, shows the normalized property variation of supercritical water around the pseudocritical point at 25 MPa (the operating pressure of the PT-SCWR) [15].

The large variation in coolant properties introduces several challenges to SCWR conceptual development. Licht et al., for example, were examining the heat transfer characteristics of supercritical water, evaluating multiple empirical correlations' ability to predict peak fuel surface temperatures in typical PHTS operating conditions, ultimately showing there were significant gaps in the existing knowledge base [15]. The changes in fluid density around the pseudocritical transition are of particular importance in SCWR neutronics, where the density of coolant nuclei necessarily affects various neutron-nuclei interaction rates and, most importantly, the fission rate in the fuel. In the case of a PT-SCWR channel, for example, the coolant density is expected to decrease by an order of magnitude between the channel inlet and outlet. The coupling between

neutronics and thermalhydraulics in SCWR concepts has been studied extensively at both the fundamental and full-core modelling levels [16, 17, 18].
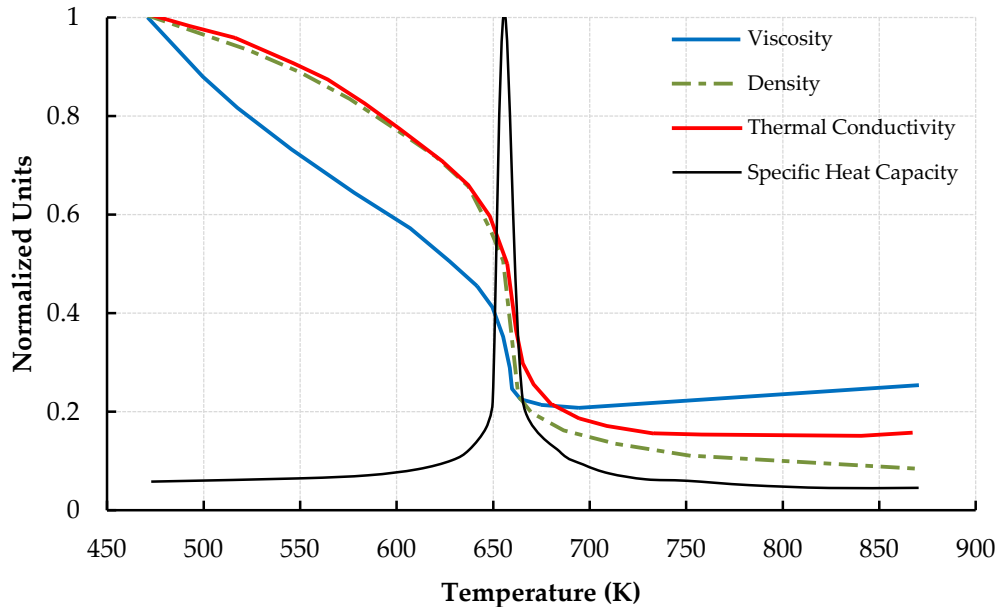
Figure 1.2: Physical property variation in supercritical water at 25 MPa

Supercritical fluid exists in a single thermodynamic phase, and even though there is a large thermo-physical property variation around the pseudocritical transition, the properties are continuous. This is contrast to boiling fluids where there is a discontinuity in properties between the liquid and vapour phases, resulting in an interface between fluids in different states. Nevertheless, Ambrosini posits that the behaviour of supercritical fluids in heated channels is in many ways analogous to boiling fluids [19, 20]. For example, the large density change expected in a SCWR channel is typical of a Boiling Water Reactor (BWR), wherein saturated liquid is heated in the channel and becomes vapour.

The similarity to BWRs is notable because, as a result of the neutronics-thermalhydraulics coupling and large coolant density changes, they are vulnerable to a special type of *instability* wherein the core power and flow oscillate out of phase with one another, potentially threatening plant operational and safety limits [21]. The potential for power and flow instabilities in SCWR concepts was identified in the Generation IV roadmap as an important technology gap requiring substantial analysis with core-level transient models [22].

1.2 Objectives of this Study

The primary objective of this work was to establish the core-level transient behaviour of the current (as of this writing) PT-SCWR conceptual design. This included determining the existence of BWR-like coupled instabilities and modelling the progression of coupled transients similar to postulated accident scenarios. The state-of-the-art in contemporary BWR stability analysis methodology would be applied to the PT-SCWR core, which requires coupled core-level neutron diffusion (with spatial kinetics) and channel-level thermalhydraulics computational models [23, 24, 25].

Such models were created as part of this work, which also required neutron transport to be modelled at the fuel lattice level (the output being necessary for constructing a core-level neutron diffusion model). The selected toolset included the DRAGON (for neutron transport), DONJON (for neutron diffusion and spatial kinetics), and CATHENA (for channel thermalhydraulics) computer codes, each developed for modelling CANDU reactors [26, 27, 28]. Although these codes are not validated for modelling SCWR conditions (which would only be possible with a future database of separate effects and integral experimental data), they are some of the best tools available as a result of recent extensions or by virtue of being open source (thus allowing any necessary modifications). A method for transient coupling of DONJON and CATHENA would also need to be created since these independently developed codes contain no native provisions for passing information to one other.

The fact that there are two opposing coolant flow paths in the HERC concept (as seen in Figure 1.1) presents additional modelling challenges since most contemporary reactors (both LWR and CANDU) have only a single flow path within any given channel. Computer codes used for core-level coupled transient analysis of these reactors thus typically contain only a single coolant reactivity feedback mechanism. As a consequence the kinetics features of the PT-SCWR were expected to be substantially different from LWR or CANDU, so a key achievement of this work would be determining the transient behaviour of a system with these multiple coolant reactivity feedbacks.

With the newly created core-level models, this work would study the coupled behaviour of the PT-SCWR by initiating transients in the PHTS, precipitating

power transients from the coupled feedbacks. Two types of transients would be studied: those meant to instigate or study coupled oscillations in the core, and those meant to be evocative of postulated accidents in the PHTS. The results of these transient tests would form the basis for analysis and conclusions on the PT-SCWR's inherent coupled stability and transient behaviour.

1.3   Outline of this Thesis

This thesis consists of six chapters (including this introduction) which detail the PT-SCWR core-level coupled transient modelling study.

Chapter 2 consists of a scientific literature review that establishes the context, motivation, and requirements for the present study. Additional information on the SCWR concept and accepted modelling methodology (including relevant past studies) is included. After demonstrating the similarity between the SCWR concept and BWRs, a review of instability phenomena and the state-of-the-art in coupled analysis is also presented.

The fundamental theory employed in reactor core modelling is presented in Chapter 3. This includes the basic theory and equations of neutron transport, neutron diffusion, and neutron kinetics, as well as the system of equations and closure relationships that describe the channel thermalhydraulics. Chapter 2 and Chapter 3 introduce several concepts necessary for interpreting the subsequent simulation results.

Chapter 4 describes how the various models were implemented in their respective computer codes (i.e. DRAGON, DONJON, and CATHENA) as well as the steady-state and transient coupling procedures. This description also includes the various assumptions and simplifications made in creating the models, including important caveats in interpreting the simulation results and subsequent analysis.

The results and analysis of various coupled transient tests, including tests on core stability and postulated accident progressions, are presented in Chapter 5. Conclusions and recommendations based on these analyses are included in Chapter 6, which also includes a summary of the contributions to knowledge resulting from this work as well as recommendations for future study.

Chapter 2

Literature Review

The Pressure Tube type SuperCritical Water-cooled Reactor (PT-SCWR) is a next-generation reactor concept that promises significant improvements over contemporary nuclear energy systems. In this chapter, the background of the PT-SCWR concept is described and the current state of knowledge reviewed, highlighting some of the technical challenges facing the development of this new technology.

2.1   The Generation IV Supercritical Water-cooled Reactor

The Generation IV International Forum (GIF) identified six reactor technologies that could achieve the goals for next generation nuclear energy systems: the Very High Temperature Reactor (VHTR), the Gas-cooled Fast Reactor (GFR), the Sodium-cooled Fast Reactor (SFR), the Lead-cooled Fast Reactor (LFR), the Molten Salt Reactor (MSR), and the SuperCritical Water-cooled Reactor (SCWR) [5]. In a critical review of these six reactor technologies, Abram and Ion conclude that the VHTR and the various fast-spectrum reactors have the best ability to meet the Generation IV goals, while the MSR likely pushes the limit of what is technically achievable [7]. On the generic SCWR concept, Abram and Ion state that it is a direct extension of well-developed Light Water Reactor (LWR) technology, and therefore the most easily realizable Generation IV concept. At the same time they believe it is poorly capable of meeting the Generation IV goals outside of improved economics [7].

2.1.1   The Generic SCWR Concept

The greatest relative advantages of the SCWR concept (increased thermal efficiency and plant simplification) are primarily economic in nature, hence Abram's and Ion's criticism [7]. Abram and Ion further observe that the materials

requirements for nuclear plants are much different from fossil plants (where supercritical fluids are already deployed), and the highly corrosive nature of supercritical water introduces a significant technological challenge for the SCWR conceptual development [7].

Materials performance is, in fact, one of the primary research areas in the SCWR conceptual development program for this very reason [8]. Ehrlich, Konys, and Heikinheim, for example, evaluated potential in and out of core materials for use in SCWR concepts [29]. Their preliminary study showed that, based on available data from both LWRs and fossil fuel plants, Ni-alloys and austenitic stainless steels may be candidate materials for in-core components (including fuel cladding), but these materials will introduce significant parasitic neutron absorption compared to the Zr-based alloys in contemporary LWRs, requiring higher fuel enrichment. Ehrlich et al. conclude that detailed experimental studies on chemistry/radiolysis in supercritical conditions, as well as irradiation on stress corrosion and deformation, are still necessary, but the materials challenges are not insurmountable [29].

As to the other Generation IV objectives, Liu and Cai studied the inclusion of thorium based fuels in an SCWR concept to improve resource utilization and proliferation resistance [30]. ^{232}Th is a *fertile* material that, after absorbing a neutron, transmutes in to the *fissile* material ^{233}U, which can be then used as a standard nuclear fuel. The ^{233}U produced in this reaction is contaminated with the highly radioactive ^{232}U, which vastly increases the difficulty of diverting spent fuel to nuclear weapons programs. Liu and Cai showed that, at least conceptually, a thorium and recycled plutonium fuel mixture could be used in an SCWR congruent to the objectives of the Generation IV program [30]. The SCWR concept evaluated by Abram and Ion was merely a contemporary LWR (i.e. using enriched uranium fuel) with higher temperature and pressure coolant. Nevertheless, the work of Liu and Cai shows that there is still potential to achieve all of the Generation IV objectives with the SCWR concept.

Fischer, Schulenberg, and Laurien describe the European Union's SCWR concept, the High Performance Light Water Reactor (HPLWR) [31]. The HPLWR concept is a direct evolution of a modern LWR (in particular, the German Gundremmingen Boiling Water Reactor) [8]. According to Fischer et al., the unique feature of the HPLWR concept is the three-pass core design, which allows

a high coolant outlet temperature while minimizing the peak fuel cladding temperature. This simplifies the materials requirements for operating in supercritical conditions, increasing the technical feasibility of the HPLWR concept [31]. Further to that end, the HPLWR concept uses low enriched uranium fuel, although mixed oxide (MOX) fuel from reprocessing remains possible [8]. According to Schulenberg et al., the HPLWR conceptual design is complete and the research and development project is now moving forward on to the fuel qualification and testing phase [32].

The Japanese SCWR concept was first introduced by Oka and Koshizuka, predating the greater SCWR collaboration under GIF [33]. The Japanese SCWR concept initially existed in several versions: a thermal spectrum SuperCritical Light Water Reactor (SCLWR), a fast spectrum SuperCritical Fast Reactor (SCFR), and higher temperature versions of each (SCLWR-H and SCFR-H, respectively). These concepts were similar in that they all used hexagonal fuel assemblies and a once-through cooling cycle (as opposed to square assemblies and three core passes in the HPLWR) [33]. The SCLWR-H concept has, however, evolved substantially since introduced by Oka and Koshizuka. Yamaji et al. presented an improved SCLWR-H concept that uses square assemblies and a two pass core, making the Japanese SCWR concept much more similar to the HPLWR [34].

While the European and Japanese designs are superficially similar (both being evolutions of LWR designs), the Canadian SCWR concept has a substantially different design history having evolved from CANDU [9].

2.1.2 The Pressure Tube type SCWR (PT-SCWR)

The initial concept presented by Torgerson et al. was a direct extension of CANDU technology to a supercritical water-cooled design (CANDU-SCWR), i.e. other than changing the coolant to supercritical water (and removing the calandria tube in favour of a ceramic insulator) the unique features of CANDU reactors were maintained [15].

The Canadian SCWR has, however, evolved substantially since the first introduction of the concept. According to Boczar et al., the mechanical requirements of a fuelling machine that can connect to channels with supercritical coolant are prohibitive, and thus online refueling was abandoned in favour of a simpler batch fueling scheme [10]. This also precludes the use of

natural uranium fuel, although with the increased parasitic neutron absorption in steel over zirconium based alloys (a requirement for supercritical coolant) this was likely to be the case regardless. In its place, Boczar et al. introduced the possibilities of either low enriched uranium (4% ^{235}U) or a homogeneous mixture of recycled plutonium and thorium [10]. Boczar et al. studied the effects of design variations in the CANDU-SCWR channel on two neutronics properties: the achievable discharge burnup (in MW·d·tonne^{-1}, maximizing the reactor economics) and the magnitude of the Coolant Void Reactivity (CVR), which was to be negative as a design requirement [10]. These two variables (discharge burnup and CVR) would become two of the key physics design parameters in Canadian SCWR conceptual development.

McDonald et al. expanded on the work of Boczar et al., introducing a viable three batch refuelling scheme and several fuel assembly conceptual designs that were evolutions of CANDU-like fuel bundles (i.e. concentric rings of small-diameter fuel pins) [35]. These fuel concepts all used a homogenous plutonium-thorium fuel mixture and included a large unfueled pin in the centre that reduced the magnitude of the CVR. According to McDonald et al., the most limiting constraint in conceptual fuel design was the peak Linear Element Rating (LER) in the outermost ring of fuel elements [35]. The radial power distribution in the bundle was skewed towards the outside of the assembly (i.e. the fuel elements closest to the moderator), and at the target fuel burnup of over 40 MW·d·tonne^{-1}, the fuel cladding integrity of these pins was not assured. McDonald et al. showed several conceptual fuel designs that subdivided the outer ring of elements (i.e. more, smaller pins) in an attempt to lower the peak heat flux on the cladding surface [35].

Three objectives were thus established for Canadian SCWR fuel design: minimize the CVR (assuring that it was negative), maximize the discharge burnup, and keep the peak LER below 40 kW·m^{-1} (a conservative value based on operating LWR data on fission gas release) [35, 36]. The complete evolution of the Canadian SCWR fuel geometry is summarized by Pencer and Colton [11]. The first 43-element concept was very similar to operating CANDU fuel bundles. The 54-element concept introduced the large diameter unfueled centre pin that reduced the CVR. The 78-element concept enlarged the centre pin and reduced the diameter of the outer pins to limit the peak LER. The current 64-element concept,

presented by Pencer and Colton, has two rings of elements (32 pins each) and a large coolant flow tube in the centre (in place of the unfueled pin). The reference fuel composition is a homogenous mixture of 15 wt% PuO_2 in the inner ring and 12 wt% PuO_2 in the outer ring, with the balance being ThO_2, although according to Pencer, Edwards, and Onder, more complex axial and radial graded enrichment schemes may be implemented in the future [11, 37]. The flow tube both balances the power profile between the inner and outer rings of fuel elements (eliminating the peak LER problem) and ensures a negative CVR [11].

The re-entrant channel (where coolant first flows downward through the centre flow tube and then upward around the fuel pins) is an integral part of the Canadian SCWR conceptual design. Yetisir, Gaudet and Rhodes state that the re-entrant flow path allows for all core inlet and outlet piping to be located above the core (advantageous for safety as it reduces the risk of leaks in the PHTS and encourages natural circulation) and drastically simplifies the piping, eliminating the large lengths of feeders typical of PHWRs [12]. Together with the ceramic insulator and pressure tube that isolate the PHTS from the moderator, the concept is generally referred to as the High Efficiency Re-Entrant Channel (HERC). A simplified schematic of the Canadian SCWR concept, henceforth the Pressure Tube type SuperCritical Water-cooled Reactor (PT-SCWR), was shown in Figure 1.1.

The HERC concept also offers potential for significant improvements to reactor safety, even relative to other Generation IV designs [38]. According to Licht and Xu, in a severe Loss of Coolant Accident (LOCA) it could be possible for 100 % of radioactive decay heat to be transmitted from the fuel via radiation through the insulator to the moderator. The moderator would then naturally circulate through an isolation condenser, rejecting the decay heat to the environment with no active components. This is notable because it was the inability to passively remove radioactive decay heat that resulted in significant core damage during both the Three Mile Island and Fukushima nuclear accidents. The HERC thus forms part of what is optimistically referred to as the "no core melt" design objective [38].

2.1.3   Neutronic-Thermalhydraulic Analyses of SCWR Concepts

The effect of this coolant density change on PT-SCWR neutronics calculations was investigated by Harrison and Marleau [16]. In their study they compared a full three-dimensional neutron transport solution of an average PT-SCWR channel to a series of two-dimensional models of *lattice cells* at multiple positions along the length of the channel with different coolant properties. They concluded that the axial coupling in the PT-SCWR channel (i.e. how the coolant density at one axial position in the channel affects the neutron flux distribution elsewhere) was very weak, and thus the channel could be accurately approximated with a series of decoupled two-dimensional lattice cell calculations [16]. A similar approach was used by McDonald et al. and Pencer and Colton in their PT-SCWR physics studies: two-dimensional models of the PT-SCWR channel at several locations (at least five equally spaced from 0 to 5 m) are used to represent the channel as a whole [35, 11].

Even within a single two-dimensional "slice" of the PT-SCWR channel there may be some radial variation in coolant density as the enthalpy in individual subchannels (i.e. the flow paths between fuel pins) differs according to the radial power profile and assembly geometry. This effect was studied by Liu et al. by coupling a subchannel thermalhydraulics solver (ATHAS) to a Monte Carlo neutron transport solver (MCNP) to model the 78-element PT-SCWR fuel concept [39]. Their models showed that the effect of changes in subchannel coolant density on the individual pin powers was negligible, especially in comparison to other neutronics parameters (including differences in fuel enrichment and lattice spacing) [39]. Based on this result, two-dimensional coupled neutronic-thermalhydraulic calculations at the lattice level are likely unnecessary for determining peak fuel and cladding temperatures for design and safety analyses since equivalent results are obtained with a uniform coolant density profile.

Neutronic-thermalhydraulic coupling at the core level has also been studied. For example, Yang et al. modeled an early concept CANDU-SCWR by coupling a three-dimensional neutron diffusion model of the core to channel thermalhydraulic models (in this case, two channels were modeled: one "average" and one "hot") [17]. The purpose of Yang et al.'s study was to find an equilibrium representation of a batch-fueled CANDU-SCWR with converged

channel power and thermalhydraulics distributions, which they successfully achieved. Later, Adouki and Marleau modeled a PT-SCWR core (with fresh fuel) using the code DONJON by adding the capability to calculate the steady-state temperature and density distributions throughout the core [40]. They found that in a real core (as opposed to an infinite lattice as assumed in the aforementioned two-dimensional calculations) differences in channel powers result in different temperature and density profiles, which in turn feedback to the power calculations through the neutron diffusion solution [40]. Adouki and Marleau concluded that three-dimensional calculation of temperature and densities is necessary for core-level simulation (i.e. average channel thermo-physical properties are insufficient) [40]. This suggests that the "average channel" approach used by Yang et al. may be inadequate outside of preliminary design and scoping calculations.

Hu and Wilson studied core level coupling in the United States' reference SCWR design (which has since ceased development as the United States chose to focus on other Generation IV reactor technologies) [41]. The U.S.SCWR concept is notable because with downward-flow moderator channels and upward-flow coolant channels the flow path was similar to the HERC concept. Unlike the PT-SCWR, however, the U.S.SCWR contained an additional low-bypass downcomer and mixing plenum at the bottom of the channels. To model the separate fluids in the moderator and coolant channels, Ho and Wilson needed to modify the RELAP5 and PARCS codes (including the coupling procedure) to account for the separate fluid cross-section feedbacks [41]. They were thus able to identify potential flow reversals within the moderator channels in both steady-state and transient simulations, something which had not observed in more simplistic models [41].

The most extensive coupled neutronic-thermalhydraulic analysis of an SCWR concept, however, was presented by Monti, Starflinger and Schulenberg for the HPLWR [18]. Their model of the HPLWR core included lattice level neutron transport models (MCNP), subchannel thermalhydraulics models (MATRA), channel thermalhydraulics models (TRACE), and a core-level neutron diffusion model (ERANOS). These models together calculate complete three-dimensional distributions of power, density, and temperature (including peak fuel cladding temperatures in subchannels) in a steady-state HPLWR core, representing in

their words "a major achievement as compared with the standard methodologies" and "a new quality in core analyses" [18]. It is likely that similar models of the PT-SCWR concept will be necessary as the design process continues.

2.1.4   Analogies to Boiling Fluids

Supercritical fluid exists in a single thermodynamic phase, and thus even though there is a large thermo-physical property variation around the pseudocritical transition, the properties themselves are continuous. This is contrast to boiling fluids, in which there is a discontinuity in properties around the phase change from liquid to vapour resulting in an interface between fluids in different states.

Nevertheless, Ambrosini posits that the behaviour of supercritical fluids in heated channels is in many ways analogous to boiling fluids [19]. For example, the large density change expected in a SCWR channel is typical of a BWR, wherein saturated liquid is heated as it passes through the channel and becomes vapour. The neutronic-thermalhydraulic coupling described previously for SCWR analysis is, in fact, the same methodology used in BWR analyses (or any reactor design that includes strong neutronic-thermalhydraulic coupling, including PWRs and PHWRs in some transients) [42]. Ambrosini takes this one step further by demonstrating that the *dynamic* behaviour of supercritical fluids (i.e. time-variant phenomena) are also analogous to boiling fluids, most notably the potential for instabilities in fluid flow [19, 20]. The following section introduces the concept of two-fluid (e.g. liquid and vapour) instabilities and demonstrates how they are relevant to supercritical fluids.

2.2   Two-Fluid Instabilities

Instabilities in a nuclear engineering context can be broadly categorized as purely thermalhydraulic phenomena or the result of neutronic feedback effects. These will be introduced separately in the following sections.

2.2.1   Instabilities in Two-Phase Flows

Boure, Burgles, and Long provide a comprehensive review of the potential instability of two-phase flows [43]. From and engineering sense, flow instabilities are undesirable because sustained flow oscillations may cause forced mechanical vibrations, system control problems and significant changes in local heat transfer

characteristics. These issues become even more important in water-cooled nuclear reactors, where the properties of the fluid may have a significant impact on the core neutronics and subsequently the power being generated from nuclear fission. Boure et al. provide the following definitions [43]:

1. A flow is *stable* if when disturbed its new operations conditions tend back to the previous steady-state conditions.
2. A flow possesses *static instability* if when disturbed its new operating conditions are not in the vicinity of the previous steady-state conditions. One example of a static instability is the *Ledinegg* instability or *flow excursion*, wherein the flow undergoes a sudden and large amplitude excursion to a new stable operating condition, potentially at a much lower flow rate. Another example of static instability is *geysering*, a periodic process of fluid super-heating and violent evaporation with possible expulsion and refilling.
3. A flow possesses *dynamic instability* if system inertia and feedback effects have an essential part in the process. The system behaves like a "servo-mechanism", where knowledge of steady-state laws alone is not sufficient to predict flow behaviour [43]. An example of a dynamic instability is the *density wave* phenomena, where there are important time-delay and feedback effects between flow rates, fluid densities and pressure drops. The coupled neutronic-thermalhydraulic instability of a Boiling Water Reactor (BWR) is another example of a dynamic instability, caused by the coupling of the coolant void reactivity feedbacks with the flow dynamics and heat transfer.

Since the focus of this thesis is dynamic instability, the mechanism of the density wave oscillation is summarized in Figure 2.1. The driver of the instability is the time delay in which the relative pressure drop between the high and low density sections responds to some flow rate perturbation. A stationary observer would see oscillations in flow rate and fluid density with a period of one to two times the transit time of fluid through the heated channel, hence the term *density wave oscillation*.

Inlet flow increases / Relative pressure drop in two-phase region increases (delayed) / Inlet flow decreases due to constraint of pressure drop / Relative pressure drop in two-phase region decreases (delayed)
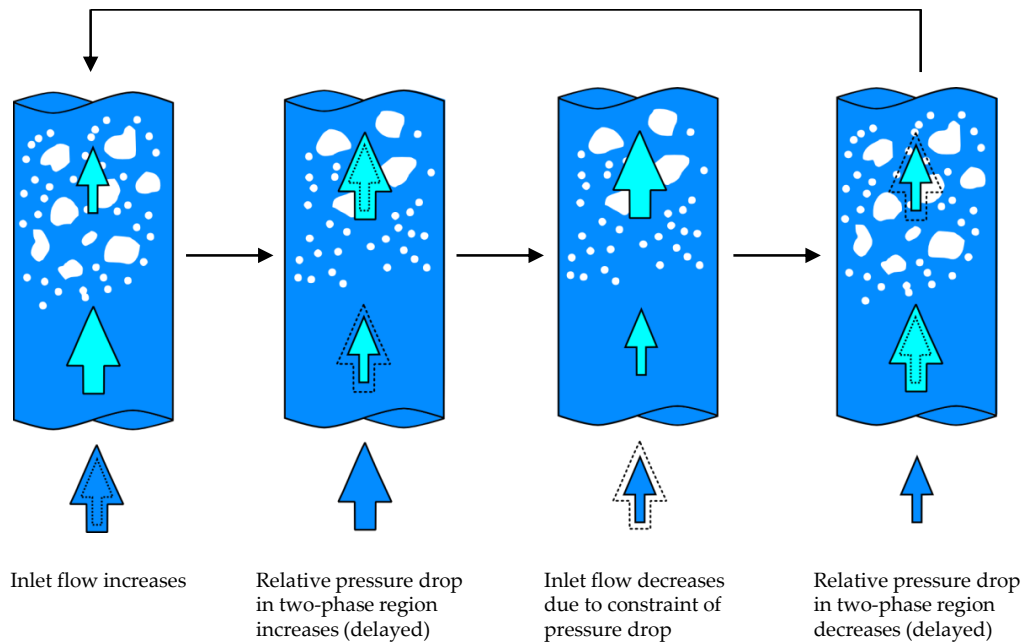
Figure 2.1: Density wave oscillation in a heated channel

According to Boure et al., some of the most important factors affecting heated channel instability from density waves are [43]:

- the *heated length* of the channel: a shorter heated length means a reduction in the delay that the inlet flow perturbations affect the pressure drop in the two-phase region closer to the outlet, stabilising the system;
- inlet and outlet *flow restrictions*: orifices or other restriction at the inlet or outlet increase the single-phase pressure drop, limiting the relative difference between the phases and stabilising the system;
- *system pressure*: higher system pressure decreases voiding and the size of the two-phase region, stabilising the system;
- *inlet subcooling*: higher inlet subcooling decreases channel voiding, stabilising the system.

Boure et al. state that analysis of two-phase flow instabilities, including density wave oscillations, is typically performed with computer codes that solve the channel thermalhydraulics (in the time domain), or using more simplistic linearized models that rely on non-dimensional quantities to determine whether the system is stable or unstable explicitly (in the frequency domain) [43].

Although several formulations for non-dimensional groups exist, according to Bourne et al. they can be generalized as one of the following [43]:

- A dimensionless velocity number, representing flow and heat input effects. An example is the Ishii-Zuber "phase change" number N_{pch} given by:

$$N_{pch} = \frac{\left(\frac{\rho_l - \rho_v}{\rho_l}\right)\Gamma_v}{\rho_v}\frac{L_c}{u_{in}} \tag{1}$$

  as a function of the liquid and vapour densities (ρ_l and ρ_v respectively), the volumetric vapour generation rate Γ_v, the characteristic length L_c, and the inlet velocity u_{in}.

- A dimensionless subcooling number. An example is the Ishii-Zuber "subcooling" number N_{sub} given by:

$$N_{sub} = \left(\frac{\rho_l - \rho_v}{\rho_v}\right)\frac{\Delta h}{h_{fg}} \tag{2}$$

  where Δh is the difference in fluid enthalpy from the latent heat of vaporization h_{fg}.

- A Froude number for dimensionless gravity, representing buoyancy effects, most relevant to natural circulation flows.
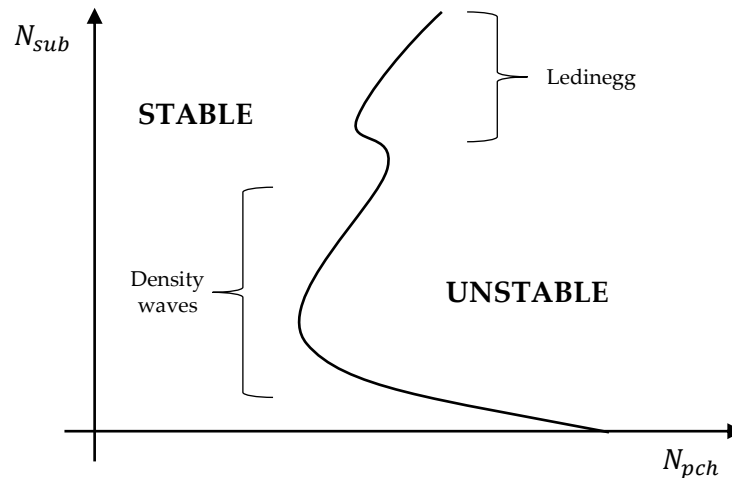
Figure 2.2: Ishii-Zuber stability plane for a heated channel with forced flow

Using these non-dimensional numbers, the stable or unstable conditions of a heated channel can be represented graphically. An example stability plane is

shown in Figure 2.2. The two "lobes" of the structure represent different methods in which the channel flow may transition from a stable condition to an unstable one.

2.2.2 The Boiling Water Reactor (BWR) Instability

The consequences of two-phase flow instabilities are significant in BWRs, where the neutronic feedbacks of fluid density changes are extremely important. According to March-Leuba and Rey, prior to the early 1990s two-phase flow instabilities were only of interest to "a few dedicated thermalhydraulicists", but after several operating BWRs underwent unstable oscillations leading to unexpected reactor scrams, the topic received renewed general interest [44].

In their review of state-of-the-art BWR stability analyses, March-Leuba and Rey identified three types of instability that BWRs are susceptible to [44]:

1. Control system instabilities: resulting from the action of out-of-core controllers attempting to regulate some variables of the reactor;
2. Channel thermalhydraulic instabilities: without any reactivity feedback, these include the static and dynamic instabilities described earlier;
3. Coupled neutronic-thermalhydraulic instabilities: instability resulting from changes in reactivity due to void fraction fluctuations.

Control system instabilities are of limited interest in this review since they don't arise out of purely physical processes and are entirely within the control of the system designer. Furthermore, according to March-Leuba and Rey, "pure" channel thermalhydraulic instabilities are not likely in a BWR due to the reactivity feedbacks [44]. The coupled neutronic-thermalhydraulic instability is therefore the most important instability, and subject to further discussion.

2.2.2.1 Mechanism for Instability

A BWR core is essentially a heated channel in which the coolant is allowed to boil. The same density wave oscillation described previously is thus possible. According to March-Leuba and Rey, the density wave is in fact the basic thermalhydraulic phenomena in BWR instability [44].

Changes in coolant and moderator density will have an associated reactivity effect in the reactor, changing the rate of nuclear fission and thus the power

generated in the fuel. In the case of a BWR, a reduction in coolant density is equivalent to a reduction in moderation (due to the reduced number of hydrogen molecules bound in water) and thus increased void in the core has a negative reactivity effect. The opposite is necessarily true as well: an increase in coolant density will result in increased moderation and a positive reactivity effect. Because there is a delay in heat generated in the fuel being transferred to the coolant (i.e. the time constant of thermal conduction), changes in void fraction and fission power may oscillate out of phase with one another. With the added effect of the density waves, the oscillation in power is accompanied by oscillations in channel flow as well (Figure 2.3). Depending on the time delay between the phenomena, these oscillations may dampen or grow with time.

March-Leuba and Rey state that the drivers of a coupled BWR instability can be summarized as [44]:

- The *neutronics* that determine the power being generated in the fuel;
- The *fuel dynamics* that determine the heat flux from the fuel to the coolant;
- The *channel thermalhydraulics* that characterize the void fraction response to changes in heat flux and include inlet flow feedback;
- The *reactivity feedback* dynamics which relate a coolant density distribution to a reactivity value.

These four drivers are typically collapsed into the "neutronic" and "thermalhydraulic" feedback paths indicated in Figure 2.3; hence the term "coupled neutronic-thermalhydraulic instability".

March-Leuba and Rey further define two types of coupled oscillations: the full-core or *fundamental mode* oscillation where the total core power and flow oscillate together, and the out-of-phase or *higher order mode* oscillations where the total core power and flow remain constant, but sections of the core oscillate in flow and power out-of-phase with one another [44]. According to March-Leuba and Huang, the behaviour of the fundamental mode oscillation is dominated by the reactivity response, and the higher order modes are largely (but not completely) determined by the thermalhydraulic response of the system [21].

Neutronic Feedback Path

Power increases   Heat flux and coolant   Void feedback lowers   Heat flux and coolant
                         void increases   power   void decreases

Inlet flow increases   Relative pressure drop   Inlet flow decreases   Relative pressure drop
                         in two-phase region   due to constraint of   in two-phase region
                         increases (delayed)   pressure drop   decreases (delayed)

Thermalhydraulic Feedback Path

Figure 2.3: Coupled neutronic-thermalhydraulic instability

March-Leuba and Rey identify the most important factors influencing both types
of oscillations. The fundamental mode oscillation is mostly strongly influenced
by [44]:

- Average void fraction: the single most important quantity since higher void means greater neutronic feedbacks and large two-phase pressure drops, both destabilising effects;
- Axial power shape: bottom peaked power shapes are more unstable since they increase the axially averaged void fraction;
- Inlet subcooling: higher subcooling reduces void and thus increases power, but decreases the time delays in the density wave effect;
- Fuel-gap conductance within the fuel sheath: higher gap conductance increases the power deposited in the coolant during a neutron flux oscillation, and is thus destabilising overall;
- Isotopic composition of the fuel: changes the coolant density reactivity coefficient.

Similarly, higher order modes of oscillation are most strongly influenced by [44]:

- Geometric buckling: larger cores are more susceptible to out-of-phase oscillations;
- Pressure drop over the core: large pressure drops increase the density wave effect are thus destabilising;
- Flow rate: higher flows increase the friction pressure drop and thus feed in to the density wave;
- Single-phase friction: flow restrictions in the single-phase regions (e.g. channel inlet orifices) dampen the effects of density wave oscillations.

It should be noted that the described instability phenomena are not exclusive to BWRs. For example, a paper by Mochizuki describes the full-scale experiments to determine the natural circulation flow instabilities of the Advanced Thermal Reactor (ATR), a pressure tube type boiling light water reactor [45]. Consistent with the previous descriptions, Mochizuki found that the density wave oscillations observed in the experiments were influenced by both the length of the two-phase region and the total power and power distribution. Mochizuki also states the the ATR was designed to have a near zero void reactivity specifically to limit the coupled neutronic-thermalhydraulic instability described previously [45]. Nayak et al. also observed similar coupled instability phenomena in the design of the Indian Advanced Heavy Water Reactor (AHWR), a conceptual evolution of a generic PHWR [46]. It can generally be said that any reactor with strong neutronics-thermalhydraulic coupling and a positive

coolant density reactivity coefficient is also potentially vulnerable to coupled instabilities.

2.2.2.2   Framework for BWR Instability Analysis

The modeling of coupled neutronic-thermalhydraulic instability is, according to March-Leuba and Huang, arguably the most complex simulation performed in reactor design [21]. They state that for most other simulations the initiating event can be realized as the application of a boundary condition (e.g. a pipe break). On the other hand, instabilities develop themselves without boundary conditions forcing them, so if every aspect of the system is not modelled correctly, the result may be "100% wrong" [21].

According to March-Leuba and Rey, predictive calculations of BWR instability require computer codes that operate in either the time-domain (i.e. solvers of reactor heat transport system thermalhydraulics and reactor kinetics) or the frequency domain (linearized models), although time-domain codes are more common [44]. A typical value of interest in BWR instability analysis is the *decay ratio*, or relative change in amplitude between subsequent power oscillations. March-Leuba and Rey state that being able to predict decay ratios from stability tests within ± 20% of the measured value is good accuracy. However, it's proven nearly impossible to predict unstable conditions in a plant without extremely good knowledge of the operating conditions, to which the solution is very sensitive [44].

In a review of the regulatory perspective of BWR instability, Huang and March-Leuba state that the primary regulatory bases for issues regarding stability in the United States of America are contained with the General Design Criteria (GDC) of regulatory document 10CFR50. Criterion 12 regarding "suppression of reactor power oscillations" specifies that [47]:

> *"…the reactor core and associated coolant, control and protection systems shall be designed to assure that power oscillations which can result in conditions exceeding specified acceptable fuel design limits are not possible or can be reliably and readily detected and suppressed."*

Furthermore, Criterion 10 regarding reactor design specifies that [47]:

"…the reactor core and associated coolant, control and protection systems shall be designed with appropriate margin to assure that specified acceptable design limits are not exceeded during any condition of normal operation, including the effects of anticipated operation occurrences."

Recent extension of BWR plant operating domains (including higher power densities and power-to-flow ratios) have, according to Huang and March-Leuba, been detrimental to the reactor's stability, as they both increase the probability of an instability event and increase the severity should one occur (for example, in the form of larger amplitude oscillations) [47].

As of 2004, there were fifteen reported instability events at BWRs around the world [23]. According to D'Auria et al. and consistent with the GDC above, the primary safety concern associated with these instabilities has been ensuring the cooling of the fuel and the fuel cladding integrity, and thus the primary objectives of BWR instability analyses are [23]:

- To assess the stability margins (i.e. the margin to an unstable condition) in normal and abnormal operation;
- To predict the transient behaviour of the reactor should an instability occur;
- To help in designing and assess the effectiveness of countermeasures meant to mitigate the effects of the instabilities.

To that end, the typical approach to performing instability analyses has been modeling the reactor through by coupling a thermalhydraulic system code to a three-dimensional neutron kinetics code. D'Auria et al. state that this approach is particularly suited towards simulating the spatially asymmetric phenomena and thermalhydraulic-neutronic feedback effects associated with the instabilities [23]. This is echoed by Ikeda et al. in their summary of BWR stability analysis in Japan, where they state that time domain models (including spatial neutron kinetics) are generally superior to linearized models in every aspect except the increased computation time and the sensitivity of the results to the time step size, which requires careful selection by the modeller [48]. Code coupling methodology is examined briefly in the following section.

2.2.3   Neutronic-Thermalhydraulic Code Coupling

Generally speaking, computer codes are coupled for the analysis of complex problems that involve multiple disciplines or different simulation domains (e.g. the PHTS and containment). Neutronic-thermalhydraulic coupling is an example of the former. In this case, a power distribution is calculated by the neutronics code and passed to the thermalhydraulics code, which calculates new material temperatures and densities, which are in turn passed back to the neutronics code to recalculate the power [42].

According to Grgic, coupling two existing codes to create a "modular code system" takes advantage of existing knowledge and user experience, with verification and validation only necessary for the coupling procedure [42]. This is opposed to creating an integrated multi-physics code or manually passing results between disparate codes, which are respectively more expensive and more prone to error than a coupled code system [42].

For temporal or time variant simulations, Grgic states the coupling can be "explicit", where one code controls the stepping forward in time as the other lags, or "implicit", where each code solves the current timestep simultaneously [42]. These same schemes can also be referred to as "asynchronous" or "synchronous" [49]. According to Downar, for coupled neutronic-thermalhydraulic safety analysis of LWRs (including BWR stability analyses) an explicit or "marching" scheme is used where the neutronics/spatial-kinetics code controls the step forward in time [50]. Grandi further defines a "mixed" scheme where one code controls the step forward in time, however if some physical parameters change too quickly between time steps (e.g. power, cladding temperature), the simulation is backed up and continued with a smaller time step. Grandi states this "mixed" (or "semi-implicit") approach requires much less computational time since the size of the time step can change with the transient, making more efficient use of computational cycles [49]. Generally speaking, most coupling implementations are either fully explicit or semi-implicit [42].

More complex coupling schemes are possible where both codes were designed to work together from the beginning. For example, Rouben describes the temporal coupling of the Canadian Industry Standard Toolset (IST) codes RFSP (for three-dimensional spatial kinetics simulation of CANDU cores) and CATHENA (for

one-dimensional pipe network simulation of CANDU PHTS), which uses a "two-tiered" time scheme [51]. According to Rouben, the three-dimensional flux in the core is factored in to amplitude and shape functions, where the latter is assumed to change much more slowly and is thus evaluated over much coarser time steps. The thermalhydraulics solution of CATHENA is coupled to the amplitude, which is evaluated over much finer steps. This method is stated to be much faster than solving for the full flux at every time step in an explicit coupling scheme [51]. There are, however, limitations to this approach. For example, in transients where the flux shape was known to be changing quickly (e.g. higher-order mode BWR instabilities) the computational savings may be minimal. Furthermore, not every 3D spatial kinetics code may assume separability of flux shape and amplitude, or may not make each accessible in isolation for coupling.

Grgic identifies several PWR transients which require neutronics-thermalhydraulics coupling, including main steam line breaks and control rod ejections [52]. According to Rouben, coupled neutron kinetics and thermalhydraulics are a critical part of CANDU large LOCA analysis owing to the positive void reactivity [51]. Due to the fundamentally coupled nature of the phenomena, neutronics-thermalhydraulics code coupling is obviously a key component of BWR instability analysis.

2.2.4   Contemporary BWR Instability Analysis

The Ringhals-1 Stability Benchmark, organized by the Nuclear Energy Agency (NEA) Nuclear Science Committee under the auspices of the Organization for Economic Co-operation and Development (OECD), represents one of the most comprehensive efforts to accurately model BWR stability [53]. The purpose of the benchmark was to distribute information on the Swedish BWR Ringhals-1 and determine if international participants could accurately model real power oscillations measured at the reactor (specifically, decay ratios and natural frequencies). The benchmark was "blind" in that the participants were given enough information to accurately model the plant, but were not given the transient measurements of the events and therefore could not "tune" their models to produce superior results. The benchmark organizers collected the computational results and concluded that most participants predicted the decay ratios within a "very small bias" and uncertainties "close" to those measured, with a general trend to slightly underestimate the oscillation frequency [53].

Nevertheless, given the age of the benchmark (published in 1996) and the majority of participants' use of linearized frequency-domain codes, the benchmark models would not qualify as modern examples of BWR instability analysis based on the description provided by D'Auria et al. [23].

The original Ringhals-1 stability benchmark specifications, however, remain available to test new models and methods. For example, Xu et al. presented a model of Ringhals-1 using the system thermalhydraulics code TRACE and the three-dimensional multigroup neutron diffusion code PARCS to test the ability of the coupled code set to accurately model a BWR instability transient [24]. TRACE and PARCS are, according to the United States Nuclear Regulatory Commission (U.S.NRC), included among the most modern computational tools in their respective fields [54]. Coupled together to simulate a transient from the Ringhals-1 benchmark, this use of TRACE/PARCS represents the state-of-the-art in BWR instability analysis. Typical for this type of study, Xu et al. examined the predicted decay ratio following perturbations to reactor control device positions and/or the inlet pressure boundary condition, concluding that coupled TRACE/PARCS was an acceptable tool for modeling instabilities [24].

The OECD's new Oskarshamn-2 BWR Stability benchmark, as described by Kozlowski et al., represents an even greater modeling challenge [25]. A decay ratio of 1.4 was measured during the 1999 stability transient at the Swedish Oskarshamn-2 BWR plant (i.e. the magnitude of the power oscillations was growing before being arrested by a reactor scram), unlike in the Ringhals-1 transient data where all measured decay ratios were below 1.0. According to Kozlowski et al., this increases the modeling difficulty substantially. Nevertheless, the results presented by Kozlowski et al. and Gajev, Ma, and Kozlowski demonstrate that coupled TRACE/PARCS is just as capable of predicting the instability in Oskarshamn-2, including oscillation frequency and decay ratio [25, 55].

Using the decay ratio as the sole measure of BWR instability is, however, not a universally accepted practice. In their critique, van der Hagen, Zboray and de Kruijf state that a BWR with a small predicted decay ratio may actually have less margin to instability than one with a large decay ratio, concluding [56]:

"…the scientific BWR-stability community is focusing too much on the [decay ratio]. It is a result of overconfidence to believe that the dynamic features of a BWR can be grasped in a single number."

Van der Hagen et al. thus advocate additional quantitative analysis from modellers, including at the very least sensitivities of decay ratios to parameters in their models [56].

The sensitivity of predicted instability parameters (e.g. decay ratio, frequency) to input parameters in the TRACE/PARCS model was thus studied by Gajev, Ma, and Kozlowski [57]. Gajev et al. used a Propagation of Input Errors (PIE) method, wherein each model input parameter was assigned an uncertainty distribution from which values were randomly sampled to create a distribution of predicted decay ratios and frequencies. From the output distribution, Gajev et al. were thus able to determine the sensitivity of the model prediction to each input parameter, or equivalently, determine which model parameters have the largest impact on the reactor stability. The input parameters they found to have the greatest effect on stability were [57]:

1. The fuel thermal conductivity, including conductance in the gas gap between fuel and cladding, which affects the rate at which heat generated in the fuel from fission is transferred to the coolant;
2. The bubbly slug wall drag coefficient, which affects the pressure drop in the two-phase region and thus feeds in to the density wave;
3. The Lower Axial Power Peaking (LAPP) factor, essentially the axial power distribution in the channel, a higher LAPP factor means more heat is being deposited to the coolant in the single phase region.

The LAPP was considered a separate input parameter for this study even though it represents the accumulated effect of several neutronics inputs. The predicted decay ratios are, according to Gajev et al., weekly sensitive to individual neutronics inputs relative to the three parameters above [57].

The sensitivity to neutronics inputs was nevertheless studied separately by Gajev et al. for the TRACE/PARCS model of Ringhals-1 [58]. While the calculated sensitivities to all neutronics inputs were small, several were smaller still such that the stability predictions are arguably independent of them. These insensitive parameters include: average energy released per fission, assembly discontinuity

factors, control rod history, and absorption cross-sections of several saturating neutron poisons (e.g. xenon and samarium) [58]. It can be assumed that all other neutronic inputs (specifically interaction cross-sections and kinetics parameters) will impact the predicted decay ratio and oscillation frequency, although only slightly compared to several thermalhydraulic inputs.

2.3   Potential Instabilities in the SCWR

As with BWRs, potential instabilities in a SCWR (regardless of type) can be categorized as either purely thermalhydraulic or coupled with neutronics. They are thus presented separately.

2.3.1   Instability in Supercritical Flows

According to Ambrosini and Sharabi, the potential for instability in heated channels with supercritical fluids was recognized early in the conceptual development of SCWRs [59]. In order to facilitate supercritical instability analysis, Ambrosini and Sharabi recognized the need for a set of non-dimensional numbers that would be relevant in the supercritical regime. The Ishii-Zuber phase change and subcooling numbers (N_{pch} and N_{sub}, respectively) used in boiling channel analyses were clearly inapplicable past the critical point where there is only a single phase and thus no discontinuity in fluid properties. Since the thermos-physical properties of the fluid vary so substantially (though continuously) near the pseudocritical point, Ambrosini and Sharabi selected it as the reference point for a new set of dimensionless numbers, namely the dimensionless density ρ^* and enthalpy h^* given by [59]:

$$\rho^* = \frac{\rho}{\rho_{pc}} \tag{3}$$

$$h^* = \frac{\beta_{pc}}{c_{p,pc}}\left(h - h_{pc}\right) \tag{4}$$

where β_{pc} is the volumetric expansion coefficient and $c_{p,pc}$ is the specific heat capacity at the pseudocritical point. Ambrosini showed that these definitions of dimensionless density and enthalpy are in fact mostly independent of dimensional quantities (most notably pressure), and thus it is usually safe to represent ρ^* as $\rho^* = \rho^*(h^*)$. The same is in fact true with very good accuracy across many different fluids, including supercritical water, carbon dioxide,

ammonia, and R23 [20]. Ambrosini and Sharabi thus introduced new non-dimensional numbers for instability analyses of (generic) supercritical fluids using these dimensionless parameters, the "trans-pseudocritical number" N_{TPC} (intentionally analogous to the Ishii-Zuber phase change number N_{pch}) and the "sub-pseudocritical number" N_{spc} (analogous to the Ishii-Zuber subcooling number N_{sub}):

$$N_{TPC} = \frac{q_0'' \Pi_h L}{\rho_{in} u_{in} A} \frac{\beta_{pc}}{c_{p,pc}} \tag{5}$$

$$N_{spc} = \frac{\beta_{pc}}{c_{p,pc}} \left(h_{pc} - h_{in} \right) \tag{6}$$

where q_0'' is the heat flux, Π_h is the heated perimeter, L is the channel length and A the channel area [59].

With these new non-dimensional numbers, Ambrosini performed several simulations of a heated channel containing supercritical fluid to examine the instability, using both a simplified Homogeneous Equilibrium Model (HEM) and a computer code using Unequal Velocity Unequal Temperature (UVUT) assumptions (RELAP5) [19]. Ambrosini found that the stability maps obtained using these non-dimensional numbers were qualitatively similar to the Ishii-Zuber plane shown in Figure 2.2, including the two-lobe structure that indicated the existence of both density wave oscillations as well as a Ledinegg instability. Furthermore, Ambrosini concluded that a HEM model produced very similar stability results as the UVUT code (RELAP5), although only experimental results (not yet gathered) would contribute any real new knowledge [19]. Ambrosini and Sharabi would later confirm their results, however noting that the amount of pseudo-subcooling necessary for a Ledinegg instability in a supercritical fluid is far greater than typical reactor operating conditions [59]. In fact, the pseudo-subcooling necessary for a Ledinegg instability in a vertical channel with supercritical fluid is equivalent to an inlet temperature below 100 °C at 25 MPa, while maintaining the outlet temperature above 800 °C [20].

Earlier, Chatoorgoon had performed a numerical stability analysis for the conceptual CANDU-X reactor, a supercritical light water-cooled pressure tube type reactor that is an early predecessor of the current reference PT-SCWR design [60]. According to Chatoorgoon, at the time both forced flow and natural

circulation for the primary heat transfer system were under consideration, and thus a stability analysis was performed for natural circulation using a non-linear thermalhydraulic stability code (SPORTS) and compared against a more simplistic analytic solution. Chatoorgoon found that both the code and analytic calculation showed the potential for instability in the supercritical flow, thinking it to be a new type of flow instability [60]. It is possible (if not likely) that the instability Chatoorgoon observed is the same density wave oscillation since proposed by Ambrosini et al.

The SCLWR-H has also undergone preliminary stability analysis by Yi, Koshizuka and Oka. [61]. The first part of Yi et al.'s study was a purely thermalhydraulic stability analysis using a specially created code in the frequency domain, consisting of a linearized single channel model with one-dimensional phase conservation equations. Yi et al. noted that the average density change through a SCLWR-H channel is five times that of a BWR. They found that the potential for flow instability indeed exists, however pure thermalhydraulic stability of the SCLWR-H could be readily achieved through proper selection of inlet orifices [61].

The U.S.SCWR concept was very similar to the SCLWR-H, and Zhao, Saha and Kazimi performed a similar linearized stability analysis as Yi et al. [62]. Zhao et al. came to the same conclusions regarding stability as Yi et al., notably that thermalhydraulic stabilities could exist in the U.S.SCWR and that they could be sufficiently dampened with inlet orifices. Zhao et al. drew special attention to the moderator channels in the U.S.SCWR assembly, which are part of a recirculating flow path similar to what was described for the PT-SCWR. Zhao et al. showed that whether or not heat transfer was modeled to the moderator channels had a significant impact on the results of the stability analysis. Specifically, heat transfer to the moderator channels was detrimental to the overall stability, even though the system could still be stabilized with proper orifices [62]. It would later be shown that this effect is even more important in the coupled neutronic-thermalhydraulic stability analysis.

2.3.2 Coupled Neutronic-Thermalhydraulic Instabilities in the SCWR

The similarity of SCWRs to BWRs was noted early in the conceptual development. According to Yang, power and flow instabilities were identified in

the Generation IV roadmap as an important technology gap in SCWR development that required serious analysis [22].

The second part of Yi et al.'s aforementioned study examined the coupled neutronic-thermalhydraulic stability of the SCLWR-H by adding additional point kinetics equations to the aforementioned linearized model [63]. They found that the water rods contributed significantly to the coupled instability due to the moderator density reactivity effects. In fact, since there is significant time delay between heat generated in the fuel reaching the water rods, the coupled instability of the SCLWR-H is in their opinion "considerable" [63].

Similarly, Zhao et al.'s study had a second part which examined the coupled instability of the U.S.SCWR compared to a BWR [64]. They found several features of the U.S.SCWR to be either beneficial or detrimental to the coupled stability. For example, the larger magnitude density change in the SCWR channel was detrimental to stability; however, the fact that most moderation takes place in the moderator channels (which have much less density variation, even with heat transfer included) was beneficial. Zhao et al. thus conclude that with this combination of effects, the U.S SCWR could be not be judged as "more" or "less" stable than a BWR [64].

Some similar analysis has also been executed for the PT-SCWR. Pan and Shan modeled a PT-SCWR channel with thermalhydraulics equations coupled to point kinetics equations [65]. Pan and Shan generated stability maps for the PT-SCWR similar to Figure 2.2 using non-dimensional numbers equivalent to N_{spc} and N_{TPC}, showing that there were regions of operation in which the PT-SCWR could be unconditionally unstable without mitigating measures [65].

Coupled neutronic-thermalhydraulic stability of the SCWR has even been examined experimentally. T'Joen and Rohde present a study in which they created a scale model of the HPLWR core with electric heaters and refrigerant coolant [66]. In their apparatus (named DeLight), neutronic feedback effects were modeled by measuring the coolant density and varying the electrical power with a feedback controller in real time. Using DeLight, T'Joen and Rohde measured decay ratios as functions of a non-dimensional number equivalent to N_{spc}. In their opinion, the results from the DeLight experiments can be used for validation of computational models of the real HPLWR [66].

While there are many similar examples of SCWR stability analysis with single channel and/or linearized models with point kinetics as above, there are conversely very few with full core coupled thermalhydraulics and spatial kinetics. Given the similarity of SCWR concepts to BWRs, it would be logical that the standard in BWR instability analysis would be applied to SCWRs. In fact, as early as 2003 Yang had identified the need for multiple channel thermalhydraulic models and space-time neutron kinetics for stability analyses [22]. This represents a significant gap in the existing knowledge base that is necessary for SCWR conceptual development.

2.4 Conclusions from Literature Review

Several conclusions can be drawn from this review:

1. The PT-SCWR is a Generation IV reactor concept that, like other SCWR concepts, is in many ways similar to contemporary BWRs because of the substantial coolant density change across the core.

2. Due to the feedback between coolant density changes and the neutronics that determine the fission power in the fuel, BWRs are vulnerable to a coupled neutronic-thermalhydraulic instability wherein the core power and flow oscillate, potentially threatening various safety limits.

3. The modern standard for BWR instability analyses is coupled computer codes that model the channel thermalhydraulics and neutron spatial kinetics in the time domain at the core level.

4. Coupled neutronic-thermalhydraulic instability analyses of SCWR concepts, consistent with the standard established for BWR instability analyses, is a necessary part of SCWR conceptual development.

Together, these lead to the further conclusion that coupled neutronic-thermalhydraulic instability analysis of the PT-SCWR is necessary. This will require core-level channel thermalhydraulics and neutron spatial kinetics models of the PT-SCWR concept to be created and coupled for transient simulation. Herein lies the primary objective of this thesis: to create the models and perform an analysis of PT-SCWR coupled (in)stability in support of the conceptual design development, with the provision that the models can be used for further coupled transient analysis.

Chapter 3

Theoretical Framework

Reactor core neutronics and thermalhydraulics are disparate fields that are derived from entirely different physical processes. Nevertheless, it is the interplay between the two that creates coupled phenomena that are the subject of this thesis. Modeling such phenomena is essentially modeling both the core neutronics and thermalhydraulics while providing a means for information to be passed between the processes. In this chapter the fundamental theory behind each model is described.

3.1 Nuclear Reactor Core Physics

The relevant nuclear processes in a reactor can be broadly categorized as either an interaction between a free neutron and an atomic nucleus or the radioactive decay of an unstable nucleus. Due to the importance of the former in creating a self-sustaining fission chain reaction, the study of "reactor physics" is also referred to as *neutronics*. The objective of this section is to provide a brief introduction to the theory of neutronics to give context to the following sections of this thesis. The physics of radioactive decay will not be described explicitly, but free neutrons released by the decay of fission products are included as an important part of transient neutronics calculations.

3.1.1 Neutron-Nucleus Interactions

The relevant nuclear processes in a reactor can be broadly categorized as *neutron absorption* (either resulting in non-productive capture or *neutron induced fission*) and *neutron scattering* (both elastic and inelastic). These are described in the following sections.

3.1.1.1   Neutron Absorption and Capture

The first interaction mechanism described is the *absorption* of a free neutron in to an atomic nucleus. A meta-stable compound nucleus is formed following the absorption, represented with the notation $\left(^{A+1}_{Z}X\right)^{*}$ where the element X initially has Z protons and an atomic mass (i.e. the sum of neutrons and protons within the nucleus) of A. This compound nucleus has excitation energy E^{*} that is necessarily the sum of the incident neutron's kinetic energy and its binding energy within the nucleus (the result of the short range strong nuclear force). The nucleus briefly remains in the excited state before de-excitation occurs through the emission of a gamma photon (called *radiative capture*) or additional nucleons [67]. Typically the term "*capture*" is reserved for interactions where free neutrons are not created by the de-excitation of the compound nucleus.

There are several interactions where additional free neutrons are created, including (n,2n), (n,3n), and etc., but few neutrons in a typical reactor possess the necessary energy to cause these reactions and their contribution to the total free neutron population is relatively small. This additional source of free neutrons is generally neglected but included in the definition of absorption [67]. Absorption of a free neutron is also a prerequisite to nuclear fission, which is the most important source of free neutrons in a reactor. De-excitation that results in the ejection of a single neutron is, however, considered a scattering interaction. Some care must thus be given to these definitions. Within the field of nuclear engineering every interaction that's not explicitly categorized as scattering can be considered absorption [68].

3.1.1.2   Neutron Scattering

An interaction between a free neutron and a nucleus that does not result in the loss of the neutron is referred to as *scattering*. As mentioned previously, after gaining a neutron to form an excited compound nucleus one of the potential avenues of de-excitation is the ejection of a single free neutron. Whether or not the ejected neutron is the same neutron that initially created the compound nucleus is irrelevant in an engineering context. Like an elastic collision in classical mechanics, if the initial kinetic energy of the neutron and nucleus is conserved after the de-excitation, it is referred to as *elastic scattering*. Similarly, if the kinetic energy of the particles is not conserved and the nucleus is left in an excited state (with a lower E^{*}) then it is *inelastic scattering* [67].

Formation of a compound nucleus is, however, only likely for specific energies of the incident neutron (with quantum mechanics, these values of E^* correspond to allowable energy states in a shell model of the nucleus). Outside of these energies there is an elastic process called *potential scattering*, which is analogous to a collision between two particles in classical mechanics (also called a "billiard ball" type collision). A simple example is the potential scattering of a free neutron off of a stationary nucleus. A free neutron that possesses energy E' before the collision will have energy E after the collision in the range $\alpha E' \leq E \leq E'$, where α is defined as [67]:

$$\alpha = \left(\frac{A-1}{A+1}\right)^2 \tag{7}$$

According to (7), the lower energy bound for a free neutron after a potential scattering interaction is inversely proportional to the atomic mass A. This is exactly what would be expected in classical mechanics; a free neutron (with $A = 1$) will transfer more momentum to a nucleus the closer that nucleus' mass is to that of the neutron itself. The span of E is attributable to the angle of collision between two moving particles [68]. Of course in a real reactor the nuclei can't be stationary since all materials have some non-zero temperature. This complicates the expression in (7) but also allows for some *upscatter* (i.e. neutrons *gaining* energy through collision, as opposed to *downscatter* defined earlier). The importance of scattering in a nuclear reactor is precisely because of the transfer of energy, which will become apparent in the following sections.

3.1.1.3   Neutron Induced Fission

The final interaction to be discussed is the *fission* of an atomic nucleus resulting from its interaction with a free neutron. After the creation of an excited compound nucleus, the most spectacular de-excitation path is for the nucleus to split in to two smaller nuclei, each close to half the size of the original. This can be visualized as the excitation energy E^* causes the nucleus to distend to the point that the strong nuclear force is overcome by the electrostatic repulsion of the constituent protons, resulting in the two *fission fragments* rapidly accelerating away from one another. The liberated binding potential thus goes mostly towards the fragments' kinetic energy [68]. If the binding energy of the original free neutron was alone sufficient to cause the fission, it is referred to as a "slow" fission (i.e. from a "slow" neutron). Conversely, if E^* required a significant

contribution from the neutron's kinetic energy, it is a "fast" fission. The useful energy released from a nuclear fission is orders of magnitude greater than any chemical reaction, which is why a nuclear fission reactor is an attractive energy source [67].

Immediately following a fission event the daughter nuclei are also in excited nuclear states (in addition to possessing substantial kinetic energy from the fission). A potential de-excitation avenue is the ejection of additional neutrons, which because of the short time scale of this de-excitation are called *prompt neutrons*. These prompt neutrons are emitted in the normalized energy spectrum $\chi(E)$ (an example spectrum is shown in Figure 3.1). The fission products are also likely to be radioactive β⁻ emitters, and after decay may still be in unstable states. This may result in the emission of additional free neutrons following the characteristic decay times, which are called *delayed neutrons* [67].
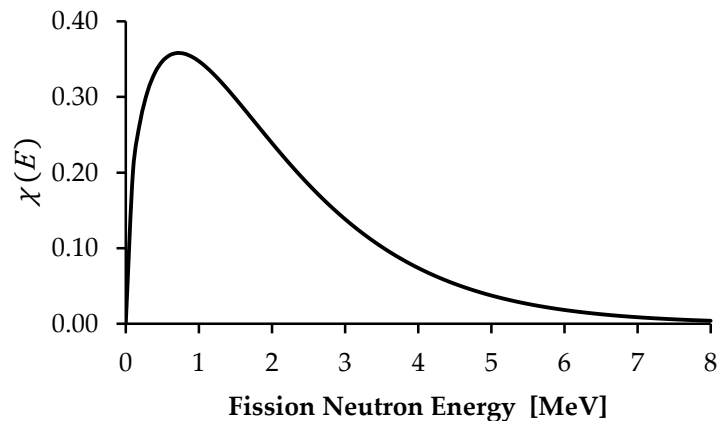
Figure 3.1: Energy spectrum of prompt neutrons released from fission of ²³⁵U

The neutrons released from fission (including prompt and delayed sources) may in turn cause additional fissions, creating what is called a *fission chain reaction*. To sustain the chain reaction it is necessary that the number of free neutrons generated in fission at least equal those that are being lost (e.g. by capture or leaking out of the system). The reactor multiplication constant k, a very important quantity in reactors physics, is thus defined as:

$$k = \frac{number\ of\ neutrons\ produced}{number\ of\ neutrons\ lost} \tag{8}$$

With this definition, the fission chain reaction is stable or *critical* when $k = 1$. In cases where $k < 1$ the reactor is *subcritical* and the chain reaction is unsustainable, eventually petering out. Conversely, in cases where $k > 1$ the number of free neutrons (and thus fissions) is constantly increasing with time. In order to harness nuclear fission as a source of energy it is necessary that a nuclear reactor remain critical in normal operation.

3.1.1.4   Neutron Interaction Cross-Sections

Consider the thought experiment shown in Figure 3.2, where a beam of neutrons with intensity I [neutrons·cm^{-2}·s^{-1}] is impinging on a surface one atom thick, over an area of N_A [atoms·cm^{-2}] [68].
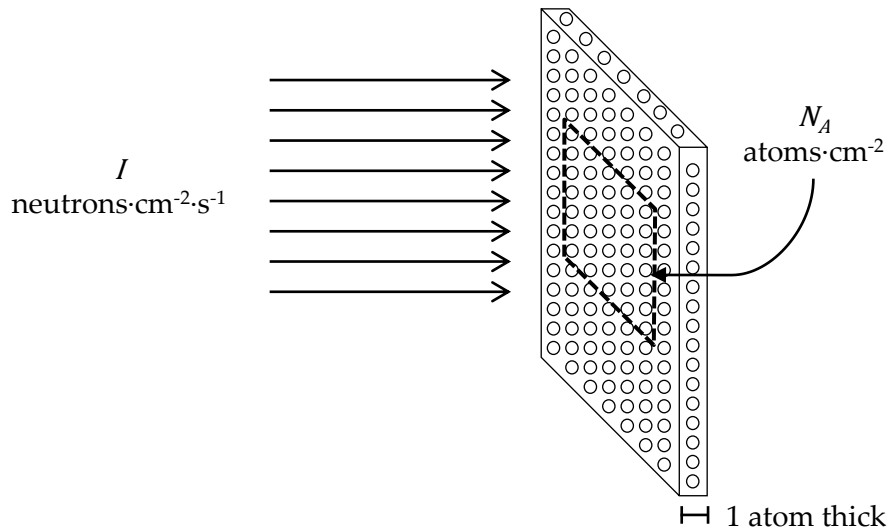
Figure 3.2: Description of microscopic cross-sections

It would be reasonable to assume that the interaction rate over the surface, in units of interactions·cm^{-2}·s^{-1}, is found as:

$$Interaction\ Rate = \sigma I N_A \qquad (9)$$

where σ is a proportionality constant for the specific interaction. It is evident that this constant must have units of cm^2, and consequently it is referred to as the *microscopic cross-section*. Each of the aforementioned neutron-nucleus interactions has an associated microscopic cross-section, which are a function of both the specific isotope and the energy of the incident neutron. Typically microscopic cross-sections are determined experimentally or with detailed nuclear models for

each isotope and interaction, and made available in nuclear data libraries in units of *barns*, such that 1 barn = 10^{-24} cm², over ranges of neutron energies.

This generic definition of cross-section is sufficient to determine the likelihood of any given interaction occurring, but if the objective is to model how neutrons move through space (as would be the case in reactor analysis) additional information is required. For scattering interactions in particular data libraries contain *differential* cross-sections which describe the likelihood of a neutron transitioning from one state (e.g. initial energy E' and direction $\vec{\Omega'}$) to another (E and $\vec{\Omega}$) in the form $\sigma_s\left(\vec{\Omega'} \to \vec{\Omega}, E' \to E\right)$ [68].

While microscopic cross-sections are useful for general data libraries, in an engineering context the important quantity is the *macroscopic cross-section* Σ defined as:

$$\Sigma\left(r, \vec{\Omega}, E, t\right) = N(r, t)\sigma\left(\vec{\Omega}, E\right) \qquad (10)$$

where the density of nuclei at position r in a volume at time t is given by N [atoms·cm⁻³]. From (10) it is seen that Σ has units of cm⁻¹, and thus represents the probability that a free neutron will undergo an interaction with a nucleus within a unit distance while passing through a volume. Most absorption cross-sections are considered to be isotropic, so this reduces to $\Sigma(r, E, t)$ for interactions that aren't scattering.

3.1.1.5   Neutron Moderation and the Thermal Spectrum Reactor

Recall that fission neutrons are emitted in the energy spectrum $\chi(E)$, with the vast majority possessing energies of 1 MeV or greater (Figure 3.1). Because of their large kinetic energy these are referred to as *fast* neutrons. Now consider that the fission cross-section for ²³⁵U (a typical nuclear fuel) is considerably higher at lower energies, as shown in Figure 3.3 [69].

Given the relatively low fission cross-section of ²³⁵U at high energies where the fission neutrons are born, the fast neutrons must somehow be robbed of their energy in order to sustain the chain reaction. In a reactor this is accomplished through a series of scattering interactions (precisely those described previously) in what is referred to as a *moderator* material. Through these scattering interactions the neutrons transfer energy to the nuclei until they are effectively in

thermal equilibrium with the moderator material, and thus have an energy distribution that follows the Maxwell-Boltzmann distribution [68]:

$$M(E) = \frac{2\pi}{(\pi k_B T)^{\frac{3}{2}}} \sqrt{E} e^{-\frac{E}{k_B T}} \tag{11}$$

where k_B is Boltzmann's constant and T is the temperature of the moderator. Figure 3.4 shows how the peak of this distribution at typical material temperatures is below 1 eV, where the fission cross-section is much higher. A reactor that requires this "thermalization" of the fission neutrons to remain critical is called a *thermal* or *thermal spectrum* reactor [67].
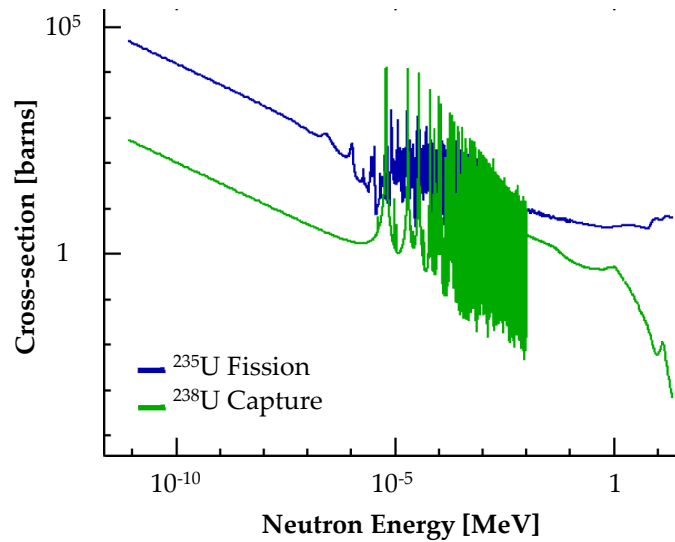
Figure 3.3: Microscopic cross-sections for ^{235}U fission and ^{238}U absorption
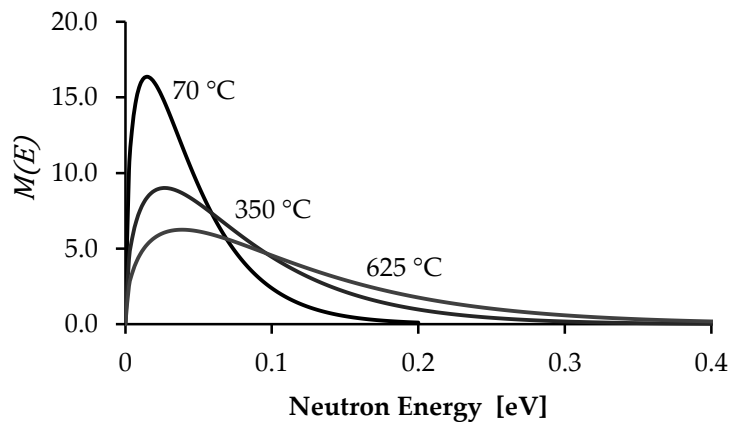
Figure 3.4: Maxwell-Boltzmann distribution of thermal neutron energies

The important properties of a moderating material are the macroscopic scattering cross-section Σ_s, the average amount of energy lost in a single scattering interaction ξ (as "logarithmic energy decrement" or *lethargy*), and the macroscopic absorption cross-section Σ_a (absorptions in the moderator being undesireable). The moderating ratio, defined in (12), is thus used to assess the effectiveness of different moderators. Some typical materials are compared in Table 3.1.

$$MR = \frac{\xi \Sigma_s}{\Sigma_a} \tag{12}$$

Table 3.1: Properties of different moderating materials

Material	Density [g·cm^{-3}]	Collisions from 2 MeV to 1 eV	MR
H_2O	1.0	16	71
D_2O	1.1	29	5670
C	1.6	91	192
^{238}U	19.1	1730	0.0092

From the table it is seen that D_2O, water that contains the hydrogen isotope deuterium rather than protium (called *heavy water*), is the most effective moderator available. The CANDU reactor is a common example of a thermal reactor that uses D_2O as a moderator [67].

3.1.1.6   Final Considerations and the Neutron Cycle

Close examination of Figure 3.3 reveals that between the fast and thermal energy ranges is a *resonance* region where the cross-section for non-productive capture is considerable. The problem of resonance absorption has a significant impact on nuclear design; fuel and moderator materials are typically lumped separately (as opposed to a homogenous mixture) to allow fission neutrons to escape resonance absorption while in the process of being moderated to lower energies. Furthermore, since the nuclei are never perfectly at rest but rather vibrate as a function of their temperature, the relative motion of the nuclei with respect to the incident neutron has an effect analogous to the Doppler shift observable in travelling waves. *Doppler broadening* increases the total absorption within a given resonance, adding what is essentially temperature dependence to the interaction cross-sections [68]. The same is necessarily true for resonances in the fission

cross-section. Nuclear data libraries thus contain cross-section data evaluated a multiple temperatures to capture this effect.

Finally, consider that the interaction cross-sections only represent the probability of interaction between a free neutron and a nucleus. It is possible that a free neutron may exit a volume without being absorbed or causing a fission. This is referred to as *leakage*. All of the pieces are now in place to describe the cycle of neutrons from one generation to the next in a fission chain reaction, shown in Figure 3.5 [70].
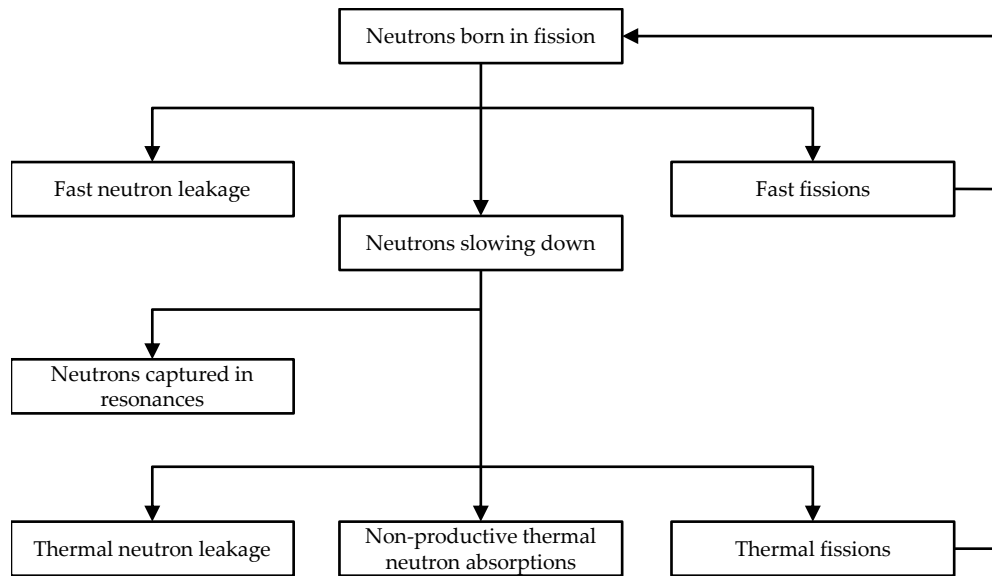
Figure 3.5: Neutron cycle in a typical thermal reactor

3.1.2   Neutron Transport

In order to fully describe the behaviour of neutrons, the angular neutron density is defined as $n(r,\vec{\Omega},E,t)d^3r\,d^2\vec{\Omega}\,dE$. This is a scalar quantity that describes the density of neutrons n [neutrons·cm^{-3}] in the volume element d^3r about position r,traveling within the solid angle $d^2\vec{\Omega}$ about direction $\vec{\Omega}$, possessing energy within the range dE about E, at time t. The angular neutron density thus exists in what is called a seven-dimensional phase space (three spatial dimensions, two angular dimensions, energy and time). A visual representation of the spatial coordinate system is shown in Figure 3.6.

The neutrons can be considered to be travelling at the scalar speed v [cm·s^{-1}], which is calculated from the neutron's kinetic energy as:

$$v = \sqrt{\frac{2E}{m_n}} \tag{13}$$

where m_n is the neutron's rest mass.
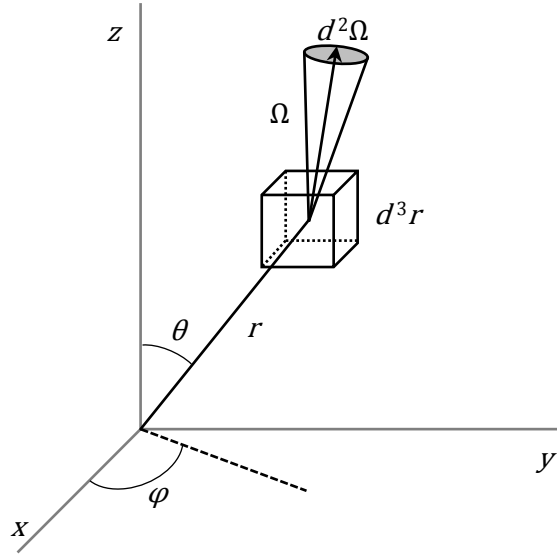
Figure 3.6: Spatial coordinate system for neutron transport

This allows definition of *angular neutron flux density* (or simply *flux*) as:

$$\Phi(r, \vec{\Omega}, E, t) = vn(r, \vec{\Omega}, E, t) \tag{14}$$

From the above definition it follows that $\Phi(r, \vec{\Omega}, E, t)$ must have units of neutrons·cm^{-2}·s^{-1}. Similar to the thought experiment in Figure 3.2, the volumetric interaction rate between neutrons and nuclei is found as:

$$Interaction\ Rate = \Phi(r, \vec{\Omega}, E, t)\Sigma(r, \vec{\Omega}, E, t) \tag{15}$$

3.1.2.1   The Neutron Transport Equation

It is reasonable to postulate that in a single element of phase space (i.e. $d^3r\ d^2\vec{\Omega}\ dE$) the neutron population is conserved. In other words, the time rate of change of the angular neutron density within the element is expressible as:

$$\frac{\delta n}{\delta t} = production - loss$$

In this relationship "production" consists of neutrons being scattered in to the element or being born from fission directly in the element. The "loss" of neutrons

will arise either from collisions with nuclei (including absorption and scattering interactions) or from neutrons that simply exit the spatial component of the element without interacting with a nucleus (leakage). Including the different interaction rates in (14) results in the *neutron transport equation* [67]:

$$\frac{\delta}{\delta t} n(r, \vec{\Omega}, E, t) = \frac{1}{v} \frac{\delta}{\delta t} \Phi(r, \vec{\Omega}, E, t)$$

$$= -\Sigma_t(r, E, t) \Phi(r, \vec{\Omega}, E, t) - \vec{\Omega} \cdot \vec{\nabla} \Phi(r, \vec{\Omega}, E, t)$$

$$+ \int_0^{4\pi} \int_0^\infty \Sigma_s(r, \vec{\Omega'} \to \vec{\Omega}, E' \to E, t) \Phi(r, \vec{\Omega'}, E', t) dE' \, d^2\vec{\Omega}$$

$$+ \frac{\chi_p(E)}{4\pi} \int_0^{4\pi} \int_0^\infty \bar{v}_p \Sigma_f(r, E', t) \Phi(r, \vec{\Omega'}, E', t) dE' \, d^2\vec{\Omega}$$

$$+ S_d(r, E, t)$$

$$(16)$$

The terms on the right side of the equation are defined as follows:

$-\Sigma_t(r, E, t) \Phi(r, \vec{\Omega}, E, t)$ is the rate at which neutrons are leaving the element through collisions with nuclei, including both scattering and absorption. The total removal cross-section Σ_t is thus defined as the sum of Σ_s and Σ_a.

$-\vec{\Omega} \cdot \vec{\nabla} \Phi(r, \vec{\Omega}, E, t)$ is the rate at which neutrons are leaking out of the element in the $\vec{\Omega}$ direction, which is assumed to be proportional to the gradient of the angular flux density in the direction of $\vec{\Omega}$.

$+ \int_0^{4\pi} \int_0^\infty \Sigma_s(r, \vec{\Omega'} \to \vec{\Omega}, E' \to E, t) \Phi(r, \vec{\Omega'}, E', t) dE' \, d^2\vec{\Omega}$ is the rate at which neutrons initially travelling in the direction $\vec{\Omega'}$ with energy E' are being scattered in to the element.

$\frac{\chi_p(E)}{4\pi} \int_0^{4\pi} \int_0^\infty \bar{v}_p \Sigma_f(r, E', t) \Phi(r, \vec{\Omega'}, E', t) dE' \, d^2\vec{\Omega}$ is the rate at which neutrons are being born in to the element from fissions caused by neutrons that were initially travelling in direction $\vec{\Omega'}$ with energy E'. $\bar{v}_p$ represents the average number of prompt neutrons born from a single fission event.

$S_d(r, E, t)$ is the rate at which delayed neutrons are being introduced in to the element. Because of the characteristic decay times of the delayed neutron

precursors, this source term is considered to be independent of the angular flux density at the current time t.

Alone, the neutron transport equation allows determination of the angular flux density in cases where the population of nuclei changes slowly with time (the time dependence of Σ would be ignored in such a case). Additional relationships are needed to account for the time variation of the macroscopic cross-sections and are discussed below.

3.1.2.2   Isotopic Depletion

Section 3.1.1 introduced the different ways that the isotopics within a reactor will change with time, including nuclear capture of neutrons to form new isotopes (*transmutation*), the destruction and production of new isotopes through fission, and the radioactive decay of unstable nuclei. Intuitively, the rate at which new isotopes are being produced or destroyed will be a function of the number of neutrons interacting with nuclei, or alternatively the variation of the nuclear density $N(r,t)$ must be a function of $\Phi\big(r,\vec{\Omega},E,t\big)$ and the individual interaction cross-sections $\sigma(E)$. As before, a conservation relationship will be assumed whereby the rate of change in nuclei density $N(r,t)$ is expressible as the sum of production and loss, resulting in what are called the *Bateman equations* [71]:

$$\frac{\delta}{\delta t}N_i(r,t) = \sum_j s^{j,i}(r,t)$$

$$-\lambda_i N_i(r,t) - N_i(r,t)\int_0^{4\pi}\int_0^\infty \sigma_{a,i}(E)\Phi\big(r,\vec{\Omega},E,t\big)dE\,d^2\vec{\Omega} \tag{17}$$

$$s^{j,i}(r,t) = N_j(r,t)\left(\sum_x Y_x^{j,i}\int_0^{4\pi}\int_0^\infty \sigma_{x,j}(E)\Phi\big(r,\vec{\Omega},E,t\big)dE\,d^2\vec{\Omega} + \lambda_j Y_\lambda^{j,i}\right) \tag{18}$$

where:

$\sum_j s^{j,i}(r,t)$ is the sum of all sources of isotope i from isotope j,

$-\lambda_i N_i(r,t)$ is the radioactive decay of isotope i with decay constant λ_i,

$-N_i(r,t)\int_0^{4\pi}\int_0^\infty \sigma_{a,i}(E)\Phi\big(r,\vec{\Omega},E,t\big)dE\,d^2\vec{\Omega}$ is the loss of isotope i resulting from interaction with a neutron,

$\sum_x Y_x^{j,i} \int_0^{4\pi} \int_0^\infty \sigma_{x,j}(E)\Phi(r,\vec{\Omega},E,t)dE\ d^2\vec{\Omega} + \lambda_j Y_\lambda^{j,i}$ is the production of isotope i from j as a result of nuclear reaction x (e.g. absorption or fission) that has a relative yield rate of Y_x,

$\lambda_j Y_\lambda^{j,i}$ is the radioactive decay of isotope j that results in i with decay constant λ_j and relative yield Y_λ.

Together the neutron transport equation and the Bateman equations form a system with which it is possible to completely describe the neutron population as it evolves in space, energy and time. This system of equations is, however, extremely difficult (if not impossible) to solve analytically, and the considerably heterogeneous geometry of a real reactor makes numerical solution extremely difficult as well. Additional simplifying assumptions are necessary if these equations are to be applied to any practical analysis.

3.1.2.3   The Steady-State Neutron Transport Equation

The first simplifying assumption will be to restrict the focus to time-invariant phenomena, which according to the definitions in 3.1.2.1 is the case where the production of neutrons exactly equals the loss within the phase space element. This results in the *steady-state* form of the neutron transport equation [71]:

$$\frac{\delta}{\delta t}n(r,\vec{\Omega},E,t) = 0$$

$$= -\Sigma_t(r,E)\Phi(r,\vec{\Omega},E) - \vec{\Omega}\cdot\vec{\nabla}\Phi(r,\vec{\Omega},E)$$

$$+ \int_0^{4\pi}\int_0^\infty \Sigma_s(r,\vec{\Omega'}\rightarrow\vec{\Omega},E'\rightarrow E)\Phi(r,\vec{\Omega'},E')dE'\ d^2\vec{\Omega} \qquad (19)$$

$$+ \frac{\chi(E)}{4\pi k}\int_0^{4\pi}\int_0^\infty \bar{\nu}\Sigma_f(r,E')\Phi(r,\vec{\Omega'},E')dE'\ d^2\vec{\Omega}$$

First note that the delayed neutron source $S_d(r,E,t)$ has been folded in to the fission source term, a consequence of the time-independent nature of the relationship. $\bar{\nu}$ now represents the average number of neutrons added by fission, including both prompt and delayed sources.

Second, note the inclusion of the eigenvalue $\frac{1}{k}$ in the fission source term. This k has the same meaning as the multiplication constant defined in (8) (Section 3.1.1.3). The criticality state of the reactor can be interpreted directly from the solution of the steady-state neutron transport equation at any instant in time, depending on both the values of the macroscopic cross-sections and the solution for the angular flux density.

Reactivity (ρ) can then defined as the relative distance from criticality in the form:

$$\rho = 1 - \frac{1}{k} \tag{20}$$

such that when $\rho = 0$ the reactor is critical, when $\rho < 0$ the reactor is subcritical and when $\rho > 0$ the reactor is supercritical. With this definition, changes to the macroscopic cross-sections that modify the value of k in the solution of the steady-state transport equation have an associated "reactivity effect". Subsequent sections will show that this is a very useful framework for safety analysis.

3.1.3   Lattice Cell Calculations

Due to the considerable geometric and material heterogeneity, it has proven computationally onerous to numerically solve even the steady-state neutron transport equation in the form of (19) over an entire reactor core. Historically the approach has been to take advantage of the fact that the reactor is constructed out of a lattice of repeating characteristic geometries, where the accurate solution of (19) over an individual *lattice cell* is achieved much easier [71]. With the appropriate selection of boundary conditions, the results of these lattice cell calculations can be applied to analysis of an entire reactor core. Figure 3.7 shows the typical features of a two-dimensional lattice cell, including a fuel region, a moderator region, and a region of structural material (in this example the "cladding" or "sheath" around the fuel).

A computer code that numerically solves the neutron transport equation and Bateman equations is used for lattice cell calculations. Examples of deterministic solvers that utilize some discretization in space, solid angle, and energy include DRAGON, WIMS-AECL, and parts of the SCALE 6 code package (e.g. NEWT) [26, 72, 73]. Stochastic solvers do not require discretization, and thus offer improved accuracy at the expense of additional computation time. Examples of

such solvers include MCNP, SERPENT, and other parts of SCALE 6 (e.g. KENO) [73, 74, 75].
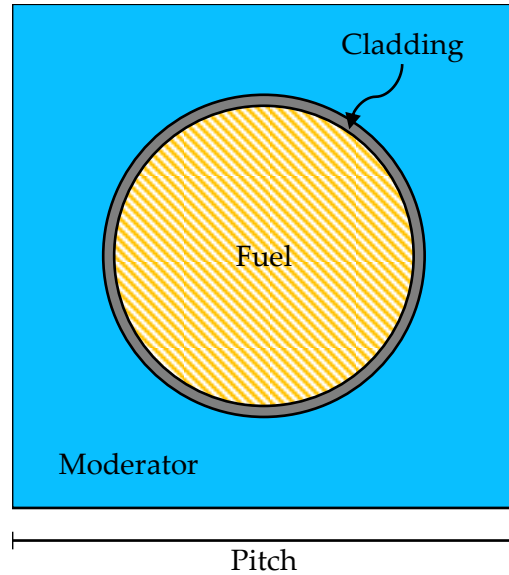
Figure 3.7: Example of a two-dimensional pin cell

3.1.3.1 Discretization of the Neutron Transport Equation

Most lattice codes use fairly straightforward discrete meshes for the space and time variables in the steady-state neutron transport and Bateman equations. In such cases the derivatives and integrals are replaced with their finite equivalents over the defined mesh [68]. The discretization of the angle and energy variables, however, merits additional discussion.

The angular variable $\vec{\Omega}$ is typically discretized in one of two ways: discrete ordinates (similar to the discrete mesh described above) or functional expansions. In the former $\vec{\Omega}$ is represented as a number of discrete directions $\vec{\Omega}_n, n = 1 \dots N$. The flux is similarly discretized:

$$\Phi_n(r, E) = \Phi(r, \vec{\Omega}_n, E) \tag{21}$$

with the property that:

$$\int_0^{4\pi} \Phi(r, \vec{\Omega}_n, E) d^2\vec{\Omega} = \sum_{n=1}^{N} \Delta\Omega_n \Phi_n(r, E) \tag{22}$$

where the *quadrature weights* $\Delta\Omega_n$ may be visualized as small "cones" around the directions $\vec{\Omega}_n$ such that $\sum_{n=1}^{N} \Delta\Omega_n = 4\pi$ [68]. The neutron transport equation is thus replaced by a system of N coupled equations for each $\Phi_n(r, E)$, with larger values of N representing increased angular resolution (at the expense of additional computation time). These are commonly referred to as the S_N equations.

In the functional expansion method the angular dependence of the flux is represented as a finite series of spherical harmonics $Y_{lm}(\vec{\Omega}) = Y_{lm}(\theta, \varphi)$ [68]:

$$\Phi(r, \vec{\Omega}, E) = \sum_{l=0}^{N} \sum_{m=-l}^{l} \Phi_{lm}(r, E) Y_{lm}(\vec{\Omega}) \tag{23}$$

where the expansion approaches the exact solution as N approaches infinity. In a cartesian lattice cell calculation there is only one angular component θ, so the spherical harmonics reduce to Legendre polynomials $P_l(\mu)$ (where $\mu = \cos\theta$) [68]:

$$\Phi(r, \mu, E) = \sum_{l=0}^{N} \frac{2l+1}{4\pi} \Phi_l(r, E) P_l(\mu) \tag{24}$$

The differential scattering cross-section is similarly expanded:

$$\Sigma_s(r, \mu_0, E' \to E) = \sum_{l=0}^{N} \frac{2l+1}{4\pi} \Sigma_{sl}(r, E' \to E) P_l(\mu_0) \tag{25}$$

where $\mu_0 = \vec{\Omega'} \cdot \vec{\Omega}$ is the scattering angle. Expanding neutron transport in this way results in a set of equations called the P_N equations, where increasing values of N mean more angular components are used in the solution (P_0 being entirely isotropic) [68].

With regards to energy, deterministic lattice codes typically make use of nuclear data libraries where the interaction cross-sections have already been discretized into a finite number of characteristic energy *groups* [68]. Within each group g the microscopic cross-sections have been averaged over the span $E^g \to E^{g-1}$ in the form:

$$\sigma^g = \frac{\int_{E^g}^{E^{g-1}} \sigma(E)\Phi(E)dE}{\int_{E^g}^{E^{g-1}} \Phi(E)dE} \tag{26}$$

where the spatial and angular dependence has been omitted for the purpose of this definition. Note that the flux $\Phi(E)$ is used as a weighting function, but the flux in the problem geometry can't be known until the transport equation is solved. In general purpose nuclear data libraries the group cross-sections are thus created with guesses for the flux spectrum based on typical reactor conditions. For example, high energy neutrons are assumed to have the fission spectrum (Figure 3.1), and low energy neutrons are assumed to possess the Maxwell-Boltzmann distribution (Figure 3.4). In intermediate energies the distribution is assumed to vary as $\frac{1}{E}$ (a slowing down spectrum), but as shown in Figure 3.8 below, this is not a good assumption near an absorption resonance [68].
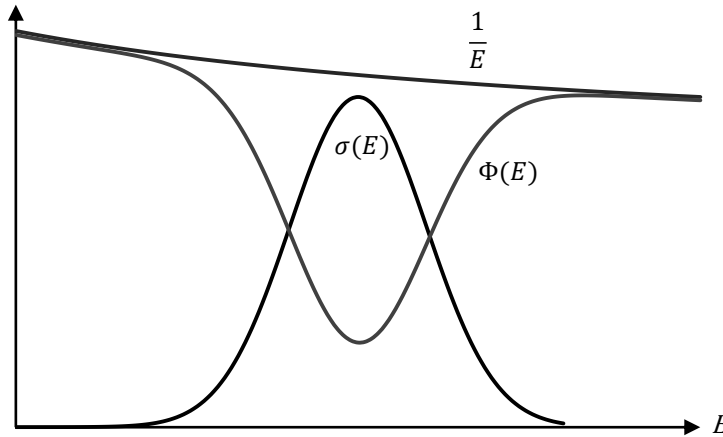
Figure 3.8: Flux depression in the neighbourhood of an absorption resonance

This phenomena is called *resonance self-shielding* [68]. To account for this effect, over a single resonance or group of resonances (depending on the width of the energy group) the *resonance integral* is defined as:

$$I^g = \int_{E^g}^{E^{g-1}} \sigma(E)\Phi(E)dE \tag{27}$$

A nuclear data library can thus contain pre-computed values of these resonance integrals, where $\Phi(E)$ is calculated in an infinite homogenous medium that

mixes the absorbing isotope with a perfect scatterer. Values of I^g are tabulated within the library as functions of temperature (to account for Doppler broadening of the resonances) and the *dilution* of the resonant absorber in the simplified geometry. A deterministic lattice code then determines the *effective dilution* of a resonant absorber in the problem geometry and relates it to a value of I^g in the data library, which is used to generate new values of σ^g by substitution in to the numerator of (26) (with the slowing down spectrum still applied in the denominator) . This is called a *resonance self-shielding correction* and is problem dependent (i.e. the calculation must be repeated for each new geometry or composition modelled with a deterministic lattice code) [71].

The end result of the energy discretization is a set of coupled equations for each *group flux* $\Phi_n^g(r)$ (with some angular discretization indicated by the subscript n). These are called the *multigroup equations*.

It's worth repeating that stochastic solvers don't rely on any discretization and are thus unaffected by any inaccuracies introduced in the above methods. The improved accuracy comes at the expense of significantly longer computation times, however. Stochastic codes have historically been reserved for benchmarking rather than production calculations, which have been the domain of much faster deterministic solvers [68]. This is starting to change with the large advances in computational power [54].

3.1.3.2   Features of Typical Lattice Cell Calculations

Because these codes are typically solving the steady-state form of the neutron transport equation, the most important output is the evaluation of the eigenvalue $\frac{1}{k}$ with geometry and materials input by the user. Nevertheless, consideration must be given to the selection of boundary conditions at the cell edges when interpreting the physical meaning of the eigenvalue [71].

Knowing that the lattice cell was specifically selected because the geometry is repeated throughout the core, it would be incorrect to assume that the solution of $\Phi(r, \vec{\Omega}, E)$ goes to zero beyond the edges of the domain (i.e. a void boundary condition). Instead it is normally assumed that an individual lattice cell exists in an *infinite lattice* of identical cells, so that any neutron crossing the edge of the domain reappears exactly as it left (i.e. a reflective boundary condition). As a consequence the neutron leakage term in (19) has no physical significance when

evaluated over the domain of the entire lattice cell. The eigenvalue thus represents the *infinite multiplication factor* of the cell designated k_∞, as opposed to the *effective multiplication factor* k_{eff} defined earlier in (8). Other possible boundary conditions include white (where neutrons crossing the boundary return isotopically) and albedo (between void and reflective).

In order to reconcile the time-dependence of the Bateman equation with the solution of the steady-state neutron transport equation, a typical approach is to assume the "quasi-static" evolution of flux and isotopics over discrete time steps within the lattice cell [71]. A solution for flux is first generated with the initial macroscopic cross-sections defined by the user. This flux solution is then fed into the Bateman equations, which are solved over a time step where the value of flux and the fission rate are assumed to be constant, in order to generate new values of $N(r,t)$. The new isotopic densities are used to calculate new macroscopic cross-sections, and the flux is recalculated at the new point in time. This is repeated until a specified value or change in k_∞ is reached, with the evolution of isotopics over the length of the calculation being one of the important outputs. This is called a *depletion* or *burnup* calculation. Implicit in the quasi-static solution approach was the assumption that the flux changes very slowly over the time step, and thus correct selection of the time step size is very important when performing a burnup calculation.

Another type of lattice cell calculation is a *perturbation*, in which a sudden change in properties within the cell is assumed to be rapid enough that the isotopic evolution as a result of nuclear interactions can be neglected [71]. In a perturbation calculation two separate solutions of the steady-state neutron transport equation are generated, each with different macroscopic cross-sections within the cell, and the difference between the corresponding values of k_∞ is interpreted as having an equivalent "reactivity worth" $\Delta\rho$:

$$\Delta\rho = \left(\frac{1}{k_{\infty_{inititial}}} - \frac{1}{k_{\infty_{perturbed}}} \right) \tag{28}$$

Perturbation calculations are used in the analysis of anticipated fast transients and are thus an important tool in reactor safety analysis.

3.1.4   Core-Level Calculations and Neutron Diffusion

Unfortunately a reactor core is not composed of an infinite lattice of identical cells. Not only is the core finite, but some cells may have different properties than others, and their relative positions within the finite core will necessarily affect the neutron flux solution. Additional simplifying assumptions are necessary if the neutron transport equation is going to be solved over this finite, heterogeneous geometry.

3.1.4.1   The Continuity Equation

It is important to note that the quantity with real physical meaning, the volumetric reaction rate, does not have an angular component. It is simply the number of interactions that are occurring within a unit volume. With this in mind the *scalar flux density* $\phi(r, E, t)$ is defined as [67]:

$$\phi(r, E, t) = \int_0^{4\pi} \Phi(r, \vec{\Omega}, E, t) d^2\vec{\Omega} \tag{29}$$

Similarly, the "net current" $\vec{J}(r, E, t)$ is defined as:

$$\vec{J}(r, E, t) = \int_0^{4\pi} \vec{\Omega} \cdot \Phi(r, \vec{\Omega}, E, t) d^2\vec{\Omega} \tag{30}$$

$\vec{J}(r, E, t)$ is a vector quantity that describes the net leakage out of the phase space element. With these definitions the time-dependent form of the neutron transport equation in (16) is rewritten as the *continuity equation* [67]:

$$\frac{\delta}{\delta t} n(r, E, t) = \frac{1}{v} \frac{\delta}{\delta t} \phi(r, E, t)$$

$$= -\Sigma_t(r, E, t)\Phi(r, E, t) - \vec{\nabla} \cdot \vec{J}(r, E, t)$$

$$+ \int_0^{4\pi} \Sigma_s(r, E' \rightarrow E, t)\phi(r, E', t)dE' \tag{31}$$

$$+ \chi_p(E) \int_0^{\infty} \bar{\nu}_p \Sigma_f(r, E', t)\phi(r, E', t)dE' + S_d(r, E, t)$$

It would appear that be eliminating the angular variable $\vec{\Omega}$ the equation would be much easier to solve, except there is no explicit relationship between $\phi(r, E, t)$ and $\vec{J}(r, E, t)$. The continuity equation is actually unsolvable in its current form, so an additional assumption regarding the relationship between the two terms is needed [67].

3.1.4.2   The Diffusion Equation

Fick's Law states that in a field of randomly moving particles the net current of particles is proportional to the gradient of the scalar concentration, where the proportionality constant D is called the constant of *diffusion*. The net current of neutrons in (30) is thus approximated as:

$$\vec{J}(r, E, t) = -D(r, E, t)\vec{\nabla}\phi(r, E, t) \tag{32}$$

where the diffusion constant is found with:

$$D(r, E, t) = \frac{1}{3(\Sigma_t - \overline{\mu}_0 \Sigma_s)} = \frac{1}{3\Sigma_{tr}} \tag{33}$$

The *transport cross-section* is defined as $\Sigma_{tr} = \Sigma_t - \overline{\mu}_0 \Sigma_s$, where $\overline{\mu}_0$ is the average cosine of the scattering angle. Σ_{tr} has physical significance as the inverse of the transport mean free path, or the average distance that a neutron travels before having an interaction.

Substituting the diffusion approximation in to (31) yields the time-dependent *diffusion equation* [67]:

$$\frac{\delta}{\delta t} n(r, E, t) = \frac{1}{v} \frac{\delta}{\delta t} \phi(r, E, t)$$

$$= -\Sigma_t(r, E, t)\phi(r, E, t) - \vec{\nabla} \cdot D(r, E, t)\vec{\nabla}\phi(r, E, t)$$

$$+ \int_0^{4\pi} \Sigma_s(r, E' \to E, t)\phi(r, E', t)dE' \tag{34}$$

$$+ \chi(E) \int_0^{\infty} \overline{v}_p \Sigma_f(r, E', t)\phi(r, E', t)dE' + S_d(r, E, t)$$

A simplified form of the neutron transport equation has finally been achieved that is applicable to larger scale analyses. Diffusion models can use similar

boundary conditions as lattice-level neutron transport models, typically reflective, void, and albedo conditions depending on the problem geometry. Examples of neutron diffusion solves used for full-core calculations include the DONJON, RFSP and PARCS computer codes [27, 76, 77].

It is worth noting that the definition of $D(r, E, t)$ in (33) makes the diffusion equation essentially a P_1 expansion of the neutron transport equation (as defined in Section 3.1.3.1). Approximating the angular dependence as diffusion thus assumes a high level of isotropy in the angular flux density, which can't be the case near material interfaces, in the vicinity of localized sources, and in highly absorbing media [67]. The next section shows that this may be compensated for when preparing macroscopic cross-section to be used in (34).

3.1.4.3   Cross-Section Homogenization and Condensation

In order to correct for the anisotropy of the flux in regions where the angular dependence is important, these regions are averaged or "smeared" over a larger area where the diffusion approximation can be used with greater accuracy (i.e. the average angular dependence is lower over larger areas). Typically this is done over the lattice cell, where the complex geometry of the cell is *homogenized* into representative macroscopic cross-sections. At the same time this is done in energy, *condensing* the multigroup discretization used in the lattice code to a significantly coarser *few groups* to simplify the solution of the diffusion equation [78]. When performing the homogenization and condensation it is necessary that the reaction rates be conserved, and thus the cell averaged macroscopic cross-section for interaction x in energy group g is defined as:

$$\Sigma_x^g = \frac{\int_{V_{cell}} \int_0^{4\pi} \int_{E^g}^{E^{g-1}} \Sigma_x(r, \vec{\Omega}, E)\Phi(r, \vec{\Omega}, E)dE\, d^2\vec{\Omega}\; d^3r}{\int_{V_{cell}} \int_0^{4\pi} \int_{E^g}^{E^{g-1}} \Phi(r, \vec{\Omega}, E)dE\, d^2\vec{\Omega}\; d^3r} \tag{35}$$

With this definition, the neutron flux acts as a weighting function, and values of Σ_x^g are consequently referred to as "flux weighted cross-sections". A lattice code is used to generate values of Σ_x^g for individual lattice cells at different values of burnup, temperature, and interesting perturbation cases for input in to a model constructed with a diffusion equation solver. This procedure is summarized in Figure 3.9.

| Lattice cell modeled | Homogenized and | Full core modeled |
| with neutron transport | condensed cross-sections | with neutron diffusion |
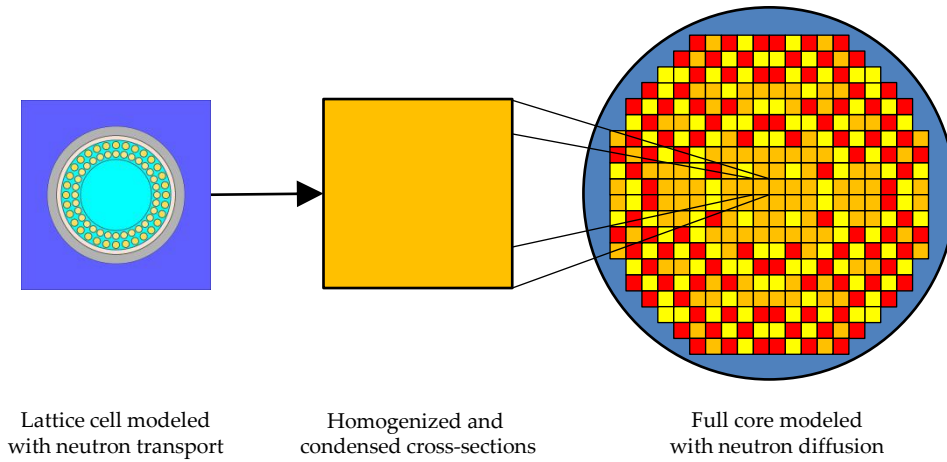
Figure 3.9: Procedure for creating a full core diffusion model

3.1.5   Neutron Kinetics

The diffusion equation is typical solved in its steady state form for preliminary design and normal operation calculations (like neutron transport, the delayed neutron source would be include in the fission source in such a case). The advantage of the diffusion approximation, however, is that the equation can be easily applied to transient safety analyses at the core level. This study of transient neutronics is called *neutron kinetics*. Solving for the transient neutron flux in a two or three dimensional space is specifically referred to as *spatial kinetics* to distinguish from fully homogenized kinetics calculations (*point kinetics*) [79].

Transient neutronics calculation requires that the delayed neutron source term $S_d(r, E, t)$ be described. This is facilitated with the definition of β as:

$$\beta = \frac{\overline{v}_d}{\overline{v}_d + \overline{v}_p} \tag{36}$$

where $\overline{v}_d$ is the average yield of delayed neutrons. β thus represents the fraction of neutrons released from fission that are from delayed sources. Similarly, $(1 - \beta)$ represents the fraction released immediately from fission.

While a given parent isotope may fission in to any number of daughter isotopes (according to the relative yield data contained within nuclear data libraries and input to the Batemen equations), it's been empirically shown that the various delayed neutron precursors (i.e. the "parent" isotopes of delayed neutrons, themselves fission products) may be combined in to a small number (L) of

characteristic groups (each denoted by the subscript l). The precursors within each group are assumed to have the same fractional yield β_l such that:

$$\beta = \sum_l^L \beta_l \tag{37}$$

and each group has a single characteristic half-life and decay constant λ_l, so that the concentration of precursor group $c_l(r, t)$ is found with:

$$\frac{\delta}{\delta t} c_l(r, t) = \beta_l \int_0^\infty \bar{v}_{d,l} \Sigma_f(r, E', t) \phi(r, E', t) dE' - \lambda_l c_l(r, t) \tag{38}$$

Typically in thermal spectrum reactors with [235]U fuel six delayed neutron groups ($L = 6$) are used [67]. The delayed neutron group parameters β_l and λ_l are stored in nuclear data libraries for each fissile isotope, much like the microscopic interaction cross-sections. These values may be homogenized over the geometry of a lattice cell for input in to a diffusion code.

The diffusion equation is modified to incorporate the delayed neutron sources explicitly as:

$$\frac{\delta}{\delta t} n(r, E, t) = \frac{1}{v} \frac{\delta}{\delta t} \phi(r, E, t)$$

$$= -\Sigma_t(r, E, t) \phi(r, E, t) - \vec{\nabla} \cdot D(r, E, t) \vec{\nabla} \phi(r, E, t)$$

$$+ \int_0^{4\pi} \Sigma_s(r, E' \rightarrow E, t) \phi(r, E', t) dE'$$

$$+ \chi_p(E)(1 - \beta) \int_0^\infty \bar{v}_p \Sigma_f(r, E', t) \phi(r, E', t) dE'$$

$$+ \sum_l^L \chi_l(E) \lambda_l c_l(r, t)$$

$$\tag{39}$$

(38) and (39) are thus a system of $L + 1$ equations describing the neutron population that can be used for core-level calculation of transient phenomena.

For practical applications, the only missing information is how the density and temperature of nuclei (and thus the macroscopic cross-sections) changes in space

and time from non-nuclear interactions. While many nuclear densities within the fuel and structure effectively remain constant, the same cannot be said for the PHTS where fluid is constantly moving and changing in temperature and density. Separate relationships are needed to describe the fluid mechanics and heat transfer (*thermalhydraulic*) phenomena so that these densities and temperatures can be determined.

3.2 Nuclear Reactor Thermalhydraulics

Thermalhydraulics refers to the modeling of fluid mechanics and heat transfer in a nuclear reactor for design, operations and safety analyses. This includes every phenomenon related to fission heat being deposited in the fuel, the heat being transferred from the fuel to the coolant, and ultimately the coolant circulating through the PHTS. For example, one of the key principles in reactor safety is to ensure sufficient cooling of the fuel at all times. This is crucial towards maintaining the integrity of the barriers that prevent the release of harmful radioactive fission products. Ensuring sufficient cooling requires thermalhydraulic models of the PHTS and other safety systems (emergency core coolant injection and shutdown cooling systems, for example) with detailed and reliable predictive capability.

Thermalhydraulics models are typically derived from the conservation of three quantities: mass, momentum, and energy. For the PHTS, conservation equations for each are defined for an individual or series of control volumes and then combined with a set of additional constitutive or *closure* equations that describe their interaction with each other and external sources or sinks [80]. Each of these will be described in turn. Examples of computer codes that solve these equations for one-dimensional pipe-network models of a reactor PHTS include CATHENA, RELAP5, and TRACE [28, 54]. Note that since supercritical fluids are typically considered to exist in a single thermodynamics phase, this description will be limited to single-phase equations (even though the aforementioned codes are capable of two-phase calculations).

3.2.1 Mass Conservation

Mass is a conserved quantity in non-relativistic reference frames (i.e. it can neither be created nor destroyed). In a fluid flow, it's reasonable to postulate that within a finite element the rate of change in mass must be the net sum of all fluid

entering and exiting the element. Consider the volume $dxdydz$ shown in Figure 3.10:
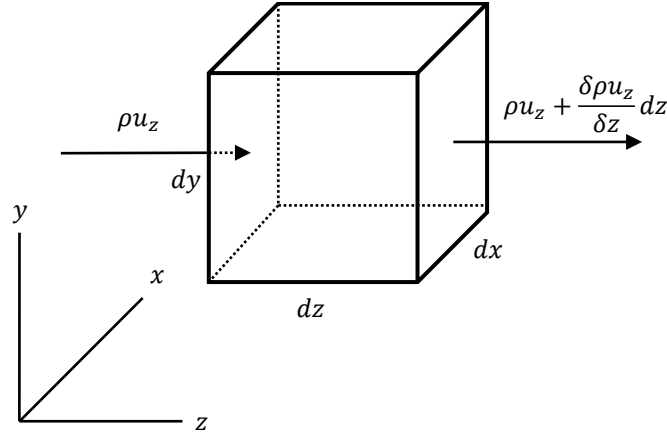
Figure 3.10: Components of mass flow in one direction

In the figure, fluid is shown to be entering the element in the z direction with density ρ [kg·m^{-3}] and velocity u_z [m·s^{-1}]. The product ρu_z is thus the *mass flux* in the z direction [kg·m^{-2}·s^{-1}]. Mass is also exiting the element in the z direction at the rate $\rho u_z + \frac{\delta \rho u_z}{\delta z} dz$. Neglecting the other dimensions for the moment, the rate of mass accumulation or loss in the element must be:

$$\frac{\delta \rho}{\delta t}(dxdydz)\bigg|_{u_x=u_y=0} = \rho u_z(dxdy) - \left(\rho u_z + \frac{\delta \rho u_z}{\delta z} dz\right)(dxdy) \qquad (40)$$

Generalizing this description to all directions and simplifying gives the mass conservation or *continuity* equation for fluid flow [81]:

$$\frac{\delta \rho}{\delta t} + \nabla \cdot (\rho \vec{u}) = 0 \qquad (41)$$

For core-level thermalhydraulics calculations, each component in the PHTS is often modeled only in one dimension (e.g. fluid flow is only considered axially down the length of a channel with no cross-flow) [80]. The continuity equation in one dimension is thus:

$$\frac{\delta \rho}{\delta t} + \frac{\delta}{\delta z}(\rho u) = 0 \qquad (42)$$

3.2.2 Momentum Conservation

Momentum conservation in a fluid flow can be considered a consequence of Newton's laws of motion. Within the element $dxdydz$ the momentum may change from the flux of fluid into and out of the element and as a consequence of forces acting on the element. A schematic of the former is shown in Figure 3.11.
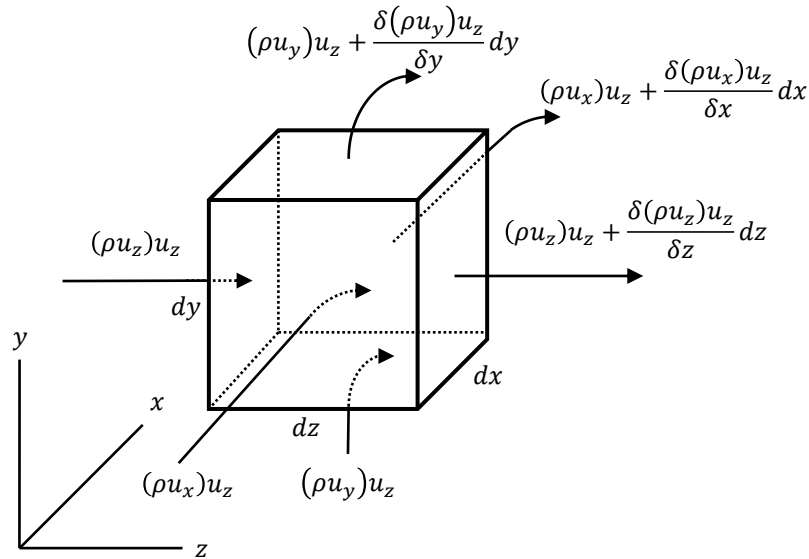
Figure 3.11: Components of momentum flux in one direction

The product $(\rho u)u$ has units of [kg·m·s^{-1}·s^{-1}] and thus represents the rate of change in momentum. The figure shows the component of momentum flux for the z direction only, but similar expressions exist for both x and y [81].

Forces acting on the element can be categorized as either *body forces* that act on the entire element (a typical example being gravity in the form $\rho\vec{g}$, where $\vec{g}$ is the gravitational vector) or *surface forces* that are either normal or tangential to the surfaces of the element. The actions of surface forces in the z direction are summarized in Figure 3.12.

Here σ_z [kg·m^{-1}·s^{-1} = Pa] is used to denote the normal stress in the z direction (i.e. on the $dxdy$ surface). For a fluid, normal stresses are caused by the pressure P and internal forces the act to elongate or compress the element τ_{zz}, such that $\sigma_z = P + \tau_{zz}$. The tangential forces cause *shear stress*, τ_{xz} and τ_{yz}, representing internal forces and interactions with other elements that act to rotate the fluid element.
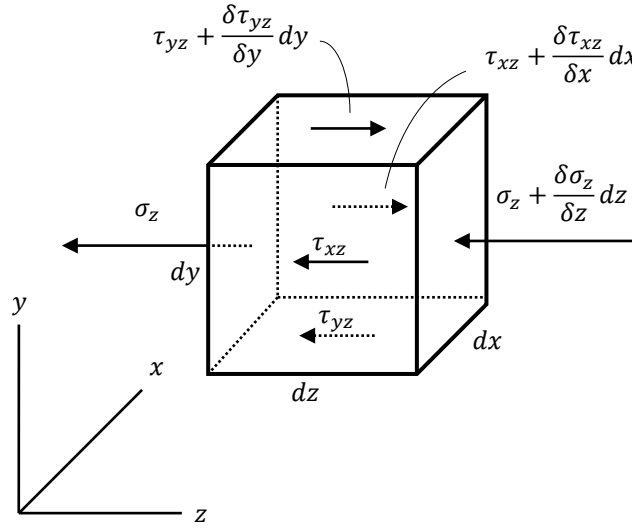
Figure 3.12: Components of stress tensor in one direction

With these definitions, the conservation of momentum in the *z* direction is [81]:

$$\frac{\delta}{\delta t}(\rho u_z) + \frac{\delta}{\delta z}(\rho u_z)u_z + \frac{\delta}{\delta x}(\rho u_z)u_x + \frac{\delta}{\delta y}(\rho u_z)u_y = \frac{\delta \sigma_z}{\delta z} + \frac{\delta \tau_{xz}}{\delta x} + \frac{\delta \tau_{yz}}{\delta y} + \rho \vec{g} \quad (43)$$

Generalizing this to all directions (and using the definition for normal stress $\sigma_i = P + \tau_{ii}$) gives a momentum conservation relationship for fluid flow [81]:

$$\frac{\delta}{\delta t}(\rho \vec{u}) + \nabla \cdot (\rho \vec{u})\vec{u} = -\nabla P + \nabla \cdot \bar{\bar{\tau}} + \rho \vec{g} \quad (44)$$

where $\bar{\bar{\tau}}$ is called the *stress tensor*:

$$\bar{\bar{\tau}} = \begin{pmatrix} \tau_{xx} & \tau_{xy} & \tau_{xz} \\ \tau_{yx} & \tau_{yy} & \tau_{yz} \\ \tau_{zx} & \tau_{zy} & \tau_{zz} \end{pmatrix} \quad (45)$$

Equation (44) can be interpreted as Newton's first and second laws applied to fluid flow. Newton related the components of the stress tensor to the fluid property *viscosity* (resistance to deformation by stress) in the form [81]:

$$\tau_{ii} = 2\mu \frac{\delta u_i}{\delta i} - \frac{2}{3}\mu \nabla \vec{u}$$

$$\tau_{ij} = \tau_{ji} = \mu \left(\frac{\delta u_i}{\delta j} + \frac{\delta u_j}{\delta i} \right)$$

$$(46)$$

where i and j are directions and μ is the dynamic viscosity of the fluid [Pa·s]. Fluids that obey Newton's law of viscosity are classified as *Newtonian*, as happens to be the case with water in a reactor PHTS. Substituting Newton's viscosity laws into the momentum conservation relationship gives [81]:

$$\frac{\delta}{\delta t}(\rho\vec{u}) + \nabla \cdot (\rho\vec{u})\vec{u} = -\nabla P - \nabla \cdot (\mu\nabla \cdot \vec{u}) + \nabla\left(\frac{4}{3}\mu\nabla \cdot \vec{u}\right) + \rho\vec{g} \qquad (47)$$

This is an expression of the *Navier-Stokes equation*. A typical approximation is that the flow is *incompressible*, i.e. the density within the fluid packet is constant and thus $\nabla \cdot \vec{u} = 0$. The Navier-Stokes equation thus simplifies to [81]:

$$\frac{\delta}{\delta t}(\rho\vec{u}) + \nabla \cdot (\rho\vec{u})\vec{u} = -\nabla P + \mu\nabla^2\vec{u} + \rho\vec{g} \qquad (48)$$

For typical thermalhydraulic analysis of the PHTS this will be limited to one dimension and the term containing μ will be generalized as a wall force F_{wall} (to be given by a separate constitutive relationship). The final result is the momentum conservation equation for core-level thermalhydraulic analysis:

$$\frac{\delta}{\delta t}(\rho u) + \frac{\delta}{\delta z}(\rho u)u = -\frac{\delta P}{\delta z} - Fwall - \rho g \cos\theta \qquad (49)$$

where θ is the angle between the gravity vector and the direction of fluid flow.

3.2.3   Energy Conservation

Conservation of energy in a fluid flow is dictated by the laws of thermodynamics. In the fluid element $dxdydz$ the rate of change in energy must be found as the net sum of energy carried in to and out of the element by the fluid flow and all internal energy sources and sinks. To assist with this description the total *specific energy* [J·kg^{-3}] is defined as:

$$e = h - \frac{P}{\rho} + \frac{u^2}{2} \qquad (50)$$

$h - \frac{P}{\rho}$ comes from the definition of *specific internal energy*: $i = h - \frac{P}{\rho}$ (where h is the *specific enthalpy*). $\frac{u^2}{2}$ represents the *kinetic energy* of the fluid in the element. The definition of e allows the energy "flux" in and out of the element to be represented as in Figure 3.13.
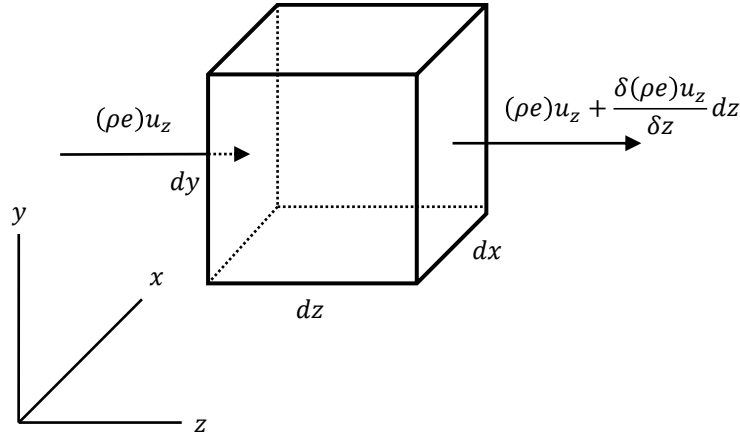
Figure 3.13: Components of energy "flux" in one direction

A derivation similar to the conservation of mass can thus be used. The resulting equation, with additional sources and sinks is [81]:

$$\frac{\delta}{\delta t}(\rho e) = -\nabla \cdot (\rho e)\vec{u} - \nabla \cdot \vec{q}'' + q''' - \nabla \cdot P\vec{u} + \nabla \cdot (\bar{\bar{\tau}} \cdot \vec{u}) + \vec{u} \cdot \rho\vec{g} \qquad (51)$$

The terms on the right side of (51) are independently defined as follows:

$\nabla \cdot (\rho e)\vec{u}$ is the transport or *convection* of energy in to and out of the element by the fluid flow;

$\nabla \cdot \vec{q}''$ is the *diffusion* of energy in to and out of the element based on the *flux* given by the field $\vec{q}''$ (in thermalhydraulics this may include heat conduction and radiation);

q''' is the internal generation of energy (for example, the heat deposited by fission);

$\nabla \cdot P\vec{u}$ is the work done on the fluid element by pressure;

$\nabla \cdot (\bar{\bar{\tau}} \cdot \vec{u})$ is the work done as a result of viscous forces (for example, the generation and dissipation of turbulent eddies in the fluid flow and friction with the pipe wall);

$\vec{u} \cdot \rho\vec{g}$ is the work done against gravity (this may be generalized to all body forces).

Additional assumptions are made for thermalhydraulic models of the PHTS. The first is that thermal diffusion (i.e. conduction) is negligible in the fluid compared

to convection, so the $\nabla \cdot \vec{q}''$ is ignored (conduction in solid materials is included as a closure relationship in the following section). The second is that viscous dissipation is negligible when averaged over sufficiently large volumes (i.e. volumes much larger than the turbulent structures themselves), so the $\nabla \cdot (\bar{\bar{\tau}} \cdot \vec{u})$ term can be ignored as well. Note that this is cannot be the case in high fidelity Computational Fluid Dynamics (CFD) models, but the approximation works well in one-dimensional thermalhydraulic models of the PHTS. Limiting the equation to one dimension and using the definition of e, the energy conservation equation can then be written as:

$$\frac{\delta}{\delta t}\left\{\rho\left[h - \frac{P}{\rho}\right]\right\} + \frac{\delta}{\delta z}(\rho h u) = q''' - \rho u g \cos\theta \qquad (52)$$

This equation describes energy conservation in a flow, but the q''' term only includes heat deposited directly to the fluid. Additional constitutive relationships are necessary to describe how heat from fission is transferred through the fuel and cladding to the coolant.

3.2.4 Closure Relationships

"Closure" or constitutive equations are additional relationships that "close" the gaps introduced by simplifying assumptions made during the derivation of practical conservation equations. Thermalhydraulic models consist of a system of conservation and closure equations that are solved either concurrently or iteratively. Some of the most important closure relationships are described here.

3.2.4.1 Wall Friction

During derivation of the momentum conservation equation, the viscous forces were collapsed in to a single term F_{wall} that represents frictional losses arising from fluid interaction with the pipe wall. This term is described by the *Darcy-Wesibach equation* [82]:

$$F_{wall} = \frac{2\rho u^2}{D_h}\left(\frac{f(\epsilon, D_h, Re)L}{D} + K\right) \qquad (53)$$

where f is the *friction factor*, ϵ is the "roughness" of the wall surface [m], D_h is the hydraulic diameter [m], Re is the non-dimensional *Reynolds number*, D is the pipe diameter [m], and K is an empirically derived minor loss term arising from changes in flow geometry.

The hydraulic diameter is a characteristic dimension of the flow geometry given by:

$$D_h = \frac{4A}{P_w} \tag{54}$$

where A is the cross-sectional area and P_w the wetted perimeter. The hydraulic diameter is used to retain some information about the flow geometry in a one-dimensional model.

The Reynolds number is defined as the ratio of inertial to viscous forces:

$$Re = \frac{\rho u D_h}{\mu} \tag{55}$$

Re is typically used to describe the level of turbulence in the flow (i.e. the higher value of Re, the more turbulent).

Friction factors are the result of empirically derived correlations represented in graphical or functional form. An example of the latter is the Chen correlation [83]:

$$f = \frac{0.25}{\left[\log \left[\frac{\epsilon/D_h}{3.7065} - \frac{5.042}{Re} \log \left(\frac{\left(\epsilon/D_h \right)^{1.1098}}{2.8257} + \frac{5.8506}{Re^{0.8981}} \right) \right] \right]^2} \tag{56}$$

There are a great number of different correlations, but the Chen correlation is notable for being used by the core thermalhydraulics code CATHENA [28].

3.2.4.2   Heat Conduction within Solids

Unlike viscous forces, heat conduction within solid materials (e.g. fission power conducted within fuel elements) is derived from first principles. The *heat equation* is a parabolic partial different equation that describes the "diffusion" of heat in a material. Given the shape of nuclear fuel elements (while assuming azimuthal symmetry and neglecting axial conduction), it is worthwhile to present the equation in radial coordinates [84]:

$$\rho c_p(r,T) \frac{\delta}{\delta t} T(r,t) = \nabla \cdot [k(r,t) \nabla T(r,t)] + q'''(r,t) \tag{57}$$

where $T(r,t)$ is the spatial and temporal distribution of temperature [°C], $c_p(r,t)$ is the *specific heat capacity* [J·g^{-1}·K^{-1}], and $k(r,t)$ is *thermal conductivity* [W·m^{-1}·K^{-1}], the latter two of which are properties of the specific material.

The first term on the right-hand-side of the equation is in fact *Fourier's law* [84]:

$$\vec{q}'' = -k\nabla T \tag{58}$$

which can be substituted in to (57) to give:

$$\rho c_p(r,t)\frac{\delta}{\delta t}T(r,t) = -\nabla \cdot \vec{q}'' + q'''(r,T) \tag{59}$$

For a nuclear fuel element $q'''(r,T)$ would be the heat deposited by fission and $\nabla \cdot \vec{q}''$ the heat being transported within and across material. Equation (59) is applicable to heat conduction at any modeling scale, including core-level and subchannel thermalhydraulics.

3.2.4.3   Heat Transfer to Fluids

Heat transfer from the fuel surface to the coolant is dominated by convection (not conduction) and is described by Newton's law of cooling [84]:

$$q'' = hA\left(T_{wall}(t) - T_{fluid}(t)\right) \tag{60}$$

where h is the *heat transfer coefficient* and A is the surface area for heat transfer. $T_{wall}(t)$ would typically be given by (59), whereas $T_{fluid}(t)$ refers to the bulk fluid temperature beyond the thermal boundary layer. Heat transfer coefficients are given by empirical correlations with differing levels of accuracy based on the local conditions. One of the most common examples is the *Dittus-Boelter correlation* [84]:

$$Nu = \frac{hL}{k} = 0.023Re^{0.8}Pr^n \tag{61}$$

where Nu is the non-dimensional *Nusselt number* (ratio of convective to conductive heat transfer), L the heat transfer length, Pr the non-dimensional *Prandtl number*, and the constant $n = 0.4$ for fluid heating and $n = 0.3$ for fluid cooling.

The Prandtl number is the ratio of momentum diffusivity (i.e. the viscous diffusion rate) to the thermal diffusivity (i.e. the thermal diffusion rate). It is given by [84]:

$$Pr = \frac{c_p \mu}{k} \tag{62}$$

The Dittus-Boelter correlation is widely applied in modeling single phase flows, as is the case in PHTS thermalhydraulic codes like CATHENA.

3.2.4.4   Equation of State

Final closure of these equations is given by the inherent physical properties of water. *Equations of state* describe the inviolable relationships between state variables. For example, given certain values of pressure and enthalpy, there must be unique corresponding values of density, temperature, heat capacity, viscosity, conductivity, and etc. [85]. The fundamental properties of water are compiled from many different experiments and distributed by recognized international organizations, such as the International Association for the Properties of Water and Steam [86]. The IAPWS fits the reduced data to several complex formulae and provides the results for general/scientific use (IAPWS-95) or industrial use (IAPWS-97) [86, 87]. The formulae in the IAPWS standard are so complex, however, that their constant re-evaluation would significantly slow down a computer code solving the aforementioned one-dimensional conservation equations. A thermalhydraulics code like CATHENA thus uses a reduced set of data based on the IAPWS standard with polynomial fits to expedite computation [85].

3.2.5   Relation to Core Neutronics

The volumetric heat generation rate q'''[W·m⁻³] in reactor thermalhydraulics is primarily the rate at which energy is deposited in the fuel from nuclear fissions. This is the means in which the reactor thermalhydraulics are linked to the core neutronics. However, recalling the definition of microscopic and macroscopic neutron interaction cross-sections in Section 3.1.1.4, the material densities and temperatures that impact the core neutronics are necessarily determined by the reactor thermalhydraulics (considering the relation between mass density ρ [g·cm⁻³] and number density n [atoms·cm⁻³], and the Doppler broadening of neutron absorption resonances). The core neutronics and thermalhydraulics are

thus *coupled*, i.e. to model the transient behaviour of the reactor it is necessary to solve both simultaneously. Typically this requires separate computational models implemented in different dedicated computer codes that pass information to one another. An example would be using DONJON to calculate the reactor power distribution, passing the information to CATHENA to solve the PHTS flow and temperature distribution, and then passing the updated thermalhydraulic information back to DONJON to update the power distribution. This is the basic method for transient simulation used in this thesis.

Chapter 4

Modelling Methodology

The disparate fundamental physics that describe reactor neutronics and thermalhydraulics detailed in the previous chapter are fittingly modelled in separate dedicated computer codes. This chapter describes how these codes were used to model the PT-SCWR as well as the method developed to couple these models for transient simulation. A novel aspect of this work was the inclusion of multiple coolant feedbacks in modelling the coupled behaviour of the PT-SCWR channel, which required additional assumptions and modifications to source code that are also described within.

4.1 Neutronics Models

The neutronics models used in this work employ multiple methods and computer codes with one ultimate goal: to simulate the transient power of the PT-SCWR core in response to changes in the thermalhydraulic parameters (including densities and temperatures). Achieving this goal required solution of the neutron transport equation (with depletion) at the lattice level, the neutron diffusion equation at the core level, and core-level spatial kinetics with transient changes to macroscopic cross-sections. The features of each of these models are described in turn.

4.1.1 Lattice-Level Neutron Transport

DRAGON is an open source computer code developed at École Polytechnique de Montréal that is capable of solving the neutron transport equation with depletion/burnup (i.e. with the Batemen equations) in two and three dimensions using a large number of discrete energy groups [26]. DRAGON makes use of the *collision probability* method to solve the steady-state transport equation, which requires discretization of the problem geometry in to small regions wherein the

solution for neutron flux is assumed to be homogeneous [88]. It is included in the Industry Standard Toolset (IST) of computer codes used for analysis of CANDU reactors, specifically for its ability to perform three dimensional neutron transport calculations to determine reactor control device reactivity worths [89]. In this work, DRAGON is used to create databases of homogenized (in space) and condensed (in energy) neutron interaction cross-sections which are necessary for core-level neutron diffusion and spatial kinetics models.

4.1.1.1   Reference Cell Creation

The reference lattice cell is a two-dimensional cross-section or "slice" of the PT-SCWR channel geometry as shown in Figure 4.1 and described in detail in Table 4.1. This cell was modelled with DRAGON 3.06K using nuclear data from the International Atomic Energy Agency (IAEA)'s WIMS-D format evaluated 172 energy group library [90]. While many nuclear data libraries are available for use with DRAGON, the IAEA evaluated library has the advantage of being extensively verified and validated (albeit for LWR applications, however other freely available data libraries cannot claim the same level of validation regardless of intended use). The absence of yttrium in the IAEA library was accomdated by creating a new material density for the ceramic insulator that conserved the number of zirconium and oxygen atoms while omitting entirely the yttrium, as indicated in the table.
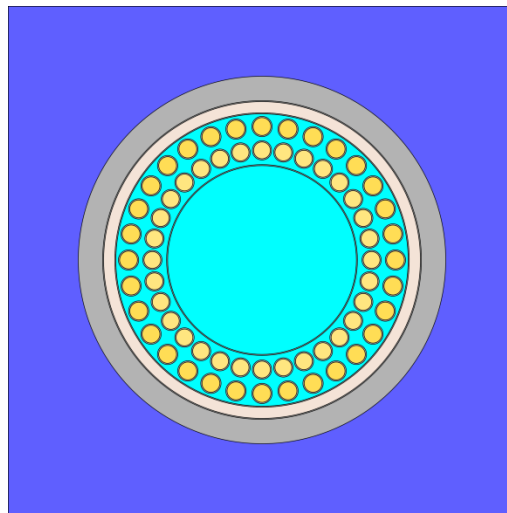
Figure 4.1: Reference PT-SCWR 64-element lattice cell

Table 4.1: PT-SCWR 64-element lattice cell description [11]

Component	Dimension	Material	Composition [wt%]	Density [g·cm⁻³]
Centre Tube Coolant	4.60 cm radius	Light Water	100% H_2O	variable
Centre Flow Tube	4.60 cm inner radius; 0.1 cm thick	Zr-modified 310 Stainless Steel	C: 0.034; Si: 0.51; Mn: 0.74; P: 0.016; S: 0.0020; Ni: 20.82; Cr: 25.04; Fe: 51.738; Mo: 0.51; Zr: 0.59	7.90
Inner Fuel Pins (32)	0.415 cm radius; 5.4 cm pitch radius	15 wt% PuO_2 in ThO_2	Pu:13.23; Th:74.70; O:12.07	9.91
Outer Fuel Pins (32)	0.440 cm radius, 6.575 cm pitch radius	12 wt% PuO_2 in ThO_2	Pu: 10.59; Th: 77.34; O: 12.08	9.87
Cladding	0.06 cm thick	Zr-modified 310 Stainless Steel	As above	7.9
Coolant		Light Water	100% $H2O$	variable
Liner Tube	7.20 cm inner radius; 0.05 cm thick	Zr-modified 310 Stainless Steel	As above	7.9
Insulator	7.25 cm inner radius; 0.55 cm thick	Yttria Stabilized Zirconia	Zr: 72.32; O: 27.68	5.37
Outer Liner Tube	7.80 cm inner radius; 0.05 cm thick	Excel Alloy	Sn: 3.5; Mo: 0.8; Nb: 0.8; Zr: 94.9	6.52
Pressure Tube	7.85 cm inner radius, 1.2 cm thick	Excel Alloy	As above	6.52
Moderator	25 cm square lattice pitch	Heavy Water	99.833 $D2O$; 0.167 $H2O$	1.0851
Plutonium Isotopics		Reactor Grade Plutonium	Pu238: 2.75; Pu239: 51.96; Pu240: 22.96; Pu241: 15.23; Pu242: 7.10	

The total cross-section of yttrium is relatively low (e.g. between that of ^{90}Zr and ^{91}Zr at thermal energies, and without the large epi-thermal resonances), so

combined with its low concentration this should serve as an acceptable approximation [69].

The procedure used was typical of most lattice-level calculations [71]. With spatial discretization, the neutron transport equation was solved for flux over the lattice geometry using the collision probability method. Reflective boundary conditions were used at the edges of the cell, implying that the cell was within an *infinite lattice* of identical cells, or more practically speaking, was in the interior of the core far from the physical boundary (treatment of lattice cells at the exterior of the core is described in Section 4.1.1.3). Using this flux solution, the cell is completely homogenized in space and condensed in energy (the few group energy structure is described in more detail with the diffusion model in Section 4.1.2.1). The Bateman equations are solved for a small time step over which the flux is assumed to be constant. The result is new atomic densities, which in turn create new macroscopic cross-sections that are used as input for the next flux calculation. The process is repeated to create a database of homogenized and condensed cross-sections tabulated as functions of burnup that input to the core-level diffusion model (according the procedure described in Section 3.1.4.3).

The variation in thermalhydraulic properties expected along the length of the PT-SCWR channel must also be accounted for in the lattice calculations. The typical approach has to been to model multiple two-dimensional lattice cells, each with different material temperatures and densities corresponding to different positions along the length of the channel. The work of Harrison and Marleau demonstrated convergence with 14 different sets of thermalhydraulic properties equally spaced along the length of the channel [16]. This work used 20 sets of thermalhydraulic properties for congruence with the diffusion calculation nodalization (described in more detail in Section 4.1.2.1). The thermalhydraulic properties were taken from a single-channel model of the PHTS described in Section 4.2.1. Table 4.2 shows the reference values for temperature and densities that are later allowed to vary in the feedback model, whereas the values in Table 4.3 are not part of the feedback model and are thus held constant in all neutronics calculations.

The thermalhydraulic parameters shown in the tables are held constant at these reference values when performing burnup calculations (deviations from the reference thermalhydraulic parameters are considered in Section 4.1.1.4). In these

calculations each position possesses the same average power density of 47.2791 Watts per gram of initial heavy elements (i.e. plutonium and thorium) calculated from the nominal core power of 2,540 MW. The results are 20 tables of homogenized and condensed cross-sections, each corresponding to a unique position in the PT-SCWR channel, which are henceforth referred to as the *reference cross-sections*.

Table 4.2: Reference thermalhydraulic conditions

Position [m]	Coolant Density [g·cm⁻³]	Coolant Temperature [°C]	Centre Fluid Density [g·cm⁻³]	Centre Fluid Temperature [°C]	Fuel Temperature [°C]
0.125	535.83	371.04	579.41	362.58	863.70
0.375	483.36	377.73	579.71	362.51	928.14
0.625	423.78	381.92	580.28	362.37	960.97
0.875	363.67	384.19	581.06	362.19	976.05
1.125	309.27	385.63	581.96	361.98	989.74
1.375	263.44	387.20	582.94	361.75	1012.56
1.625	225.71	389.65	583.97	361.51	1039.10
1.875	194.84	393.65	585.05	361.25	1072.57
2.125	169.72	399.82	586.23	360.96	1108.63
2.375	149.33	408.64	587.56	360.64	1147.47
2.625	132.66	420.49	589.10	360.26	1192.24
2.875	119.03	435.48	590.92	359.81	1234.75
3.125	107.80	453.57	593.07	359.27	1278.42
3.375	98.51	474.52	595.61	358.62	1321.33
3.625	90.78	497.88	598.60	357.85	1358.70
3.875	84.32	523.08	602.06	356.93	1393.28
4.125	78.90	549.43	606.03	355.85	1418.73
4.375	74.38	576.04	610.54	354.59	1427.54
4.625	70.68	601.61	615.57	353.14	1403.79
4.875	67.71	625.07	621.09	351.50	1352.73

Table 4.3: Reference structural material temperatures

Position [m]	Cladding Temperature [°C]	Liner Tube Temperature [°C]	Insulator Temperature [°C]	Pressure Tube Temperature [°C]
0.125	411.20	364.68	262.68	136.62
0.375	416.13	372.37	267.53	138.22
0.625	411.54	377.59	270.81	139.30
0.875	406.84	380.56	272.67	139.91
1.125	405.36	382.22	273.72	140.25
1.375	412.25	383.12	274.28	140.43
1.625	423.55	384.52	275.16	140.71
1.875	439.48	387.13	276.79	141.25
2.125	459.51	391.67	279.64	142.17
2.375	483.15	398.65	284.02	143.59
2.625	510.65	408.47	290.18	145.57
2.875	540.35	421.30	298.18	148.12
3.125	571.86	437.14	308.05	151.25
3.375	604.23	455.85	319.65	154.90
3.625	636.02	477.02	332.69	158.95
3.875	667.12	500.19	346.89	163.29
4.125	696.35	524.65	361.99	167.86
4.375	722.45	549.62	377.36	172.45
4.625	742.14	573.79	392.23	176.83
4.875	754.71	595.62	405.65	180.74

4.1.1.2 Spatial and Temporal Discretization

In order to judge if the chosen spatial and temporal discretization is sufficient, the inherent assumption of numerical discretization will be exploited: as the discretization becomes smaller, the discrete numerical solution should converge on a single value (which is ideally the real solution, but this may be limited by the accuracy of the modelling equations and input data).

In the case of DRAGON, more (smaller) spatial regions and time steps should result in increased numerical accuracy at the expense of additional computation time. The challenge is thus finding a discretization that is both acceptably

accurate and computationally efficient. For this work, an optimization strategy was adopted where a super-fine discretization, with an impractically long computation time, was created and used as a "benchmark" for evaluating simpler, more practical discretizations.

The calculated infinite lattice k_{inf} was used as a convenient measure of accuracy for comparison. The spatial discretization was optimized first, followed by an independent optimization of time step sizes (i.e. the spatial discretization was optimized only for fresh fuel). These are both simplifying assumptions. In the case of the former, it would also be possible to compare discretizations based on relative reaction rates or homogenized and condensed cross-section values. The value of k_∞, however, conveniently summarizes many properties of the lattice cell in a single number and is commonly used in code-to-code benchmark comparisons [91]. In the case of the latter, optimizing time step size *concurrently* with spatial discretization would be a significantly complicated and time-consuming multi-variable optimization problem. This would only be necessary if the neutron flux shape was expected to undergo extreme changes with burnup, and there is no evidence that this is the case in the PT-SCWR or with and other water-cooled reactor [71].

Three variables can be independently varied for spatial discretization in DRAGON: the size of the flux regions (wherein the solution for flux is assumed to be homogeneous), the number of tracking angles used in calculating the collision probabilities between regions, and the density of tracking lines used when evaluation the collision probability integrals between regions. The "benchmark" model was the discretization that had the smallest (most) regions, the most tracking angles, and the most tracking lines.

An important point is that these parameters were being studied for the flux solution geometry only. DRAGON allows a separate spatial mesh to be defined for the resonance self-shielding cross-section correction calculation. In DRAGON, the self-shielding module calculates the fuel-to-fuel collision probability only, which does not require a fine spatial mesh and is typically performed with only the material regions themselves defined [16, 26, 79]. This work will thus use fewer spatial regions for the self-shielding calculation, but will keep the determined tracking parameters (angles and lines) consistent between the geometries.

This optimization used a phased approach where the entire lattice cell was first meshed with the same sized regions, and in subsequent phases the mesh spacing in different parts of the cell (e.g. fuel, coolant, moderator, etc.) were changed separately from one another. The number of tracking angles and lines are, however, "global" properties of the geometry. The values for each were established from past experience with the DRAGON code. While any integer (in the case of the former) or decimal (in the case of the latter) numbers would be allowable, this optimization selected from a small population for simplicity and expediency. Table 4.4 shows the results from the first phase of the optimization. Differences of a few pcm (<0.05 mk) were considered good agreement. Based on the decrease in computation time, the final discretization (Test 27 in the table) was chosen as the basis for the next phase of the optimization. The tracking parameters would be held constant as the size of the spatial regions was refined.

In the next phase, the size of the mesh spacing was gradually increased in each region (Table 4.5). The final result has a discrepancy of less than 2 pcm from the benchmark model (Test 23), but with a significantly shorter calculation time. This final discretization is very similar to one of the first tests in Table 4.4. Evidently the solution for k_∞ is weakly sensitive to the spatial discretization past a certain threshold, which is exactly the convergent behaviour that was expected. This meshing (Figure 4.2) was held constant over the time step optimization.

The procedure for optimizing the time step sizes in the burnup calculation was slightly different. In order to accurately capture the initial rapid accumulation of saturating fission and activation products, the first time steps in the calculation are relatively small (on the order of hours). Conversely, later during the fuel's residency in the core the relationships between time, burnup, and k_∞ are nearly linear (or at least monotonic). This allows much larger time steps (on the order of several days or months) to be used. In a typical lattice-level burnup calculation, the time step size is thus accelerated as a function of time [71]. Since each time step requires a new flux calculation, the total calculation time is directly proportional fo the number of steps. An optimal temporal discretization thus minimizes the total number of burnup steps without sacrificing accuracy.

Table 4.4: Lattice cell spatial discretization optimization

Test Number	Mesh Size [cm]	Tracking Angles	Line Density [cm⁻¹]	k_∞	Discrepancy [mk]	Duration [min]
1	0.1	20	35	1.178799	-0.103	7
2	0.1	20	45	1.17876	-0.075	9
3	0.1	20	25	1.178775	-0.086	9
4	0.1	24	35	1.178753	-0.070	9
5	0.1	24	45	1.178756	-0.072	11
6	0.1	24	25	1.178729	-0.053	6
7	0.1	14	35	1.178726	-0.050	5
8	0.1	14	45	1.178724	-0.049	6
9	0.1	14	25	1.178694	-0.027	3
10	0.2	20	35	1.179208	-0.397	2
11	0.2	20	45	1.179175	-0.373	3
12	0.2	20	25	1.179188	-0.383	2
13	0.2	24	35	1.179165	-0.366	3
14	0.2	24	45	1.179173	-0.372	3
15	0.2	24	25	1.179144	-0.351	2
16	0.2	14	35	1.179136	-0.345	1
17	0.2	14	45	1.179139	-0.348	2
18	0.2	14	25	1.179109	-0.326	1
19	0.05	20	35	1.178696	-0.029	23
20	0.05	20	45	1.178659	-0.002	32
21	0.05	20	25	1.178676	-0.014	18
22	0.05	24	35	1.178651	0.004	31
23	*0.05*	*24*	*45*	*1.178656*	*-*	*34*
24	0.05	24	25	1.178628	0.020	23
25	0.05	14	35	1.178624	0.023	17
26	0.05	14	45	1.178622	0.024	18
27	0.05	14	25	1.178595	0.044	11

Table 4.5: Second spatial discretization optimization

Test Number	Fuel Mesh [cm]	Centre Mesh [cm]	Coolant Mesh [cm]	Moderator Mesh [cm]	k_∞	Discrepancy [mk]	Duration [min]
28	0.10	0.10	0.05	0.10	1.178596	0.043	3
29	0.05	0.10	0.10	0.10	1.178721	-0.047	3
30	0.10	0.05	0.05	0.10	1.178565	0.066	4
31	0.10	0.10	0.05	0.20	1.178581	0.054	2
32	0.20	0.20	0.05	0.20	1.178722	-0.048	1
33	0.10	0.20	0.05	0.20	1.178702	-0.033	1
34	0.10	0.10	0.10	0.20	1.178679	-0.017	1
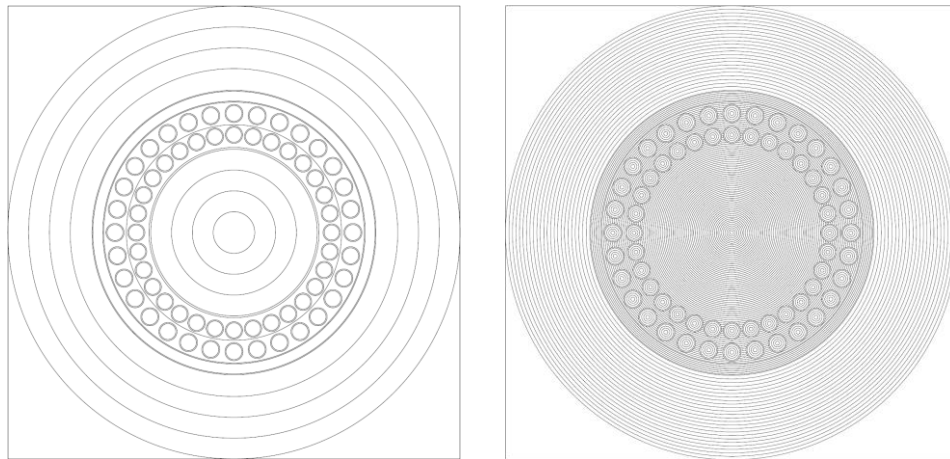
Figure 4.2: DRAGON discretization for self-shielding (left) and flux (right)

A temporal discretization considered impractically long for the reference calculation was used as a "benchmark" basis for comparison. The sizes of the time steps and the times at which the time step size increased were adjusted. Discretization schemes were compared based on the discrepancy in the infinite lattice k_{inf} from the benchmark at each instant in time. Since each scheme does not necessarily evaluate steps at the same residence times, linear interpolation was performed on the available steps to match the benchmark scheme. Table 4.6 shows the different discretization schemes tested and the interpolated reactivity discrepancies. The final discretization scheme (Test 13) was judged to possess sufficient accuracy despite requiring only 60%of the steps in the benchmark model (Test 3).

Table 4.6: Burnup time step size optimization

Test	Time and Time Step Size [d]															Number of Steps	Maximum Deviation [mk]	Integrated Deviation [mk·d]
	0	0.5	1	1.5	2	4	5	6	10	50	100	200	500	2000	2500			
1	0.1				1				10	50	100					50	5.03	-115.88
2		0.2			2				10		50					68	29.08	21.52
3			0.1			1			10		50					113	-	-
4	0.1	0.5			2				10	50	100					43	5.03	-115.61
5		0.1			2				10	50	100					55	5.03	-113.32
6	0.2			1					10		100					48	29.08	-89.15
7	0.2		1		2				10	50	100					52	29.08	-69.88
8	0.1	0.5			2				10	50						66	0.38	-6.96
9	0.1	0.5			2				20		50					64	0.38	-7.71
10	0.1	0.5			2				10	50						74	0.22	-3.04
11	0.1	0.5	1		2				10	50						76	0.22	-1.63
12	0.1	0.5	0.5		2				15	50						71	0.22	-3.77
13	0.1	0.5		0.5	2				15	50						68	0.13	-1.23

4.1.1.3   Lattice Cells near the Core Boundary

Fuel channels at the periphery of the core must be modelled different than those in the interior. Being adjacent to the reflector, it would be incorrect to approximate that the cell is within an infinite lattice of identical cells and so reflective boundary conditions cannot be used. Furthermore, the adjacency of the reflector would impact the flux solution within the cell, so it would be incorrect to use the homogenized infinite cell cross-sections for these *edge* cells in the full-core neutron diffusion calculation. In this work these edge cells were modelled as special *multicells* which include multiple fuel channels and part of the heavy water reflector.

An independent study found that a minimum two additional homogenized fuel lattice cross-sections are required: "corner" cells which see fuel and reflector on two sides each, and "side" cells which see fuel on three sides and reflector on one. This study also showed that these cells could be included in the same calculation geometry, the 4×4 cells shown in Figure 4.3 (with four fuel channels and twelve "reflector cells") [92].
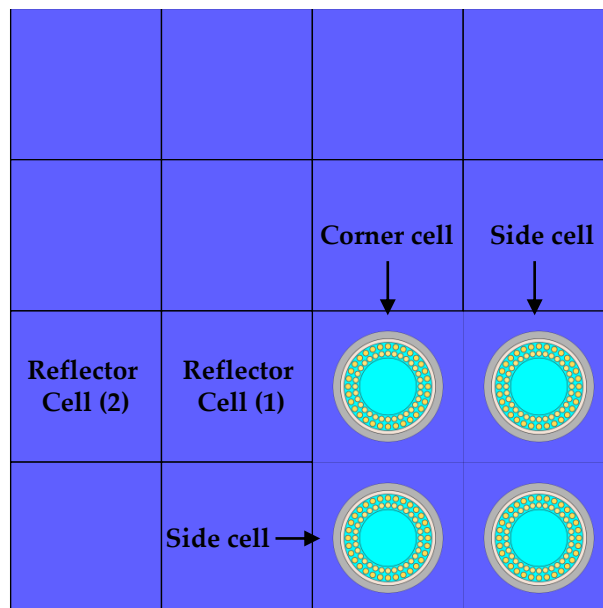
Figure 4.3: Reflector multicell near the core boundary

This calculation geometry was also used to create homogenized cross-sections for the heavy water reflector material. The aforementioned study also recommended that the heavy water reflector closest to the fuel should be homogenized

separately from that further (at least one lattice spacing) away, and that recommendation was followed for this work.

This geometry was modelled in DRAGON to create additional tables of burnup dependent homogenized and condensed cross-sections for the corner and side cells. The spatial discretization in each of the fuel cells was identical to the reference discretization establish in Section 4.1.1.2. The same time step scheme for the burnup calculation was also used. The spatial meshing for the reflector cells, however, needed to be established. A similar optimization approach was attempted, however "superfine" meshing like that in Table 4.4 results in an extremely large number of calculation regions that is beyond the capability of the DRAGON code. Nevertheless, the tests in Table 4.7 give some insight into the sensitivity of the result to the spatial meshing and the large computation time required. The meshing shown in Figure 4.4 (Test 4 in Table 4.7) was adopted as a practical compromise between accuracy and simulation time.

Table 4.7: Multicell spatial discretization optimization

Test Number	Regions in Closest Reflector	Regions in Furthest Reflector	Total Number of Regions	k_∞	Duration [min]
1	100	100	1200	1.227006	223
2	240	80	1520	1.225509	359
3	240	240	1680	1.227402	477
4	160	160	1020	1.227094	174
5	160	80	940	1.225550	152

It was also necessary to reevaluate the boundary conditions applied to the edge of the multicell. For the "interior" (i.e. inward-facing) edges, reflective boundary conditions were deemed an acceptable approximation. This would be not be acceptable for the "exterior" (i.e. outward-facing) edges, however, since neutrons that pass through the reflector are the very definition of leakage. On the other hand, a void boundary condition on the exterior edges would not be acceptable either since the real reflector is 105 cm thick, more than double that included in the multicell model [93]. An albedo boundary condition presents a compromise. Duderstadt and Hamilton state that the albedo of a homogeneous neutron reflector can be calculated with [68]:

$$\alpha = \frac{1 - \left(\frac{2D}{L}\right) \coth\left(\frac{a}{L}\right)}{1 + \left(\frac{2D}{L}\right) \coth\left(\frac{a}{L}\right)} \tag{63}$$

where D is the diffusion coefficient, L is the diffusion length, and a is the width of the reflector. The value of albedo, α, is between 0 and 1, respectively representing an equivalent void and reflective boundary condition. The only challenge in using this relationship is finding the correct values of D and L, but after exploring several calculation options it was found that the expression was completely dominated by the width of the absent reflector, a = 55 cm. An albedo value of α = 0.93 was ultimately settled and used as the boundary condition for the exterior edges.
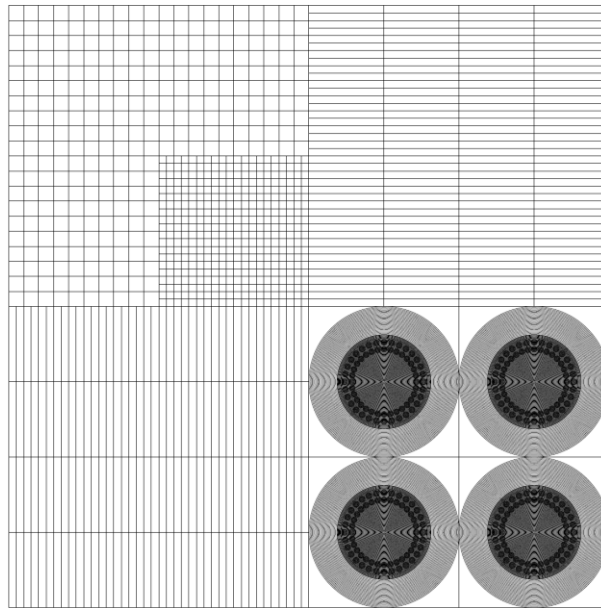
Figure 4.4: DRAGON discretization for multicell flux calculation

Like the infinite lattice cell, the reflector multicell was evaluated for each of the 20 thermalhydraulic conditions described in Table 4.2. The result is two additional sets of homogenized and condensed cross-sections as functions of burnup, one set of 20 for the corner cell and one set of 20 for the side cell, in addition to the set of 20 for the infinite lattice cell. With the two homogenized reflector cells (assumed to be independent of axial position and burnup), these 62 sets of reference fuel cross-sections are the basis for the reference core-level diffusion model described in Section 4.1.2.1.

4.1.1.4   Feedback Database Creation

The purpose of the feedback model is to capture how the homogenized cross-sections change with perturbations to the thermalhydraulic parameters. In DRAGON this is facilitated with the CFC module, which takes reference and perturbed cross-sections as inputs and creates a database of first and second order coefficients that describe how each homogenized value (including cross-sections and diffusion coefficients) changes with each thermalhydraulic parameter [26]. The CFC module requires 28 CPO data structures as input. These are homogenized and condensed values from previous flux calculations tabulated as functions of burnup by the CPO module. Table 4.8 describes each of these structures and how there were implemented for the model.

Note that the burnup calculation was performed exclusively at the reference thermalhydraulic conditions. At each burnup step a specific thermalhydraulic parameter was changed and a new flux calculation was performed to create an entry in the corresponding CPO structure. The only exceptions are the perturbed power histories, where each is a separate burnup calculation with a different power density. Although all 28 CPOs are required input to the CFC module, DONJON does not necessarily use all of them when applying the feedback model. Section 4.1.3.2 contains more details on how the feedback database (FBM data structure) was used in the PT-SCWR core model.

A key feature of this work is that the coolant in the centre flow tube and in the fuel region is modelled separately. Although they are clearly related by the movement of fluid through the fuel channel and heat transfer through the flow tube, on short time scales (i.e. on the scale of neutron kinetics) their temperatures and densities may change independently. This has significant impact on the lattice neutronics, so it was critically important to include these separate effects in the feedback database. The database structure used by DRAGON and DONJON, however, only has subdirectories for a single "coolant" material [94]. Flow tube coolant feedbacks are thus stored under "moderator" material subdirectories in the database. This allows the temperature and density variation in the centre flow tube to be included, with the caveat that the actual moderating material (the heavy water outside the pressure tube) is assumed to be constant during any transient. With the thermal isolation provided by the YSZ insulator, this assumption is reasonable for the short transients modelled in this work.

Table 4.8: Perturbed parameters used to create the feedback database

CPO Signature	Perturbed Variables	Value	Comments
REF MODREF	None	Reference values	"Moderator" not used in this work
CDEN-D	Coolant density	0.02 g·cm⁻³	
CDEN-UP	Coolant density	0.75 g·cm⁻³	
CTEMP-D	Coolant temperature	300 °C	
CTEMP-UP	Coolant temperature	1200 °C	
FTEMP-D	Fuel temperature	600 °C	
FTEMP-UP	Fuel temperature	2100 °C	
MIXMD	Coolant density and temperature	0.02 g·cm⁻³; 1200 °C	
MIXFD	Fuel temperature and coolant density	2100 °C, 0.02 g·cm⁻³	
MDEN-D MODDEN-D	Flow tube fluid density	0.02 g·cm⁻³	
MDEN-UP MODDEN-U	Flow tube fluid density	0.75 g·cm⁻³	
MTEMP-D MODTP-D	Flow tube coolant temperature	300 °C	
MTEMP-UP MODTP-UP	Flow tube coolant temperature	1200 °C	
PURITY MODPUR	Flow tube D_2O concentration	1 wt% D_2O	Not used
BORON MODBOR	Flow tube boron concentration	0.1 wt% B10	Not used
POWERUP	Power density	94.5582 W·g⁻¹	Not used
POWERIN	Power density	23.6396 W·g⁻¹	Not used
POWERD	Power density	11.8198 W·g⁻¹	Not used
NP239	Activation product concentration	1.0×10^{-12} wt% Np239	Not used
SM149	Fission product concentration	1.0×10^{-12} wt% Sm149	Not used
XENON	Fission product concentration	1.0×10^{-12} wt% Xe135	Not used

The edge cells described in Section 4.1.1.3 must also be included in the feedback database since their reference homogenized cross-sections are different from the infinite lattice. The length of time required to perform a single multicell calculation (as shown in Table 4.7), combined with the large number or

perturbation calculations necessary for constructing the feedback database, makes the feedback calculation impractical, however (i.e. over 10,000 processor hours). It was therefore assumed that the feedback coefficients from the infinite lattice could be applied to the reference cross-sections of the edge cells. The strength of this assumption was tested for fresh fuel at a single axial location, where it was found that the group feedback coefficients determined in a multicell calculation differed from the corresponding infinite lattice results by approximately 5% on average. Applying the infinite lattice feedback coefficients to the edge cells thus saved considerable computation time without a significant reduction in accuracy. To construct the database in this manner, "dummy" CPO structures were given as input to the CFC model to create the database structure. An external script (not part of the DRAGON code) was then created to modify the database file and overwrite the feedback entries for the edge cells with the corresponding infinite lattice values.

The resulting feedback database thus contains 60 top level directories for each of the 60 reference fuel types (20 infinite lattice cells, 20 corner cells, and 20 side cells). Each fuel type directors contains a subdirectory for each burnup step, which in turn contains subdirectories for the reference cross-section values and coefficients for those cross-sections change with perturbations to the thermalhraulic variables. The database is stores as a single file (nearly 1 GB in size) that is readable by DONJON.

4.1.2 Core-Level Neutron Diffusion

DONJON is an open source computer code also developed at École Polytechnique de Montréal that solves the neutron diffusion equation at the core level [27]. It makes use of a finite difference spatial discretization to solve neutron diffusion in three dimensions. DONJON is closely integrated with DRAGON, which provides homogenized and condensed cross-sections and thermalhraulic feedbacks in the form of CPO and FBM data structures. In this work, DONJON is primarily used to calculate the power distribution in the PT-SCWR core. This section specifically describes steady-state calculations (i.e. using the steady-state form of the neutron diffusion calculation). Transient procedures (or "neutron kinetics") are described in Section 4.1.3. The base code version used was DONJON 3.02g, however some changes to the source code were made

specifically for this work, including bug fixes and special extensions to the feedback model.

4.1.2.1   Reference Core Creation

The general properties of the reference PT-SCWR core are summarized in Table 4.9 [93]. The three batch refuelling scheme defined for the reference core is quarter-symmetric. To fit within the limitations of CATHENA (used for modelling the channel thermalhydraulics and described in detail in Section 1.1), this symmetry was exploited and only one-quarter of the core was modelled with DONJON. This geometry, including the three batch refuelling scheme, is shown in Figure 4.5. With quarter symmetry the boundary conditions on the "interior" of the core are reflective. The "exterior" edges, as well as the top and bottom, were given void boundary conditions to represent the physical limit of the reactor. Note that no control or reactivity hold-down devices were included in this model. These devices were not part of the PT-SCWR reference conceptual design during the course of this work.

Table 4.9: PT-SCWR core summary

Number of Channels	336
Thermal Power	2,540 MW
Thermal Efficiency	>45%
Fuel Composition	≈13 wt% PuO_2 in ThO_2
Core Dimensions	5 m (axial) × 5 m (radial)
Reflector Dimensions	55 cm radial, 50 cm axial
Refuelling Scheme	3-cycle batch
Cycle length	>400 Full Power Days (FPD)
Discharge Burnup	>40 MW·d·kg^{-1}

Figure 4.5 shows that each fuel assembly was modelled with 20 axial nodes. Typically pressure tube type heavy water moderator reactors (i.e. CANDU) have been modelled with each node corresponding to a single fuel bundle (of which there are usually 12 in a single channel) [51, 95]. The PT-SCWR channel concept does not contain a string of short bundles but rather a single long assembly. The concept thus closely resembles a batch-fuelled LWR (specifically a BWR given the similar large coolant density changes). BWR assemblies are typically meshed

with over 20 axial nodes when performing coupled simulations [52, 24]. Given the 25 cm lattice spacing, splitting the 5 m PT-SCWR fuel channel in 20 results in cubic 3D cells (25×25×25 cm), which is convenient for visualization. Furthermore, it is within the range of established standards for nodalization when creating 3D coupled neutron kinetics and thermalhydraulics models. The same sized nodes are used in the reflector region, thus making the mesh uniform over the entire calculation geometry.
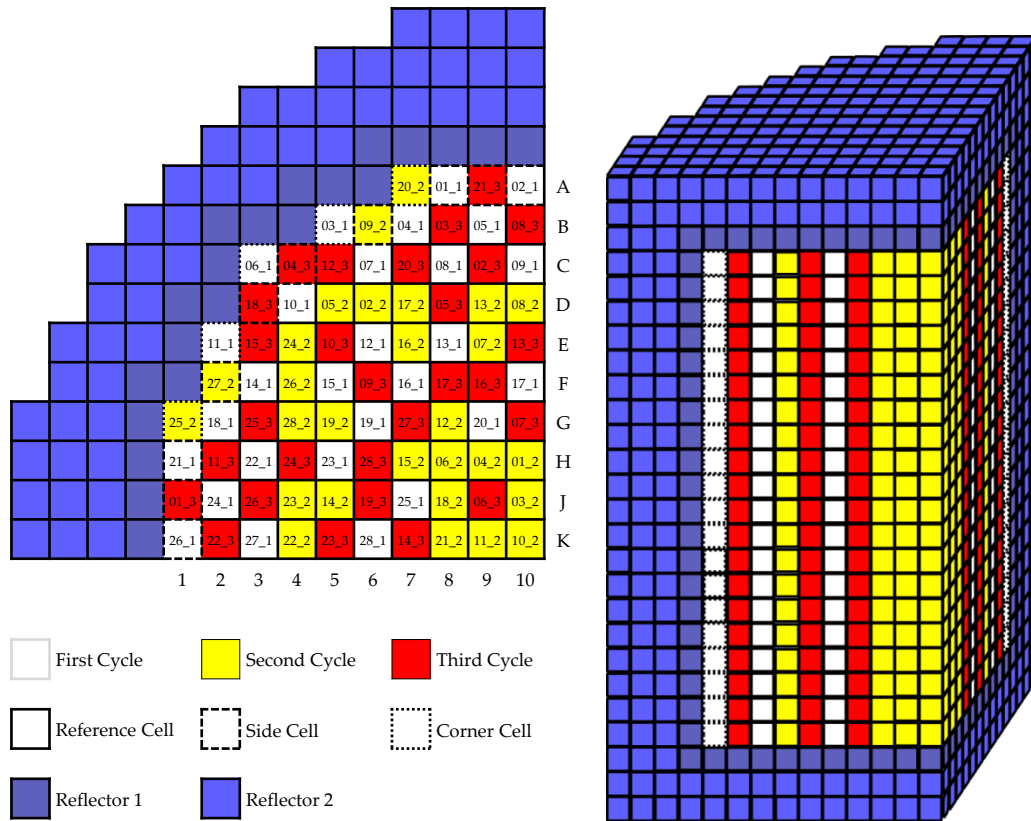
Figure 4.5: PT-SCWR core as modelled in DONJON

Homogenized and condensed cross-sections were taken from CPO data structures created with DRAGON. These are used by DONJON to create burnup-dependent fuel tables from which each node is given interpolated cross-section values. The model contains 60 such fuel tables: 20 for the interior cells, 20 for the side cells, and 20 for the corner cells (each corresponding to a unique axial location). The two sets of homogenized reflector cross-sections were not functions of burnup or axial position.

The DONJON model uses an eight group energy structure (the lattice cells having been condensed from 172 groups by DRAGON). Although two groups are typically used for core-level diffusion calculations, there is evidence that more energy groups are required to model the PT-SCWR [96]. For example, the near-thermal (0.3 eV) resonance in the ^{239}Pu fission cross-section may be especially important in coupled transients, but a two group structure will miss its effect. The optimal few-group energy structure (i.e. the number of groups and their limits) for PT-SCWR analysis is still undetermined. Nevertheless, it's reasonable to assume that energy group structures used in past analyses of other high plutonium content fuels could be applicable to PT-SCWR fuel. The eight group structure shown in Table 4.10 was previously used in an international benchmark for LWR MOX fuel [97]. This group structure correctly bounds the aforementioned fission resonance, and thus has been used in this DONJON model.

Table 4.10: Eight group neutron energy structure

Group Number	Lower energy cut-off [eV]
1	2.2313×10^6
2	8.2085×10^5
3	9.1188×10^3
4	1.3007×10^2
5	3.9279×10^0
6	6.2506×10^{-1}
7	1.4572×10^{-1}
8	0.0000×10^0

Some initial core condition is also required to being the flux calculation procedure. It would be incorrect to begin with a batch fuelled core that has fresh (i.e. zero burnup) fuel in every node. Such a core would be very far from critical, which is clearly unrealistic and imposes additional difficulties on the DONJON flux solver. A nearly sinusoidal burnup distribution was thus imposed in the second and third cycle locations based on the expected value of average discharge burnup. This was a more realistic initial condition representing the beginning of a fuelling cycle, and well within the capabilities of DONJON to find

a 3D flux solution. The next section, however, illustrates that this is still not an acceptable initial condition for transient analysis.

4.1.2.2 Fuelling Cycle Iterations

Whatever initial guess is provided for the core beginning-of-cycle burnup distribution is very unlikely to be correct (i.e. representative of a real core). The core power distribution, calculated with the burnup dependent cross-sections, is also unlikely to be correct. Since power directly determines the burnup progression in the fuel, the initial burnup guess will affect the power distribution at all points during the cycle and subsequent cycles. Consider that a refuelling operation shuffles two thirds of the fuel assemblies while replacing the spent (i.e. end-of-life) fuel with fresh assemblies. The power (and subsequently burnup) in the fresh fuel is necessarily affected by the burnup of adjacent fuel from the previous cycles. The core could therefore be in a different state at any prescribed time after refuelling (e.g. 0 days, 10 days, 100 days, etc.) in different cycles.

This work, however, assumes that there is an *equilibrium* core where the burnup and power distribution as functions of time are identical between subsequent cycles. Further, it's assumed that this equilibrium should be approached after many refuelling cycles regardless of the initial conditions, although the quality of the initial guess will affect how many cycles are required to reach equilibrium.

An algorithm (Figure 4.6) was thus implemented in the DONJON model to determine the equilibrium core. In this algorithm the cycle is split in to discrete time steps (Δt). For each step the flux and power distribution is updated and then used to advance the fuel burnup over a (small) time step where the power is assumed to be constant. This is similar to the lattice cell burnup calculation in DRAGON. A cycle reaches its end when the calculated core k_{eff} drops below a set criterion (in this case $k_{eff,end}$ = 1.010, a value that has been used in other PT-SCWR core calculations [35]). The fuel assemblies are then removed, shuffled, and replaced according to the scheme in Figure 4.5 and a new cycle is began.

The algorithm as implemented in DONJON has no decision logic to determine if equilibrium has been reached. Rather, it's up to the user to compare subsequent cycles and decide if any differences are acceptably small. This work compared the maximum difference in power for all nodes at beginning and end-of-cycle core states (the cycle length should be identical in subsequent cycles when the

core is at equilibrium). For node powers averaging hundreds of kilowatts, discrepancies of less than one per cent are on the order of watts. Relative to the total core power of 2,540 MW, differences this small are comparable to the converge criteria of the flux solution and are considered sufficient evidence that equilibrium was achieved.
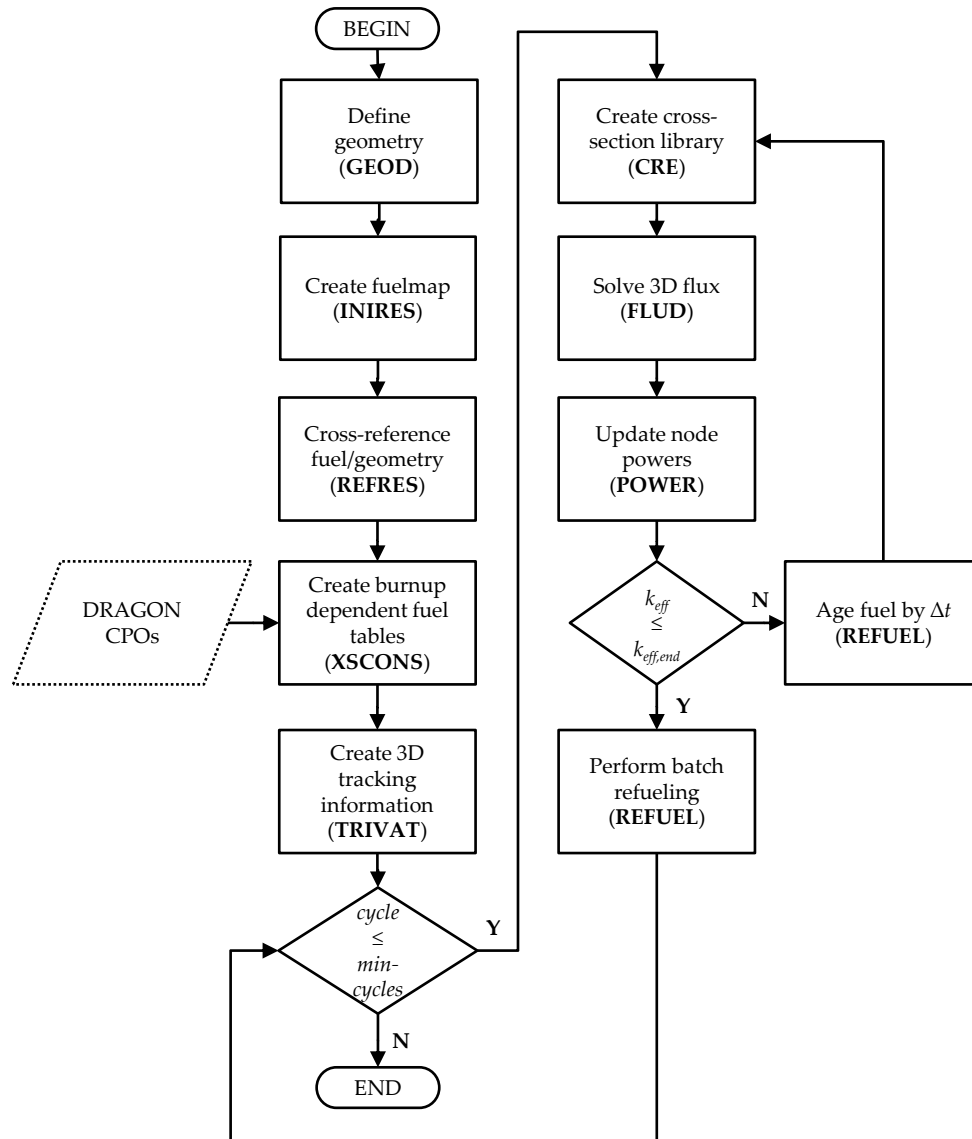
Figure 4.6: Algorithm for batch fuelling cycle iteration

Given the method in which the homogenized and condensed cross-sections were prepared with DRAGON, there is an inherent assumption about the thermalhydraulic conditions in each node of the DONJON diffusion model.

Specifically, it's assumed that the reference thermalhydraulic conditions in Table 4.2 are maintained at every instant during the cycle. Nevertheless, as the core power distribution evolves the fuel temperature distribution, and subsequently all other thermalhydraulic parameters, should be evolving with it. Capturing this effect would require a special application of a feedback model called a *history* calculation, which was not done for this work. Rather, it was assumed that a future reactivity control system would act to maintain the reference power distribution (and thus the distribution of thermalhydraulic parameters) at all points in the cycle, making a burnup history calculation unnecessary. It's not certain that such an ideal control system is realizable, but this serves as a simplifying assumption for this work. The feedback database is thus only applied to the coupled calculations.

The steady DONJON model described in this section, using the equilibrium core states at different points during the cycle (e.g. beginning, middle, or end), creates the initial conditions for transient spatial kinetics calculations. The kinetics simulation procedure is described in the next section.

4.1.3   Core-Level (Spatial) Neutron Kinetics

Neutron kinetics is used to model the transient behaviour of core power. This is distinct from the fuel cycle calculations described in Section 4.1.2.2 which solved the steady-state neutron diffusion equation at discrete steps (with new cross-sections) to model the passage of time over a relatively long scale. Kinetics calculations are truly time-variant and are used in this work to determine the PT-SCWR core power, and power distribution (i.e. "spatial kinetics"), in coupled neutronic-thermalhydraulic transients where the fuel isotopics can be considered constant. DONJON 3.02g was used as the tool for spatial kinetics simulation, and the previously described steady-state DONJON models create the initial conditions for the selected transients [27].

4.1.3.1   Spatial Kinetics Simulation Procedure

DONJON uses the Improved Quasi-Static (IQS) method for spatial kinetics. In this method the time-dependent flux is factored in to a time-variant amplitude function and a slowly-varying shape function (hence "quasi-static") [98]. Since the amplitude function is independent of geometry or flux shape, it is essentially a point kinetics approximation of the core. The coupling methodology used in

this work does not take advantage of this separation, i.e. both the amplitude and shape are re-evaluated at every time step (unlike coupling between RFSP and CATHENA, for example, where the shape and thermalhydraulics are evaluated at coarser time steps than the amplitude) [51]. More details about the coupling procedure are located in Section 4.3.1.

The required inputs for DONJON's IQS module are the forward (i.e. normal) and adjoint steady-state flux solutions, and the perturbation in macroscopic cross-sections over which the transient is to be calculated. Both flux solutions are produced simultaneously during the steady-state neutron diffusion calculation. The cross-section perturbation is determined by simply calculating the difference between two macroscopic cross-section libraries, each corresponding to an instant in time. These libraries are generated by the AFM module using the feedback database (more details about this procedure are in the next section). The general transient flux calculation procedure is shown in Figure 4.7. The FUELMAP data structure contains power and thermalhydraulic state data for each node in the 3D model.

The solution of the amplitude function, being essentially an application of point kinetics, can only have one set of kinetics parameters (i.e. delayed neutron fractions and precursor lifetimes). This is contrary to the differences in flux spectrum and fuel burnup within the core, which would be expected to add some spatial dependence to the neutron kinetics. The work of Schwanke and Nichita, however, demonstrates that the kinetics parameters in the PT-SCWR core are weakly sensitive to the local thermalhydraulic conditions [99]. A single set of kinetics parameters is thus an acceptable approximation for the PT-SCWR.

Table 4.11: Kinetics parameters used in the DONJON model

Group	β	λ [s^{-1}]
1	7.180×10^{-5}	0.0117727
2	7.410×10^{-4}	0.0277209
3	5.467×10^{-4}	0.1151299
4	1.002×10^{-3}	0.2993739
5	3.615×10^{-4}	1.0469525
6	9.070×10^{-5}	2.5418856
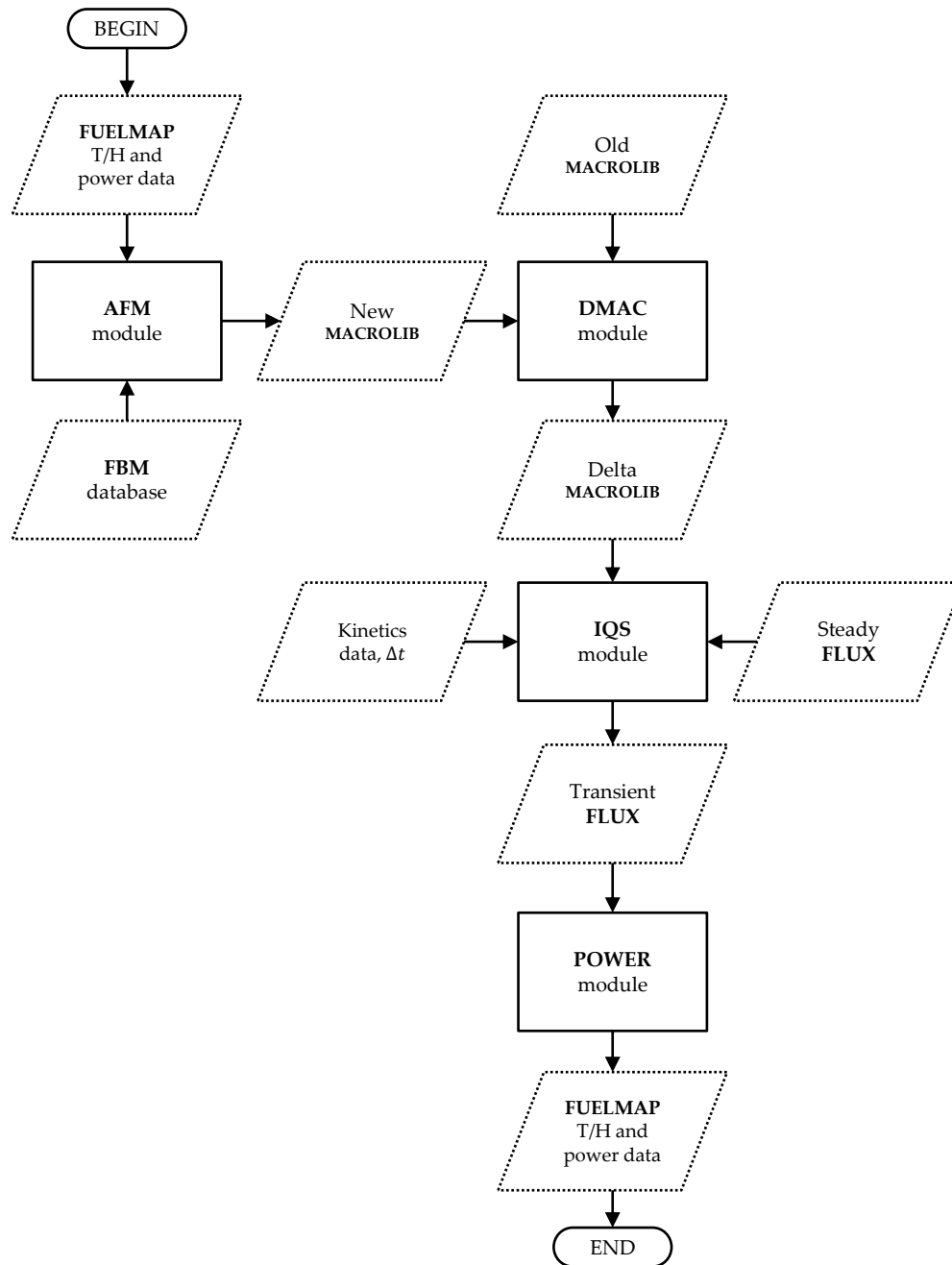
Figure 4.7: DONJON kinetics calculation procedure for a single time step

The kinetics parameters used for this work (Table 4.11) were taken from a SCALE model of the PT-SCWR lattice cell at the core mid-plane (DRAGON does not natively calculate kinetics parameters) [92].

4.1.3.2   Integration of the Feedback Database

The feedback database (discussed in Section 4.1.1.4) is used by DONJON's AFM module to create new macroscopic cross-sections for each node based on the local thermalhydraulic conditions. The new cross-sections are used to advance the spatial kinetics calculation such that each time step in a transient has an associated library of cross-sections. Aside from the database itself, the only other input to AFM is the FUELMAP data structure. For each node in the DONJON model, the FUELMAP contains values for:

- Power [kW]
- Burnup [MW·d·tonne^{-1}]
- Coolant density [g·cm^{-3}]
- Coolant temperature [K]

- Fuel temperature [K]
- Flow tube density [g·cm^{-3}]
- Flow tube temperature [K]

In the original version of AFM the moderator properties (where the "flow tube" data is stored in this work) were global rather than by node, so only one value could be accepted by AFM. One of the modifications made to the AFM source code in this work was expanding this functionality so that the moderator / flow tube properties could vary spatially.

For each node in the FUELMAP, AFM interpolates between burnup values in the database and applies the feedback model, returning macroscopic cross-sections (in the form of a MACROLIB data structure) that can be used in a new flux calculation. The differences between two libraries constructed in this manner are what are used to drive the kinetics calculation, with each library corresponding to an instant in time. The process is thus repeated at every time step.

There are certain fission, decay, and neutron activation products that are constantly created and destroyed while the reactor is operating. These products have a specific steady-state concentration based on the rate that they're produced and destroyed (i.e. the reactor power). For this reason that are called *saturating isotopes*. Saturating isotopes that have significant neutron capture cross-sections are obviously important in neutronics calculations (examples include ^{135}Xe, ^{149}Sm, and ^{239}Np). AFM is capable of calculating new saturated concentrations of these isotopes based on the powers in the FUELMAP and applying the appropriate feedback to the cross-sections. There is an important caveat, however, in the AFM will calculate *only* the saturated concentrations at steady-state. Physically,

these concentrations should be strong functions of time due to their own half-lives and those of their precursors, so it would be incorrect to update the concentration immediately to the saturated value after a small time step. The AFM module does not accept any time input, and it was decided that adding this functionality would be too onerous within the scope of this work. The calculation of saturating concentrations was thus disabled entirely in the source code.

This is partially justifiable because the aforementioned half-lives are measured in hours while the studied transients last seconds or minutes. The change in concentrations should be minimal over these short durations. This neglects the change in production rate directly from fission (a function of the instantaneous power), but this loss was judged insignificant relative to the much larger error of immediately stepping to the saturated concentration. Further, there is evidence that the results of these short transients (including BWR-like instabilities) are weakly sensitive to the neutron capture in saturating fission products regardless, strengthening the case for disabling the calculation outright [58].

4.2   Thermalhydraulics Models

CATHENA (Canadian Algorithm for THErmalhydraulic Network Analysis) is a thermalhydraulics code developed by AECL primarily for LOCA analysis of CANDU reactors [28]. It uses a one-dimensional, two-fluid representation to calculate transient two-phase flows in piping networks. The included GENeralized Heat Transfer Package (GENHTP) facilitates calculation of convective, conductive, and radiative heat transfer. In this work CATHENA MOD-3.5d/Rev 3 was used to model the thermalhydraulics of the PT-SCWR heat transport system for both steady-state and transient simulations.

The CATHENA code was recently enhanced to function in supercritical flow regimes with an expanded set of fluid properties [100]. This does not mean that its capability to model supercritical water is as mature as its subcritical two-phase and single-phase models. MOD-3.5d/Rev 3 treats supercritical water as a single-phase fluid and exclusively uses the single-phase friction factor and Dittus-Boelter heat transfer coefficient in calculations (i.e. there are no dedicated correlations for supercritical water). There are also documented code problems when crossing below the supercritical point (around 22.1 MPa) to two-phase fluid during transients, although the code is stable when operating exclusively in

the supercritical or two-phase regimes. These limitations had to be considered when creating the PHTS model and designing transient tests.

Many of the finer details of the PHTS geometry are undefined as of this writing, which is understandable given the early conceptual state of the PT-SCWR design. Considering the limitations of a one-dimensional thermalhydraulics system code like CATHENA, it would not be possible to resolve all the fine details of the flow path in the model regardless. Typically these fine features are represented as irrecoverable minor losses (i.e. *K* factors), and in this work considerable effort was put towards identifying descriptive minor loss terms. Without measured data to validate the CATHENA model, however, this work relies on simple comparison with other CATHENA results available in literature to determine if the new model is appropriate [100]. Specifically, if it can be observed that the total flow, temperature, and density distributions from the newly created CATHENA model match the expectations of the conceptual design and are similar to other published CATHENA simulation results, then the new model is judged sufficient for performing coupled transient simulations in this work.

4.2.1   Single-Channel Reference Model

CATHENA can model "virtual" parallel flow paths, wherein it's assumed that each parallel channel possesses the exact same flow characteristics. The advantage of this approach is that it's only necessary to solve one set of flow field equations while the total flow through the combined virtual parallel channels remains the same. The model is thus much simpler and faster to execute. Modelling the 336 channels of the PT-SCWR as a single channel provides information on the average flow behaviour in the core (the single channel being equivalent to an average channel in this case). While this approach would be inappropriate for three-dimensional coupled simulations, the average temperature and density distributions from the single-channel model can be used as the reference thermalhydraulic conditions in the lattice-level neutronics calculations (Section 4.1.1). For such calculations average properties are required, and it's more expedient to model a single average channel rather than model every channel and perform the averaging after the fact. Further, because each channel geometry is identical, the only practical difference between single and multi-channel models are the number of parallel components defined through the core pass (all out-of-core components being the same). Since the single-

channel model was used to generate the reference thermalhydraulic conditions for the neutronics calculations, some description of the model is warranted.

4.2.1.1 Hydraulic Components

Several out-of-core components in the PHTS circuit were omitted from the CATHENA model for simplicity, most notably the coolant pumps and turbines. Fluid pressure and temperature boundary conditions were instead imposed at the locations corresponding to the outlet of the primary heat transport pump (the core inlet boundary condition) and the inlet of the first turbine stage (the core outlet boundary condition). This approach was consistent with early CATHENA models of the PT-SCWR concept as well as modern BWR instability analysis [24, 100]. The steady-state conditions were specified as 350 °C at 25.8 MPa at the inlet and 625 °C at 25.0 MPa at the outlet [100]. Without any reactivity control devices included in the spatial kinetics model, changes to these boundary conditions were the primary means of initiating power transients through thermalhydraulic feedbacks.

The core inlet and outlet plena were represented as one-dimensional 'VOLUME' components in the CATHENA model. This precludes any simulation of the flow distribution within the plena since each is represented by a single hydraulic node. Using one-dimensional volumes in this manner is nevertheless consistent with other CATHENA modelling efforts [100].

The remainder of the PHTS flow path could be represented with 'PIPE' components. The component geometries are summarized in Table 4.12. Each component had an absolute surface roughness of 4.5×10^{-5} m in lieu of more detailed specification. The centre flow tube and fuel channel were each represented with 20 equally sized nodes for congruence with the DONJON model. This allowed the DONJON node powers to be transferred directly to the CATHENA model, and similarly CATHENA temperatures and densities to be used directly in the DONJON feedback model.

The CATHENA component dimensions were well defined within the core using the lattice cell description in Table 4.1. Other component lengths and volumes were taken either from literature or correspondence with the designers [100]. A "dead volume" around the connection between the riser and outlet plenum was also included as a hydraulic component. Including this dead volume facilitates

future expansion of the CATHENA model to simulate transients where the heat transfer across the riser pipe wall may be important. The details of the flow path as modelled in CATHENA are shown in Figure 4.8.

Table 4.12: CATHENA component geometry definitions

Label	Length [m]	Area [m²]	D_h [m]	K factor	Nodes	Parallel Components	Volume [m³]
PUMPDIS	0.500	2.761×10^{-1}	5.929×10^{-1}	0	3	4	0.138
INPLEN							68.719
INNOZZLE	1.697	1.614×10^{-2}	9.992×10^{-2}	1.2	3	336	9.205
FLOWTUBE	5.000	6.648×10^{-3}	9.200×10^{-2}	0	20	336	11.168
RVRSEVOL	0.250	1.629×10^{-2}	1.440×10^{-1}	1.2	1	336	1.368
FUELCHAN	5.000	4.565×10^{-3}	6.742×10^{-3}	20	20	336	7.669
OUTNOZLE	1.697	3.136×10^{-3}	6.319×10^{-2}	1.15	3	336	1.788
RISER	0.927	2.992×10^{-3}	6.172×10^{-2}	0	3	336	0.932
OUTPLEN							14.232
DEADVOL	0.927	2.274×10^{-2}	1.407×10^{-1}	0	3	336	7.082
TRBPIPE	0.990	1.257×10^{-1}	4.000×10^{-1}	0	3	4	0.498

While the in-core flow areas (i.e. within the flow tube and around the fuel) were easily representable as one-dimensional components, the complex geometries of the channel inlet/outlet nozzle and the flow reversal at the bottom of the pressure tube presented additional challenges. The flow areas and hydraulic diameters shown in Table 4.12 for these components are approximations based on engineering drawings and include significant averaging of three-dimensional features over the length of the volume. The attached *K* factors were determined using Idelchik's *Handbook of Hydraulic Resistance.* Specifically, the inlet nozzle *K* factor was determined from reduced data for the "merging of flow streams", the flow reversal from "flow with changes in stream direction", and the outlet nozzle from "flow past obstructions in a tube" [101]. The *K* factor for the fuel channel itself was selected based on previous experience modelling flow through annular fuel bundles [102]. The results were found to be insensitive to the values of these *K* factors within significant variance (i.e. halfing or doubling the *K* factors varied flows, densities and temperatures by less than 0.1%), and limited (if any) sensitivity of the coupled transient results to these approximations was expected.
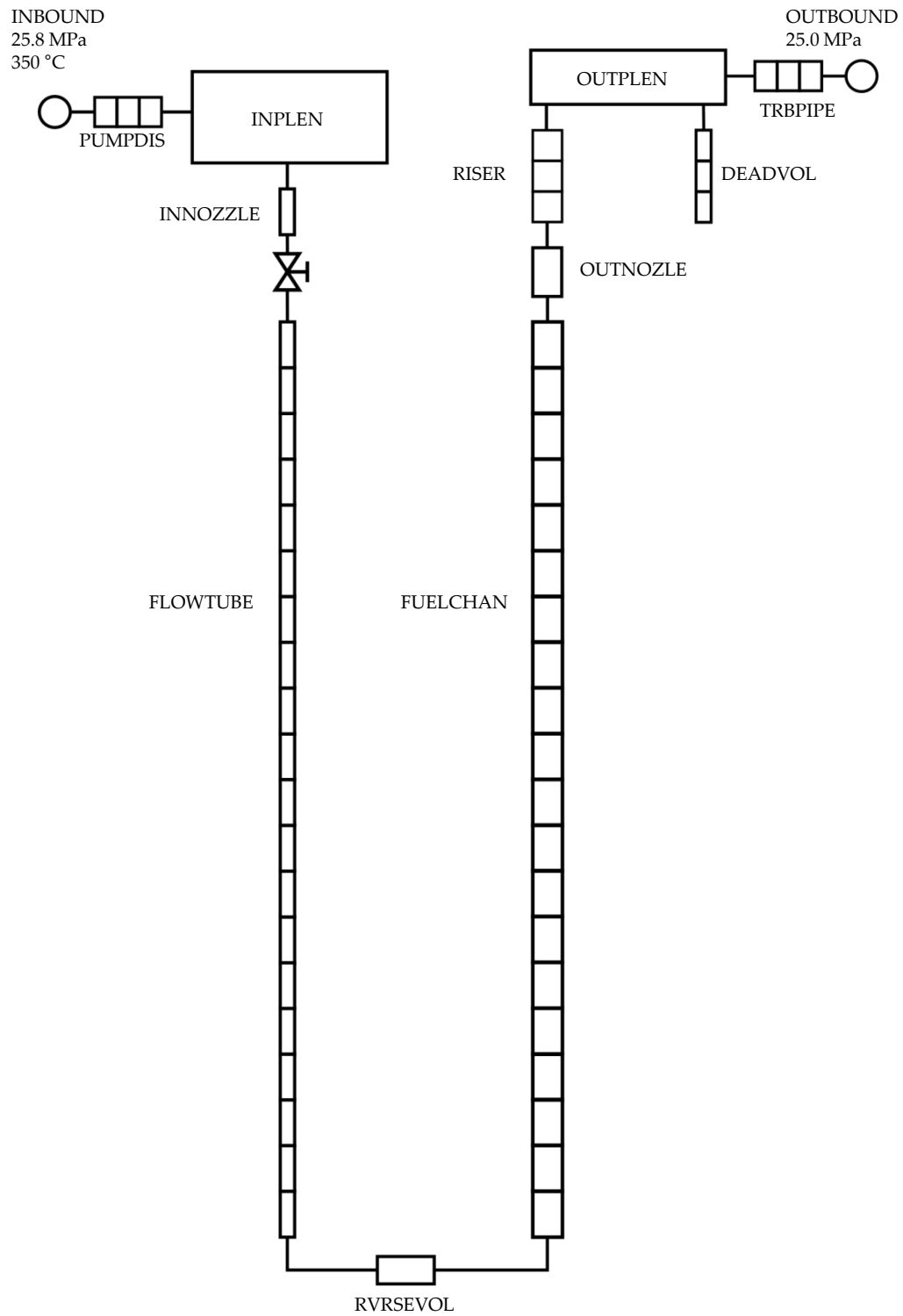
Figure 4.8: CATHENA single-channel hydraulic components

According to the conceptual design specifications, the inlet of each channel is to include a flow-limiting orifice that matches the channel flow to the channel power so that the coolant temperature at the outlet is within a small tolerance of 625 °C [100]. This orifice was assumed to be coincident with the inlet nozzle in this work (more details about the orifice sizing procedure are presented in Section 4.2.3). These orifices are likely the source of the aforementioned insensitivity to the geometry and K factor approximations. Even at high channel powers the majority of pressure drop (i.e. well over 50% or 0.4 MPa) was observed over these orifices, indicating that they were significantly restricting the channel flows at the prescribed boundary conditions of 25.8 MPa (inlet) and 25.0 MPa (outlet) and largely determining the flow behaviour on their own. This raises the question if the imposed 0.8 MPa pressure differential was appropriate, but it was decided that these boundary conditions were to be kept to maintain consistency with other PT-SCWR models.

4.2.1.2 Heat Transfer Components

The single channel PHTS model includes four GENHTP models representing the inner and outer rings of fuel elements, the pipe wall of the centre flow tube, and the pressure tube (including the ceramic insulator). Each of these is described in turn.

The inner and outer rings of fuel elements were modelled separately but similarly, differing only in the geometry and relative share of the reactor power. Each ring of fuel elements was represented as a cylinder corresponding to a single fuel pin. CATHENA replicates this geometry according to the number of pins defined in a ring (each pin in a ring is assumed to be identical in the solution, similar to the treatment of parallel channels). The pin model used 20 axial nodes matching the hydraulic discretization of the fuel channel, with the exterior boundary condition of each axial node coupled to the corresponding hydraulic volume. The radial nodalization is shown in Figure 4.9.

The pin radial geometry is shown to consist of three material regions: fuel, gas gap, and cladding. The thermophysical properties of PuO_2-ThO_2 fuel were received from AECL and input to the GENHTP model (Table 4.13). Heat generated from fission was deposited in the fuel material and distributed evenly within the region.
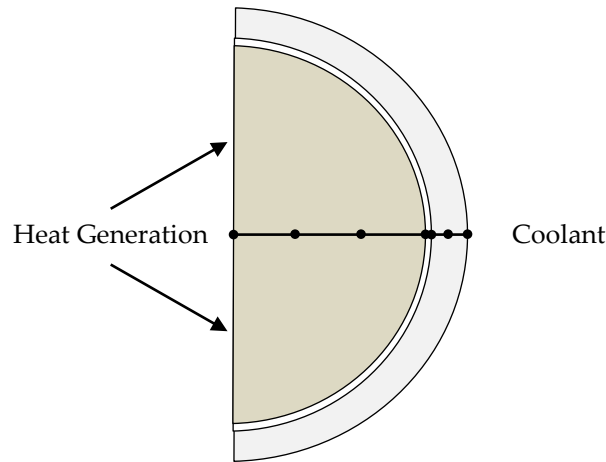
Figure 4.9: Fuel element GENHTP radial nodalization

The gas gap does not exist in the formal specification of PT-SCWR fuel. It's possible that the concept will make use of a "collapsible" fuel sheath that ensures direct contact between fuel and cladding at all times. Nevertheless, it's intuitive that coupled transient results should be sensitive to the rate at which heat is transferred from fuel to coolant, and there will be some contact resistance even with a collapsible sheath, so it was decided that a small gap (0.082 mm thick) should be included to at least explore the results' sensitivity to these assumptions. The gap was included using CATHENA's 'GAP' material specification with a defined thermal conductance. The reference model possessed an extremely large conductance (50,000 $W \cdot m^{-2} \cdot °C^{-1}$) to approximate the collapsible sheath being in contact with the fuel. These values (both gap thickness and conductance) were typical of LWR fuel [103]. The cladding material itself used the built-in thermophysical properties of stainless steel.

The power of a single node in the DONJON model must be distributed between the inner and outer rings of fuel elements. Lattice-level calculations (using DRAGON) showed that slightly more power is consistently generated in the outer ring at every axial location and fuel burnup state. The maximum outward skew was, however, within 5% of being evenly split in the worst possible case (fresh fuel at the channel outlet), and in the majority of the core within 2.5%. Rather than implementing a complex function with external tools that modified the radial power distribution as functions of axial location and fuel burnup within the CATHENA model, a constant average power skew was implemented (51.9% outer ring, 48.1% inner ring).

Table 4.13: Thermophysical properties of PuO_2-ThO_2 fuel

Temperature [°C]	Inner Ring		Outer Ring	
	Thermal Conductivity [W·m^{-1}·°C^{-1}]	Volumetric Heat Capacity [J·m^{-3}·°C^{-1}]×10^6	Thermal Conductivity [W·m^{-1}·°C^{-1}]	Volumetric Heat Capacity [J·m^{-3}·°C^{-1}]×10^6
27	3.80	2.18	4.77	2.17
127	3.42	2.39	4.20	2.38
227	3.11	2.51	3.75	2.50
327	2.86	2.60	3.39	2.59
427	2.64	2.66	3.10	2.64
527	2.45	2.70	2.85	2.69
627	2.29	2.72	2.63	2.71
727	2.15	2.74	2.45	2.73
827	2.02	2.75	2.29	2.74
927	1.91	2.75	2.15	2.74
1027	1.81	2.75	2.03	2.74
1127	1.72	2.75	1.92	2.74
1227	1.64	2.75	1.82	2.74
1327	1.57	2.76	1.73	2.75
1427	1.50	2.76	1.65	2.75
1527	1.44	2.78	1.58	2.77
1627	1.38	2.79	1.51	2.79
1727	1.33	2.82	1.45	2.82
1827	1.28	2.86	1.39	2.86
1927	1.23	2.91	1.34	2.91
2027	1.19	2.98	1.29	2.98
2127	1.15	3.06	1.24	3.06
2227	1.11	3.15	1.20	3.16
2327	1.08	3.26	1.16	3.27
2427	1.05	3.40	1.12	3.41
2527	1.01	3.55	1.09	3.57
2627	0.99	3.73	1.06	3.75
2727	0.96	3.93	1.03	3.96

The GENHTP model for the "centre flow tube" pipe wall was relatively simply by comparison. The tube was modelled as a cylinder with 20 axial nodes, corresponding to the 20 hydraulic volumes in both the flow tube and fuel channel, with which the inner and outer surface were respectively coupled. The model consisted of a single material region, represented with three equally spaced radial nodes, using the built-in stainless steel thermophysical properties. The model geometry contained no insulator to thermally isolate the flow tube and fuel channel, consistent with the reference conceptual design specifications [11].

The radial geometry of the "pressure tube" GENHTP model (Figure 4.10) contained four material regions representing (from inside to out) the inner liner tube, ceramic insulator, outer liner tube, and pressure tube. The inner liner tube region utilized the built-in thermophysical properties of stainless steel. The properties of YSZ needed to be determined from literature [104, 105]. The yttrium content specified in the PT-SCWR conceptual design was equivalently 5.71 mol% yttria. The data was processed to create the thermophysical property input shown in Table 4.14. The outer liner tube and pressure tube itself used the built-in properties of zircalloy.
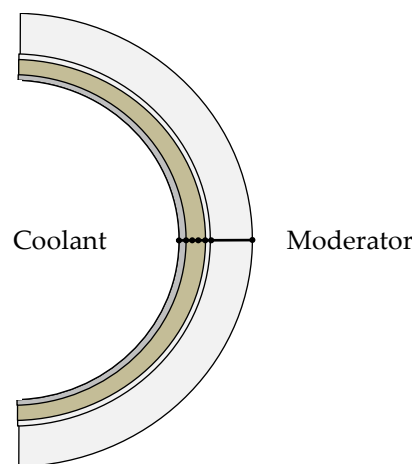
Figure 4.10: Pressure tube GENTHP radial nodalization

Table 4.14: Thermophysical properties of the ceramic insulator

Temperature [°C]	Thermal Conductivity [W·m^{-1}·°C^{-1}]	Volumetric Heat Capacity [J·m^{-3}·°C^{-1}]×10^6
50	2.51	2.75
100	2.52	2.90
150	2.47	3.05
200	2.39	3.18
250	2.31	3.28
300	2.22	3.35
350	2.15	3.43
400	2.09	3.51
450	2.03	3.55
500	1.99	3.56
550	1.96	3.58
600	1.93	3.64
650	1.91	3.67
700	1.90	3.70
750	1.90	3.72
800	1.92	3.77
850	1.94	3.76
900	1.97	3.81
950	2.00	3.84
1000	2.06	3.86

Rather than explicitly modelling the liquid moderator, a constant pressure and enthalpy boundary condition (or 'LIQUID-BATH' as implemented in CATHENA) was instead coupled to the outer surface of the pressure tube. This was done mostly for simplicity in the model. For the relatively short transients studied in this work the heat transfer between the coolant and inner liner may not be negligible (necessitating its inclusion in the model). Nevertheless, in such transients any variation in the heat transferred to the moderator is likely insignificant given the thermal inertia associated with the significant volume of (insulating) material. In parametric studies where the core pressure drop was varied by 25% (200 kPa), for example, the pressure tube surface temperature only

varied by a few degrees (< 4 °C) within 30 s of the step change in core flow. The constant moderator properties were defined as 336 kPa and 231 kJ·kg^{-1} in the model.

Generally speaking, GENHTP input in CATHENA contains many options to control and adjust convective heat transfer between surfaces and fluid. The vast majority of these controls, however, are only relevant towards two-phase heat transfer. In cases of single-phase wall-to-fluid heat transfer (as in the supercritical region), the states of these controls is irrelevant and thus were left with their default values. A multiplier can nevertheless be applied to the single-phase convective heat transfer coefficient for sensitivity analysis. Note that no radiative heat transfer was included in the model. It was decided that radiation would be insignificant in the short coupled transients studied in this work where sheath temperatures remain below 1000 °C for most cases.

4.2.2   Quarter-Core (84-Channel) Model

Modelling each of the 336 channels separately was determined to be beyond the capability of the CATHENA code. The reference batch refuelling scheme of the PT-SCWR, however, results in a core that is quarter symmetric (or eighth symmetric if half-channels are allowable) [93]. There are 84 unique channels in the quarter core, and if each is modelled as four parallel channels that possess the same power and flow distributions, the total core power and flow is conserved. This was found to be within CATHENA's capability. As a consequence, however, the core-level model could no longer capture the higher-mode coupled oscillations described in Section 2.2.2, and is thus constrained to the fundamental mode. This sacrifice of capability was deemed necessary to fit within the limitations of the toolset.

The hydraulic and GENHTP components in the 84 channel model were practically identical to those described for the single channel mode apart from the number of parallel components (4 each instead of all 336) and the specification of power in each node. The plena and core inlet/outlet piping were consistent with the single channel model. There is thus significant repetition in the CATHENA component definition (i.e. 84 each of the described components and GENHTP models), with each only differing in the channel label and corresponding node powers taken from the DONJON model (match precisely to

the CATHENA nodalization without merging or mapping). It was thus expedient to create a template for each component and a script to generate the CATHENA input file.

The resulting model (Figure 4.11) consists of 1,014 unique components (comprised of 4,124 hydraulic volumes), attached to 336 GENHTP models, and includes 84 special control connections that represent the flow-limiting orifices (described in detail in the next section). The input file itself exceeds 50,000 lines.

4.2.3 Channel Inlet Flow-Limiting Orifices

From a reactor design perspective, it's desirable that there be a uniform coolant enthalpy (or temperature) increase in each channel. For channels that have different powers (from different fuel burnups or positions in the core), this is achieved by matching the channel flow to the channel power to produce the desired outlet temperature. In a typical PHWR the flow-power matching is achieved through a combination of orifices and variations in each channel's feeder pipe geometry, thus introducing hydraulic losses that produce the desired channel flows [106]. The PT-SCWR concept, however, includes no feeders so the requisite hydraulic losses need to be created entirely with flow-limiting orifices installed at the inlet of each channel [12].

The dimensions of each orifice will necessarily be a function of the corresponding channel powers. The typical approach to model the PT-SCWR PHTS has been to use variable orifices that dynamically match the specified channel powers at runtime [100]. Once the orifice sizes are determined in a steady-state model, they are held fixed for subsequent transients. This approach was used in this work as well.

In a batch fuelled reactor like the PT-SCWR, each channel's power is a function of time, varying from beginning to end of cycle as the fuel depletes. The channel flows required to achieve a uniform outlet temperature are thus also changing during the cycle. The proposed orifices are static features, however, so some deviation from the desired outlet temperature would be expected over the course of a fuel cycle.
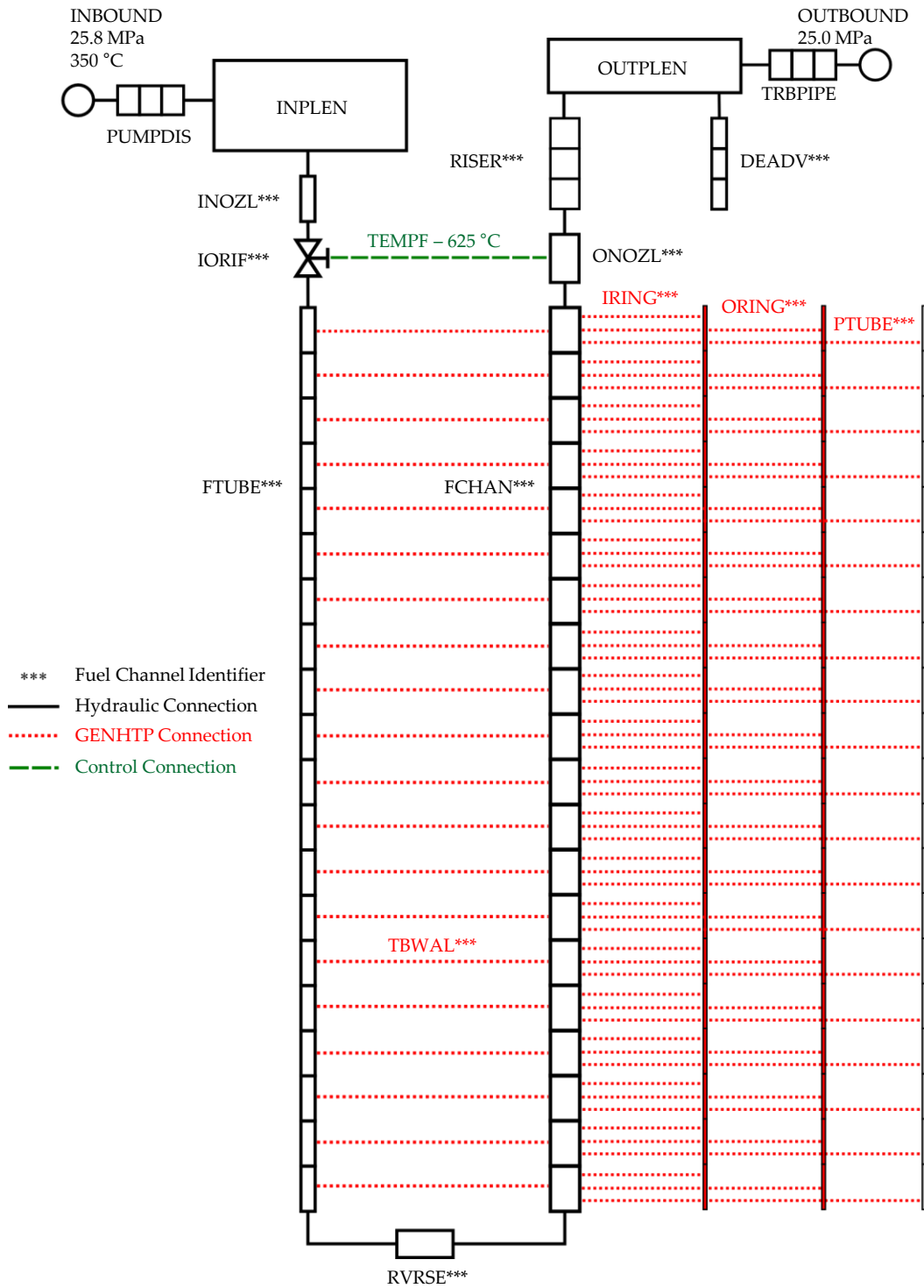
Figure 4.11: Quarter Core CATHENA model nodalizataion

Attempts to find optimal orifices that minimized the outlet temperature deviation over an entire cycle were unsuccessful since even the minimum achievable deviations were unacceptably large departures from the PT-SCWR design specifications [107]. Some reactivity and power levelling control system will be necessary to minimize the channel power variation during a cycle, but no such system was part of the PT-SCWR reference conceptual design as of this writing.

To mimic the control system's impact on channel powers, this work assumed that at the start of each transient the flow-power characteristics were balanced such that the outlet temperature in each channel was at the design target of 625 °C. To accomplish this, unique orifices sizes were determined for each initial condition (i.e. steady-state core power and burnup distribution at an instant during the batch cycle, or core "snap shot").

Within the CATHENA model the variable orifices were implemented as 'VALVE' components that controlled the flow area between the inlet nozzles and centre flow tubes. Since the valves are entirely artificial, the model used the CATHENA defaults for valve discharge coefficient and orifice type. The valve flow area was controlled by a 'CONTROL DEVICE' component that was an idealized implemented of a PI (proportional-integral) controller in the form:

$$A_{orifice}(t) = P_K\big(T_{out}(t) - T_{setpoint}\big) + \frac{P_K}{T_i} \int \big(T_{out}(t) - T_{setpoint}\big)\, dt \qquad (64)$$

The temperature setpoint ($T_{setpoint}$) was the reference core outlet temperature of 625 °C. Technically this was the desired temperature at the turbine inlet, but since the CATHENA model did not calculation flow distribution within the outlet plenum or heat loss through the pipe walls, this was equivalent to specifying the temperature at the outlet of each channel. The proportional gain (P_K) and integral time (T_i) were determined through trial-and-error to be 5.643×10⁻⁴ and 3.000 s respectively, which typically gave adequate performance by converging to steady values within a few hundred seconds of simulation time. The controller was not unconditionally stable for the lowest channel powers and occasionally experienced low frequency oscillations, but averaging the output of these oscillations provided adequate results with the channel outlet temperatures falling within the allowable deviation about 625 °C.

4.3 Code Coupling and Transient Simulation Procedures

The DONJON and CATHENA codes were developed independently without consideration towards coupling with one other. One of the key accomplishments of this work was establishing a method to transfer information between the two disparate codes, thereby allowing simulation of coupled neutronic-thermalhydraulic transients. In this section the coupling and transient calculation procedures are described.

4.3.1 Mechanism for Code Coupling

The key facilitator of passing data between codes was DONJON's FUELMAP data structure. As described in Section 4.1.3.2, the FUELMAP contains burnup, power, and thermalhydraulic data for each node in the DONJON model. Saved as a file, the power data can be read from the FUELMAP and written to a CATHENA input file (specifically the heat generation entries in the fuel pin GENHTP models) by a relatively simple script. Similarly, CATHENA output of temperatures and densities can be read by a script and used to modify thermalhydraulic entries in the FUELMAP. When the following iteration of DONJON reads the FUELMAP, new macroscopic cross-sections are created based on these thermalhydraulic conditions.

This passing of information is illustrated in Figure 4.12. Process inputs and outputs are clearly specified in the chart to show the flow of information. Additional details in the DONJON procedure, including geometry specification and tracking definition, are omitted from the figure for brevity.

Note that this method of coupling requires data to be written and read from the hard disk for every iteration. This is inefficient compared to the codes using a shared memory space, but given their independent developments it was the most straightforward way of passing information between without making significant changes to the source code.
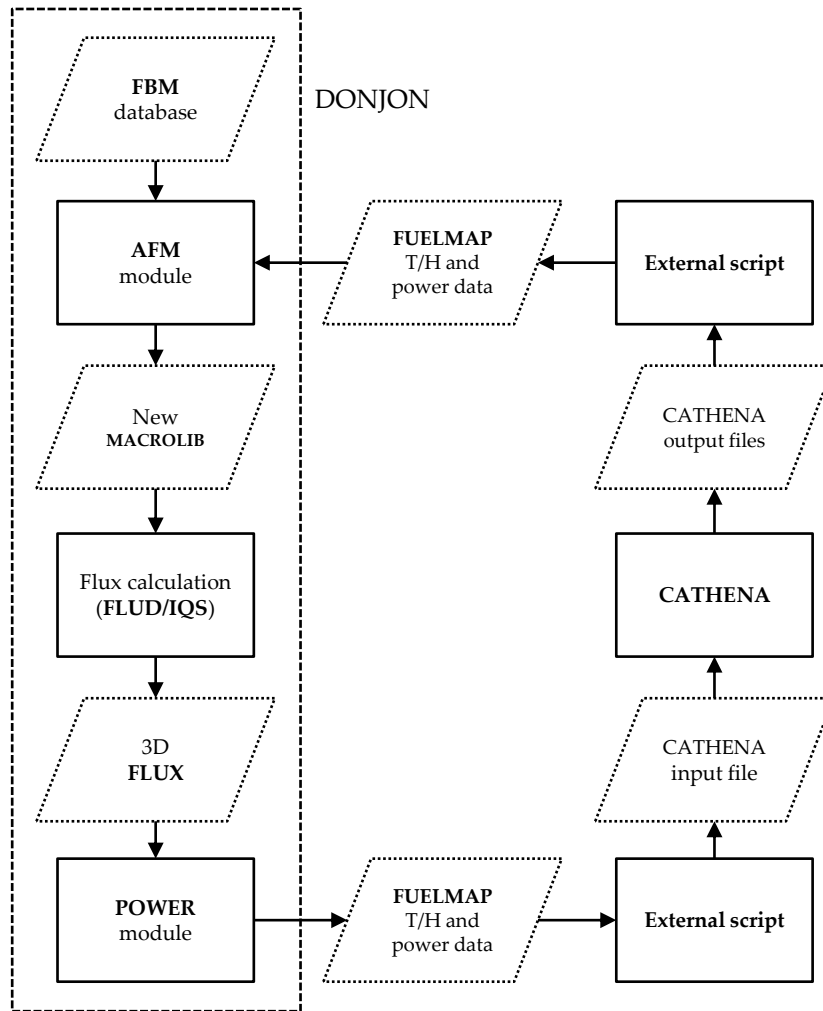
Figure 4.12: Generalized DONJON/CATHENA coupling procedure

4.3.2   Steady-State Iterations for Initial Conditions

Before beginning a transient, it's necessary to have valid initial conditions. For the coupled code set, valid initial conditions should have self-consistency between the distributions of power and thermalhydraulic parameters. Furthermore, in the case of the PT-SCWR model, the thermalhydraulic property distribution should be very close to the reference property distribution used in generating the reference cross-sections.

An iterative procedure was developed to converge on self-consistent three dimensional power and thermalhydraulic power distributions. Beginning with an initial guess of thermalhydraulic properties, new powers are calculated by

DONJON and then used to form new CATHENA input. CATHENA then finds the inlet orifices that give a coolant outlet temperature of 625 °C in each channel. These properties are used to create new DONJON input, which is then used to generate new power for the next iteration. Applying successive under-relaxation of the power distribution in the form:

$$P^i = rP^i + (r - 1)P^{i-1} \tag{65}$$

with a value of $r = 0.2$, gives convergence typically with a few (< 10) iterations.
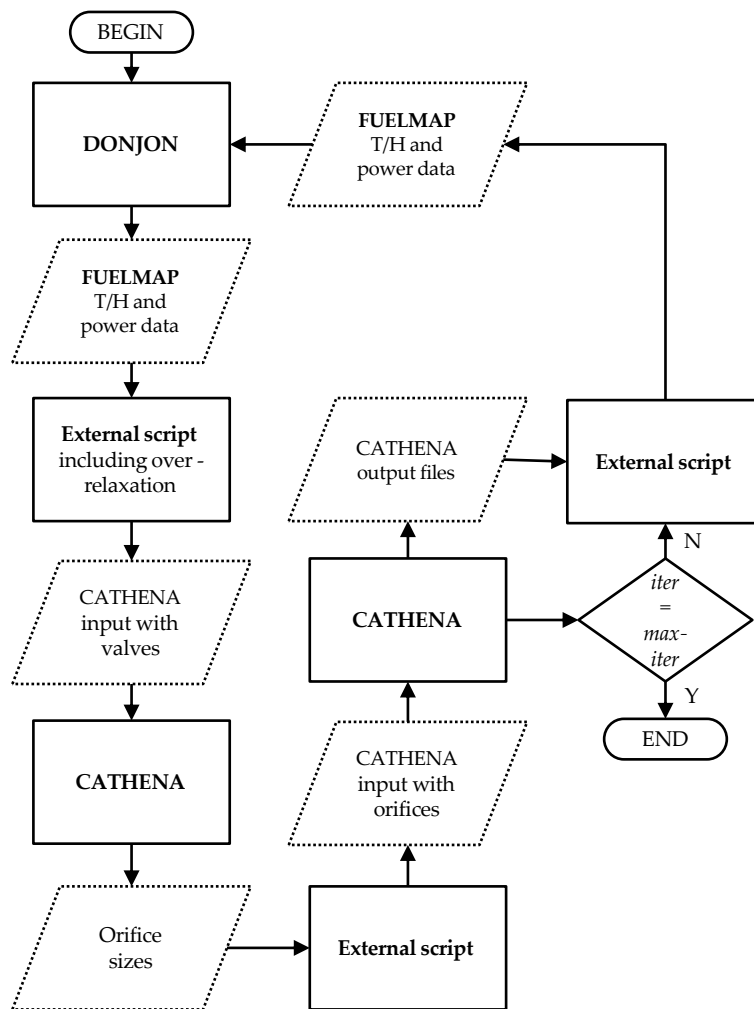
Figure 4.13: Iterative procedure for generating initial conditions

The procedure is summarized in Figure 4.13. The process needs to be repeated for every initial core state that is used in transient calculation (e.g. beginning,

middle, and end of cycle) or following any changes to the steady-state DONJON or CATHENA models.

4.3.3   Coupled Transient Simulation Procedure

The coupling procedure for transient calculation was conceptually similar as for the steady-state, but additional consideration needed to be made for the spatial kinetics and time step selection. Consistent with the description given by Downar, in the transient procedure the kinetics calculation will be "leading" the simulation's march through time, with the thermalhydraulic calculation "lagging" or "catching up" at each step [50]. This is best visualized in Figure 4.14.
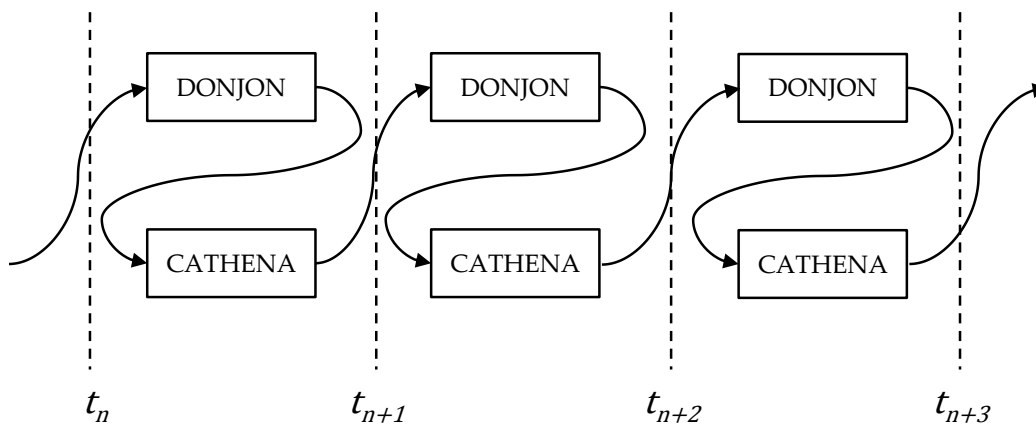
Figure 4.14: Coupled-code transient marching procedure

Since the kinetics is always one step ahead of the thermalhydraulics, feedbacks in the cross-sections will always be artificially delayed by one time step. The effect on the results can be mitigated by using very small time steps, but exclusively using small time steps would be computational inefficient in slowly progressing transients. The time step size was thus allowed to change dynamically according to transient rate of change. This would be consistent with what Grgic and Grandi respectively described as "semi-implicit" or "mixed synchronous-asynchronous" code coupling [42, 49].

Since the kinetics calculation was "leading" the transient, the logical choice for determining the time step size was the maximum power change in each node. For this work the maximum allowable relative change in node power was 0.5%. If this was exceeded, the time step size was halved and the step was reattempted. If the criterion was satisfied for more than four consecutive steps, the time step size was doubled. Maximum and minimum allowable time step sizes were

defined as 1.0 s and 0.0005 s, although in practice the lower limit was rarely reached. CATHENA is also capable of dynamically adjusting time step sizes, but in this coupling procedure it was forced to use the externally determine time step in order to maintain synchronicity with the DONJON model. The transient coupling procedure is shown diagrammatically in Figure 4.15.
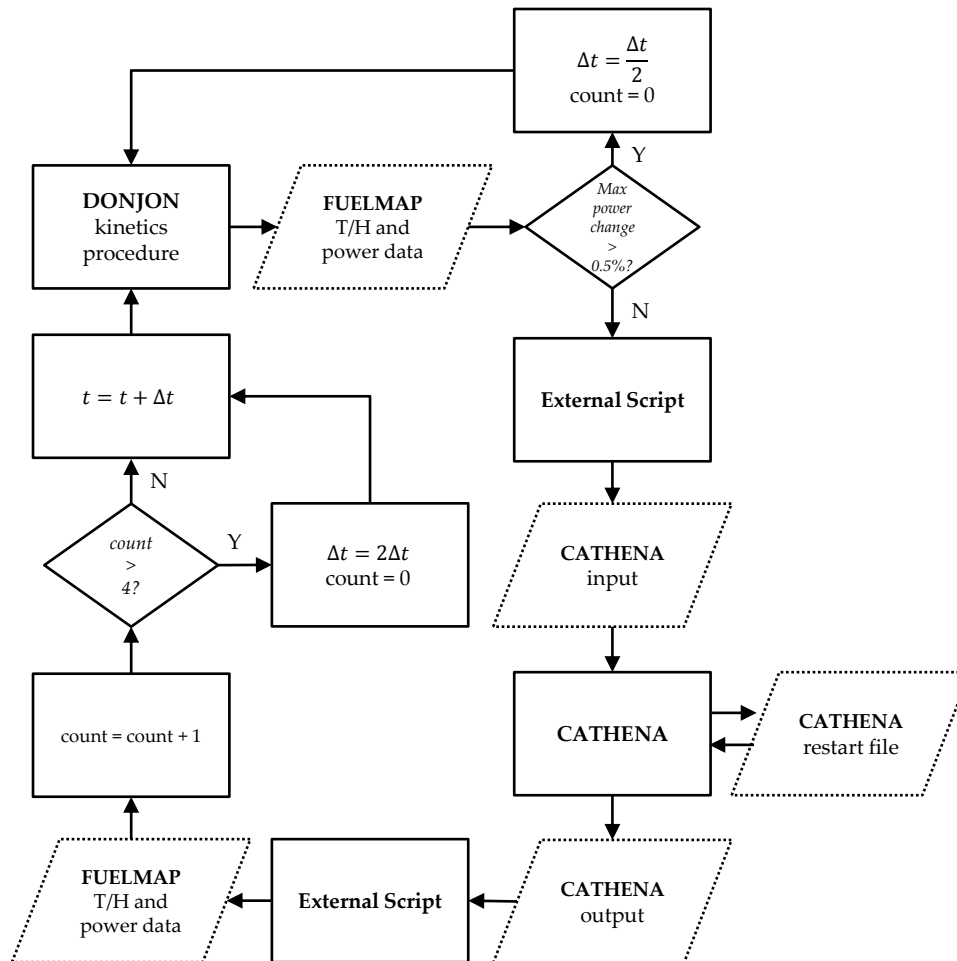
Figure 4.15: Transient code-coupling procedure with time step selection

The transients studied in this work were initiated by changes to the core inlet and outlet boundary conditions contained within the CATHENA model. These were modified as function of time within the script that generated the CATHENA input file. Before beginning a transient the system was allowed to run for several seconds of simulation time with the boundary conditions held constant. This "null" transient ensured that the kinetics parameters were properly initialized and the reactor was perfectly stable before initiating a true transient test.

Chapter 5

Simulation Results

The models described in Chapter 4 have been used to study the steady-state and transient three-dimensional coupled neutronic-thermalhydraulic behaviour of the PT-SCWR concept. This is notable for: 1) being the first application of this level of analysis to the PT-SCWR, and 2) being among the first applications of coupled spatial kinetics and thermalhydraulics that includes multiple coolant feedbacks. In this chapter, simulation results are presented and discussed from the lattice to core level. Section 5.3 presents results for two types of coupled transients: tests on the PT-SCWR's inherent coupled stability, and imposed flow transients meant to be evocative of postulated accident scenarios. This section also includes a partial model parameter sensitivity analysis to elucidate how some assumptions and simplifications made during creation of the core models affect the coupled transient results.

5.1 Lattice-Level Results

Power transients in the full-core coupled model are determined through a spatial kinetics calculation. The kinetics calculation is turn governed by the supplied cross-section feedback database. Since the feedback database is the product of lattice-level neutron transport calculations, the lattice models alone can provide some insight in to the behaviour of the coupled system.

Lattice-level benchmark code-to-code comparisons often examine calculated parameters including k_∞, coolant void reactivity (CVR), and fuel temperature reactivity coefficient (FTC) [91, 108]. The latter two are especially relevant to a system with strong thermalhydraulic feedbacks. The CVR value is essentially a special case of the coolant density reactivity coefficient since it is always calculated with a reduction in density (albeit with the opposite sign: a *negative* CVR indicates a *positive* coolant density coefficient). These common parameters

were thus calculated for the 64-element PT-SCWR fuel using the lattice models created with DRAGON 3.06K and the IAEA nuclear data library. Three separate CVR calculations were performed: where only the centre flow tube was voided, where only the fuel region was voided, and where both were voided. The results for fresh fuel, approximately mid-life fuel, and end-of-life fuel are shown in Figure 5.1 through Figure 5.4 for each of the 20 axial locations.

Note that the presented reactivity coefficients are not explicitly part of the thermalhydraulic feedback database. As described in Section 4.1.1.4, the database contains information on how each macroscopic cross-section changes with each thermalhydraulic parameter in each of the eight energy groups. This is distinct from the reactivity change calculated from a perturbation to the lattice cell. Nevertheless, these values provide some insight to the aggregate effect on the lattice cell caused by changes in the thermalhydraulic parameters from which changes to the local power may be extrapolated (if only approximately).

Figure 5.1 shows that a reduction in coolant density exclusively around the fuel has a positive reactivity effect regardless of burnup state or axial position within the channel. The magnitude of the CVR is notably higher near the *inlet* but, as noted in a previous benchmark study, the reference coolant density (Table 4.2) is much higher near the inlet so the magnitude of the density change over which the void reactivity worth is calculated is correspondingly larger [91]. Transforming this into a coolant density reactivity coefficient (which has opposite sign and is evaluated per unit density change), as in Figure 5.5, shows that the marginal reactivity worth is in fact larger near the *outlet* with fresh fuel.

It's reasonable to postulate that significant contributors to the fuel region CVR being positive are the downscattering of fast neutrons and upscattering of thermalized neutrons into capture resonances that occurs in the presence of coolant. When the coolant is removed, more fast and thermal fissions can occur. It follows that in Figure 5.5 the coolant density reactivity coefficient would be largest in magnitude near the outlet (for fresh fuel) where the coolant temperature and fuel temperature are highest (respectively shifting the thermalized spectrum upward and Doppler-broadening the capture resonances). The fact that coefficient decreases most rapidly with burnup near the outlet would indicate that the absorbing isotope is depleting most rapidly where more resonance captures are taking place, lending credence to this theory.
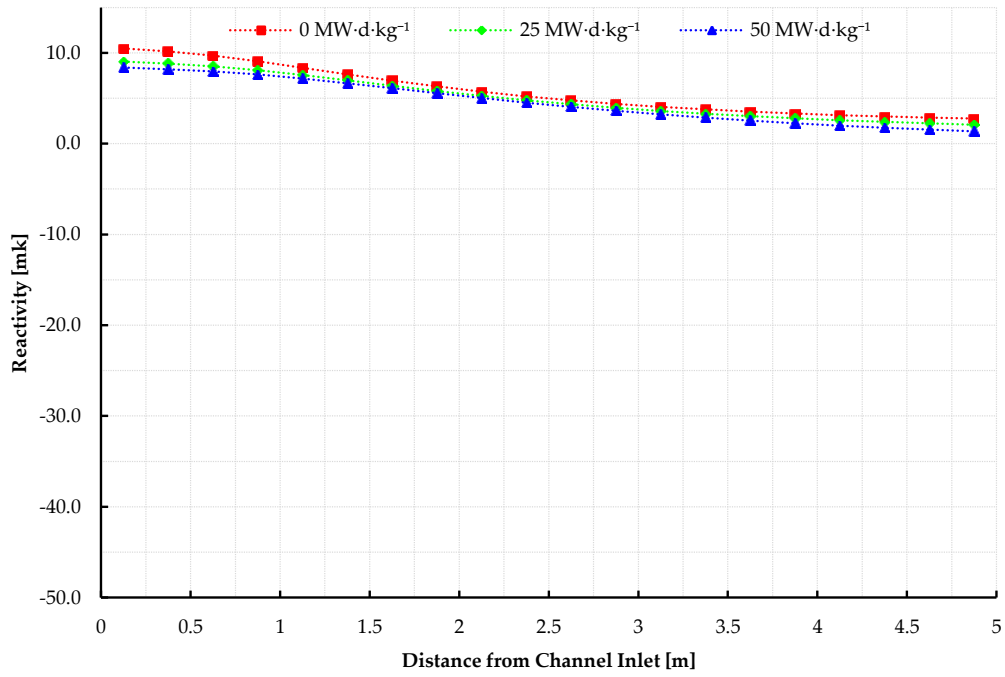
Figure 5.1: Coolant void reactivity in fuel region
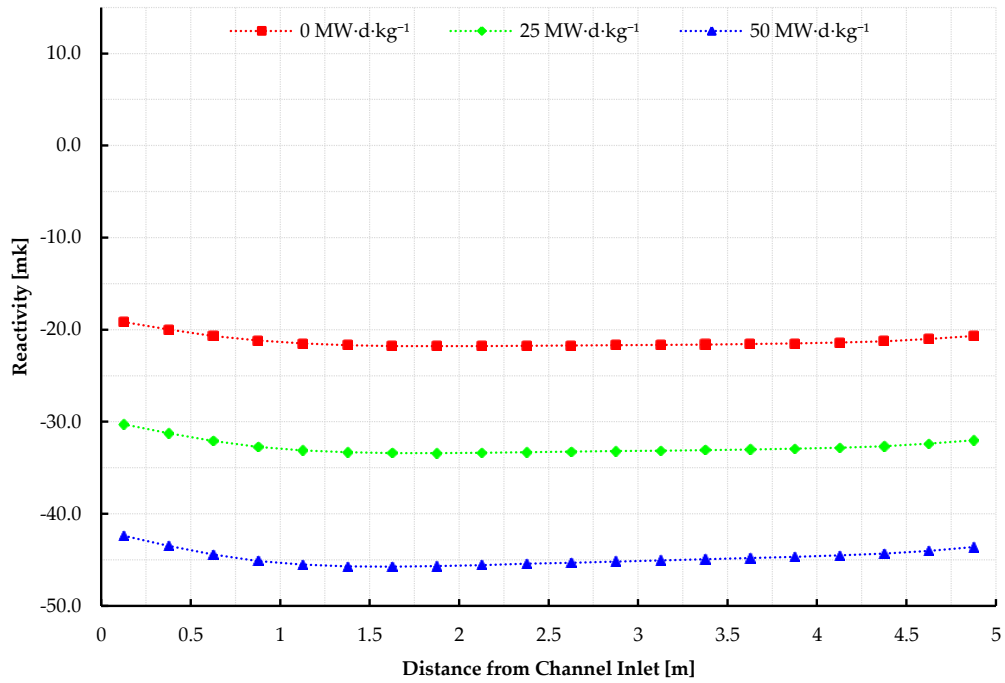
Figure 5.2: Coolant void reactivity in flow tube

D. W. Hummel
Ph.D. Thesis

Chapter 5
Simulation Results

McMaster University
Engineering Physics
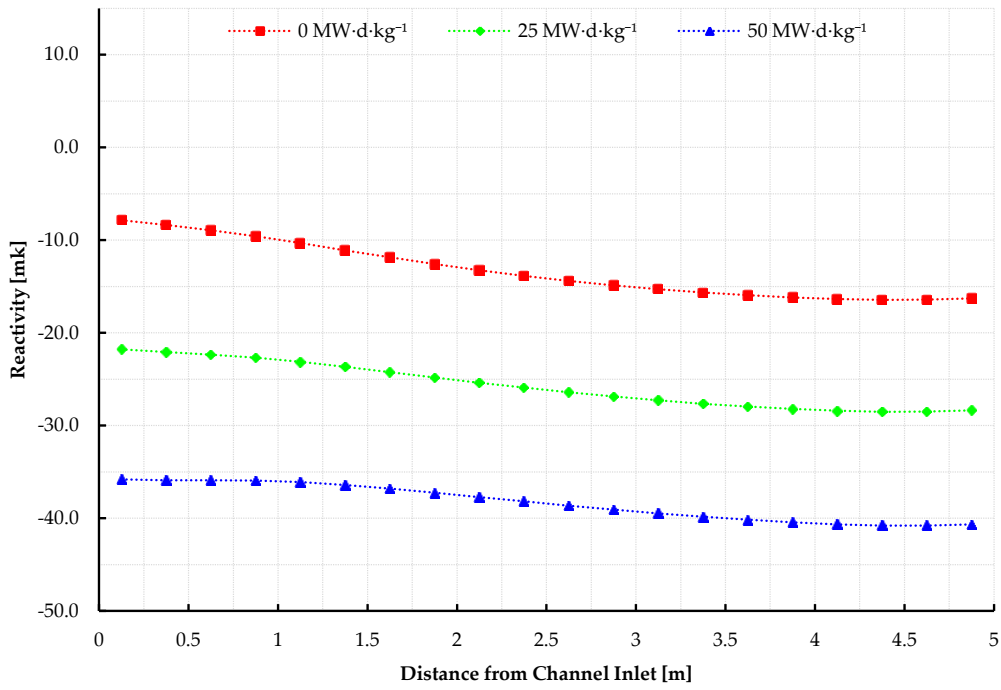
Figure 5.3: Total coolant void reactivity
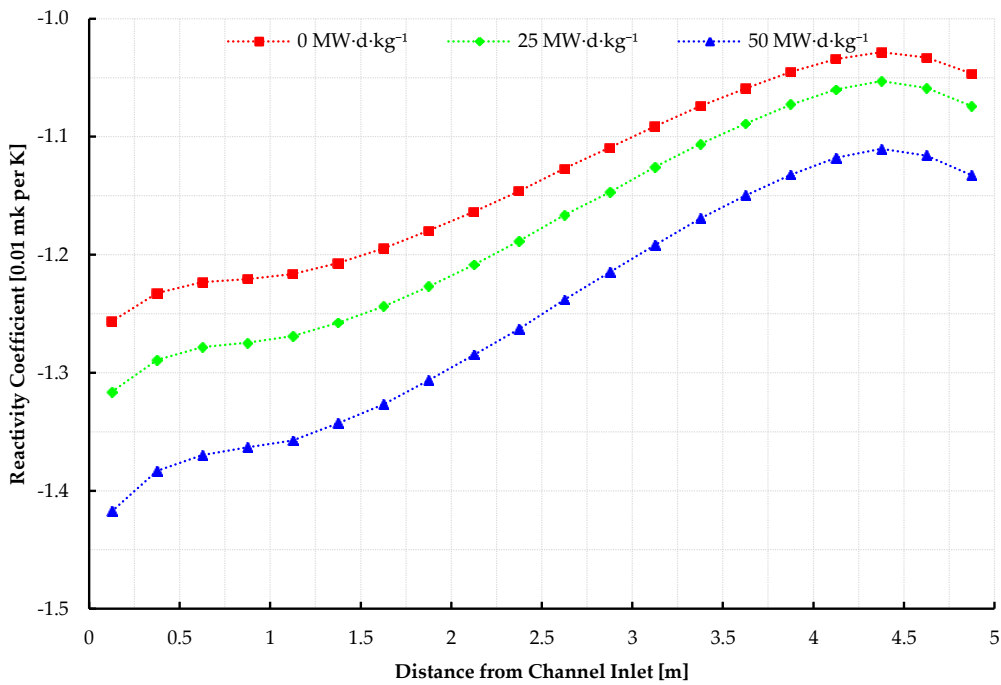
Figure 5.4: Fuel temperature reactivity coefficient
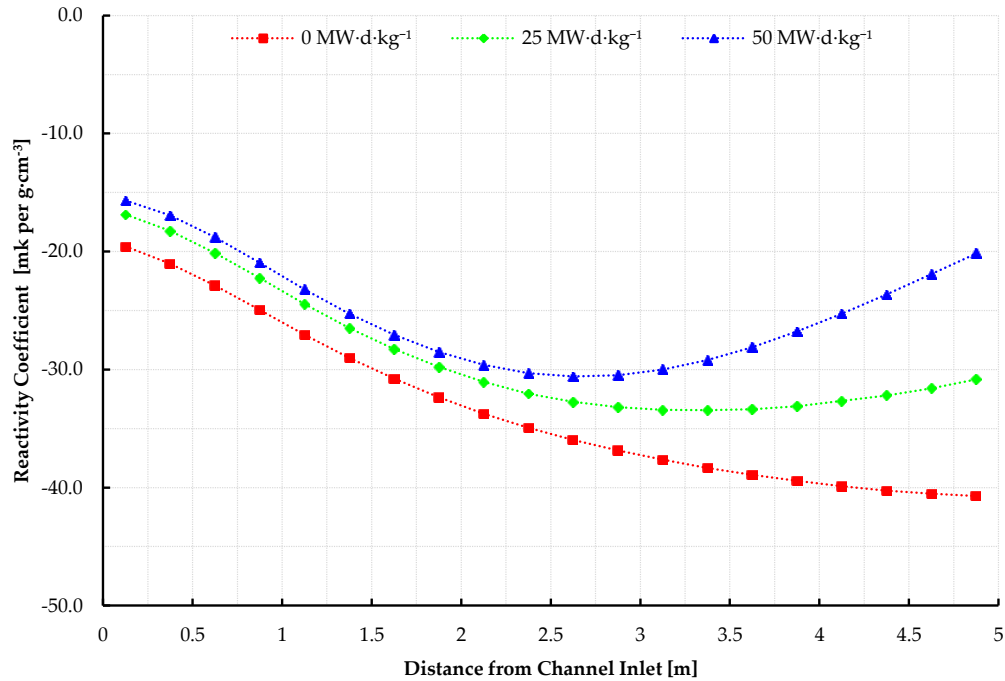
Figure 5.5: Coolant density reactivity coefficient in fuel region

Conversely, reducing the coolant density in the centre flow tube is consistently a very large *negative* reactivity effect which dominates when both regions are voided at the same time. The coolant in the flow tube must therefore be contributing significantly to the neutron moderation within the lattice cell. It's worth noting that the total CVR very nearly matches the linear sum of the separate fuel region and flow tube CVR values. Higher order effects on the flux solution from voiding both regions (as opposed to one or the other) are evidently minimal. This partially validates the implementation of the feedback database wherein each coolant region's feedback was calculated entirely separate with no higher-order cross-terms.

The positive void reactivity in the outer/fuel region raises the possibility of a positive power excursion in cases of flow stagnation or reversal (where low density fluid re-enters the channel from the outlet plenum). Such transients are necessarily self-limiting since under homogeneous or equilibrium conditions the centre flow tube density will eventually equilibrate causing a large negative reactivity insertion. Some of these postulated transients are studied in more detail in 5.3.2.

Another observation from the lattice data is that the reactivity values are consistently decreasing with burnup, including the fuel temperature coefficient (note that only the fuel region CVR is reducing in magnitude, the others are becoming *more negative*). A likely explanation is the depletion of ^{239}Pu and the diminishing effect of its low-energy fission resonance (around 0.3 eV). Based on the initial fuel composition in Table 4.1, the dominant fissile isotope by a significant margin should be ^{239}Pu (in fresh fuel the only other fissile isotope would be the small concentration of ^{241}Pu). Removing this resonance through depletion would affect both the FTC (since less fissions are being caused by absorptions in the Doppler-broadened resonance) and the CVR (since fewer thermal neutrons are being upscattered in to the fission resonance in the presence of coolant). This is counter to the behaviour of water-cooled reactors that are initially fueled with enriched or natural uranium, where the accumulation of ^{239}Pu through neutron capture makes the FTC and CVR behave the opposite with increasing burnup [70]. These explanations are, however, merely theories based on integral properties (i.e. reactivity) of lattice cells. Further investigation of isotope-specific reaction rates in PT-SCWR fuel would definitively find the cause of these observed trends, and are recommended for future work.

5.2 Core-Level Coupled Steady-State Results

Examination of the steady-state core-level simulation results serves two important purposes. First, the steady-state results necessarily form the initial conditions used to initialize transients and are thus extremely relevant to the transient results (e.g. the consequences of a LOCA towards fuel integrity are directly affected by the initial fuel temperature). Second, the steady-state core power and thermalhydraulic parameters can be used to provide assurance that the DONJON and CATHENA models are descriptive of the PT-SCWR concept by comparing the results to those available in literature.

Core-level studies on the PT-SCWR concept have typically focussed on the Beginning-of-Cycle (BOC) and End-of-Cycle (EOC) core states, and so these states were included in this study as well. Neither of these discrete states is truly representative of the "typical" core over the length of the cycle, however (with the BOC state being an especially poor representation of the average core power distribution) [107]. This work will therefore include an additional Middle-of-Cycle (MOC) core state for analysis. Control system proposals for the PT-SCWR

are considering active and passive systems that minimize the channel power deviation from the MOC state, so examination of MOC is considered most representative of the typical core [109].

Figure 5.6 through Figure 5.9 show the steady-state channel power and flow distributions for the selected core states, with additional core properties summarized in Table 5.1. There are several caveats when interpreting these results.

First, the channel power distribution is largely determined by the fuel burnup distribution and the imposed refuelling scheme. Although the channel power and flow distributions are self-consistent for the discrete states shown (determined using the iterative process described in Section 4.1.2.2), recall that history effects were not considered in the core-level burnup calculation. The effect of the local thermalhydraulic conditions on isotopic depletion was considered solely within the two-dimensional lattice calculations at constant power (the large axial property variation necessitating the simulation of multiple positions along the length of the channel). The feedback database only contains information for instantaneous perturbations from the reference conditions.

Second, since the channel flows in the CATHENA model are matched to the channel powers via the action of the inlet orifice controllers, discrepancies between the presented results and those available in literature can be largely attributed to the power distribution rather than the CATHENA model itself.
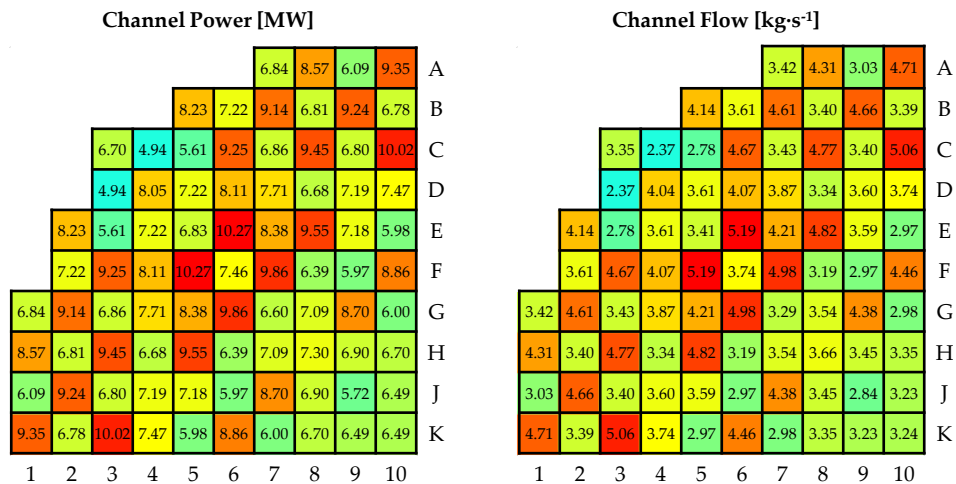
Figure 5.6: BOC core power and flow distribution

Channel Power [MW]

	1	2	3	4	5	6	7	8	9	10	
							6.55	7.76	5.66	8.20	A
					7.72	6.96	8.49	6.48	8.46	6.38	B
			6.52	5.01	5.64	8.75	6.70	8.86	6.61	9.26	C
			5.01	7.91	7.35	8.07	7.75	6.70	7.41	7.65	D
		7.72	5.64	7.35	6.76	9.62	8.25	9.25	7.52	6.30	E
		6.96	8.75	8.07	9.62	7.21	9.42	6.58	6.32	9.00	F
	6.55	8.49	6.70	7.75	8.25	9.42	6.79	7.66	9.15	6.65	G
	7.76	6.48	8.86	6.70	9.25	6.58	7.66	8.28	8.01	7.98	H
	5.66	8.46	6.61	7.41	7.52	6.32	9.15	8.01	6.93	8.07	J
	8.20	6.38	9.26	7.65	6.30	9.00	6.65	7.98	8.07	8.23	K

Channel Flow [kg·s⁻¹]

	1	2	3	4	5	6	7	8	9	10	
							3.27	3.90	2.81	4.12	A
					3.88	3.48	4.27	3.23	4.26	3.18	B
			3.25	2.44	2.80	4.41	3.35	4.46	3.30	4.67	C
			2.47	3.97	3.68	4.05	3.89	3.35	3.71	3.84	D
		3.88	2.80	3.68	3.38	4.86	4.15	4.66	3.77	3.14	E
		3.48	4.41	4.05	4.86	3.61	4.75	3.28	3.15	4.54	F
	3.27	4.27	3.35	3.89	4.15	4.75	3.39	3.84	4.61	3.32	G
	3.90	3.23	4.46	3.35	4.66	3.28	3.84	4.16	4.02	4.01	H
	2.81	4.26	3.30	3.71	3.77	3.15	4.61	4.02	3.46	4.05	J
	4.12	3.18	4.67	3.84	3.14	4.54	3.32	4.01	4.05	4.14	K

Figure 5.7: MOC core power and flow distribution

Channel Power [MW]

	1	2	3	4	5	6	7	8	9	10	
							6.64	7.86	5.70	8.20	A
					7.93	7.01	8.63	6.54	8.59	6.40	B
			6.94	5.24	5.81	8.86	6.71	8.93	6.61	9.27	C
			5.24	8.24	7.48	8.03	7.70	6.66	7.44	7.66	D
		7.93	5.81	7.48	6.71	9.45	8.06	9.16	7.52	6.30	E
		7.01	8.86	8.03	9.45	6.98	9.23	6.47	6.26	9.00	F
	6.64	8.63	6.71	7.70	8.06	9.23	6.64	7.55	9.07	6.57	G
	7.86	6.54	8.93	6.66	9.16	6.47	7.55	8.16	7.89	7.88	H
	5.70	8.59	6.61	7.44	7.52	6.26	9.07	7.89	6.81	7.94	J
	8.20	6.40	9.27	7.66	6.30	9.00	6.57	7.88	7.94	8.06	K

Channel Flow [kg·s⁻¹]

	1	2	3	4	5	6	7	8	9	10	
							3.31	3.95	2.83	4.12	A
					3.98	3.51	4.34	3.26	4.32	3.19	B
			3.47	2.62	2.89	4.46	3.35	4.50	3.30	4.67	C
			2.64	4.14	3.75	4.03	3.86	3.33	3.73	3.84	D
		3.98	2.89	3.75	3.35	4.77	4.05	4.62	3.77	3.14	E
		3.51	4.46	4.03	4.77	3.49	4.65	3.23	3.12	4.53	F
	3.31	4.34	3.35	3.86	4.05	4.65	3.31	3.79	4.57	3.28	G
	3.95	3.26	4.50	3.33	4.62	3.23	3.79	4.10	3.96	3.96	H
	2.83	4.32	3.30	3.73	3.77	3.12	4.57	3.96	3.40	3.99	J
	4.12	3.19	4.67	3.84	3.14	4.53	3.28	3.96	3.99	4.05	K

Figure 5.8: EOC core power and flow distribution

Recall that the core fuel loading scheme also has one-eighth symmetry along the diagonal. This means that in the steady-state core each channel on one side of the diagonal should have an exact duplicate in power and flow on the opposite side. This is indeed the case with the highest power channels (E6/F5) and lowest power channels (C4/D3). Since this symmetry was not defined explicitly in the computational models, one channel in a mirrored pair may possess slightly higher power and flow than the other within the convergence criteria of the numerical solutions.
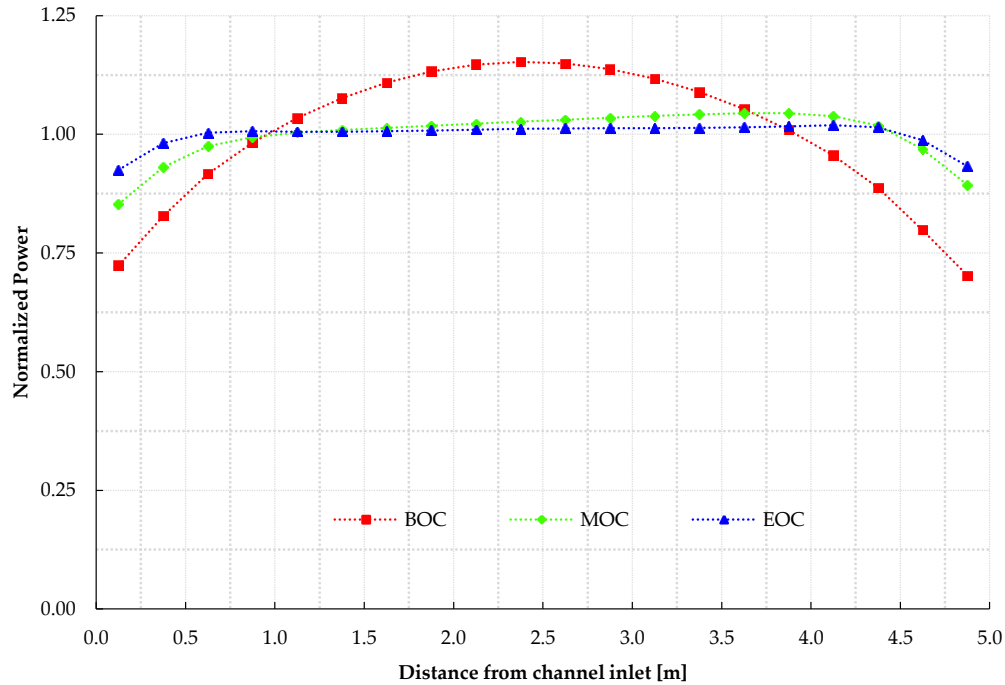
Figure 5.9: Average steady-state axial power profiles

Table 5.1: Steady-state core summary

	BOC (0 FPD)	MOC (224 FPD)	EOC (447 FPD)
Total Core Power [MW]	2540	2540	2540
Maximum Channel Power [MW]	10.27 (E6)	9.62 (F5)	9.45 (E6)
Minimum Channel Power [MW]	4.94 (D3)	5.01 (D3)	5.24 (C4)
Core Excess Reactivity [mk]	116.01	59.91	9.80
Avg. Discharge Burnup [MW·d·kg^{-1}]	-	-	63.401
Total Core Flow [kg·s^{-1}]	1,272.75	1,273.59	1,273.96
Maximum Channel Flow [kg·s^{-1}]	5.19 (E6)	4.86 (F5)	4.77 (E6)
Minimum Channel Flow [kg·s^{-1}]	2.37 (D3)	2.44 (C4)	2.62 (C4)
Peak Cladding Temperature [°C]	746.66 (D3)	773.72 (J10)	776.18 (J10)
Peak Fuel Centreline Temperature [°C]	2,657.56 (E6)	2,491.55 (F5)	2,433.39 (E6)

The calculated channel power distribution is qualitatively similar to simulation results presented by Pencer et al. (average channel power discrepancy 8.82% at

BOC and 3.06% at EOC) [93]. Since the channel power distribution is largely determined by the fuel burnup distribution, this is strong evidence that the geometry and batch refuelling sequence were correctly implemented in the DONJON model. The locations of the maximum and minimum channel powers are similar in both models, but the results presented by Pencer et al. show slightly lower peak channel powers (9.90 MW at BOC, 9.22 MW at EOC) [93]. The trends in the average axial power distribution are also similar.

The DONJON results also exceed those presented by Pencer et al. for the initial core excess reactivity (108 mk), cycle length (425 FPD), and average discharge burnup (58.6 MW·d·kg^{-1}), although these parameters are obviously closely related [93]. Both results are much higher than the target discharge burnup of ≈40 MW·d·kg^{-1}. According to Pencer and Colton, the progression of the conceptual fuel design has introduced significantly more moderator to the lattice cell, raising the fissile content utilization [11]. Given the requirements for SCWR materials exposed to high neutron fluxes, future changes to the SCWR neutronics design are likely in order to return to the target value.

There are some discrepancies between the DONJON model results and those presented by Pencer et al. The intent of this work was to model the core concept as accurately as possible with the chosen tools, so the core models may possess several fundamental differences, including (but not limited to):

- source of nuclear data / cross-section library;
- treatment of the reflector in lattice models;
- the number of axial positions modelled in the lattice and core-level models;
- the number of energy groups used in the diffusion calculation;
- the computer codes themselves.

Demonstrating that the core model developed for this work produces results that qualitatively and quantitatively resemble other simulation results presented in literature demonstrate that the model and initial conditions are valid representations of the PT-SCWR concept for performing transient analysis. While some parameters may differ by several per cent, the differences are within those expected given the higher fidelity simulations performed here.

The CATHENA results presented by Wang and Wang serve as a similar point of comparison for the core thermalhydraulics model, although the previously discussed caveat of the channel power-flow matching must be recognized [100]. Wang and Wang used a similar approach to match the channel power to flow in using a variable inlet orifice and the channel outlet temperature as the controlled parameter, but their model only contained five channels with maximum and minimum powers of 9.975 MW and 7.144 MW respectively. Their model also included heat transfer between the wall separating the inlet and outlet plena, so their channel outlet temperature set point was 652 °C in order to achieve 625 °C at the turbine inlet [100]. Wang and Wang report a total core flow of 1,254 kg·s^{-1}, highest power channel flow of 4.98 kg·s^{-1}, maximum cladding temperature of 806 °C, and maximum fuel centreline temperature of 2,389 °C [100]. For channels at comparable powers (e.g. J5 at MOC almost exactly matches Wang and Wang's "average channel" of 7.52 MW) the flow rates are systematically 1.62% higher in the present model, which is expected given the 8.94% lower dictated temperature increase in the channel (i.e. 275 °C as opposed to 302 °C). This can be considered reasonably close agreement.

Given the strict control imposed on the channel temperature and density distributions by the outlet temperature set point, and the evidence in Figure 5.6 through Figure 5.8 that the channel flow distribution exactly matches the channel power distribution, the CATHENA model created for this work can be considered to be working as intended. The same logic as used for the neutronics model can thus be applied: the CATHENA thermalhydraulics model is a valid representation of the PT-SCWR concept and is suitable for transient analysis.

5.3   Core-Level Coupled Transient Results

The coupled transient test results have been separated in to two sections for presentation in this thesis: the study of coupled instability/oscillations, and flow-induced coupled transients meant to parametrically examine progression of postulated accident scenarios.

To ensure that the core model was truly in a steady state prior to each transient, the coupled system was simulated for 100 s with the boundary conditions held at their reference values (as shown in Figure 5.10). These first 100 s are truncated

from the presented results for brevity, and most transients will appear to begin at 5 s in the figures.
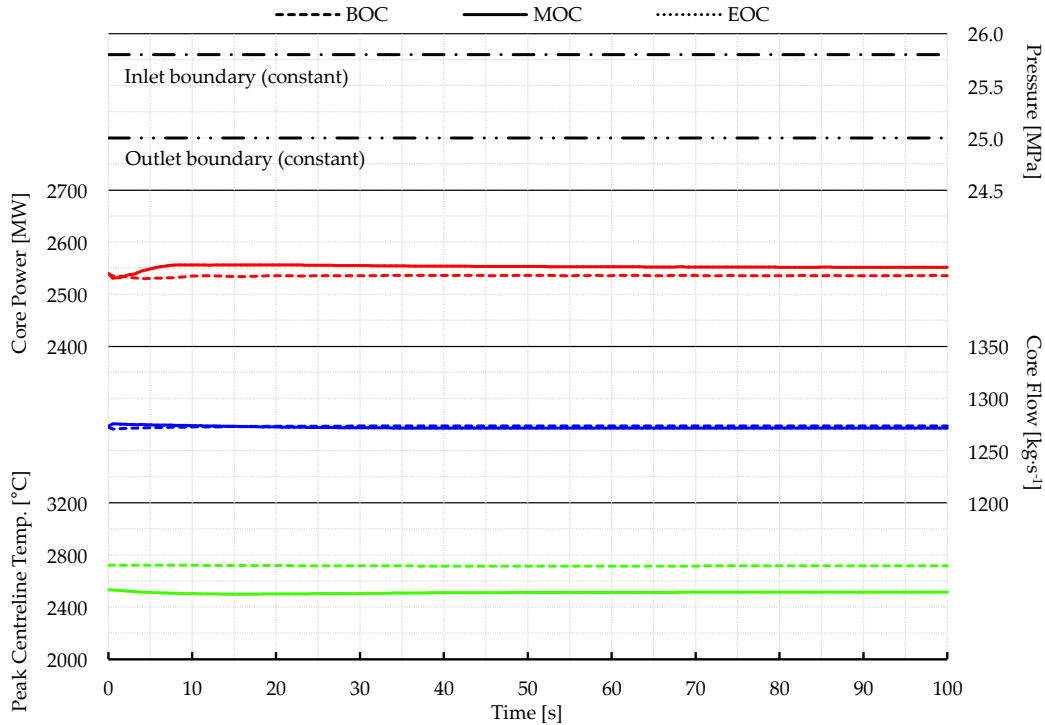
Figure 5.10: Null transient at each initial core state

In these initial core states DONJON determined the mean neutron generation time Λ (the average time between neutron emission and capture resulting in fission) to be $\Lambda_{BOC} = 2.21\times10^{-4}$, $\Lambda_{MOC} = 2.22\times10^{-4}$, and $\Lambda_{EOC} = 2.33\times10^{-4}$.

There is a significant amount of data generated for each time step in a simulation. For example, each of the 1,680 nodes in the core model has a unique flux/power, coolant density and temperature, fuel temperature, centre tube fluid density and temperature, and so on. It would be impractical to plot all of these parameters for even a single transient. Most of the presented results are thus integral parameters for the whole core (e.g. total core power, total core flow, peak fuel centreline temperature, etc.) or averaged by axial plane. Three channels have been isolated for cases where planar averaging may obfuscate relevant spatial distributions. These are:

- C4, a third cycle channel at the edge of the core and the lowest power channel in each core state;
- E6, a first cycle channel in the core interior and the highest power channel in each core state;
- G8, a second cycle channel near the centre of the core that is close to the average channel power in each core state.

These three channels, combined with the average distributions, are meant to provide a comprehensive description of the core while keeping the amount of plotted data practical. Plots of axial distributions are given for specific instants during a transient and contain the normalized power and the largest thermalhydraulic feedbacks: (average) fuel temperature, coolant density in the fuel region, and coolant density within the flow tube.

5.3.1   Coupled Stability Investigation

Time domain stability analyses of BWRs have typically relied on perturbations to the reactor operating conditions to initiate oscillations [24, 55, 56]. In full-core coupled neutronics-thermalhydraulics models, these perturbations can be implemented through the movement of control devices or by changes to the model boundary conditions [24, 55]. Since the current PT-SCWR model does not contain the former, this study relies on the latter. Specifically, tests on the coupled stability of the PT-SCWR were initiated by changing the core inlet pressure, inlet temperature, and outlet pressure as functions of time in the coupled model.

The tests performed through variation of these boundary conditions can be generally categorized as one of two types. In the first, a parameter is briefly perturbed and then returned to its reference value. This tests the transient response of the coupled system and its inherent stability (i.e. will the system return to its original operating condition, attain a new quasi-stable operating condition, or begin oscillating with some growth or decay rate). In the second test category, oscillations are *imposed* on the coupled system by controlling a boundary condition with a sinusoidal time function. This also tests the stability of the system (e.g. will the power variation amplitude grow or remain stable) and its inherent damping characteristics. The following two sub-sections describe the

various transient tests and results. Overall analysis on the PT-SCWR coupled stability is contained within Section 5.3.1.3.

5.3.1.1 Temporary Perturbations to Operating Conditions

Figure 5.11 shows the coupled transient initiated by a sudden drop and recovery in the core inlet pressure at the MOC core state. In this test the inlet pressure was decreased by 400 kPa in 2.5 s, and then returned to the initial value of 25.8 MPa in the following 2.5 s. The sudden decrease in the imposed pressure drop results in a flow transient which, as indicated in the figure, is accompanied by an increase in core power that peaks at approximately 130% (3,330 MW) of the nominal value.

The axial distributions presented in Figure 5.12 shows how the decrease in core flow results in a decrease in the average coolant density in the fuel region. The density in the flow tube essentially remains constant. Based on the lattice results in Section 5.1, this is a positive reactivity insertion that creates the aforementioned power excursion. The flow recovery brings more high density coolant in to the fuel region, which has the opposite (negative) reactivity effect and the power reduces quickly.

The fuel temperature transient is shown to lag behind the power transient, likely due to the combined effects of the fuel heat capacity, thermal conductivity and convective heat transfer to the coolant (i.e. the "thermal inertia" of the system). The delayed peak fuel temperature is likely responsible for the slight "overshoot" of the total core power below the initial steady-state value. Approximately 7.0 s after initiating the transient the fuel temperature decreases and the system returns to the original steady-state conditions.

Figure 5.13 through Figure 5.15 show the axial distribution in the selected channels during the transient, and the quarter-core channel power distribution is shown in Figure 5.17. Each channel is shown to exhibit similar behaviour and no substantive changes in the quarter-core channel power distribution (i.e. the radial power shape) are observable. Since each channel's initial flow was scaled to its initial power by the variable sizing of the inlet orifices, and a significant fraction of the total pressure drop occurs at these orifices (as mentioned in 4.2.1.1) it's not surprising that each channel would behave similarly in a flow induced transient and the initial relative power shape would remain constant throughout.
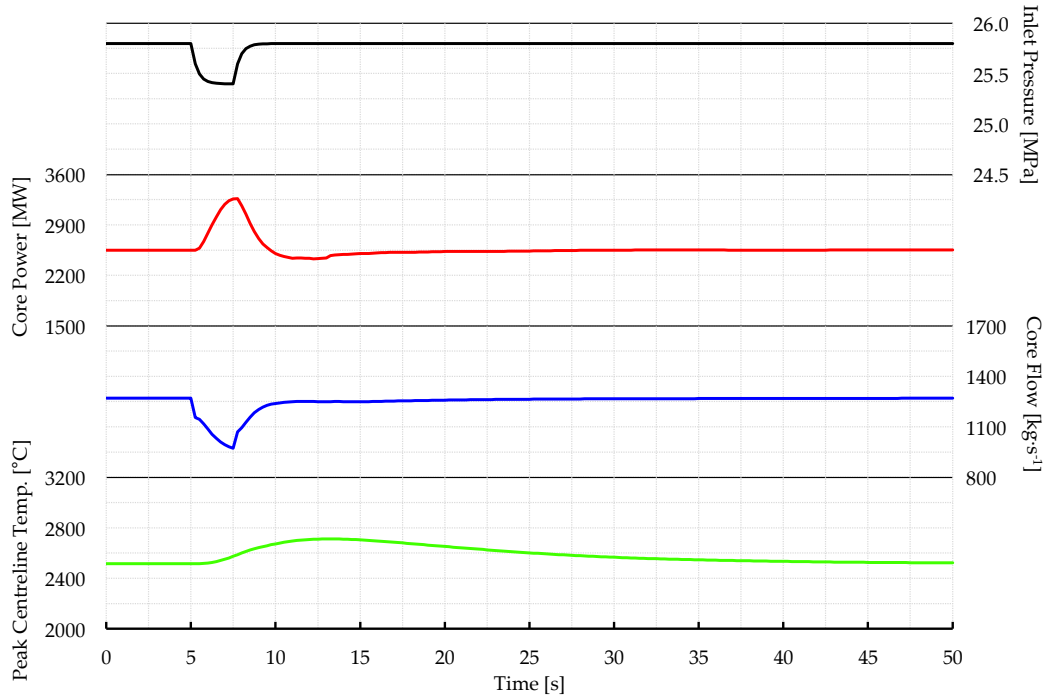
Figure 5.11: Inlet pressure perturbation transient at MOC
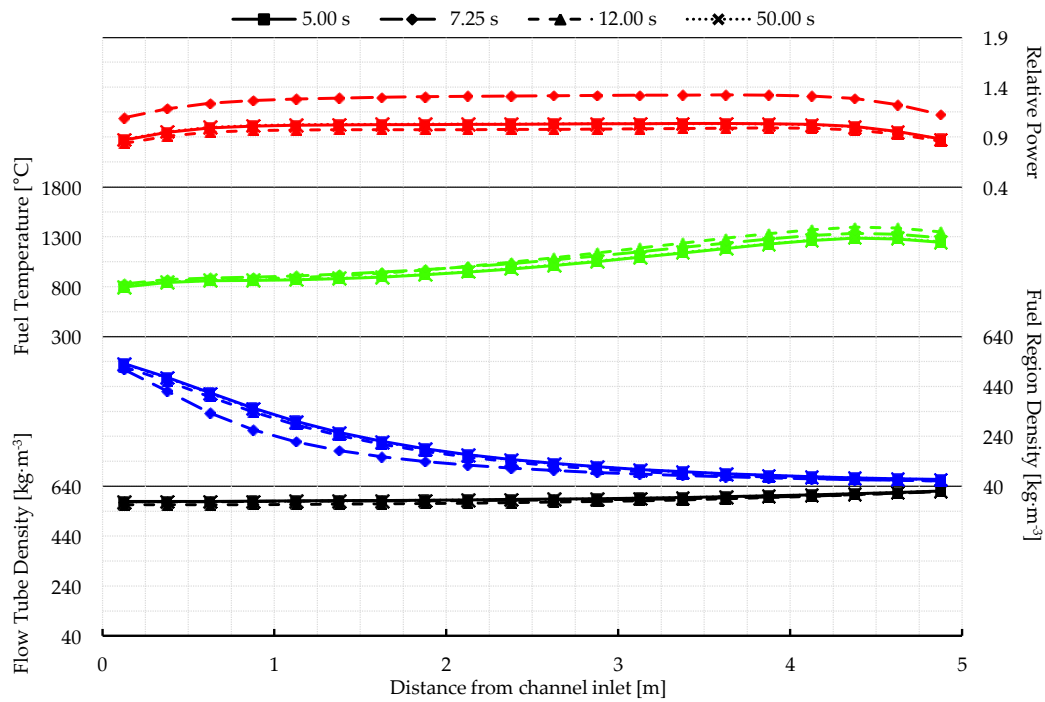
Figure 5.12: Average axial profiles in inlet pressure transient at MOC
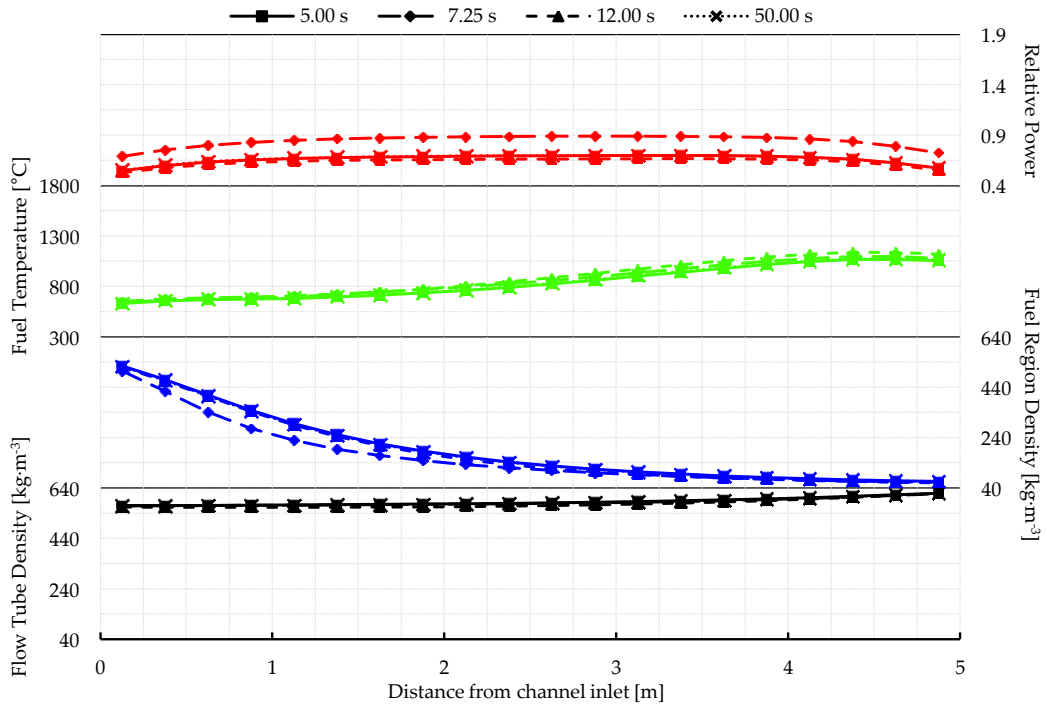
Figure 5.13: Axial profile in C4 during inlet pressure transient
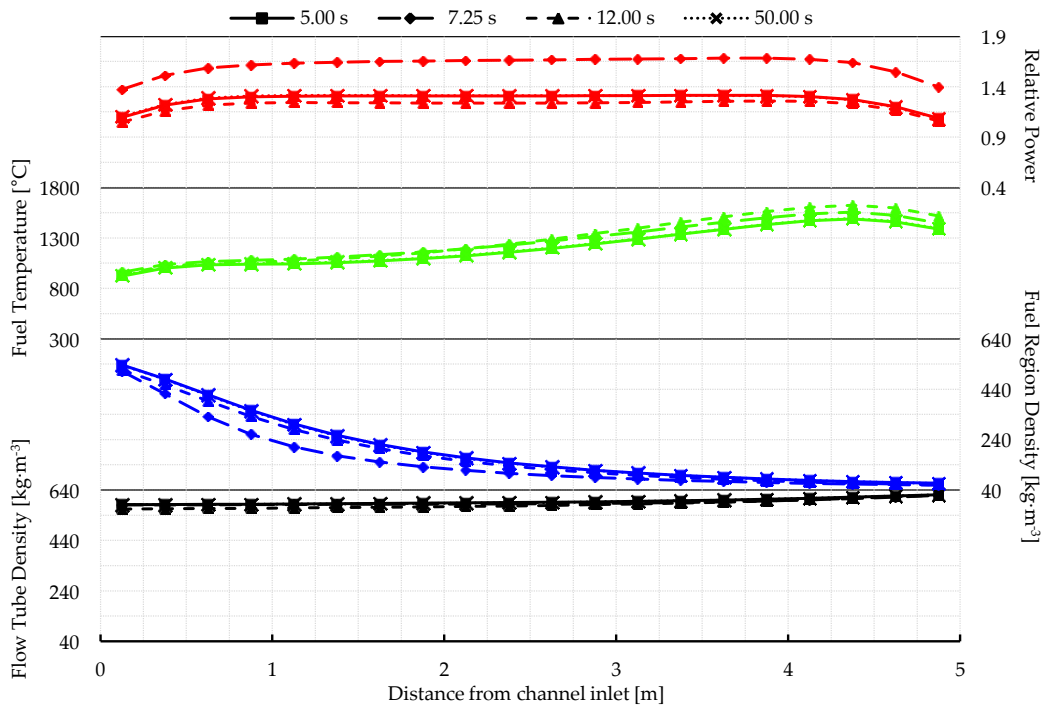
Figure 5.14: Axial profile in E6 during inlet pressure transient
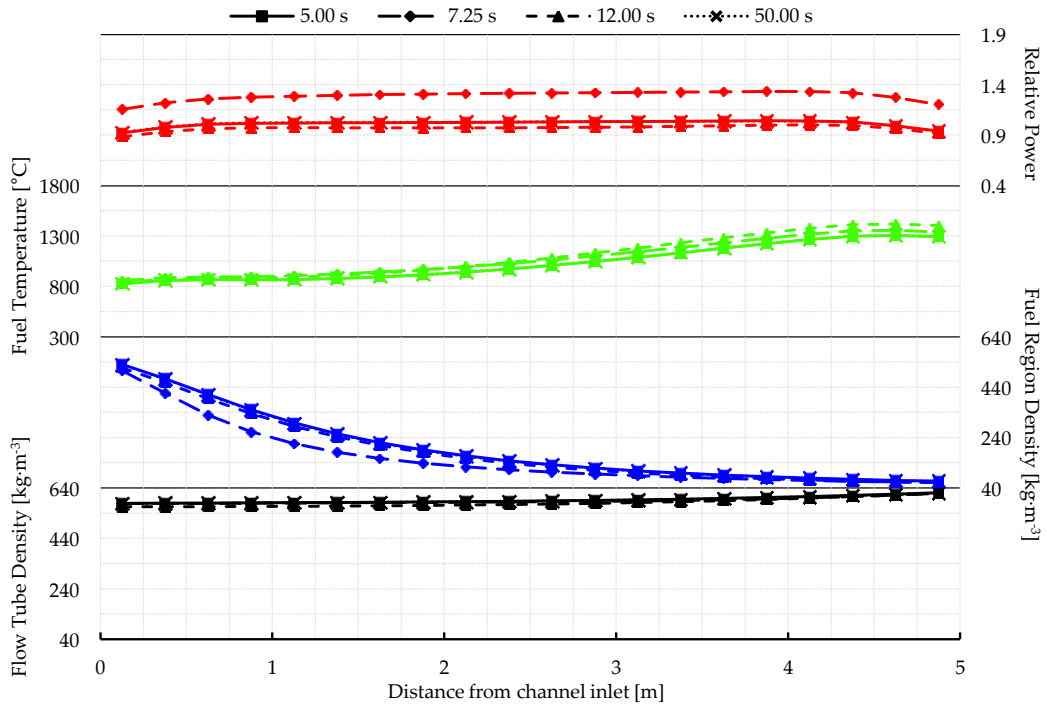
Figure 5.15: Axial profile in G8 during inlet pressure transient
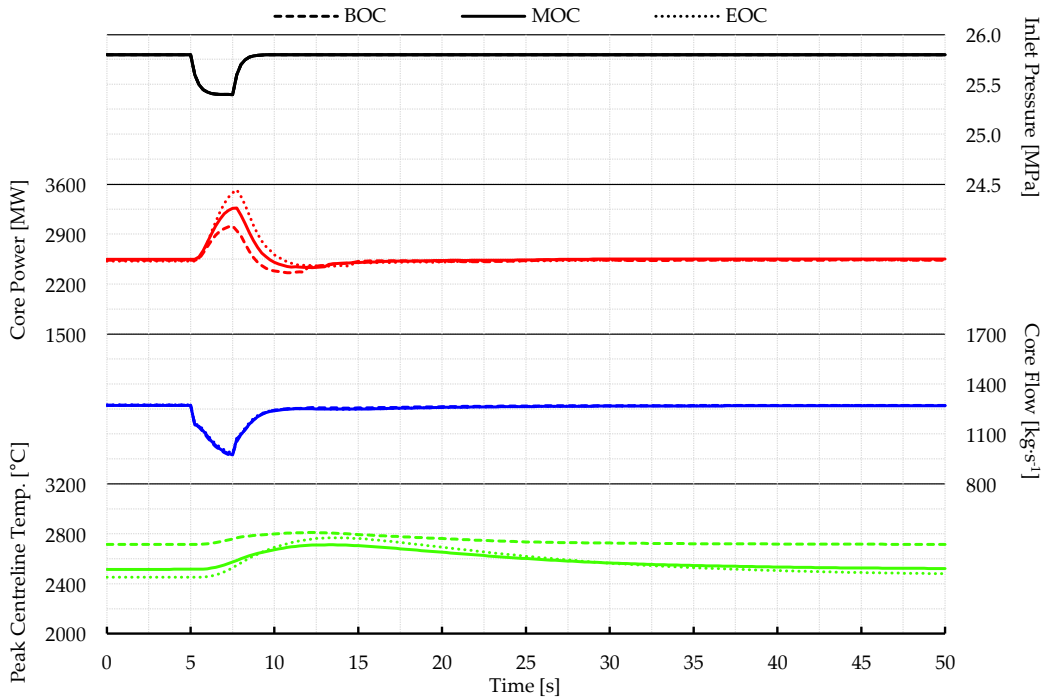
Figure 5.16: Inlet pressure perturbation transient at BOC, MOC, and EOC

Channel powers at 5.00 s [MW]

	1	2	3	4	5	6	7	8	9	10	
A						6.58	7.80	5.68	8.23		A
B					7.76	6.99	8.53	6.51	8.50	6.41	B
C			6.55	5.03	5.67	8.79	6.73	8.90	6.64	9.31	C
D			5.03	7.94	7.38	8.10	7.79	6.73	7.44	7.68	D
E		7.76	5.67	7.38	6.79	9.66	8.29	9.29	7.55	6.33	E
F		6.99	8.79	8.10	9.66	7.24	9.46	6.61	6.34	9.04	F
G	6.58	8.53	6.73	7.79	8.29	9.46	6.82	7.69	9.19	6.68	G
H	7.80	6.51	8.90	6.73	9.29	6.61	7.69	8.32	8.04	8.01	H
J	5.68	8.50	6.64	7.44	7.55	6.34	9.19	8.04	6.96	8.10	J
K	8.23	6.41	9.31	7.68	6.33	9.04	6.68	8.01	8.10	8.26	K

Channel powers at 7.25 s [MW]

	1	2	3	4	5	6	7	8	9	10	
A						8.35	9.88	7.21	10.43		A
B					9.84	8.87	10.80	8.26	10.77	8.13	B
C			8.30	6.39	7.19	11.13	8.54	11.28	8.43	11.79	C
D			6.39	10.06	9.36	10.27	9.88	8.55	9.45	9.75	D
E		9.84	7.19	9.36	8.62	12.24	10.51	11.78	9.59	8.04	E
F		8.87	11.13	10.27	12.24	9.19	11.99	8.40	8.07	11.48	F
G	8.35	10.80	8.54	9.88	10.51	11.99	8.67	9.78	11.67	8.49	G
H	9.88	8.26	11.28	8.55	11.78	8.40	9.78	10.57	10.23	10.19	H
J	7.21	10.77	8.43	9.45	9.59	8.07	11.67	10.23	8.86	10.31	J
K	10.43	8.13	11.79	9.75	8.04	11.48	8.49	10.19	10.31	10.51	K

Channel powers at 12.00 s [MW]

	1	2	3	4	5	6	7	8	9	10	
A						6.31	7.46	5.45	7.88		A
B					7.43	6.70	8.15	6.24	8.13	6.14	B
C			6.28	4.82	5.43	8.40	6.44	8.50	6.36	8.88	C
D			4.82	7.60	7.06	7.74	7.44	6.44	7.12	7.34	D
E		7.43	5.43	7.06	6.50	9.21	7.91	8.86	7.22	6.05	E
F		6.70	8.40	7.74	9.21	6.92	9.02	6.32	6.07	8.63	F
G	6.31	8.15	6.44	7.44	7.91	9.02	6.52	7.35	8.77	6.38	G
H	7.46	6.24	8.50	6.44	8.86	6.32	7.35	7.94	7.68	7.65	H
J	5.45	8.13	6.36	7.12	7.22	6.07	8.77	7.68	6.65	7.73	J
K	7.88	6.14	8.88	7.34	6.05	8.63	6.38	7.65	7.73	7.89	K

Channel powers at 50.00 s [MW]

	1	2	3	4	5	6	7	8	9	10	
A						6.60	7.81	5.69	8.25		A
B					7.78	7.01	8.54	6.53	8.52	6.42	B
C			6.56	5.04	5.68	8.81	6.74	8.92	6.65	9.32	C
D			5.04	7.96	7.40	8.12	7.80	6.74	7.45	7.70	D
E		7.78	5.68	7.40	6.80	9.67	8.30	9.30	7.56	6.33	E
F		7.01	8.81	8.12	9.67	7.25	9.47	6.62	6.35	9.06	F
G	6.60	8.54	6.74	7.80	8.30	9.47	6.83	7.70	9.20	6.68	G
H	7.81	6.53	8.92	6.74	9.30	6.62	7.70	8.33	8.05	8.02	H
J	5.69	8.52	6.65	7.45	7.56	6.35	9.20	8.05	6.96	8.11	J
K	8.25	6.42	9.32	7.70	6.33	9.06	6.68	8.02	8.11	8.27	K

Figure 5.17: Channel powers during the inlet pressure perturbation transient

Figure 5.16 shows a comparison of the same transient executed at the BOC and EOC core states. The average axial profiles for the BOC and EOC cases are shown in Figure 5.18 and Figure 5.19 respectively (recall that the MOC profiles were in Figure 5.12). The flow transient is identical in each case, but relative to the MOC power pulse the peak power at BOC is lower and at EOC it is higher (no differences in the channel power distribution were observed in either the BOC or EOC transients, so these plots were omitted for brevity). The integrated relationships between burnup, power, feedbacks, and initial conditions, evidently result in amplified thermalhydraulic feedback later during a batch cycle.
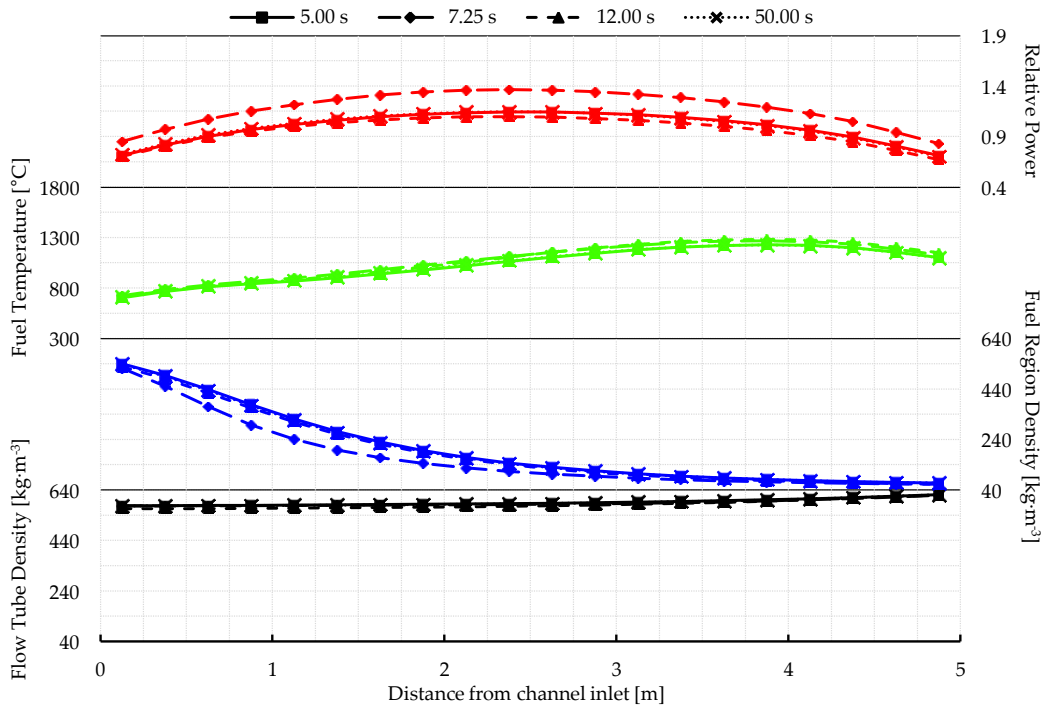
Figure 5.18: Average axial profiles in inlet pressure transient at BOC
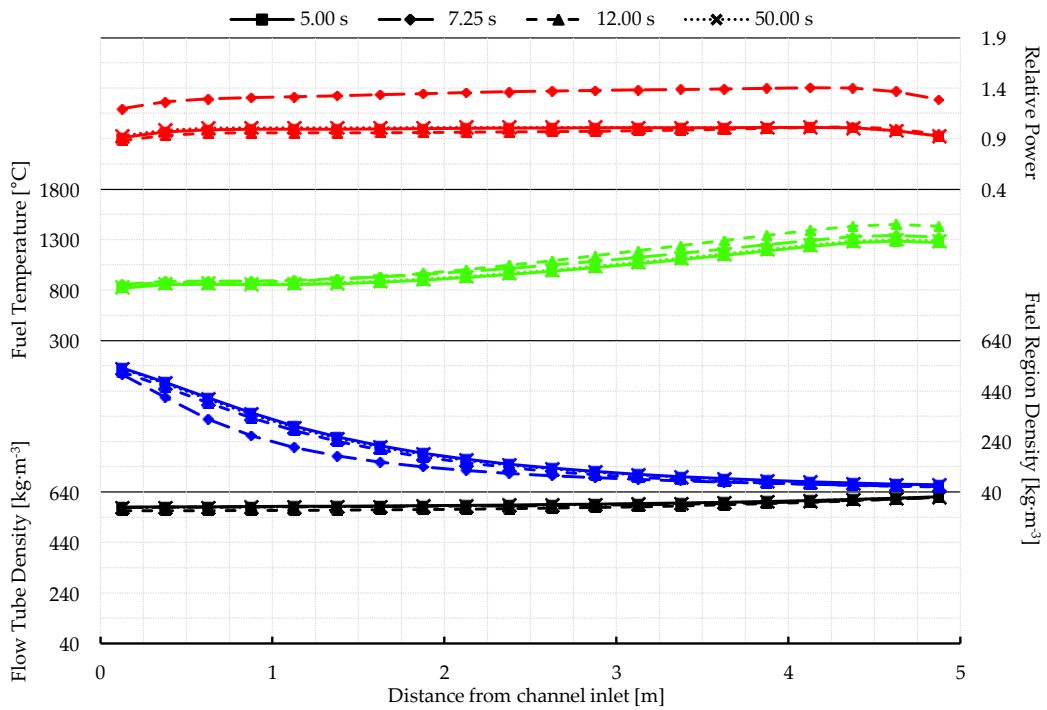
Figure 5.19: Average axial profiles in inlet pressure transient at EOC

This result is somewhat counter-intuitive considering that the lattice-level calculations show decreasing reactivity worths at higher burnups. In the core-level coupled model, however, where neither the local power or thermalhydraulic conditions are specified (but rather calculated), there are several potential contributors to this behaviour:

1. The refuelling scheme was primarily devised to limit the peak channel power, which typically occurs in fresh or low-burnup fuel immediately after a refuelling operation (i.e. BOC) [37]. The imposed channel age distribution thus suppresses flux/power in fresh and low-burnup assemblies at BOC. As fuel depletes over the course of a cycle the power redistributes from the "older" to "younger" fuel and by EOC more power is being generated in these relatively "younger" channels (the evolution of the channel power distribution is evident in Figure 5.6 through Figure 5.8). The lattice-level results show that the magnitude of the fuel region coolant density reactivity feedback is larger for low-burnup fuel, so the relative redistribution of flux toward lower burnup fuel makes the core-wide coolant density reactivity feedback larger towards the end of a cycle.

2. The average axial power profile in the core is centre-peaked at BOC but significantly flatter at EOC (Figure 5.9). As a consequence the relative power and flux near the channel outlet at EOC is much higher. Figure 5.5 shows that the coolant density reactivity coefficient is largest near the outlet. Similar to the above case, the relative redistribution of flux in to this region will correspondingly increase the core-integrated reactivity worth.

3. The peak fuel temperatures are significantly lower later during the cycle (Figure 5.16). The increased Doppler-broadening of capture resonances near BOC may have the net effect of making the core less reactive in response to coolant density changes.

Ultimately all three effects (and potentially others not listed) may be contributing to the observed behaviour. Their relative impact could be established by analysis of isotope-specific reaction rates and lattice-level sensitivities. Since such a detailed investigation of lattice-level effects was outside the scope of this study, this is recommended for future work.

Figure 5.20 shows a similar coupled transient at MOC except the 400 kPa pressure decrease is imposed on the core outlet. The transient is thus mirrored: the total core flow briefly *increases* which results in a power *drop* to approximately 80% of full power (2,050 MW).

Most of the same underlying phenomena as in the inlet pressure transient are observed, except the feedback is in the opposite direction. Figure 5.21 shows the increased core flow bringing more high density coolant in to the fuel region. This negative reactivity insertion causes a decrease in power. When the flow recovers the density decreases and the positive reactivity causes the power to rebound upwards. The fuel temperature transient again lags the power transient, so the power "overshoots" above the initial power before eventually settling to the steady-state conditions. Figure 5.22 through Figure 5.25 show no substantive changes to the channel power distribution. Figure 5.26 shows how the same power transient is magnified when performed later in the batch cycle (i.e. BOC is less severe than MOC, which is less severe than EOC).
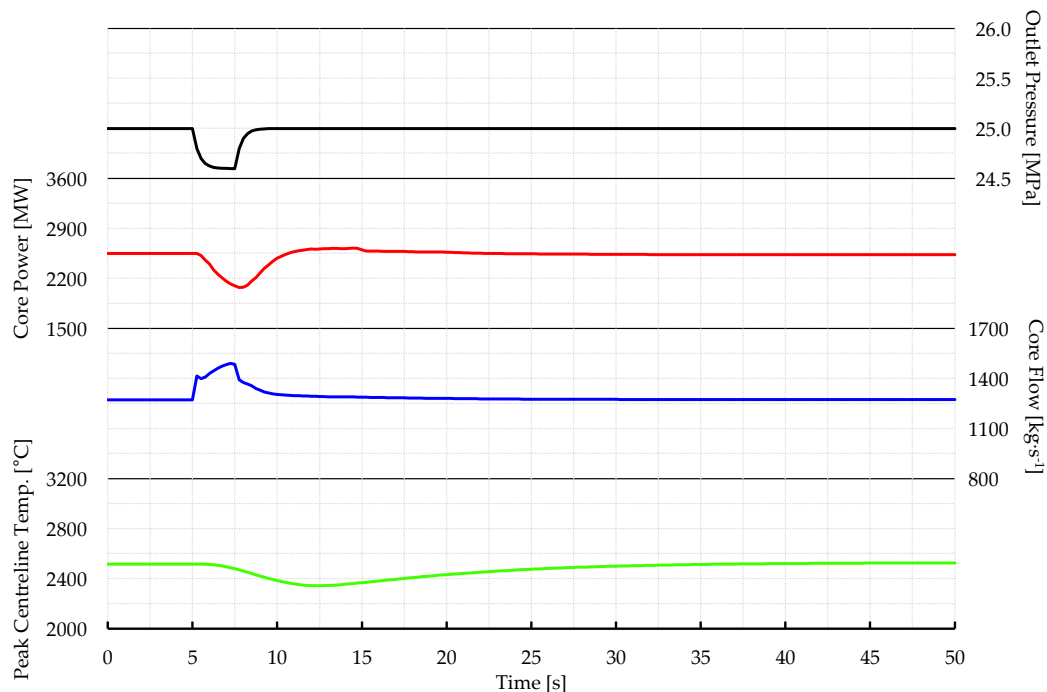
Figure 5.20: Outlet pressure perturbation transient at MOC
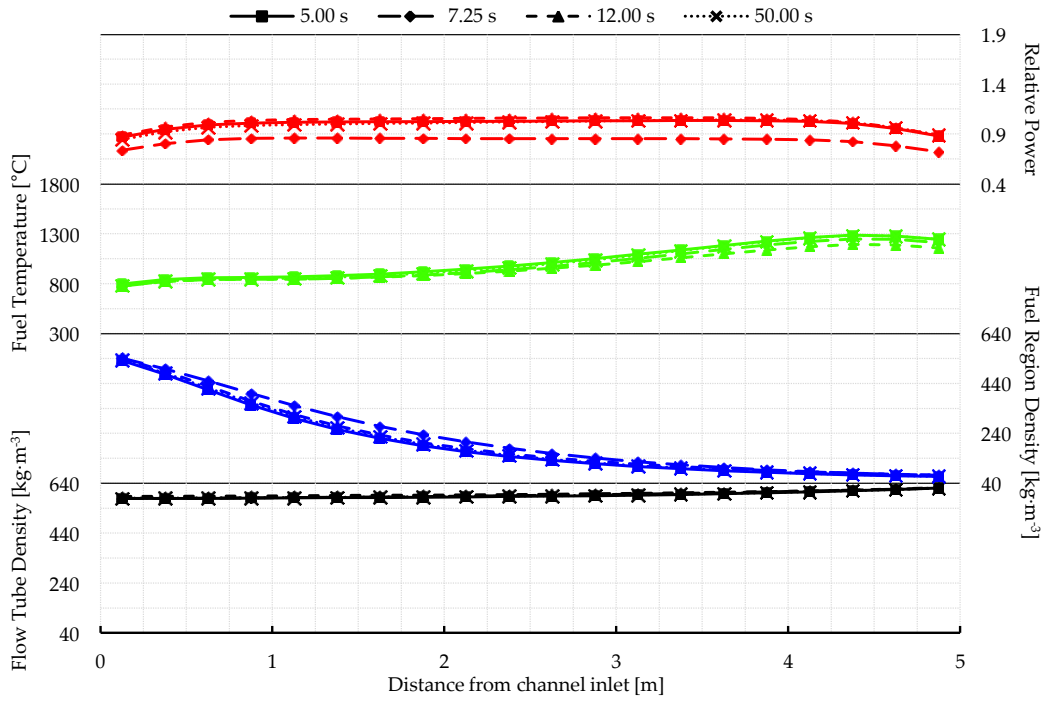
Figure 5.21: Average axial profiles in outlet pressure transient at MOC
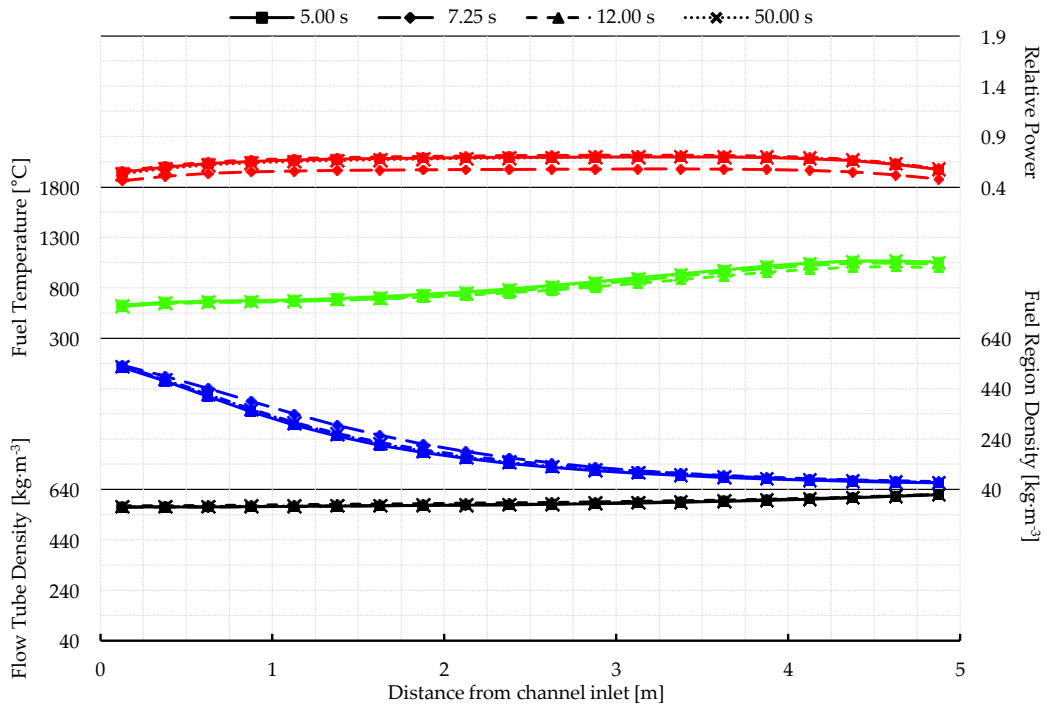
Figure 5.22: Axial profiles in C4 during outlet pressure transient
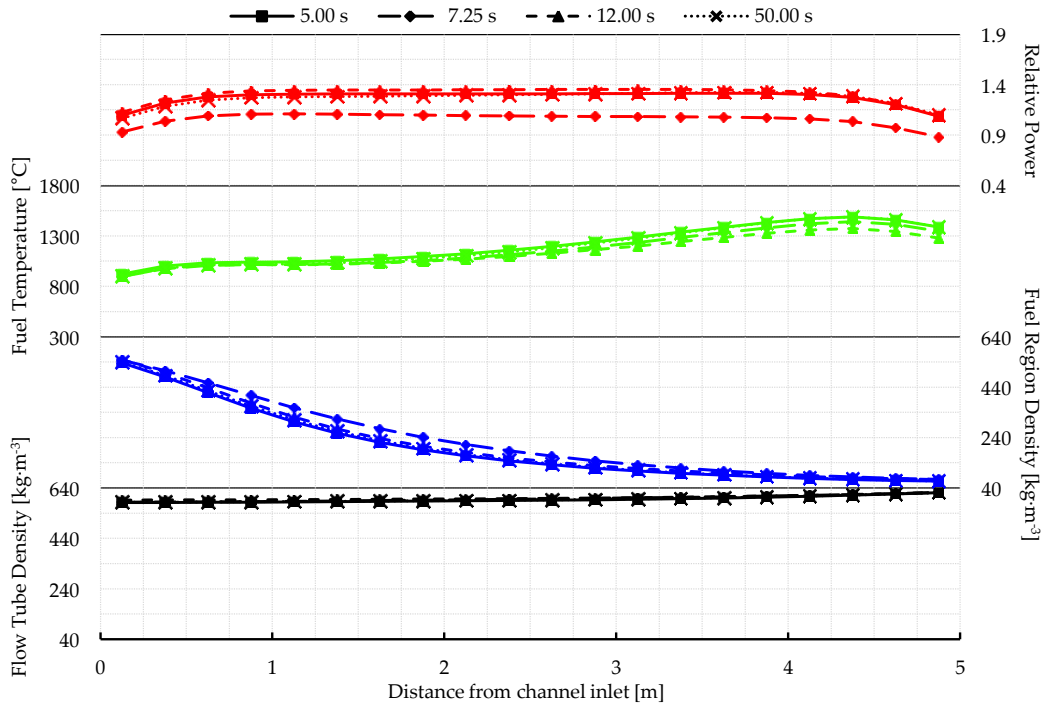
Figure 5.23: Axial profiles in E6 during outlet pressure transient
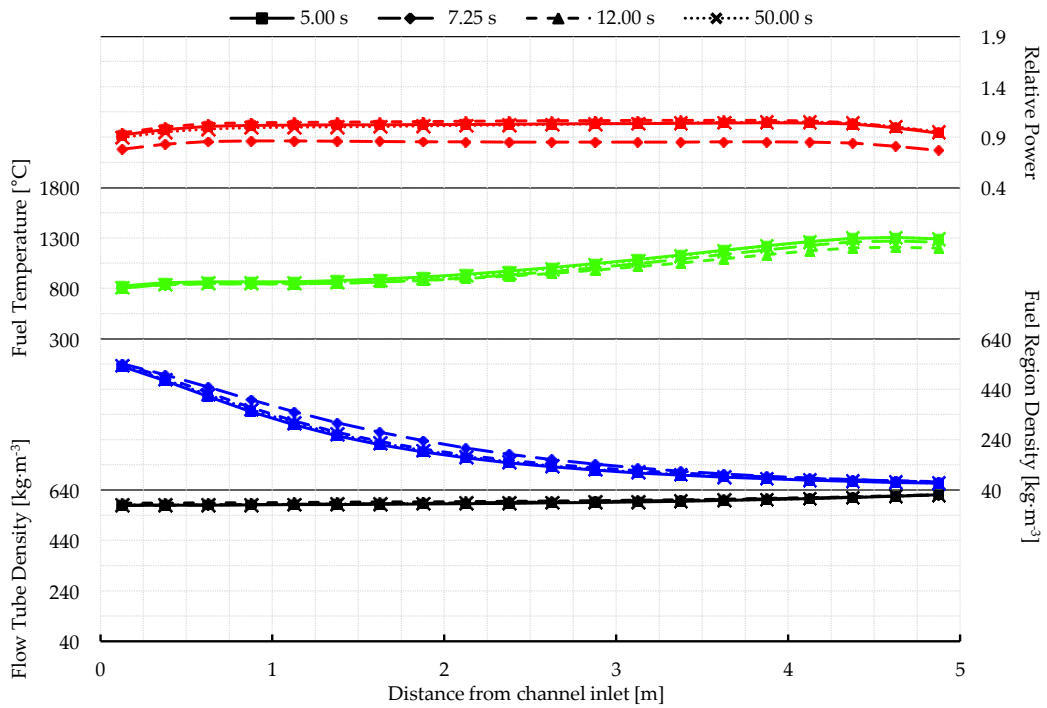
Figure 5.24: Axial profiles in G8 during outlet pressure transient

Channel powers at 5.00 s [MW]

	1	2	3	4	5	6	7	8	9	10	
A					6.58	7.80	5.68	8.23			A
B			7.76	6.99	8.53	6.51	8.50	6.41			B
C		6.55	5.03	5.67	8.79	6.73	8.90	6.64	9.31		C
D		5.03	7.94	7.38	8.10	7.79	6.73	7.44	7.68		D
E	7.76	5.67	7.38	6.79	9.66	8.29	9.29	7.55	6.33		E
F	6.99	8.79	8.10	9.66	7.24	9.46	6.61	6.34	9.04		F
G	6.58	8.53	6.73	7.79	8.29	9.46	6.82	7.69	9.19	6.68	G
H	7.80	6.51	8.90	6.73	9.29	6.61	7.69	8.32	8.04	8.01	H
J	5.68	8.50	6.64	7.44	7.55	6.34	9.19	8.04	6.96	8.10	J
K	8.23	6.41	9.31	7.68	6.33	9.04	6.68	8.01	8.10	8.26	K

Channel powers at 7.25 s [MW]

	1	2	3	4	5	6	7	8	9	10	
A					5.49	6.51	4.74	6.87			A
B			6.47	5.83	7.11	5.43	7.09	5.34			B
C		5.46	4.19	4.72	7.33	5.61	7.42	5.53	7.75		C
D		4.19	6.62	6.15	6.75	6.48	5.60	6.19	6.39		D
E	6.47	4.72	6.15	5.65	8.04	6.90	7.73	6.28	5.26		E
F	5.83	7.33	6.75	8.04	6.02	7.87	5.49	5.27	7.52		F
G	5.49	7.11	5.61	6.48	6.89	7.87	5.67	6.39	7.64	5.54	G
H	6.51	5.43	7.42	5.60	7.73	5.49	6.39	6.91	6.68	6.65	H
J	4.74	7.09	5.53	6.19	6.28	5.27	7.64	6.68	5.77	6.72	J
K	6.87	5.34	7.75	6.39	5.26	7.52	5.54	6.65	6.72	6.86	K

Channel powers at 12.00 s [MW]

	1	2	3	4	5	6	7	8	9	10	
A					6.73	7.98	5.81	8.43			A
B			7.94	7.16	8.73	6.66	8.71	6.56			B
C		6.69	5.14	5.79	9.00	6.89	9.12	6.80	9.54		C
D		5.14	8.13	7.56	8.30	7.97	6.89	7.62	7.87		D
E	7.94	5.79	7.56	6.95	9.90	8.49	9.52	7.73	6.47		E
F	7.16	9.00	8.30	9.90	7.41	9.69	6.76	6.49	9.27		F
G	6.73	8.73	6.89	7.97	8.49	9.69	6.98	7.88	9.42	6.83	G
H	7.98	6.66	9.12	6.89	9.52	6.76	7.88	8.52	8.24	8.21	H
J	5.81	8.71	6.80	7.62	7.73	6.49	9.42	8.24	7.12	8.30	J
K	8.43	6.56	9.54	7.87	6.47	9.27	6.83	8.21	8.30	8.46	K

Channel powers at 50.00 s [MW]

	1	2	3	4	5	6	7	8	9	10	
A					6.53	7.74	5.64	8.17			A
B			7.70	6.94	8.47	6.47	8.44	6.36			B
C		6.50	4.99	5.62	8.73	6.68	8.84	6.59	9.24		C
D		4.99	7.88	7.33	8.05	7.73	6.69	7.39	7.63		D
E	7.70	5.62	7.33	6.74	9.59	8.23	9.22	7.50	6.28		E
F	6.94	8.73	8.05	9.59	7.19	9.39	6.56	6.30	8.98		F
G	6.53	8.47	6.68	7.73	8.23	9.39	6.77	7.64	9.13	6.63	G
H	7.74	6.47	8.84	6.69	9.22	6.56	7.64	8.26	7.99	7.96	H
J	5.64	8.44	6.59	7.39	7.50	6.30	9.13	7.99	6.91	8.04	J
K	8.17	6.36	9.24	7.63	6.28	8.98	6.63	7.96	8.04	8.20	K

Figure 5.25: Channel powers during the outlet pressure transient

Figure 5.27 shows a power transient initiated by a step reduction in the core inlet temperature (from 350.0 °C to 347.5 °C) executed at each of the three core states. At 300 s the inlet temperature was stepped back up to the reference value. With the inlet pressure remaining constant, the small temperature reduction must be accompanied by a modest increase in coolant density. The lattice-level results indicate that increasing coolant density in the flow tube has a positive reactivity effect, and in the fuel region the effect is negative. The figure shows that in this transient the net effect is a gradual power decrease. The total core flow increases slightly as a result of the power decrease under the constraint of constant pressure drop, which bring more high density fluid in to the fuel region and further negative reactivity feedback.
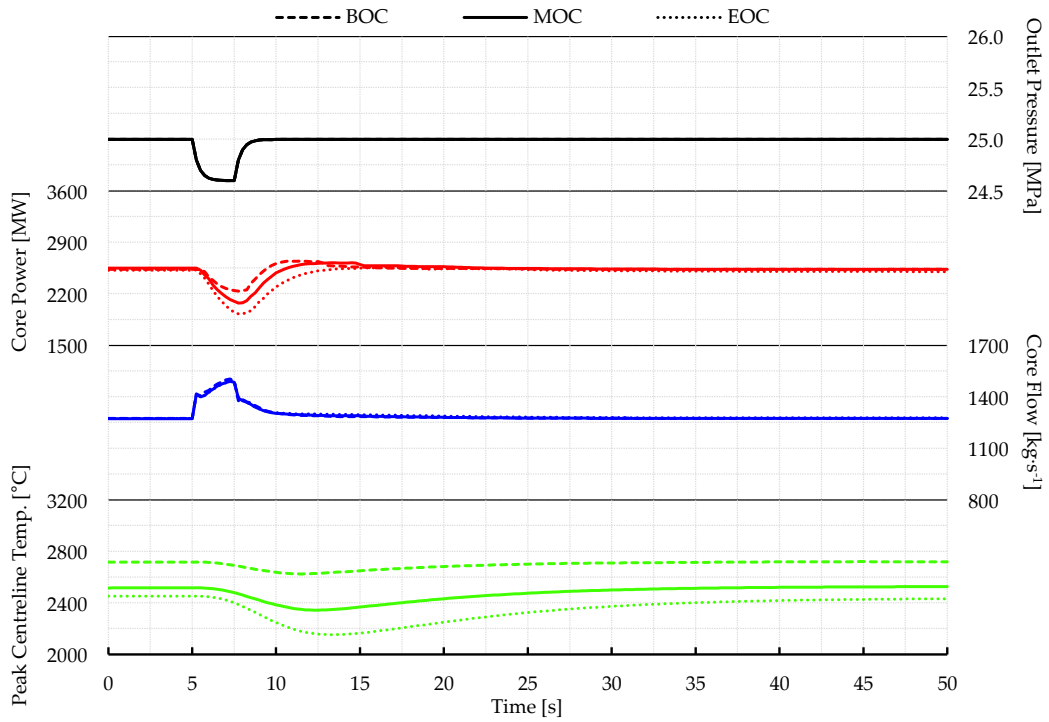
Figure 5.26: Outlet pressure perturbation transient at BOC, MOC, and EOC
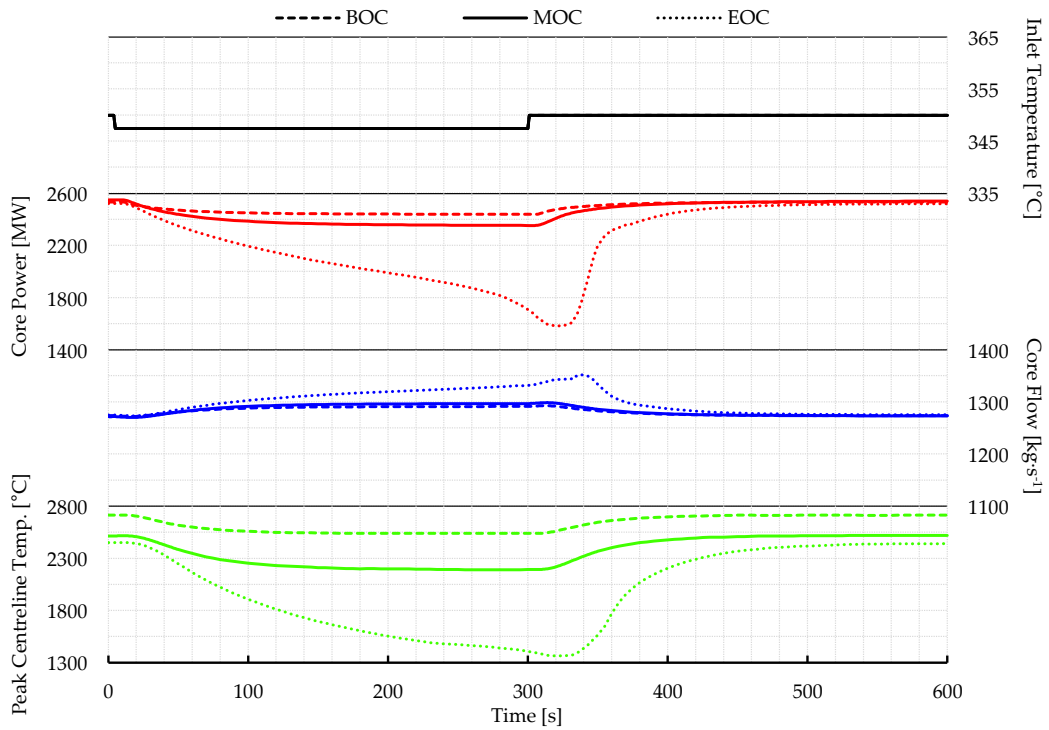
Figure 5.27: Inlet temperature step down transient at BOC, MOC, and EOC
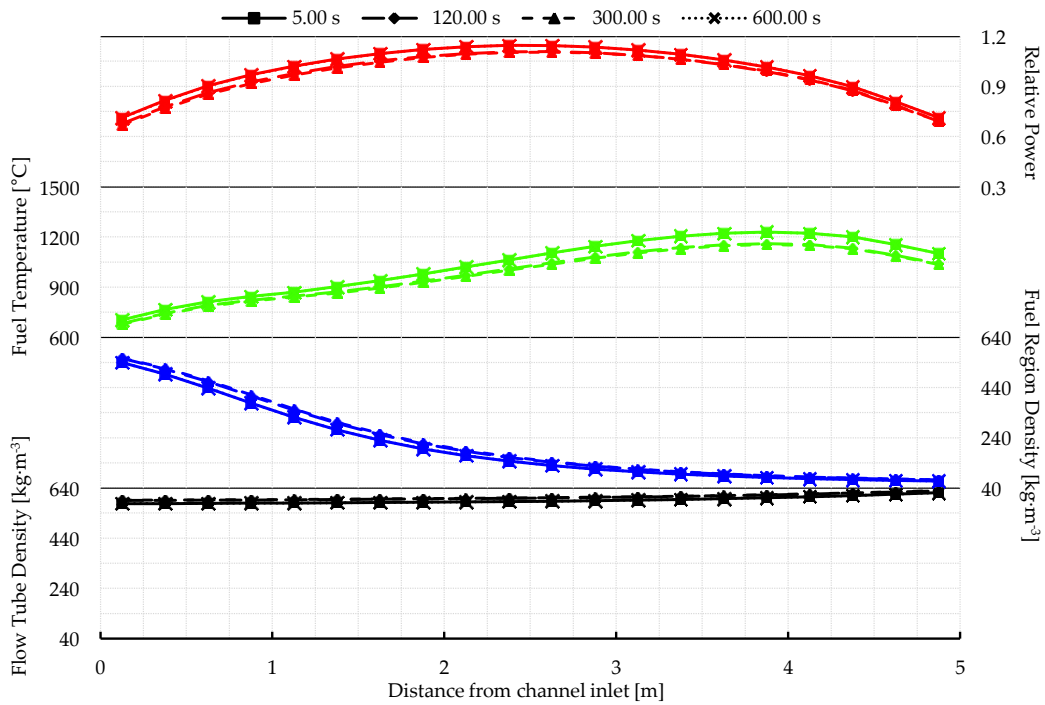
Figure 5.28: Average axial profiles during temperature step down at BOC
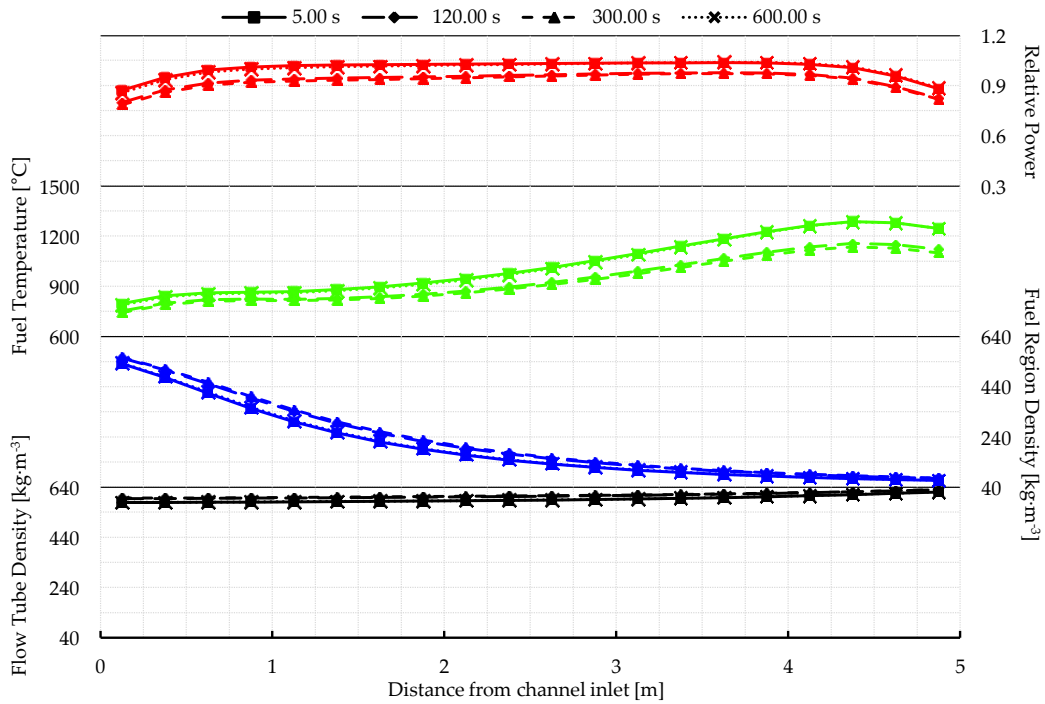
Figure 5.29: Average axial profiles during temperature step down at MOC
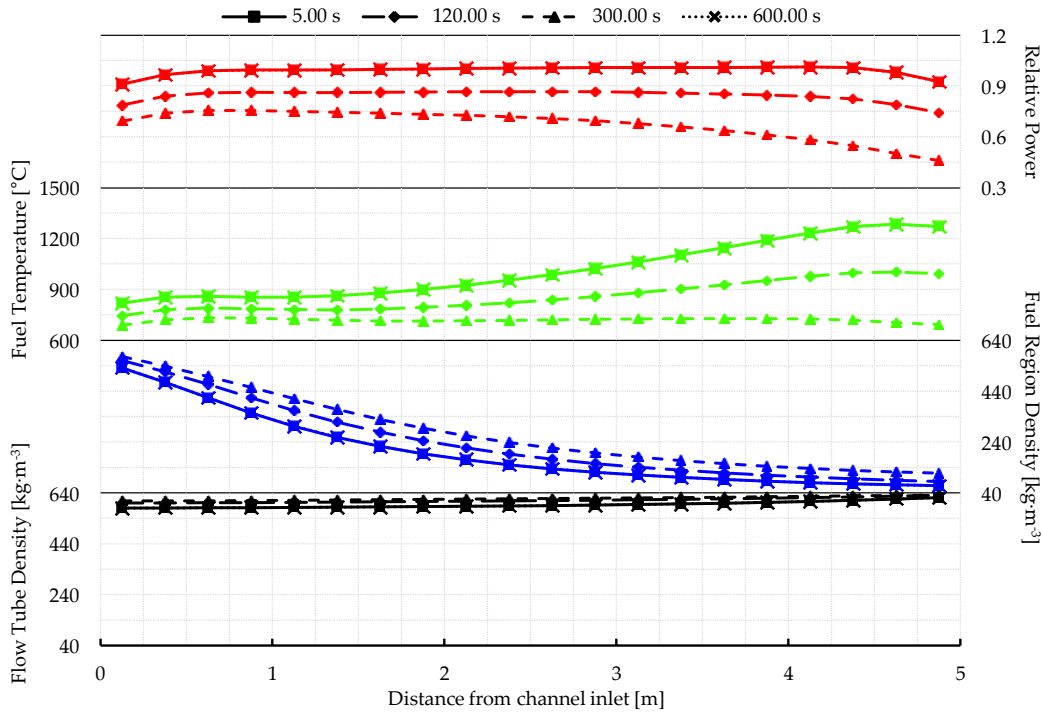
Figure 5.30: Average axial profiles during temperature step down at EOC

For both the BOC and MOC core states the reactor power eventually reaches equilibrium at a new steady value (≈2,440 MW / 96% full power in the case of the former, ≈2,350 MW / 92% full power in the case of the latter). At EOC, however, the greater negative reactivity feedbacks cascade (i.e. lower temperatures result in higher densities, which leads to lower powers and even lower temperatures) and the core power has an accelerating downward trajectory. Evidently the fuel temperature decrease does not provide enough positive reactivity to compensate for the cascading negative effects. The power transient is arrested when the inlet temperature returns to the reference value and the core begins to return to the initial steady-state conditions. Without increasing the inlet temperature the reactor would likely have shut down from the negative reactivity feedbacks.

Figure 5.28 through Figure 5.30 show the average axial distribution for each core state during the transient. The BOC and MOC figures show the new steady operating conditions corresponding to the new steady inlet temperature. The EOC figure shows the progression of the negative feedback cascade. The local power is shown to decrease faster near the outlet of the core at EOC, likely a result of the greater coolant density feedbacks near the outlet.

Figure 5.31 shows a similar transient initiated by an equally sized step *increase* in the core inlet temperature (from 350.0 °C to 352.5 °C). Again, at 300 s the inlet temperature was stepped back to the reference value. The progression of the transient is the exact opposite as in Figure 5.27. The small temperature increase results in a modest decrease in coolant density. A coolant density decrease in the flow tube has a negative reactivity effect and in the fuel region a positive reactivity effect. The net result in this case is gradual power *increase* accompanied by a corresponding decrease in the total flow under the constraint of constant pressure drop.

Unlike the temperature step down transient, however, there is no reactivity feedback cascade at EOC and at each initial core state the reactor reaches a new equilibrium condition. The new steady axial profiles are evident in Figure 5.32 through Figure 5.34. The initial coolant density change near the outlet (where the feedback is largest) at EOC (Figure 5.34) caused by the temperature step up is clearly much smaller than when the temperature was stepped down (Figure 5.30), which is likely a key contributor to why there is no positive reactivity cascade in this case.
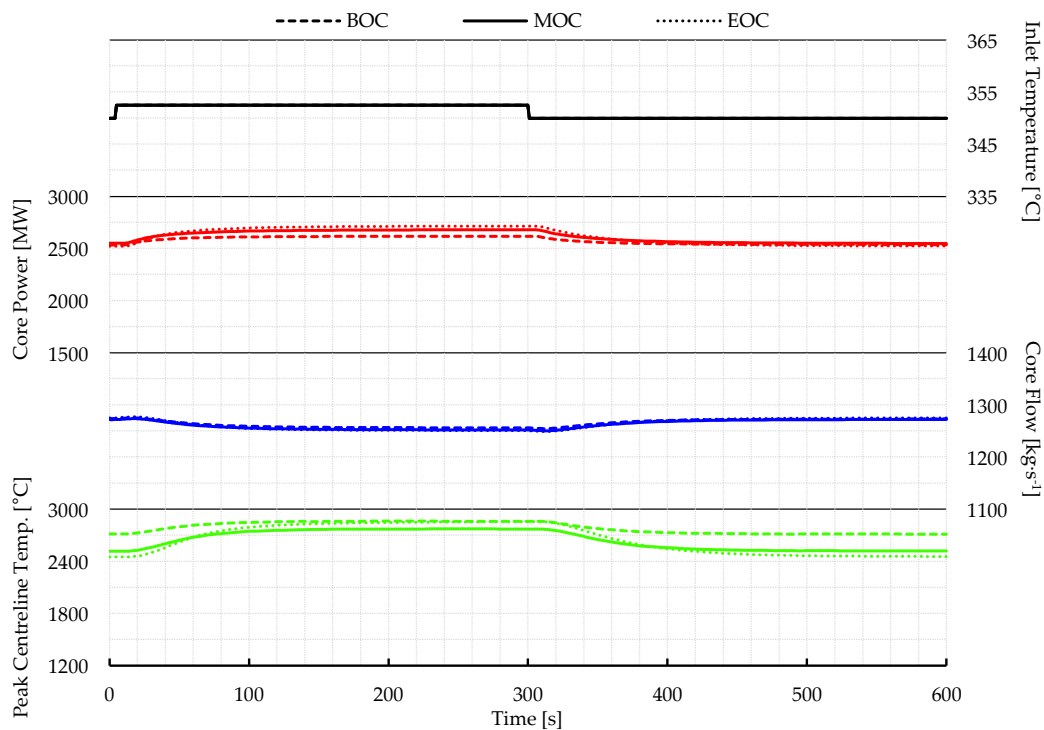
Figure 5.31: Inlet temperature step up transient at BOC, MOC, and EOC
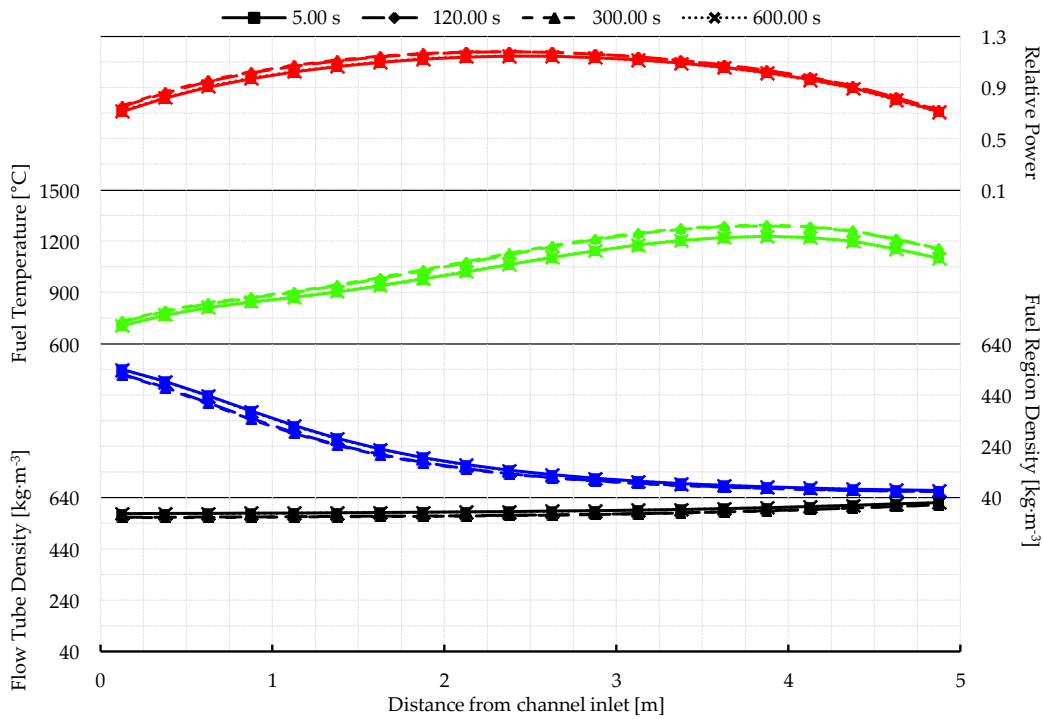
Figure 5.32: Average axial profiles during temperature step up at BOC
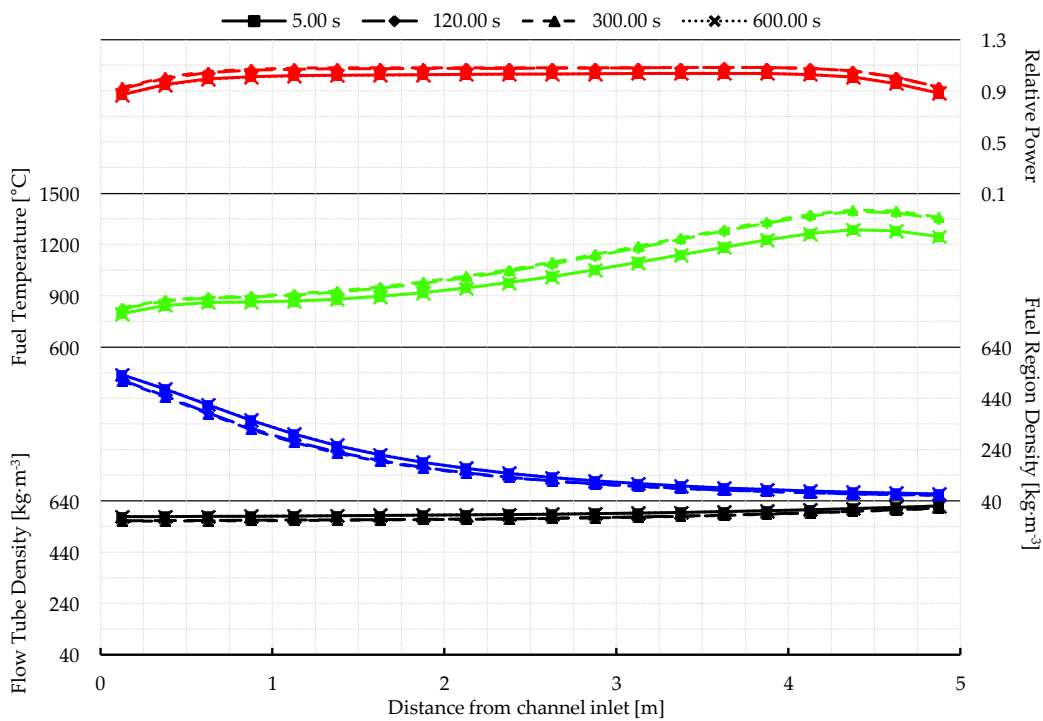
Figure 5.33: Average axial profiles during inlet temperature step up at MOC
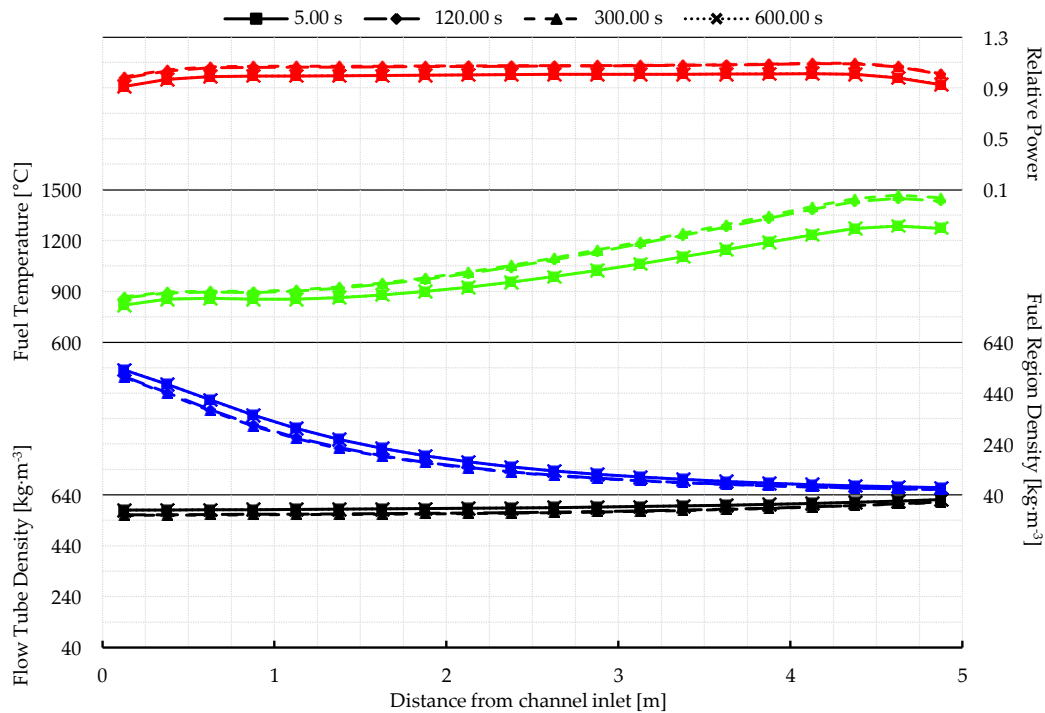
Figure 5.34: Average axial profiles during inlet temperature step up at EOC

5.3.1.2   Imposed Oscillations

Figure 5.35 through Figure 5.37 show a transient where power and flow oscillations were imposed on the core by varying the core inlet temperature as a sinusoidal function. The sinusoid used in these first tests had a 10.0 °C amplitude and a 10.0 s period. The inlet temperature was returned to its steady reference value (350 °C) at 200 s and the transient was allowed to continue for an additional 200 s. Note the magnified vertical scale used in these plots compared to the previous section since the magnitude of the power and flow variations were much smaller.

Similar to the inlet temperature step change, there is a slight delay after varying the inlet temperature (≈5 s) before any changes in the core power are realized. This is likely due to the large fluid volume in the inlet plenum and the transit time for fluid leaving the pump and reaching the channels. After this short delay there is a power increase resulting from the initial coolant temperature increase (and density decrease) and the associated positive reactivity insertion. The magnitude of this initial power deviation is larger later in the batch cycle, which is consistent with the previous results.
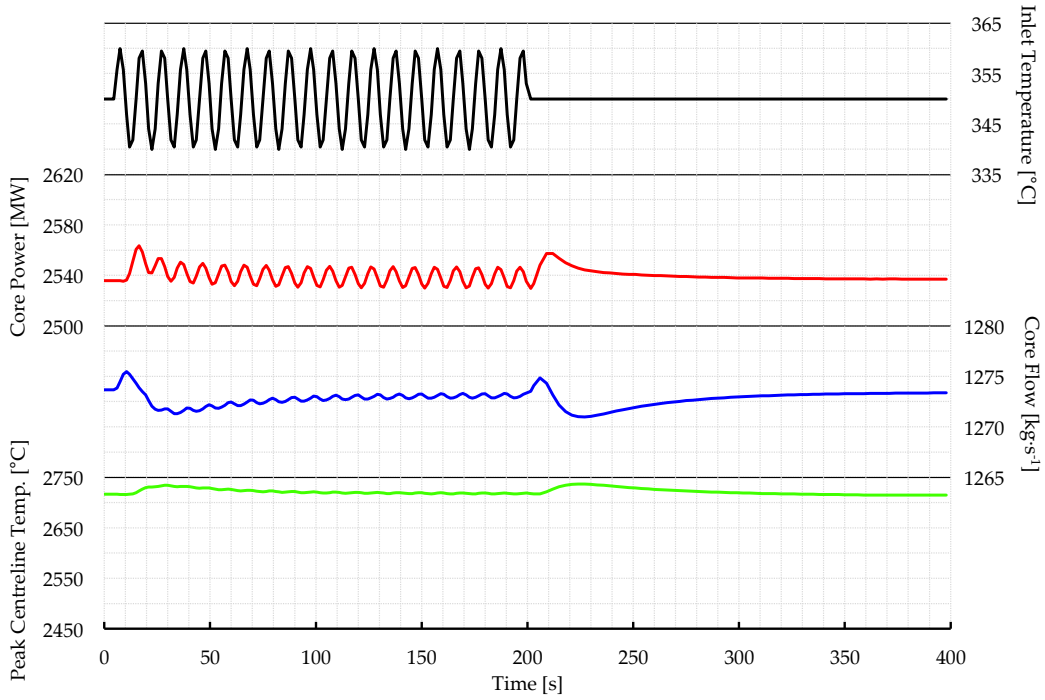
Figure 5.35: Inlet temperature oscillation at BOC
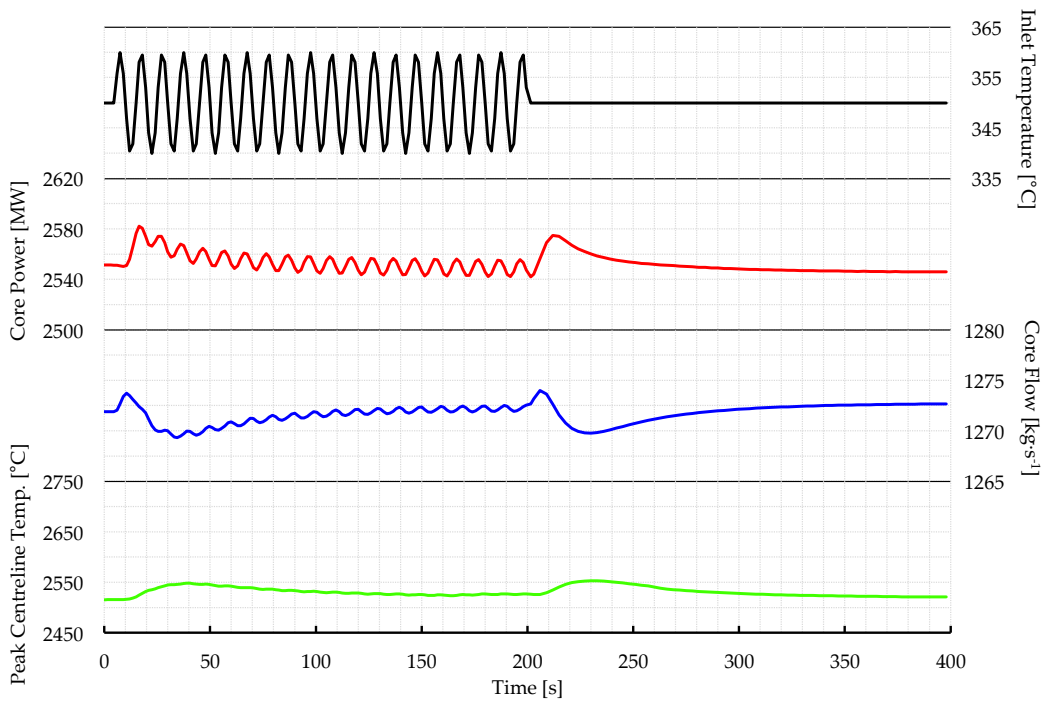
Figure 5.36: Inlet temperature oscillation at MOC
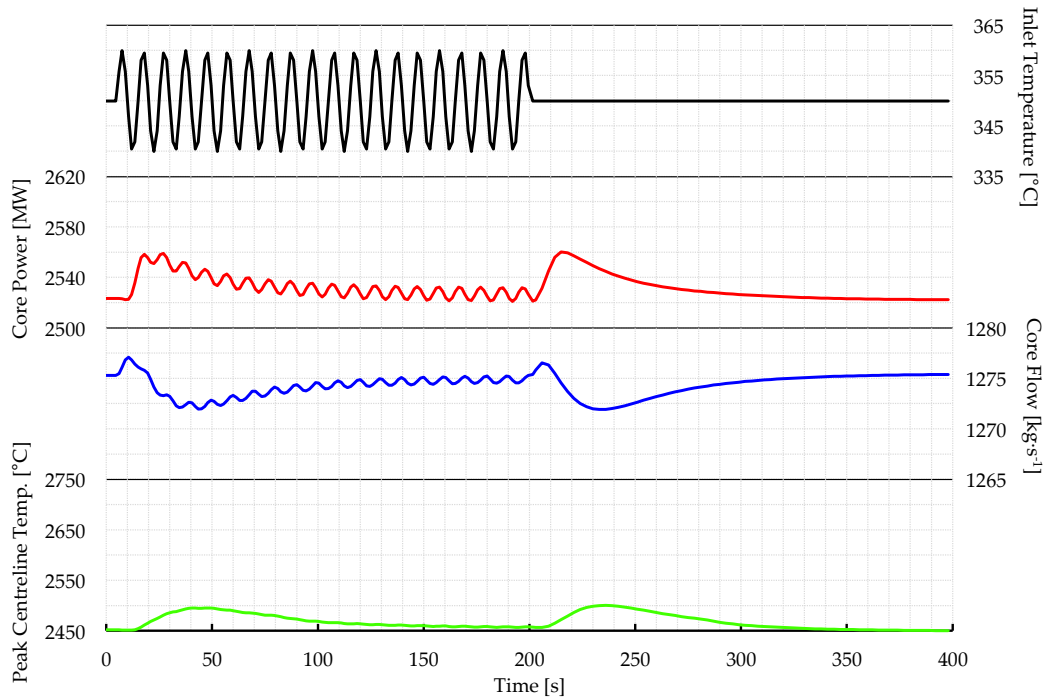
Figure 5.37: Inlet temperature oscillation at EOC

There is a similar transient (including the ≈ 5 s delay) after the oscillations have ceased, after which the core slowly returns to the steady-state reference conditions. Considering the magnitude of the power transients observed in the inlet temperature step change tests, the power transients in this case are clearly being limited by the sinusoidal temperature function.

After the initial power ramp the core starts oscillating in-phase with the inlet temperature. These oscillations begin with an upward bias from the initial reactivity transient, but this bias slowly decays and the power oscillations become centred approximately on the initial steady power level. The total core flow oscillates as well, but the magnitude of the oscillation (< 1 kg·s^{-1} or 0.1% of total flow) is extremely small.

The inlet temperature signal is strongly attenuated in the core power response. For example, at BOC a 2.5 °C temperature step reduction produced a new steady power nearly 100 MW below the initial condition, but a 10.0 °C amplitude oscillation produces a power oscillation of ≈ ±7.5 MW. The oscillation magnitude at EOC is slightly smaller, suggesting that the greater feedbacks later in the batch cycle are increasing the attenuation. The kinetics parameters were the same in

each core state (those in Table 4.11), so these differences in the transient response can only be explained by differences in core power/burnup distribution and feedback coefficients.

Figure 5.38 and Figure 5.39 show the results of similar transients executed at MOC, except in the case of the former the oscillation period was reduced to 7.5 s, and in the later the period was lengthened to 15.0 s. The amplitude remained 10.0 °C in both cases. The results are consistent with what could be inferred by the step change and 10.0 s period oscillations, i.e. the power response to changes in the boundary conditions is more attenuated at higher frequencies. This is an intuitive result: the core power has a transient response so it can't immediately change to match the new operating conditions, and the less time the operating conditions are consistently perturbed away from the initial value (either above or below), the less time the core power has to change according to the cross-section feedbacks and kinetics parameters. Note that the 15.0 s period transient begins with the temperature decreasing rather than increasing, so the initial power bias is negative rather than positive. The initial bias nevertheless decays in the same way as in the other transients.
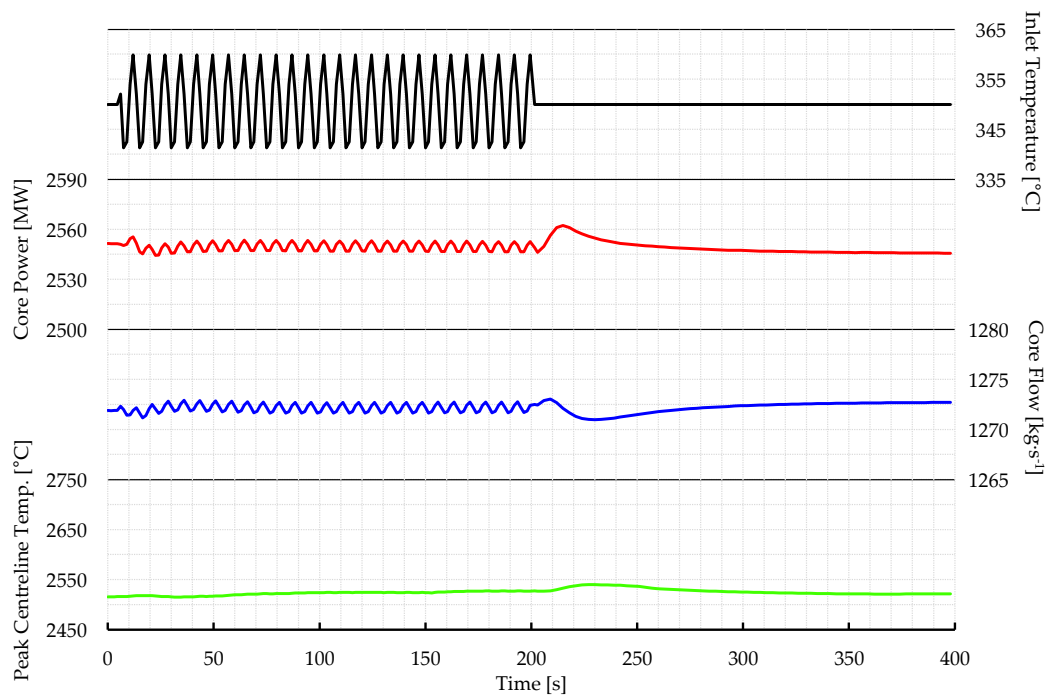
Figure 5.38: Higher frequency inlet temperature oscillation
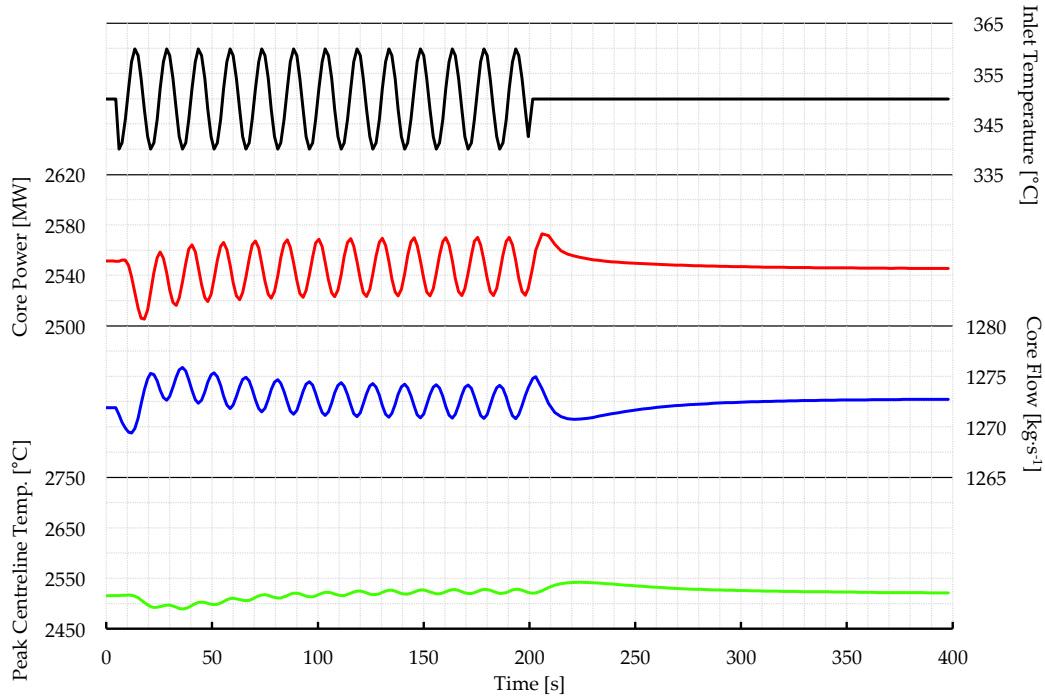
Figure 5.39: Lower frequency inlet temperature oscillation
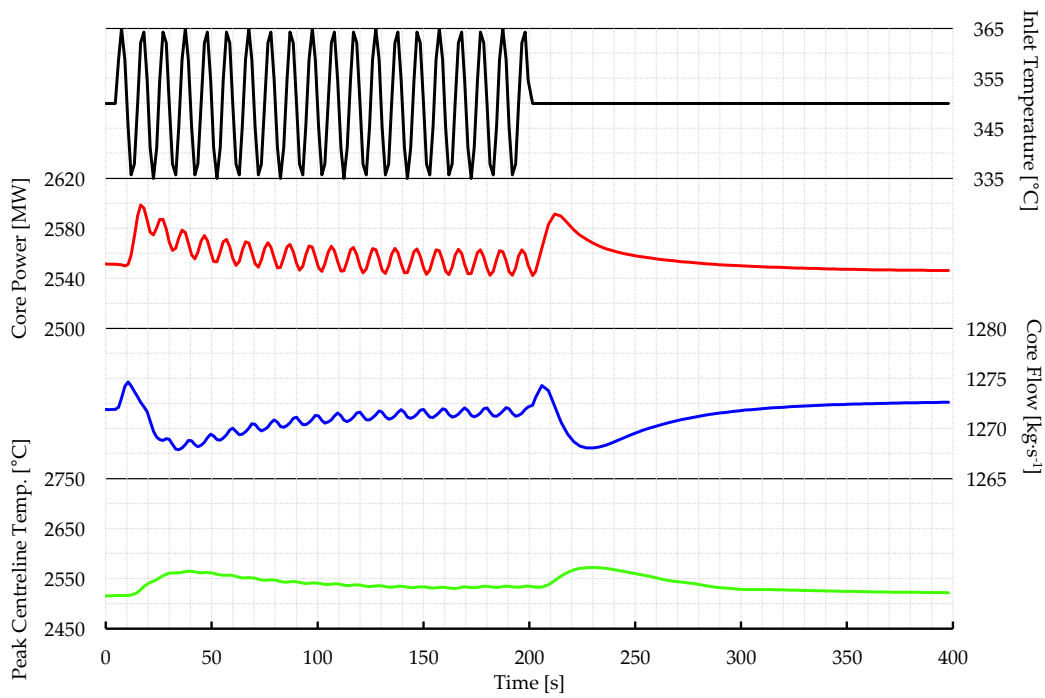
Figure 5.40: Larger magnitude inlet temperature oscillation

As a final test, the magnitude of the temperature oscillation was increased to 15.0 °C while maintaining the 10.0 s period at MOC. The transient results are shown in Figure 5.40. Compared to the 10.0 °C amplitude oscillation shown in Figure 5.36, the initial reactivity transient and power bias is larger, and so is the amplitude of the power oscillation. The increase in amplitude is less than proportional to the temperature increase, however, which is further evidence that the core transient response to these types of oscillations is significantly attenuated.

5.3.1.3   Analysis of Coupled Stability Test Results

The transient tests performed in Section 5.3.1.1 suggest that when perturbed from its steady-state operating conditions the PT-SCWR core will generally: 1) return to its previous steady-state after a short transient if the perturbation was relatively brief, or 2) attain a new steady-state corresponding to new steady-state boundary conditions. The only exception to the latter was when a cascade of negative reactivity feedbacks caused the core power to accelerate downward, but this transient could be arrested by returning the perturbed parameter back to its reference condition (or in a real reactor, presumably through the action of a reactivity control system). In neither case were significant BWR-like core power and flow oscillations observed.

The tests in Section 5.3.1.2 demonstrate that when oscillations are imposed on the PT-SCWR core by varying the boundary conditions with a sinusoidal function the power response is significantly attenuated. The level of attenuation is largely frequency dependent and most likely determined by the combined thermal and kinetic response of the reactor, with the cross-section feedback playing only a small role in determining the power amplitude (which essentially remains constant during any given transient). The power oscillations ceased after returning to the reference boundary conditions.

Taken together, this is strong evidence that the PT-SCWR core cannot experience BWR-like power oscillations and coupled neutronic-thermalhydraulic instability. There are probably many small contributors to the relative stability of the PT-SCWR, which based on BWR literature likely include the severe inlet orifices and lack of a gas gap between the fuel and cladding. The largest stabilizing effect, however, is likely the fuel channel design and its effect on the lattice physics. In

none of the typical stability tests did changes in core power have any significant observable impact on the fluid density in the centre flow tube (which has a *negative* CVR as required for the coupled instability). Conversely, coupled effects between power and coolant density in the fuel region were abundantly clear, but the CVR in this region is *positive*. A key driving mechanism for the coupled instability is thus absent.

Consider that in a BWR additional heat being removed from the fuel, leading to decreased coolant density, has a negative reactivity effect. A power decrease conversely results in lower heat, higher coolant density, and positive reactivity. In the current PT-SCWR concept the reactivity effects are reversed, so the driving mechanism of coupled oscillation and instability are removed. This is true even though the PT-SCWR fuel has a negative (total) CVR as a design requirement.

The lattice results demonstrate that with multiple flow paths this requirement does not preclude positive "partial" or "differential" CVR values. The progression of fuel design concepts presented by Pencer and Colton show that this was not always the case with PT-SCWR fuel [11]. Fuel channel concepts that contained only a single flow path but had negative CVR could have, in theory, experienced coupled oscillations. The positive partial CVR around the fuel makes the PT-SCWR unique among SCWR concepts and likely immune to coupled instability, but as the next section shows, potentially vulnerable to power pulses in flow induced reactivity transients.

5.3.2   Imposed Flow Transients

The simulation results presented in this section are meant to illustrate the behaviour of the coupled system for stylized transients representing postulated accidents in the PHTS. These include large LOCAs and flow rundowns (or LOFAs: Loss of Flow Accidents) without reactor trips. There are a number of caveats to be had when interpreting the results. First, since there are no safety systems included in the PHTS model (e.g. pressure relief and discharge vales, emergency coolant injection, etc.) these transients can't be considered true representations of postulated accident progressions in the complete PT-SCWR conceptual design. Second, radiation heat transfer from the fuel through the pressure tube to the moderator is a key component of the PT-SCWR safety design, but radiation heat transfer was omitted from the CATHENA model. The

peak fuel temperatures shown in the transients are thus likely to be over-estimated. Finally, the imposed transients themselves are abstract creations and possibly non-physical. These cases are meant to create an understanding of how the core may perform under specific (and stylized) circumstances.

5.3.2.1   Flow Reversals and LOCA-like Transients

The positive CVR in the fuel region suggests that the PT-SCWR may exhibit power excursions in cases where the coolant density around the fuel decreases rapidly before a corresponding reduction occurs in the centre flow tube. A flow reversal, for example, causing a front of low density fluid to travel from outlet to inlet, could occur during a LOCA with a sufficiently large break in the core inlet piping. The transient depicted in Figure 5.41 is a stylized case where the core outlet pressure remains high, thus giving the maximum possible negative pressure differential. The inlet pressure undergoes an exponential decrease to 23.0 MPa, which was the lowest pressure imposed in any transient to prevent CATHENA from cross over to subcritical fluid at 22.1 MPa.

The figure shows how the flow rapidly decreases and eventually reverses. There is a power excursion (160% full power or 4,070 MW) that peaks before there is any reverse flow. The coolant density reduction and positive reactivity insertion must therefore be caused by the slowly moving coolant increasing in enthalpy from sustained contact with the fuel. After the flow reverses, however, the reactor power drops rapidly.

The axial distributions in Figure 5.42 through Figure 5.45 show the progression of the low density fluid front and the power transient. The peak of the power pulse at approximately 6.50 s is precipitated by the loss of coolant within the fuel channel. At this point the power is clearly tilted towards the top of the channel as low density fluid has started to enter the bottom of the centre flow tube. In the subsequent seconds the low density fluid continues moving up the flow tube, providing the large negative reactivity that essentially shuts down the reactor.

The channel power distribution during the transient is shown in Figure 5.46. There are no substantive changes to the channel power shape, although there is evidence the distribution is slightly flatter (at 6.50 s the total power is 156% full power, whereas the maximum channel power is only 152 percent of its nominal value).
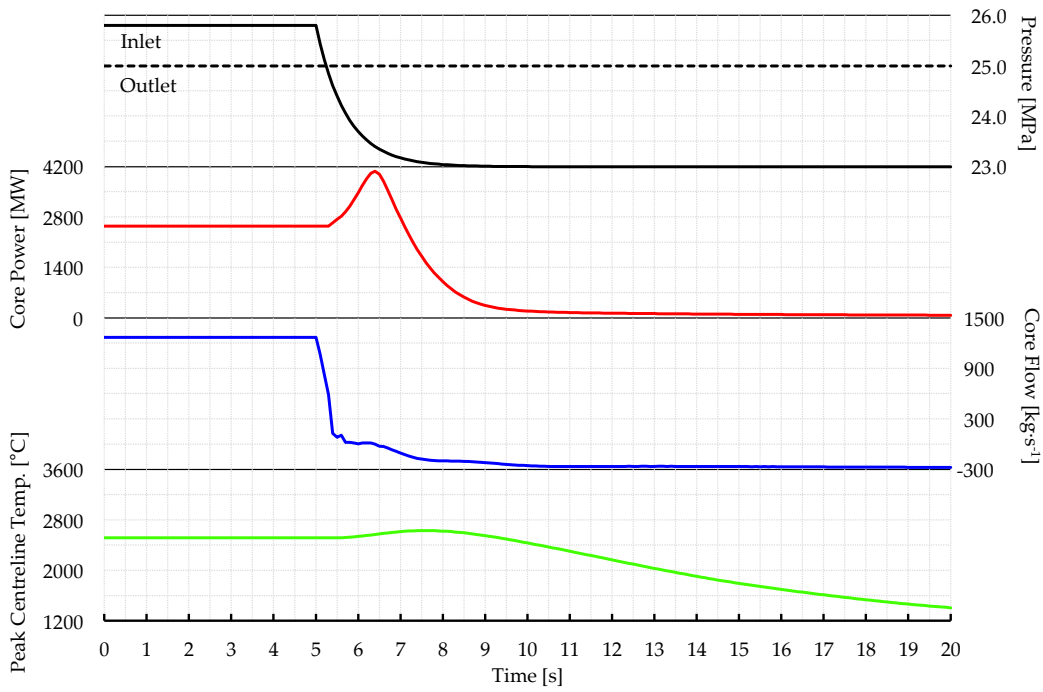
Figure 5.41: Flow reversal transient at MOC
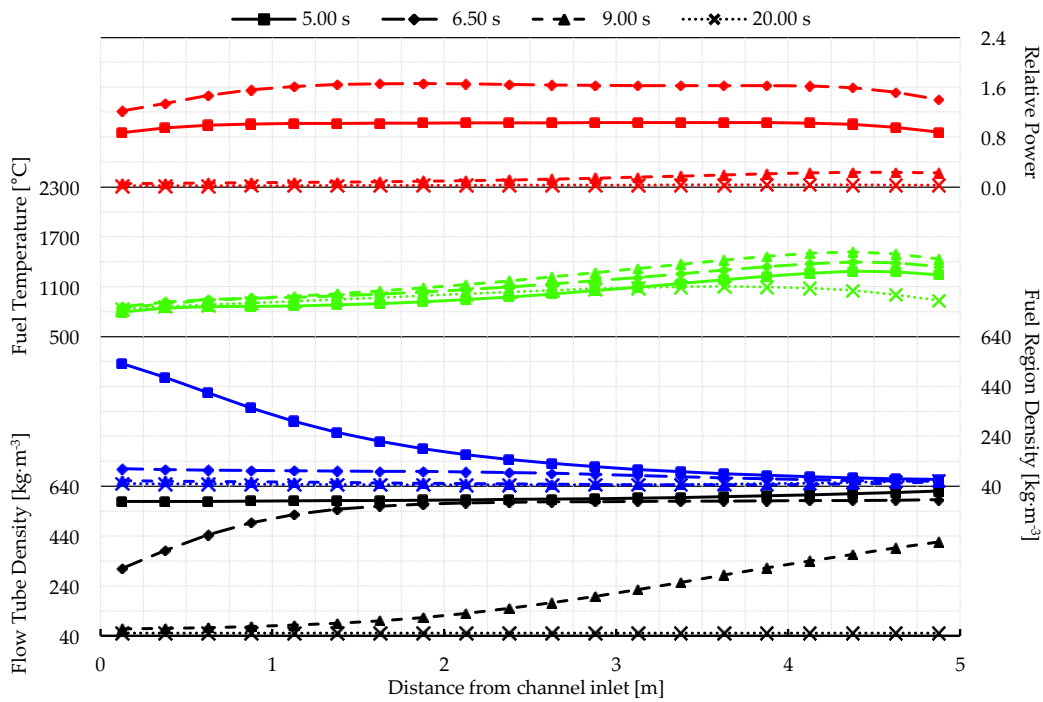
Figure 5.42: Average axial profiles during flow reversal transient
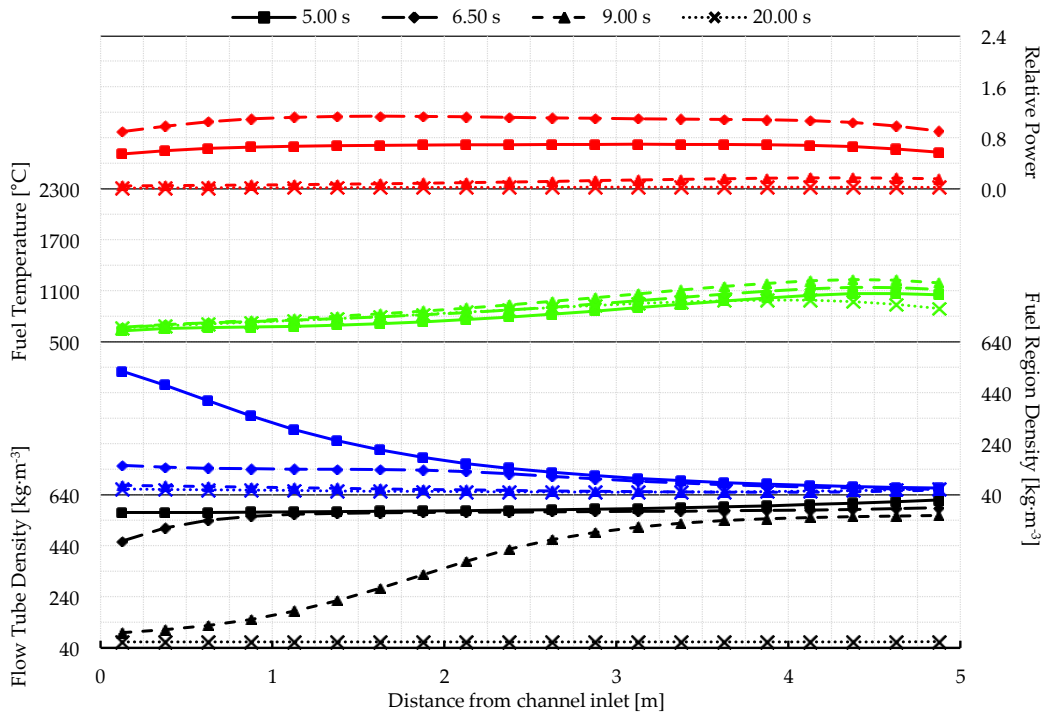
Figure 5.43: Axial profiles in C4 during flow reversal transient
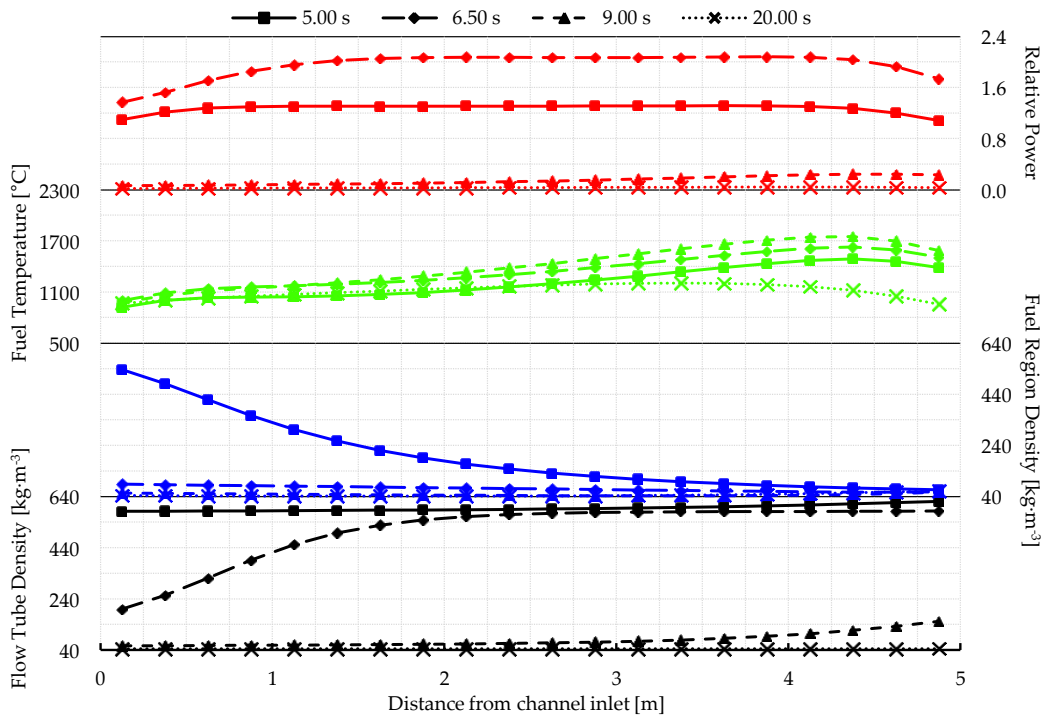
Figure 5.44: Axial profiles in E6 during flow reversal transient
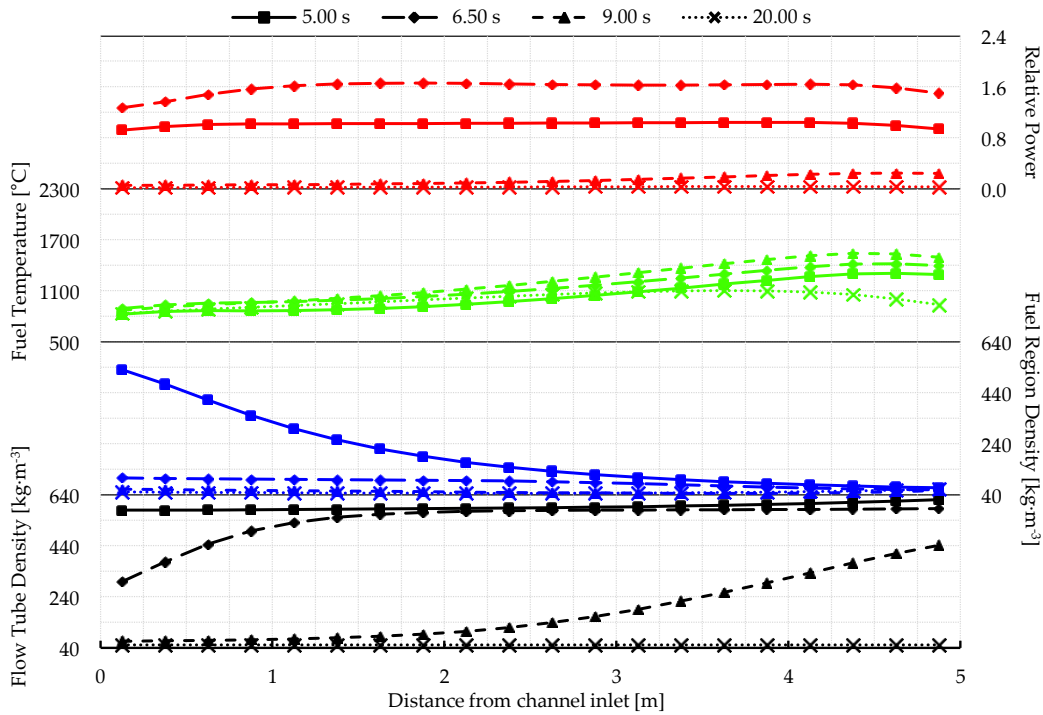
Figure 5.45: Axial profiles in G8 during flow reversal transient

Figure 5.47 shows a similar transient except the inlet pressure decrease is slightly slower. This delays the time at which low density fluid enters the centre flow tube, but instead of resulting in a larger power pulse the progression of the entire transient is slower. The peak power is in fact slightly lower than in the faster transient, but only marginally so (158% or 4,022 MW). The integrated area under the power curve is visibly larger, however, and considering the greater energy deposition this is arguably worse in terms of fuel integrity and overall safety.

Figure 5.48 through Figure 5.51 show the axial distribution for the slower flow reversal transient. Many of the underlying phenomena are exactly the same, except the transient progresses slower and the power peak is delayed by approximately 1.0 s. Again, the channel power distribution does not change substantially, so the maps have been omitted for brevity.
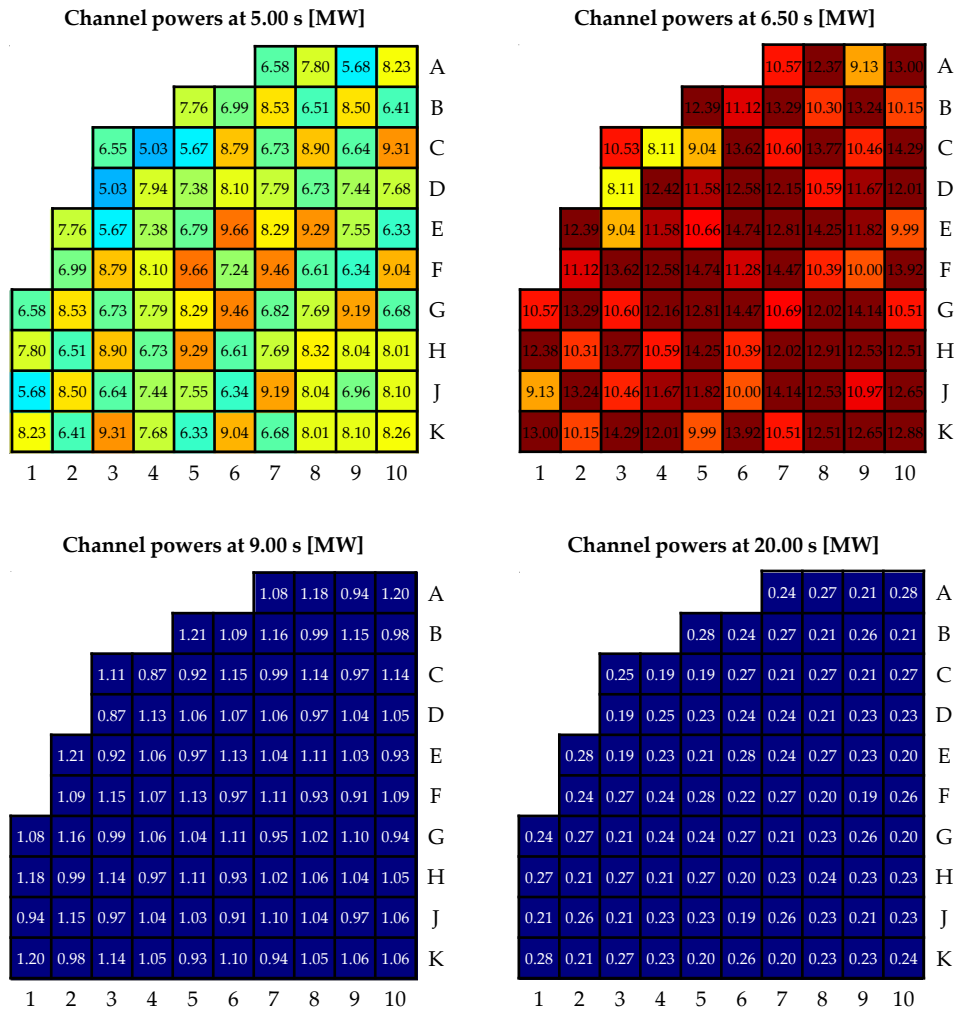
Figure 5.46: Channel powers during the flow reversal transient
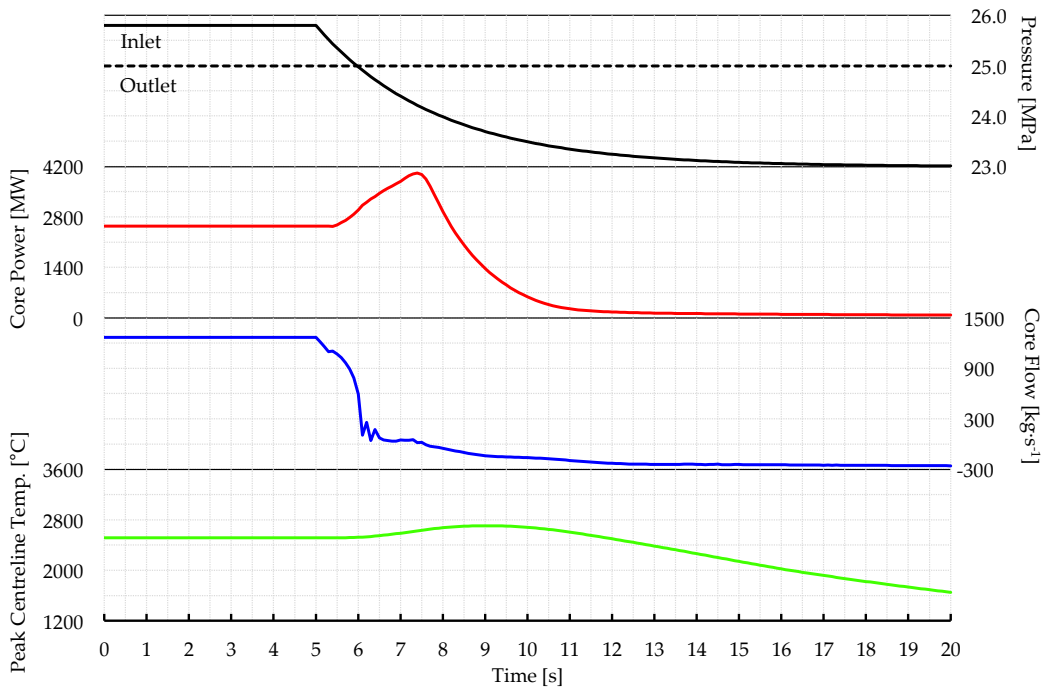
Figure 5.47: Slower flow reversal transient at MOC
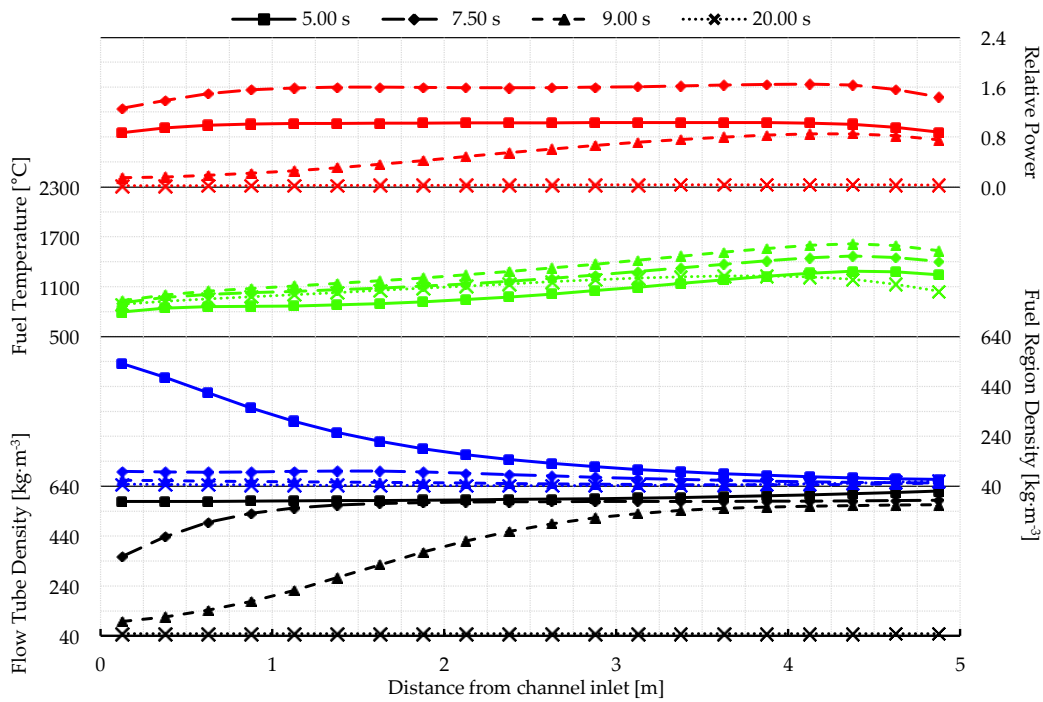
Figure 5.48: Average axial profiles during slower flow reversal transient
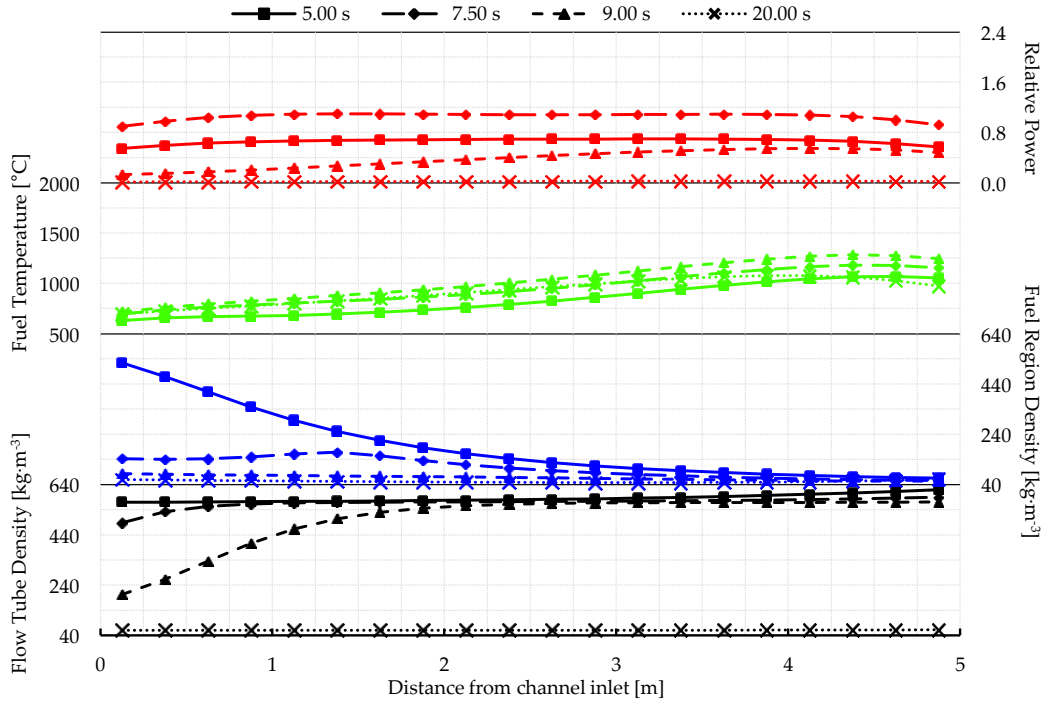
Figure 5.49: Axial profiles in C4 during slower flow reversal transient
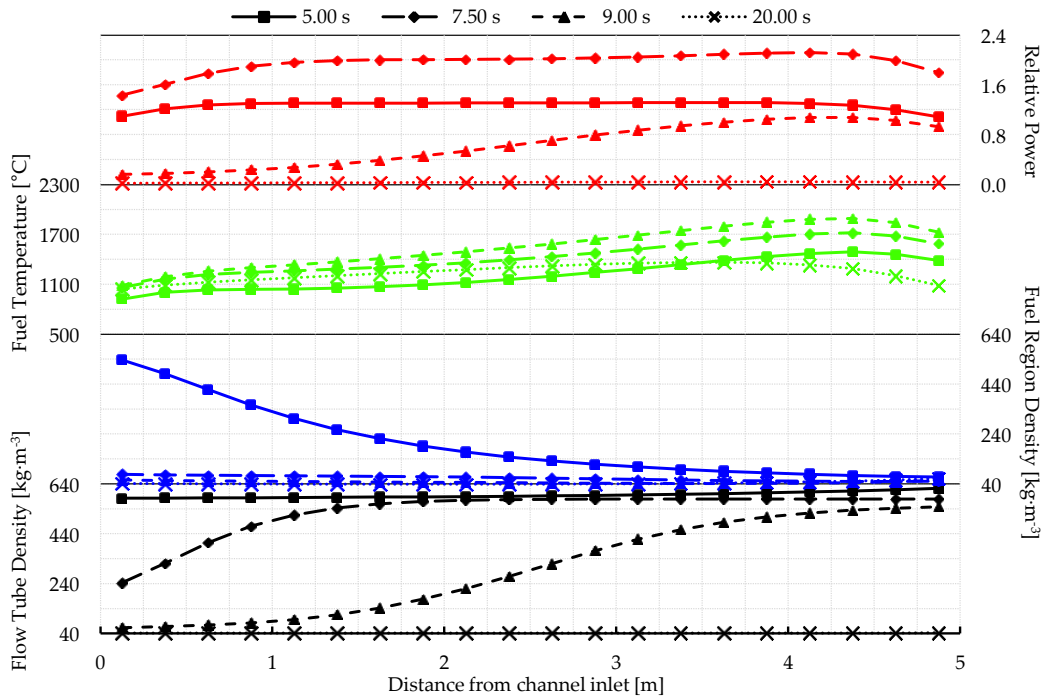
Figure 5.50: Axial profiles in E6 during slower flow reversal transient
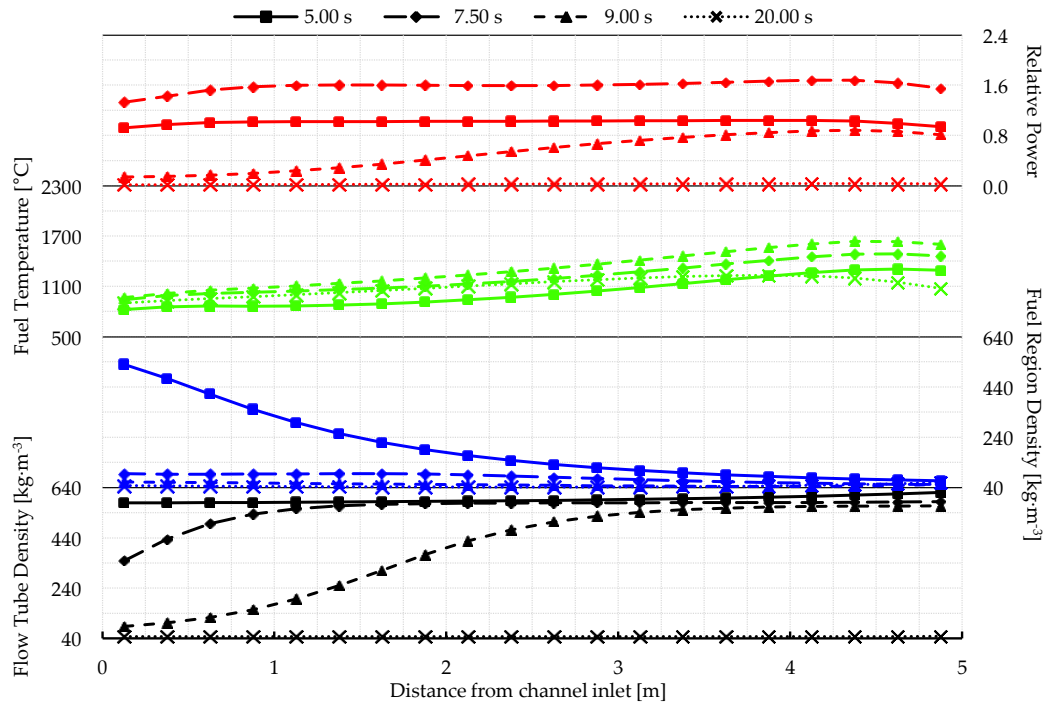
Figure 5.51: Axial profiles in G8 during slower flow reversal transient

In Figure 5.52 a more realistic LOCA-like transient is depicted where the outlet pressure falls with the inlet pressure after a short delay. The reverse flow is thus much smaller than in the previous cases where the outlet pressure remains high. After ≈10 s both the inlet and outlet pressure near the imposed limit of 23.0 MPa, but a small reverse flow is still maintained. The peak of the power pulse is lower still in this case (150% full power or 3,838 MW).

With smaller reverse flow the low density fluid front is much slower to travel up the centre flow tube, and the reactor power tails off much slower than in the other transients. This is evident in the axial distributions shown in Figure 5.53 through Figure 5.56. Despite the lower peak power the final average fuel temperatures are markedly higher than in the previous cases due to the reduced reverse flow.
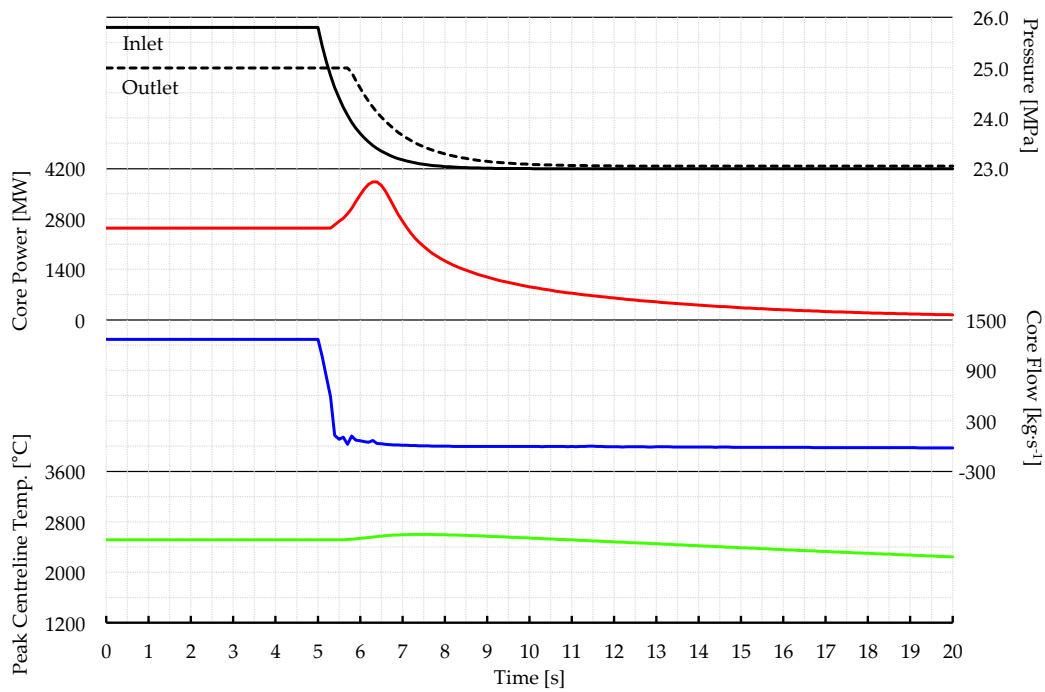
Figure 5.52: Realistic flow reversal transient at MOC
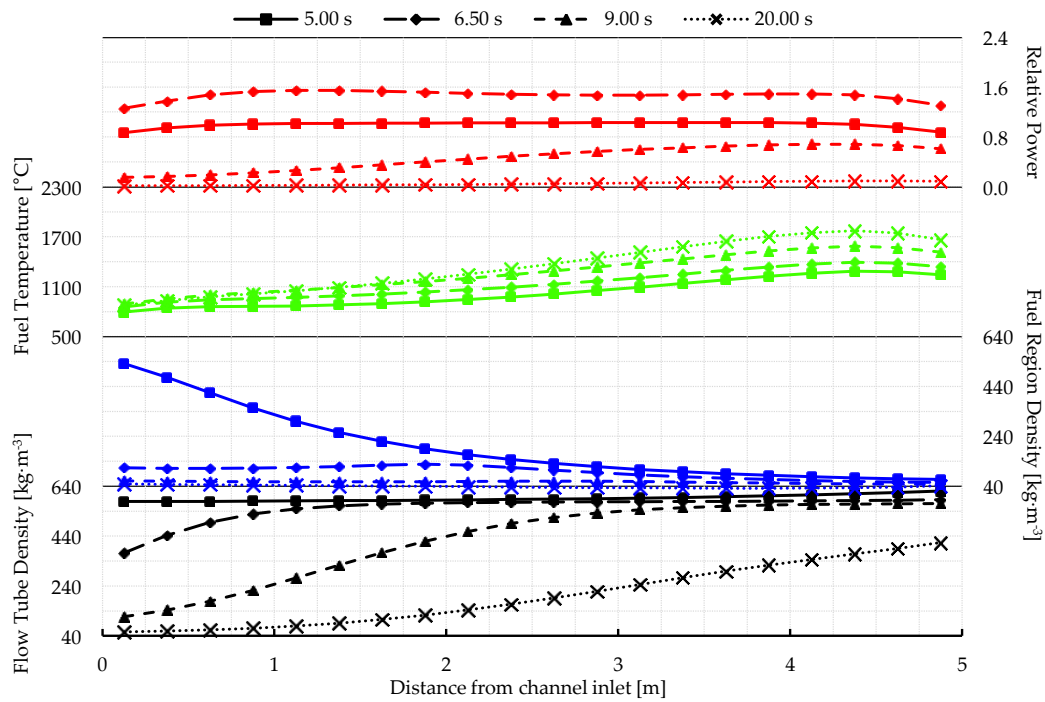
Figure 5.53: Average axial profiles during realistic flow reversal transient
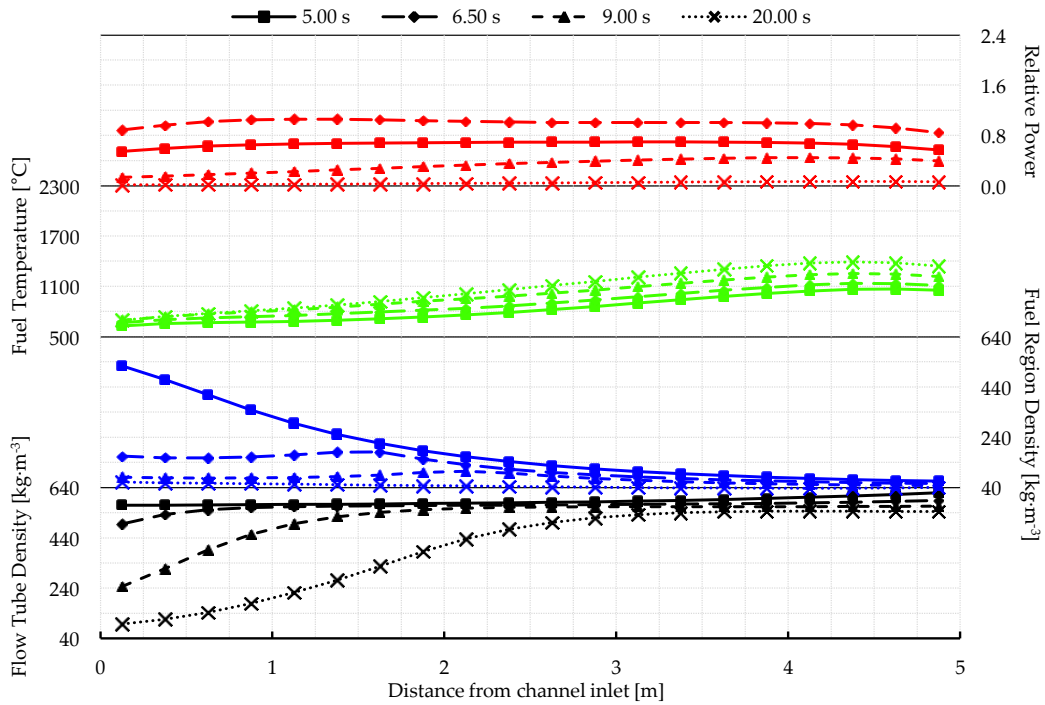
Figure 5.54: Axial profiles in C4 during realistic flow reversal transient
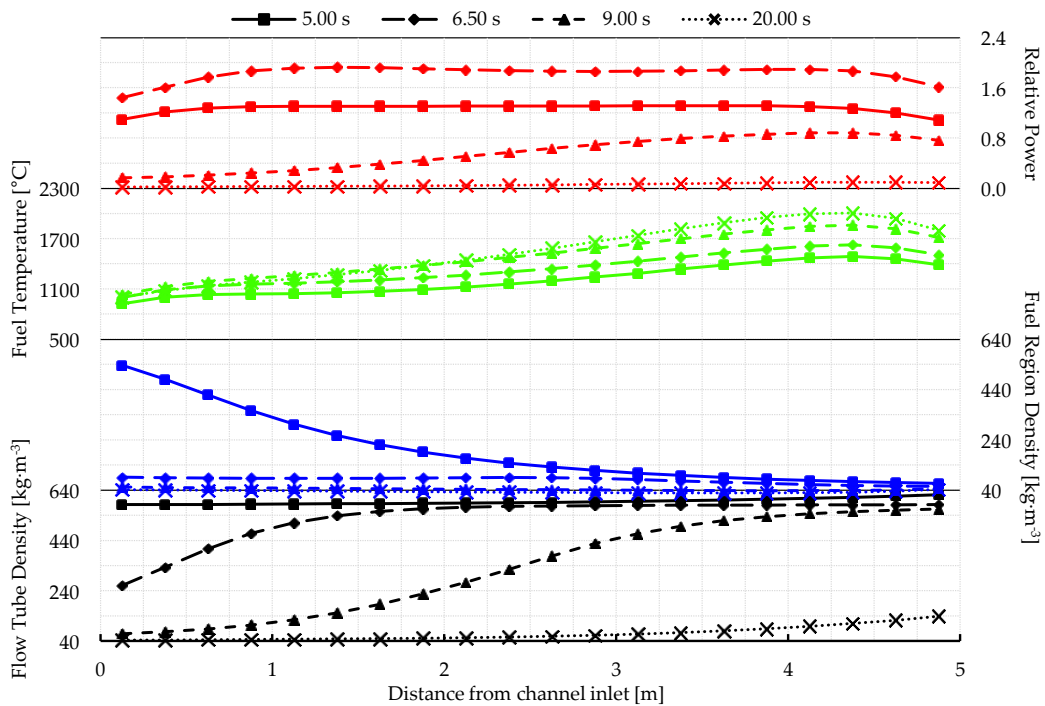
Figure 5.55: Axial profiles in E6 during realistic flow reversal transient
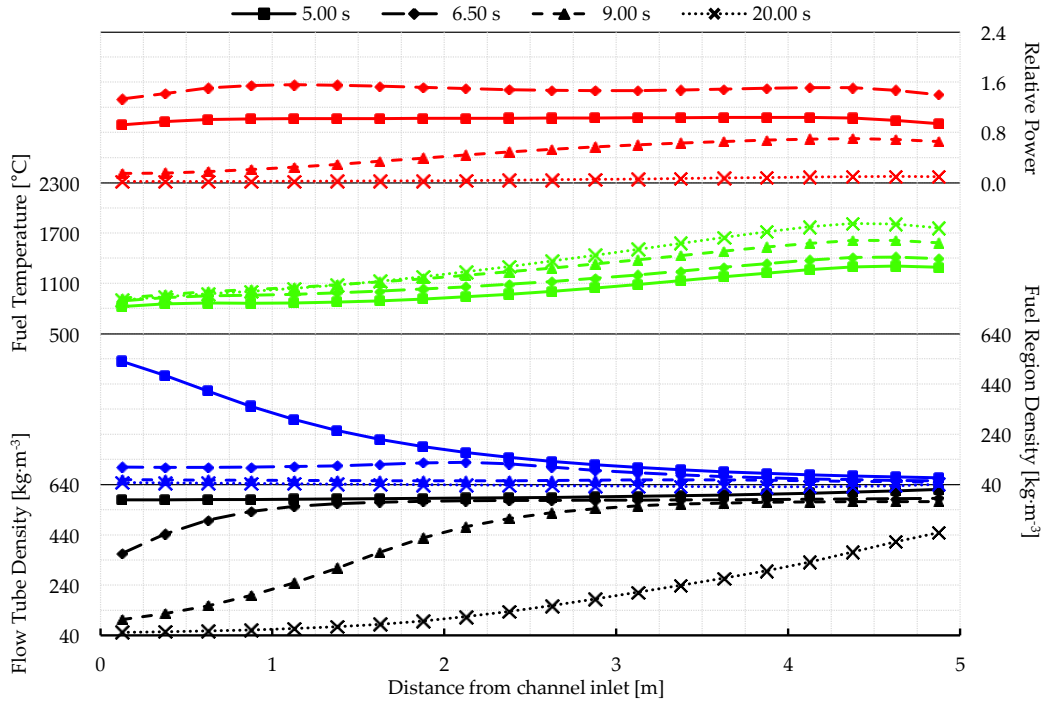
Figure 5.56: Axial profiles in G8 during realistic flow reversal transient

5.3.2.2 Flow Rundown and Stagnation

Figure 5.57 shows a transient where the inlet pressure exponentially decreases to match the outlet pressure over a ≈15 s period. This pressure transient was intended to qualitatively resemble a rundown of the primary heat transport pumps without reactor trip or any action by relief vales or other safety systems. The falling inlet pressure causes the total core flow to decrease and, as shown in the figure, the power to increase to 120% (3,055 MW) within 5 s. After reaching this peak the negative reactivity feedback causes the power to ramp down and 30 s after initating the transient it is at less than 10% full power. By this point the flow has nearly stagnated in the channels, but some heat is still transferred to the coolant as the fuel temperature continues to decrease with the lower power.

Figure 5.58 through Figure 5.62 show the thermalhydraulic property and power distributions within the core. The flow decrease causes a coolant density decrease in the fuel region that is the source of positive reactivity. The fuel temperature reactivity feedback plays a key role in arresting the power pulse, and the eventual density decrease within the flow tube causes the subsequent power ramp-down (as discussed in detail below).
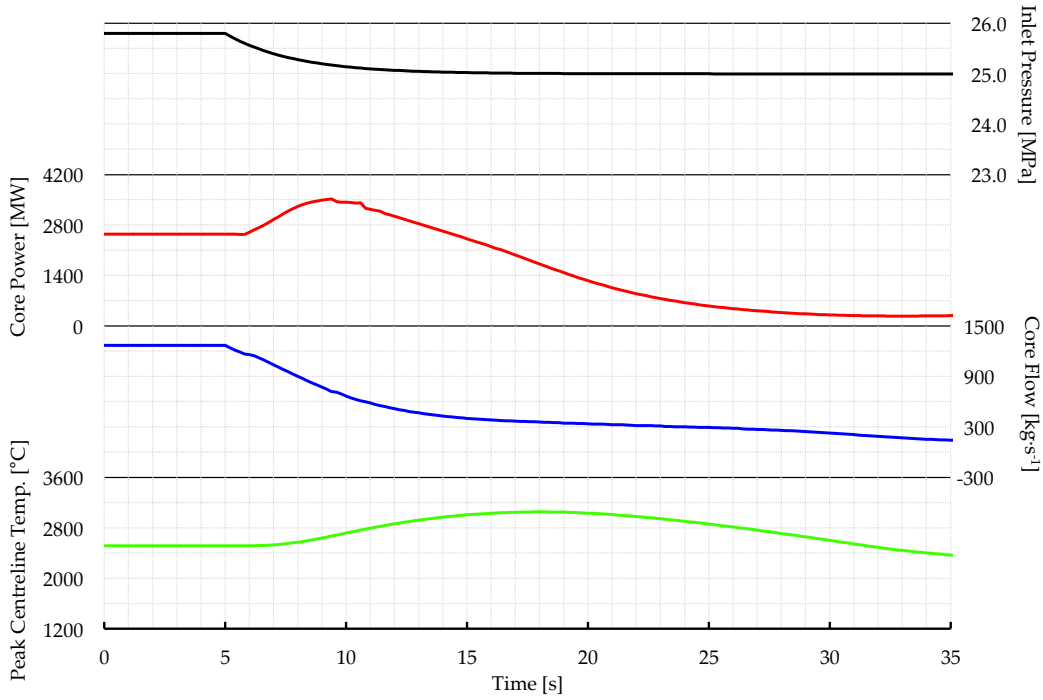
Figure 5.57: Flow rundown transient at MOC
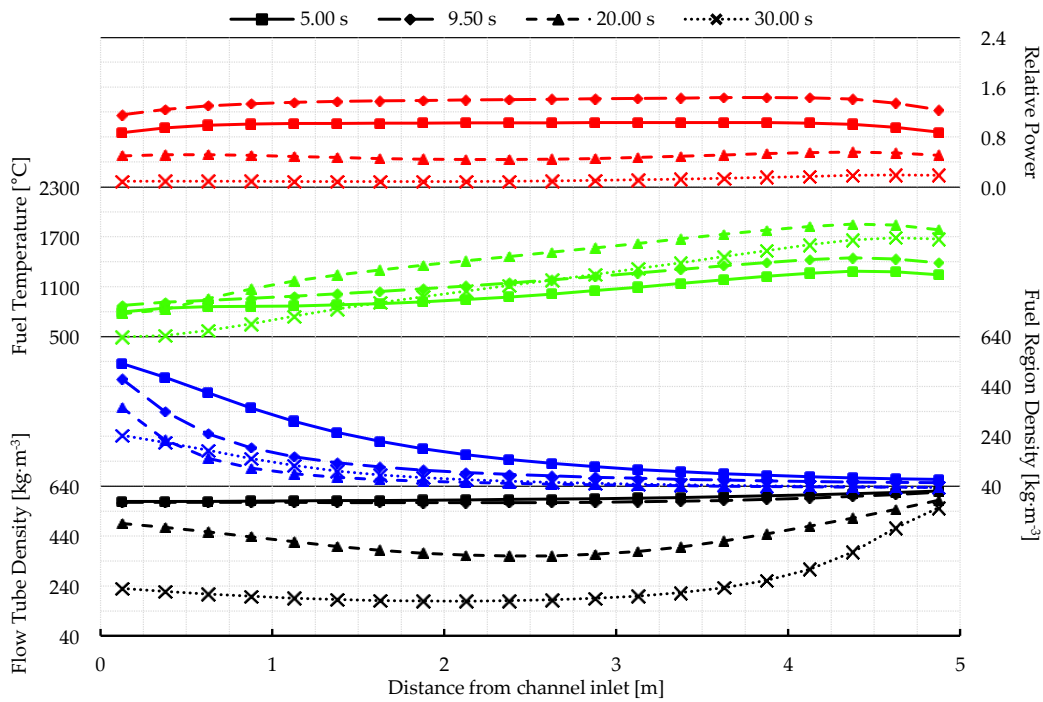
Figure 5.58: Average axial profiles during flow rundown transient
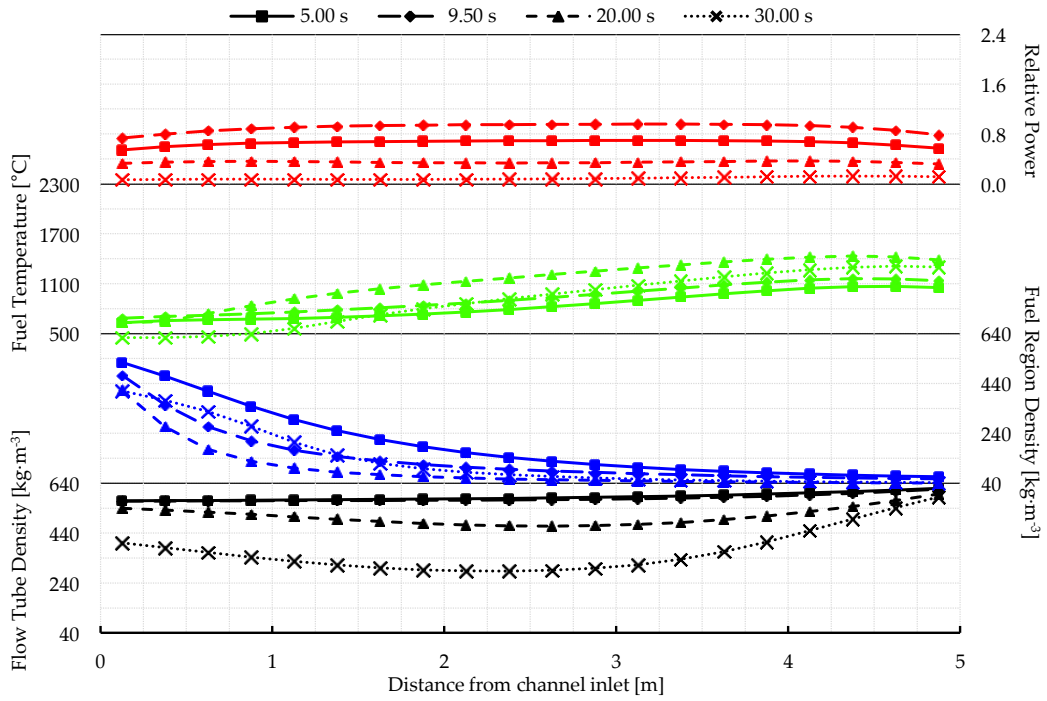
Figure 5.59: Axial profiles in C4 during flow rundown transient
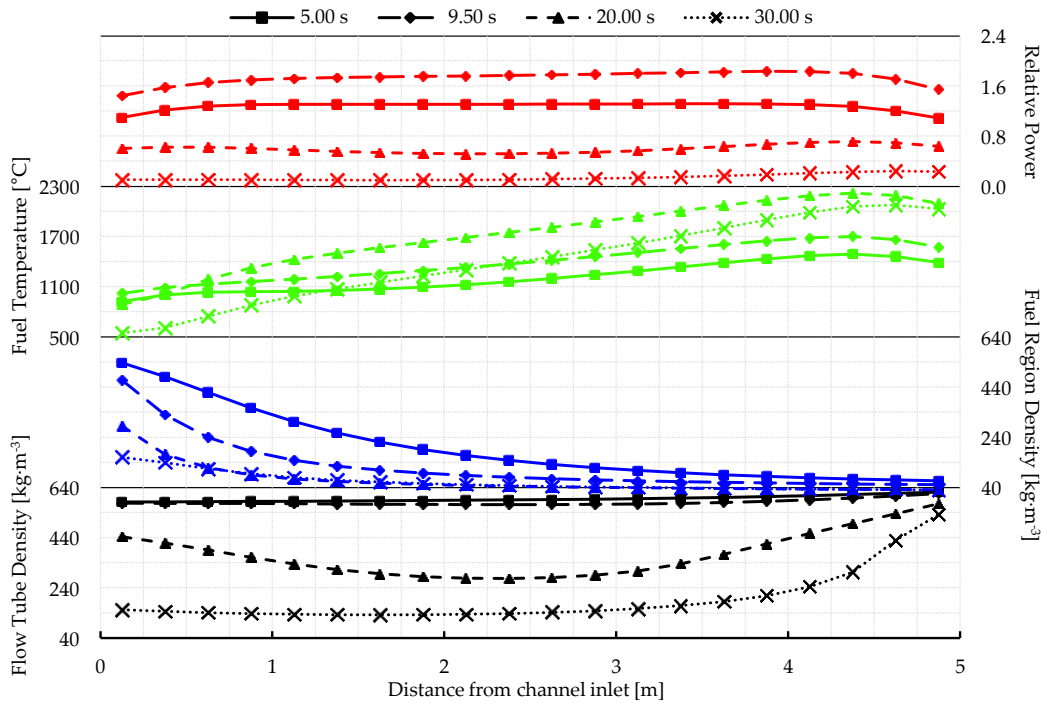
Figure 5.60: Axial profiles in E6 during flow rundown transient
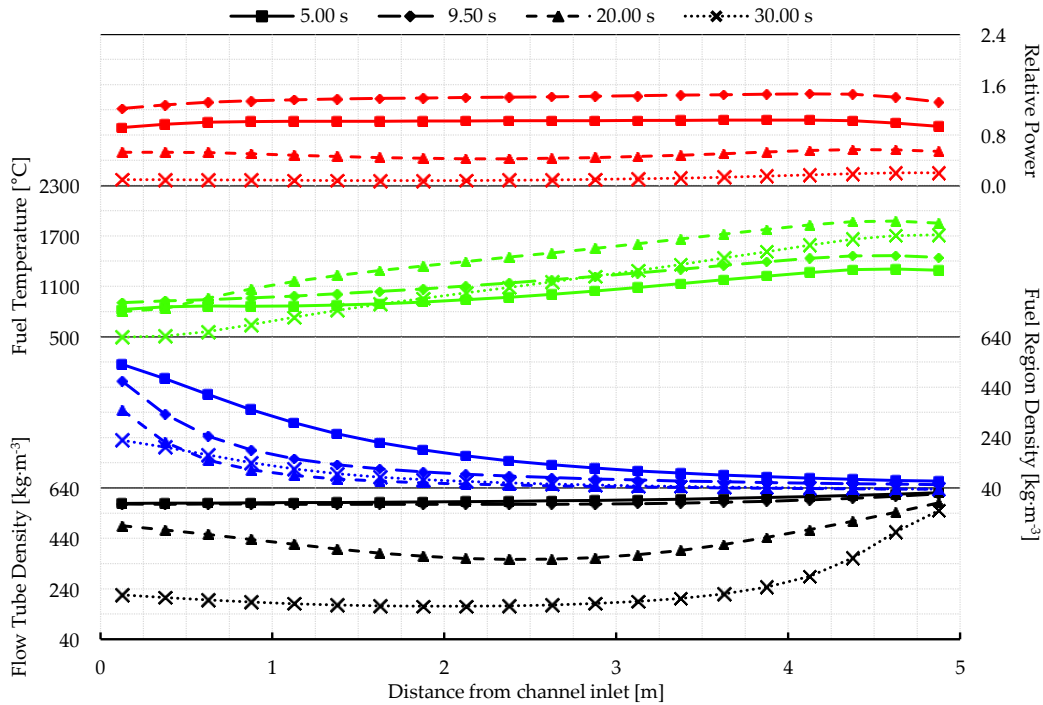
Figure 5.61: Axial profiles in G8 during flow rundown transient

The flow tube coolant density profiles shown at 20.0 s (dipped in the centre of the channel) may at first seem counter-intuitive but are consistent with the low channel flows. The average fluid velocities within the flow tube by this point in the transient are fractions of a metre per second, and the enthalpy of the slowly moving fluid increases via contact with the flow tube pipe wall (much more so than in the steady-state core where the velocities are significantly higher). The initial temperature of the flow tube pipe wall is lowest at the bottom of the channel, so the stagnant fluid in contact with the wall maintains its higher density longer. At the flow tube inlet the fluid entering from the inlet plenum always has high density, thus creating the momentary "dipped" shape in the fluid density distribution. By 30.0 s this dip has mostly disappeared except in the lowest power channels which also have the lowest flows.

There was no reverse flow in this transient, so it was solely the heat conduction across the flow tube pipe and convective heat transfer to the coolant that decreased the centre channel coolant density and provided the negative reactivity that essentially shuts down the reactor.
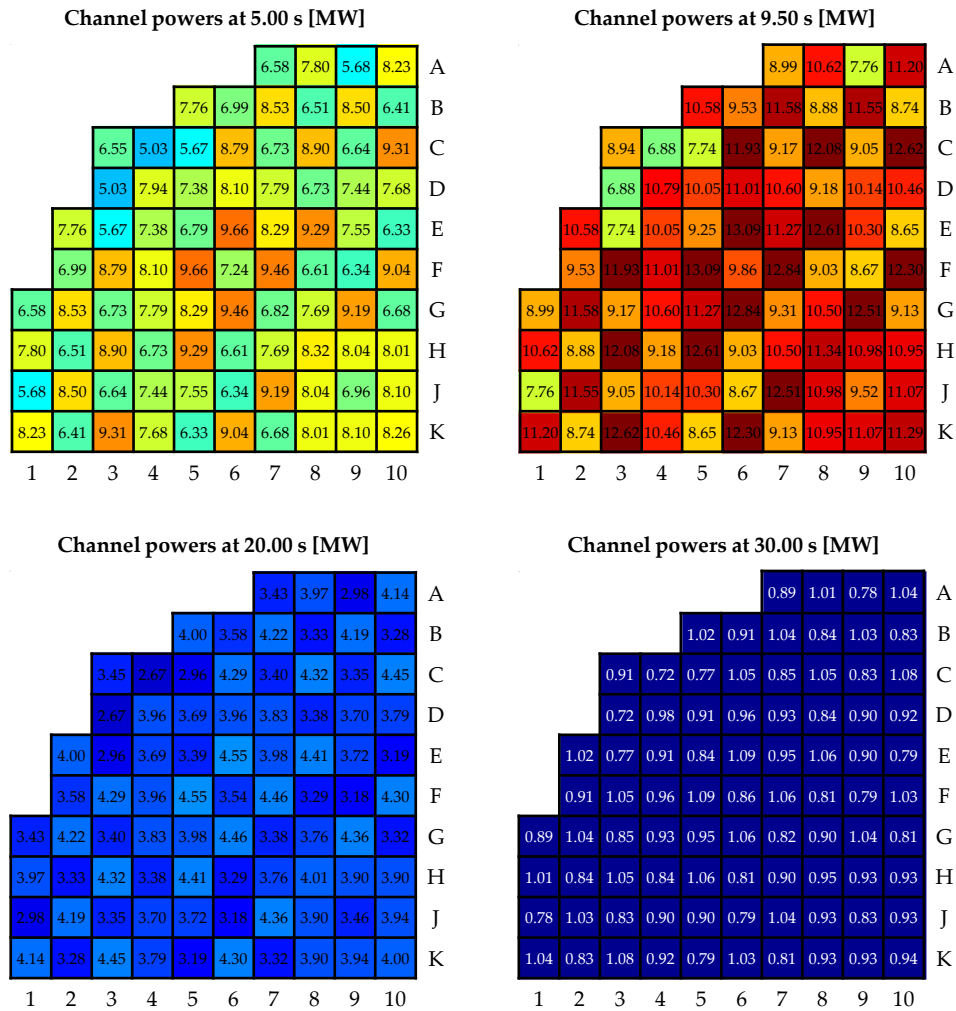
Figure 5.62: Channel powers during flow rundown transient

5.3.2.3 Analysis of Flow Transient Tests

Although the preceding core transients were heavily stylized, taken together they can provide some insight in to the coupled neutronic-thermalhydraulic behaviour of the PT-SCWR concept during a postulated accident. Even without inclusion of reactivity devices, safety systems, or radiation heat transfer, the physics of the spatial kinetics and thermalhydraulics coupling are sound. This analysis focuses on these coupled effects rather than trying to force any conclusions on the PHTS safety design on the inherent safety of the PT-SCWR concept.

First, the concern of flow reversal bringing low density fluid back in to the channel from the outlet plenum, thereby causing a large positive reactivity insertion and power excursion, is somewhat misplaced. In even the most aggressive pressure transients the very act of the fluid slowing down (and thus decreasing in density from heat being delivered from the fuel) is sufficient to initiate a power excursion prior to any flow reversal. One general trend that can be extrapolated from the transient tests is that the faster the flow decreases, the faster the power increases and the higher the peak of the pulse. Nevertheless, with the sign of the feedbacks being as they are, *any* flow reduction should result in temporary positive power feedback.

Second, the flow induced transients were found to be self-limiting due to the very large negative reactivity associated with fluid density reduction in the centre flow tube. In these transients without reactor trip, the negative reactivity is large enough to shut down the reactor on the order of seconds. The transient tests show that the faster the density in the flow tube decreases, the faster the reactor power drops. In cases of reverse flow this happens quite quickly, whereas in flow stagnation the process is much slower since heat needs to be conducted through the centre flow tube pipe wall.

The greater implication of these results is that power excursion transients are clearly possible, and while extensions to the core model to include safety systems, radiation heat transfer, and etc. will affect the calculated magnitude and duration of these pulses, they will not change the fact that they exist. This is dictated by the fundamental physics and the design of the fuel channel. The reason the power pulse exists is the same reason the core is immune to BWR-like power oscillations: the positive coolant void reactivity in the fuel region (in spite of the total negative CVR).

The relative magnitude of these power excursions in the context of reactor safety merits some additional discussion. A CANDU reactor, for example, has positive CVR and will thus experience a significant power pulse in a large-break LOCA. Coupled transient analysis of a CANDU-6 predicts power pulses of 400% to 500% full power which are terminated by fast-acting shutdown systems [110]. These systems bring the reactor to shutdown conditions within two to three seconds of initiating the transient. The transient predicted in this work for the PT-SCWR show peak powers of 160% or less, so it's reasonable to postulate that

if a similarly capable shutdown system was deployed in the PT-SCWR the net energy deposited in the fuel in a large LOCA or LOFA would be significantly less than in a CANDU large LOCA. The requirements of a fast-acting shutdown system in the PT-SCWR will need to be established in future work.

5.3.3 Coupled Model Parametric Sensitivities

The models used in the study were, as detailed in Chapter 4, created with many assumptions and approximations. The purpose of this section is to establish how much the transient results are affected by some of the most uncertain model parameters and those parameters identified in literature as being especially impactful on coupled neutronics-thermalhydraulics simulations. For this study these have been identified as:

- Neutron interaction cross-sections
- Kinetics parameters
- Fuel-to-coolant heat transfer
- Fuel-clad gap conductance
- Fluid friction factor
- Time step size

Unfortunately, it was impractical or impossible to test that parametric sensitivity of some of the above. The effect of the chosen nuclear data library on lattice-level results is known to be significant, but generating reference cross-sections and the feedback database in DRAGON requires several thousand processor-hours [91]. The complete act of changing the data library (or even a single value within) and following through to new transient results requires an investment of over a month real time, and was thus deemed impractical. Another difficulty was that the single-phase friction factor calculation is locked by CATHENA as part of its recent extensions for supercritical water. This means that friction in supercritical flows is always calculated with the Chen friction factor and there are no provisions in the CATHENA input for modifying it. The remaining parameters could be tested relatively easily.

The most straightforward way of assessing parametric sensitivity is to execute the same transient multiple times while varying a single parameter and observe how the results change. This is not meant to be a true sensitivity analysis, but simply a source of insight in to how the transient results presented in the

previous section may be affected by uncertain modelling parameters. A single transient was thus selected for the sensitivity study: the flow rundown presented in Section 5.3.2.2. The flow rundown is a good general test because it includes a power excursion but the flow behaviour is not dominated by an aggressive pressure transient. This parametric sensitivity study will focus specifically on the magnitude of the power excursion.

5.3.3.1 Kinetics Parameters

The kinetics parameters used in the reference DONJON model (Table 4.11) were taken from an independent SCALE/TRITON calculation and used in every transient for each initial core state (i.e. BOC, MOC, EOC). Pencer, McDonald, and Anghel also evaluated the PT-SCWR core kinetics parameters, however, and presented core-averaged values for the three core states separately [111]. Since the kinetics parameters determine the time response of the core, it would be useful to see how the power pulse is affected. The BOC and EOC core states presented by Pencer et al. (Table 5.2) serve as convenient upper and lower bounds for the parametric test (the MOC state simply falls in between). Note that the reference kinetics parameters have an effective delayed neutron fraction of β = 2.82 mk, so the BOC and EOC data represent increases of approximately 19% and 25%, respectively.

Table 5.2: Kinetics parameters used in the sensitivity study

| | β = 3.35 mk | | β = 3.52 mk | |
Group	β_i	λ_i [s^{-1}]	β_i	λ_i [s^{-1}]
1	8.850×10^{-5}	0.0133000	9.890×10^{-5}	0.0133000
2	8.130×10^{-4}	0.0302000	8.390×10^{-4}	0.0304000
3	5.450×10^{-4}	0.1140000	5.620×10^{-4}	0.1140000
4	1.130×10^{-3}	0.3030000	1.180×10^{-3}	0.3030000
5	5.590×10^{-4}	0.8560000	5.820×10^{-4}	0.8530000
6	2.170×10^{-4}	2.7700000	2.600×10^{-5}	2.7100000

The power excursion transient is shown in Figure 5.63, and the plane-averaged axial profiles at the approximate time of the power peak are shown in Figure 5.64. As would be expected with higher effective delayed neutron fraction, the new kinetics parameters result in a slower power increase and also a lower peak

power. These differences are extremely small, however. On one hand this indicates that the transient results are only weakly sensitive to the kinetics parameters within a reasonably expected variance. On the other, this suggests that the shape of the power pulse is dominated by the thermal characteristics and cross-section feedbacks rather than the kinetics response. Nevertheless, based on this result there is no reason to expect that the exact kinetics parameters are having any significant impact on the presented transient results.

5.3.3.2   Fuel-to-Coolant Heat Transfer

The heat transfer coefficient between the cladding surface and the coolant plays a significant role in determining the transient progression and is, according to literature, one of the most impactful model parameters subject to large uncertainty [112]. The CATHENA model is restricted to using the Dittus-Boelter correlation for determining the heat transfer coefficient under supercritical conditions, but CATHENA nevertheless allows a constant multiplier to be applied to the result.

Figure 5.65 shows the transient results when executed with 1.2 and 0.8 times the reference heat transfer coefficients (HTC). The peak of the power excursion is shown to be higher when the heat transfer coefficient is higher and lower when it is lower. Greater fuel-to-coolant heat transfer necessarily results in more heat being delivered to the coolant (lowering its density) and lower fuel temperatures, both of which have positive reactivity effects as reflected in the results. The magnitude of the power variation is quite small, however, when weighed against the imposed 20% difference on the heat transfer coefficient.

Figure 5.66 shows the average axial distributions during the power peak. Greater heat transfer clearly results in greater power being generated near the outlet, but there's relatively little difference closer to the inlet of the channel. The differences in coolant density are extremely small when weighed against the normal inlet-to-outlet variation in the channel, but differences in the fuel temperature are clearly visible near the outlet. The fact that even small changes in the coolant density have the highest marginal reactivity worth near the outlet, combined with the effect on the fuel temperature being largest near the outlet, explains the axial biases in these results.
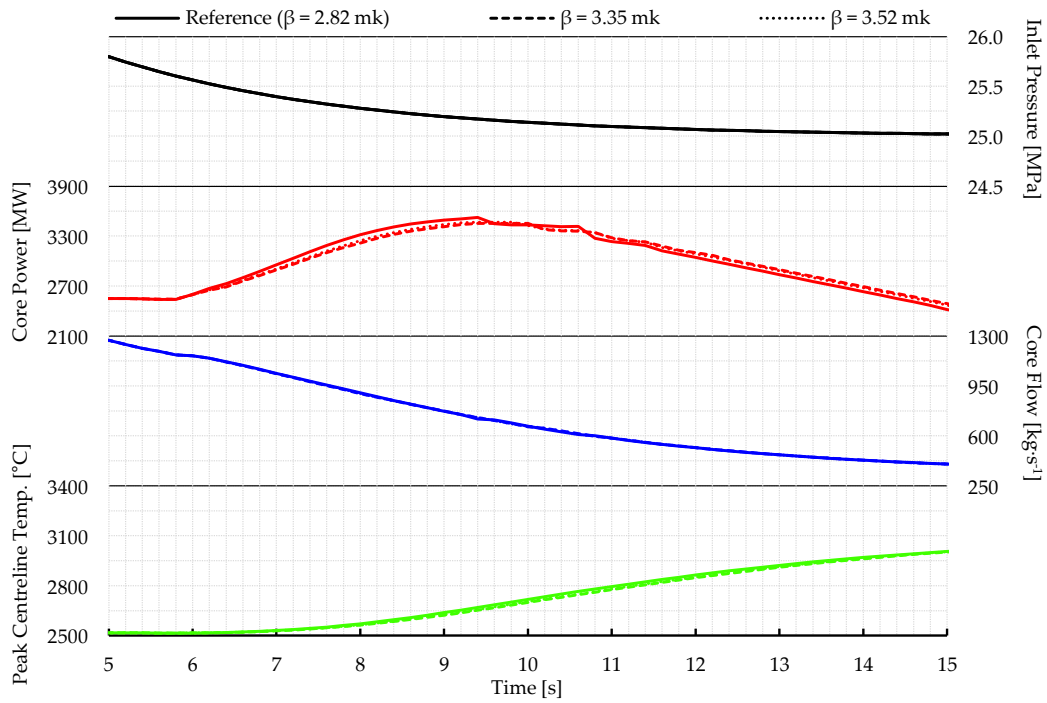
Figure 5.63: Power excursion transient with varied kinetics parameters
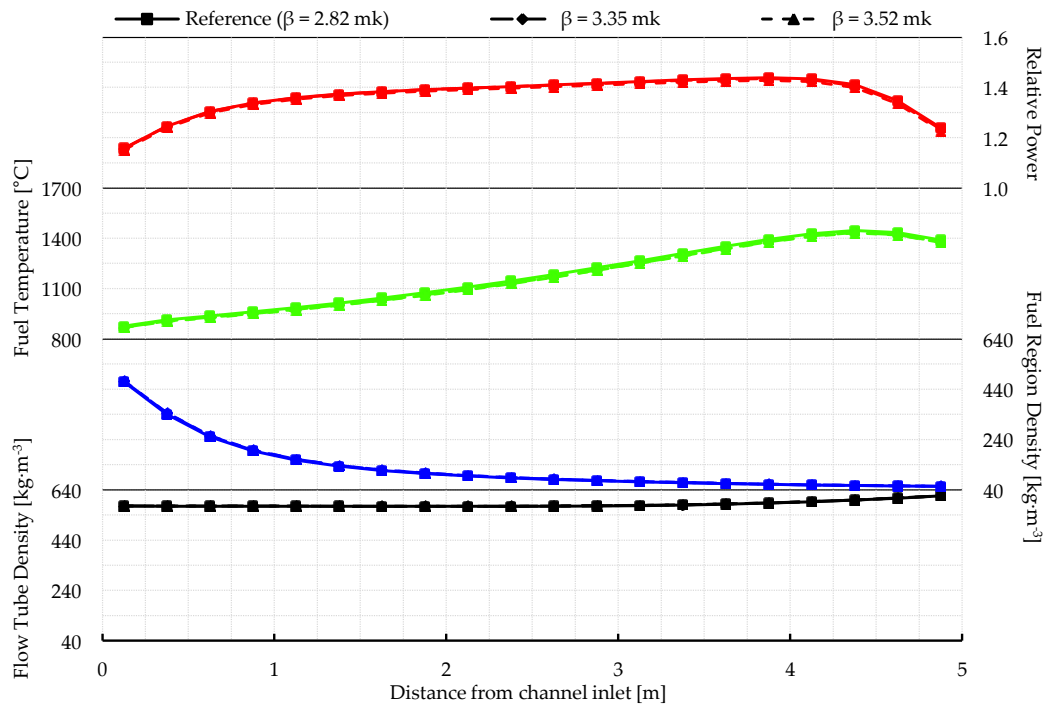
Figure 5.64: Peaked excursion profiles with varied kinetics parameters
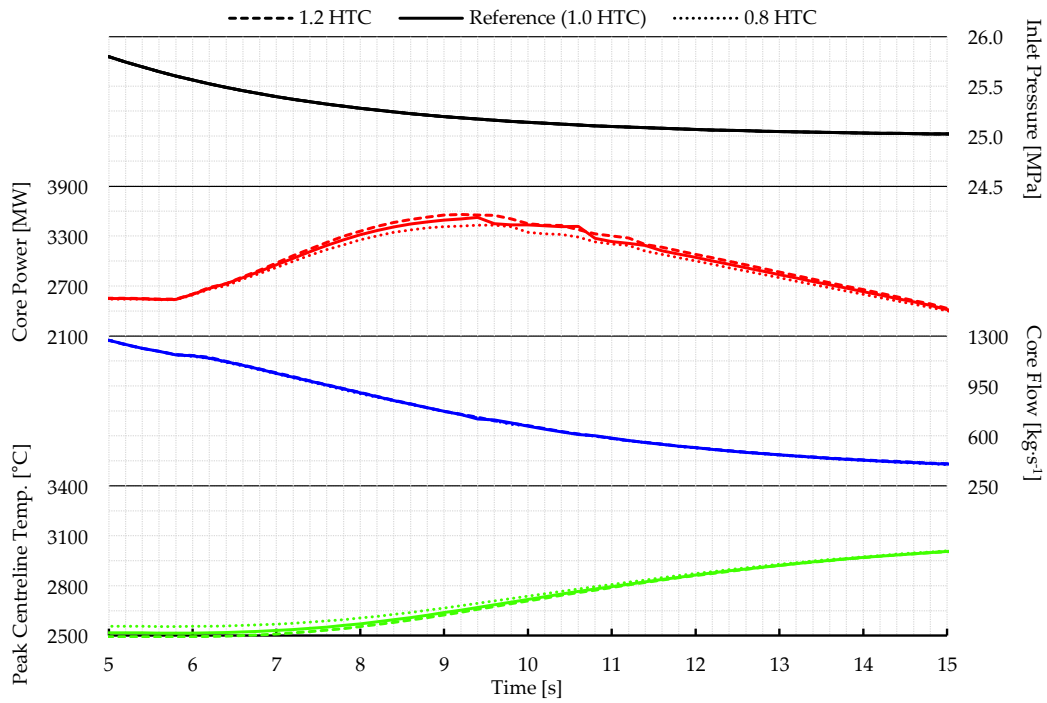
Figure 5.65: Power excursion transient with varied heat transfer coefficient
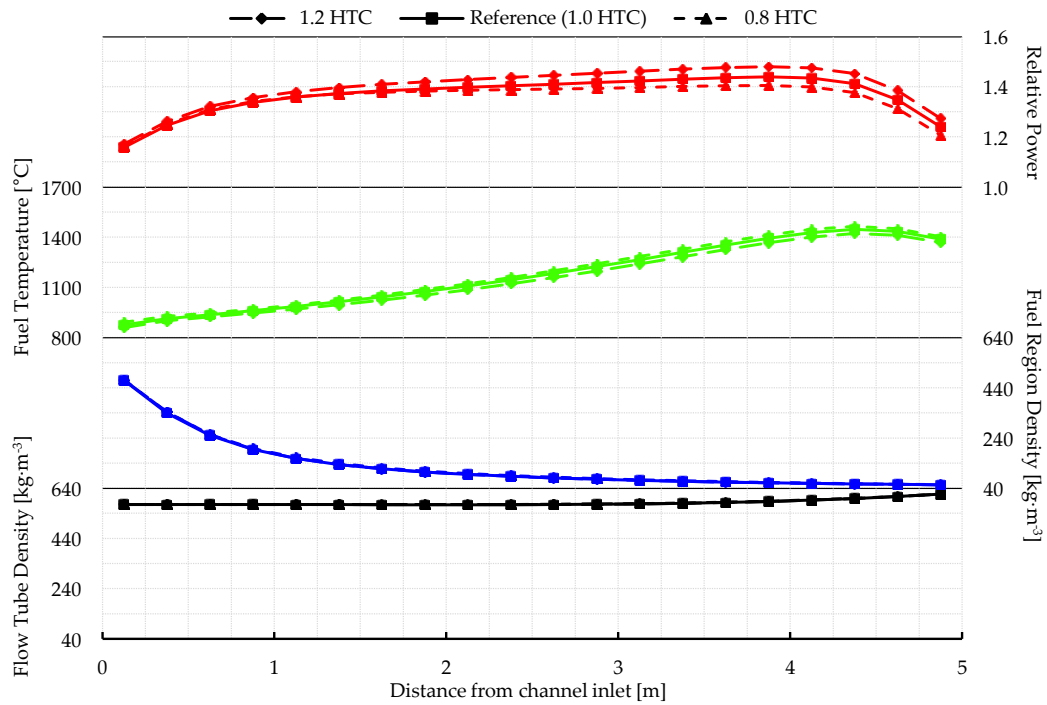
Figure 5.66: Peaked excursion profiles with varied heat transfer coefficient

This implies that the difference in the total core power is the result of variations in local power at a single location (the channel outlet, in this case) rather than a global change to the reactor power. While the sensitivity of the integral core parameters (e.g. total core power, total flow, etc.) to the heat transfer coefficient are almost negligible within the chosen variance (± 20%), the same cannot be said of the extremal values (e.g. peak node power, peak fuel centreline temperature, etc.) found near the channel outlet in the selected transient. This result underlines the need for three-dimensional spatial kinetics in modeling the PT-SCWR.

5.3.3.3   Fuel-Clad Gap Conductance

The fuel cladding of the PT-SCWR is intended to be collapsible, so there is no specification for a "gas gap" between fuel and cladding in the reference conceptual design. In coupled BWR models (which were the basis for this study methodology), however, prediction of heat transfer across the gas gap is an extremely important part of simulating any transient. The CATHENA model created for this work included a small gas gap modelled with a thermal conductance, but in the reference model the conductance was extremely high (50,000 $W \cdot m^{-2} \cdot °C^{-1}$) to represent the cladding being in contact with the fuel. This value could easily be adjusted for parametric sensitivity study.

Figure 5.67 shows the flow rundown transient executed with two additional gap models: one with a realistic value of gap conductance (8,000 $W \cdot m^{-2} \cdot °C^{-1}$, which is typical of pressurized LWR fuel), and one with no gap at all [103]. The most notable variations are in the magnitude of the power excursion and the peak fuel centreline temperature (approximately +300 °C with the realistic gap model), but the other parameters (including the axial distribution in Figure 5.68) show little sensitivity to the gap model.

It's intuitive to relate changes in the gap model to variations in the total fuel-to-coolant heat transfer coefficient. For example, with low gap conductance less heat can be delivered from the fuel to the cladding, and in turn less heat from cladding to coolant. The fuel temperatures shown reflect this. It then follows that some variation in the convective heat transfer coefficient should have some associated variation in gap conductance that has equivalent effect on the fuel temperatures.
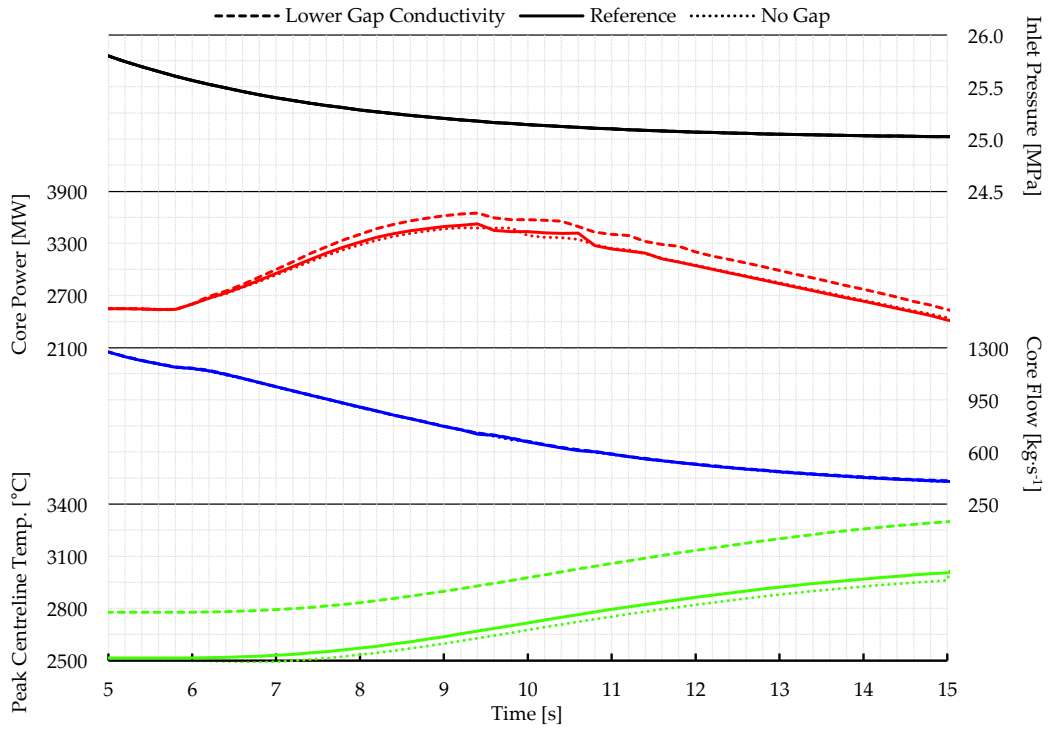
Figure 5.67: Power excursion transient with varied gap conductance
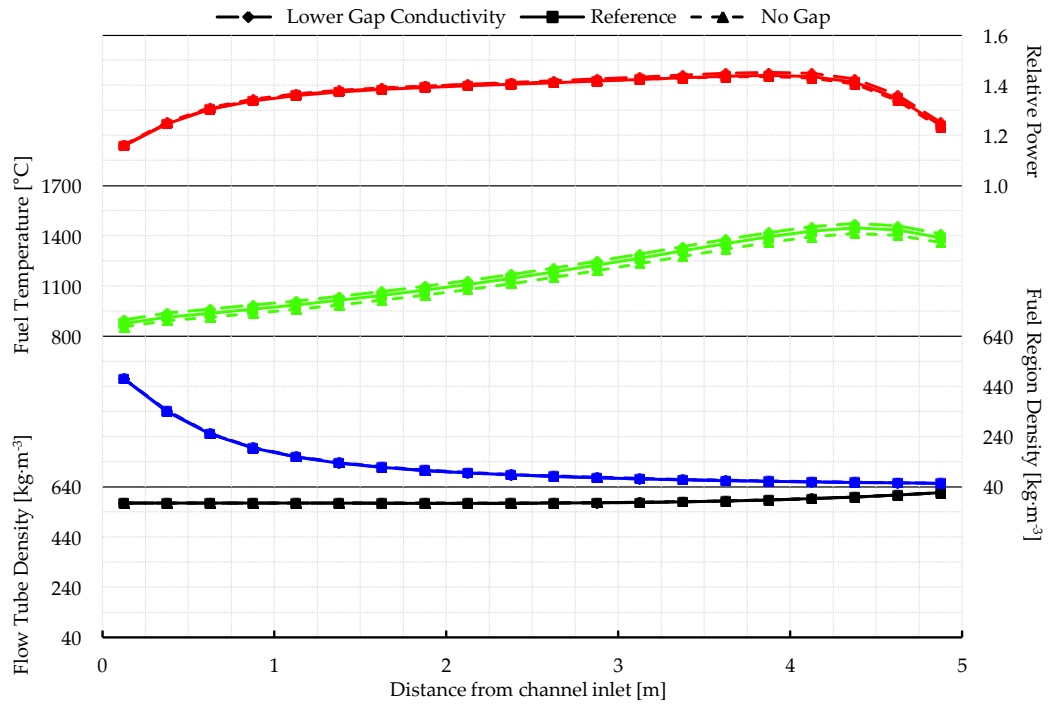
Figure 5.68: Peaked excursion profiles with varied gap conductance

Nevertheless, the case with no gap shows lower powers during the transient, and with lower gap conductance the power is higher. The sensitivity of the power transient to the gap conductance is then seemingly the *opposite* of varying the convective heat transfer coefficient to the same effect on fuel temperature.

The effect of the initial conditions on the transient results can't be ignored, however. It would have been incorrect to create an initial condition (using the procedure described in 4.3.2) with the reference gap conductance and then use a new value for the transient. Rather, the initial condition must be created with the perturbed value, so the initial equilibrium property distributions for each transient are necessarily different as well (but still under the constraint of a 625 °C coolant outlet temperature). Such variations in the transient power, with all the effects that come from having different initial conditions, cannot be so easily related to the relatively large magnitude variations in gap conductance that were imposed. It is reasonable to conclude that the transient results are sensitive to the value of gap conductance, but it is difficult to isolate the effect from the variation in initial conditions. On a side note, the sensitivity to the initial distribution of local parameters further underlines the need for the three-dimensional spatial kinetics as implemented in this study.

5.3.3.4   Time Step Size Selection

As described in Section 4.3.3, the time step size in transient calculations is dynamically selected according to the rate of change in node powers, and thus may assume several different values during a single transient. The reference calculation varied the step size by a factor of 0.50 or 2.00 if the decrease or increase criteria were respectively met. In order to assess the sensitivity of the results to the time step size, the magnitude of the size variation was decreased to 0.67/1.50 and increased to 0.33/3.00, thus ensuring different time steps during the transient. The results of these variations are shown in Figure 5.69 and Figure 5.70. There is practically no deviation from the reference calculation apart from a slight variance around the peak of the power excursion. The solution is evidently most sensitive to the temporal discretization around the extremal values of power (i.e. at the peak of the pulse), but the observable differences are objectively small (less than 2%). The sensitivity to the temporal discretization was thus judged to be small with the range of time step sizes studied.
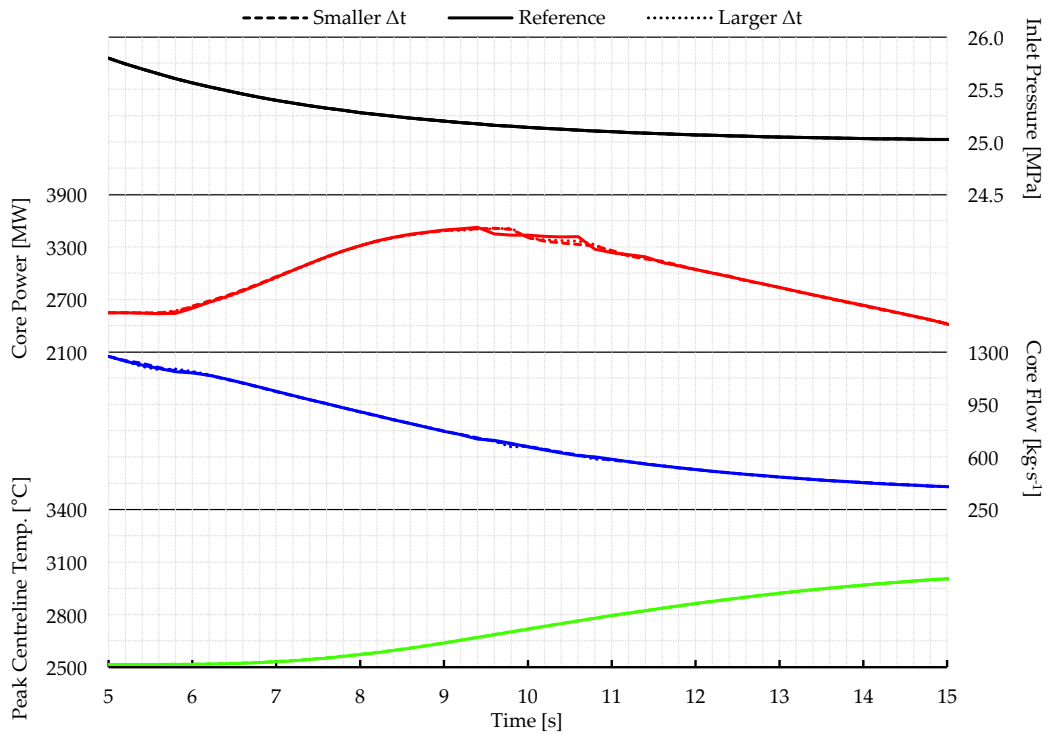
Figure 5.69: Power excursion transient with varied time step size
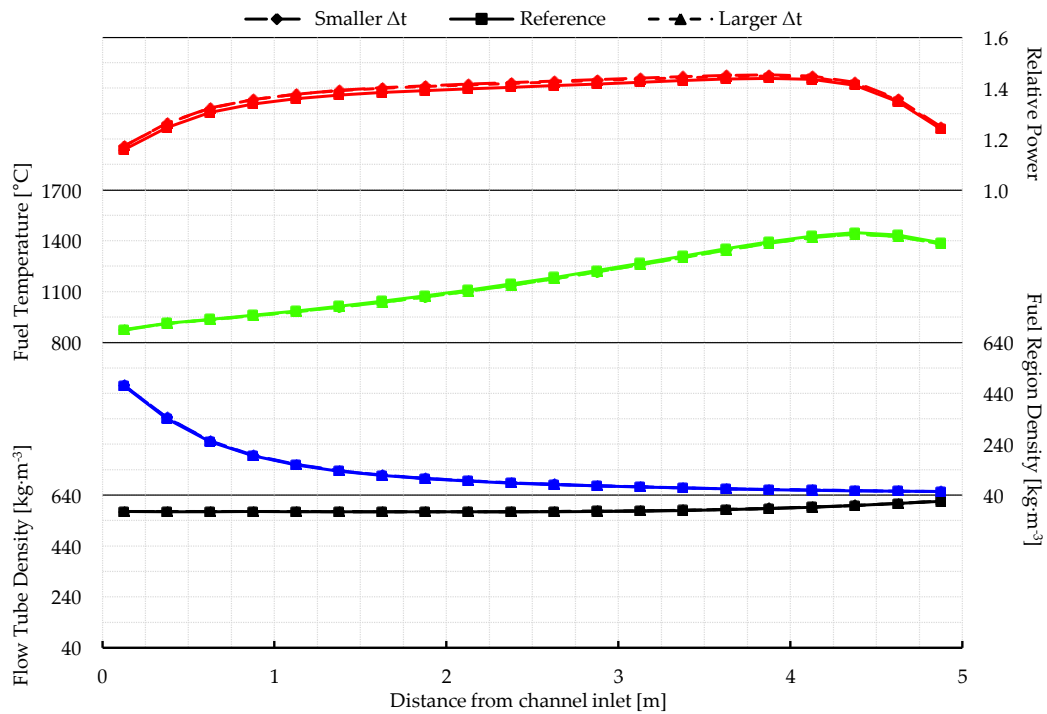
Figure 5.70: Peaked excursion profiles with varied time step size

Chapter 6

Conclusions and Recommendations

This dissertation presented the means and methods in which a coupled neutronics-thermalhydraulics model of the PT-SCWR concept was created and used for safety-related transient analyses. To accomplish the goals set forth in Chapter 1, the physics modelling included multiple coolant reactivity feedbacks coupled to individual hydraulic paths. Such models are unique to this study. The results of these analyses lead to several conclusion on the coupled stability and transient behaviour of the PT-SCWR core in specific accident-like conditions, which are summarized here. This chapter also contains recommendations for future analysis as well as a brief summary of the novel contributions to knowledge generated over the course of this work.

6.1 Summary of Study Methodology

Chapter 1 and Chapter 2 of this thesis introduced the Generation IV PT-SCWR concept and, through the large expected coolant density variation and negative CVR, its similarity to contemporary BWRs. This introduced the possibility that the PT-SCWR concept could experience BWR-like coupled neutronic-thermalhydraulic transients, most notably unstable oscillations in core power and flow, which potentially threaten the safety of the reactor. A literature review found that such transients were also a concern in other SCWR concepts, prompting substantial study (both computational and experimental) on coupled transients and stability. The PT-SCWR, as an evolution of the CANDU reactor, has a substantially different design pedigree than these other SCWR concepts which, in addition to several other design features (most notably the multiple coolant flow paths within the channel), affects the determinant physics and postulated transient progression. The purpose of this study was thus to model

178

the coupled transient behaviour of the PT-SCWR for both stability and other transient analyses related to reactor safety.

Given the similarities between the PT-SCWR concept and BWRs, it was decided that commonly accepted BWR modelling and analysis methodology would be the basis for studying the PT-SCWR. The state-of-the-art in BWR stability analysis is core-level coupled neutron diffusion (with spatial kinetics) and individual channel thermalhydraulics models (the fundamental theory behind neutronics and thermalhydraulics modelling was described in Chapter 3 of this thesis). In the coupled model created for this study the core diffusion and kinetics calculation was performed by the DONJON computer code, and the channel thermalhydraulics by CATHENA. DRAGON was used to model lattice-level neutron transport and create homogenized cross-sections and a thermalhydraulic feedback database for input to DONJON. A novel method for passing information between the disparate DONJON and CATHENA computer codes was implemented as part of the transient code-coupling procedure. These models were described in Chapter 4.

Transients were initiated by modifying the core inlet and outlet boundary conditions within the thermalhydraulics model (i.e. coolant pressure and temperature), thereby creating power transients from the cross-section feedback. For testing coupled stability the imposed transients included brief property perturbations (to see if and how the reactor would return to its original state), step changes to new values (to see if and how the reactor would attain a new steady state), and sinusoidal time-functions (to impose oscillations on the reactor). The inlet and outlet pressure boundary conditions were also used to initiate flow transients evocative of accident scenarios in the PHTS, including (stylized) large-break LOCAs and LOFAs, in order to study the coupled behaviour of the PT-SCWR in transients without reactor shutdown. Results and analysis for these simulated transients were presented in Chapter 5.

6.2   Conclusions from the Coupled Analysis

Several conclusions can be drawn from the results and analysis presented in Chapter 5. These are organized under the umbrellas of "coupled stability" and other "coupled transient" analysis in this section (similar to the structure of Chapter 5).

6.2.1 On the Potential for Coupled Instabilities in the PT-SCWR

This study found no evidence that BWR-like coupled instabilities or core power-flow oscillations could occur in the current PT-SCWR conceptual design. Under the prescribed test conditions it was observed that:

- The core returns to its initial state if the PHTS boundary conditions are briefly perturbed. There will be a short power transient (upward or downward according to the initiating parameter change) but no oscillatory behaviour.
- The core will typically attain a new steady power after a step-change in the boundary conditions that corresponds to the new thermalhydraulic parameters. The only exception is if the initial step change has too large of a reactivity worth to be countered by opposing feedbacks. In such a case the core power ramp will accelerate from the reactivity feedback cascade unless acted upon by a control system or additional changes to the PHTS. Because of this the PT-SCWR can't be considered *unconditionally* stable under the strictest definitions of stability (as presented in Section 2.2), but there remains no evidence of *dynamic* instability (e.g. naturally occurring power and flow oscillations).
- If oscillations are imposed by sinusoidal variations in the thermalhydraulic boundary conditions, the power response in the core is significantly attenuated by the reactor kinetics and thermal response (i.e. inertia) of the system. It's reasonable to conclude that the core power will be effectively stable in the presence of minor parameter "noise" in the PHTS.

Despite the aforementioned similarities between the PT-SCWR concept and BWRs, the lattice physics results show that there are unique features of the PT-SCWR fuel channel design that make BWR-like oscillations unlikely. While the reactivity worth of voiding the entire channel is negative (as required), with multiple flow paths like in the current HERC configuration the void reactivity exclusively around the fuel is positive. Additional heat being delivered from the fuel to the coolant, decreasing its density near the fuel, thus has the opposite reactivity effect as in a BWR. One of the necessary drivers for power and flow oscillations is thus removed. It can be concluded that the PT-SCWR is inherently stable with respect to dynamic BWR-like coupled oscillations.

6.2.2   On Coupled Transients Initiated by Perturbations in the PHTS

The fact that the void reactivity is positive around the fuel introduces the possibility of coupled transients where changes in the PHTS result in rapid positive power excursions, potentially requiring safety system intervention similar to CANDU designs. In the imposed PHTS transients it was found that:

- Flow reductions will result in a power transient as positive reactivity is added from the accompanying coolant density decrease. In the most extreme transient modelled in this work the power peaked at 160% of the nominal value.
- In a LOCA-like or LOFA transient without reactor shutdown the power transient will be arrested by low density fluid eventually reaching the centre flow tube. The negative reactivity resulting from decreased coolant density in the centre flow tube is large enough that in most cases the reactor will essentially shut itself down within seconds of initiating the power transient.
- Transients with flow reversal possess higher peak powers but are shorter lived since low density coolant reaches the centre flow tube faster. In transients where there is no reverse flow, heat conduction through the flow tube pipe wall is sufficient to lower the centre coolant density and provide large negative reactivity.

Generally speaking, the configuration of multiple flow paths within the current HERC concept creates a situation where power excursions can be initiated by perturbations in the PHTS, but such transients are inherently self-terminating (i.e. the reactor will be pushed deeply sub-critical within several seconds without action by a control or shutdown system). The integrated energy deposition in the fuel and peak material temperatures in such transients will need to be studied in more detail to establish the requirements of a fast-acting shutdown system. The peak powers found in this work were significantly lower and the power ramps slower than in similar transients in a PHWR, however, so it's reasonable to assume that a CANDU-like fast-acting shutdown system would be capable of arresting any power excursion without detrimental effects to the fuel integrity.

6.3 Recommendations for Future Work

PT-SCWR conceptual development is an ongoing project with many participants at research institutions and universities. Based on the conclusions of this study and the experience gather in modelling the current PT-SCWR concept, several recommendations are made for future work.

6.3.1 Improvements to the Computer Code Toolset

The modelling methodology described in Chapter 4 includes several instances where the fidelity of the model or the scope of the transient tests was limited by the capability of the selected toolset (DRAGON/DONJON and CATHENA). These limitations were considered when designing the current study, so the presented results and conclusions are valid within their intended scope. Nevertheless, there are several areas where the toolset could be improved specifically for PT-SCWR analysis:

- In DRAGON/DONJON, the CFC/AFM modules could be extended to include additional coolant feedbacks rather than relying on centre flow tube variations to be calculated as "moderator" feedbacks. This would allow the real heavy water moderator (outside the pressure tube) to change during coupled transients.
- In DRAGON/DONJON, the CFC/AFM modules could be extended to include additional branch cases for the insertion and removal of control rods within the lattice cell. This would be similar to how control devices are modelled for coupled analysis in other 3D neutron diffusion codes (e.g. PARCS) [77].
- The AFM module in DONJON could be extended to accept time input for calculating true time-dependent concentrations of important fission and activation products rather than immediately stepping to saturated concentrations.
- Dedicated heat transfer and friction correlations for supercritical water could be added to CATHENA.
- CATHENA should be able to reliably cross from supercritical to subcritical water during transients.

6.3.2   Extensions to the Coupled Steady-State and Transient Models

There are several ways in which the coupled DONJON and CATHENA models created for this study could be extended to perform other steady-state and transient analyses. Some features of the PT-SCWR concept were omitted from the models because they were irrelevant to the coupled stability and flow-induced transients studied in this work, and would have added needless complexity to already large models. Potential areas for expansion in the models include:

- The addition of reactivity hold-down and power-levelling control devices to the DRAGON and DONJON models: If movable control rods and/or burnable neutron absorbers are going to play a role in levelling the channel power variations during a batch cycle, then these devices should be included in the models. No such mechanisms were part of the reference PT-SCWR conceptual design during the course of this work, but their requirements were inferred from the steady-state core diffusion results. This study used artificial variable inlet orifices for channel flow-power matching when generating each initial steady-state, but fixed orifices could be used if the channel powers were controlled in such a manner.
- Additional components in the CATHENA model: The CATHENA model could be extended to include radiation heat transfer within the channels as well as out-of-core components (rather than inlet/outlet boundary conditions) including control valves and potentially pumps and turbines. This would facilitate higher fidelity safety analysis for coupled transients including realistic LOCAs.

6.3.3   PT-SCWR 64-Element Fuel Neutronics Sensitivity Study

In Chapter 5 several conjectures on the causes of the positive CVR and its relation to axial position and burnup were made based on information that could be gleaned from a set of lattice-level benchmark calculations. A thorough examination of isotopic-specific reactions rates and flux spectra effects, or a true sensitivity analysis performed with a robust computational tool like TSUNAMI (part of the SCALE code package), would yield much more useful information on the various contributors and their relative magnitudes. Furthermore, a mechanistic understanding of the relevant processes would positively impact the

conceptual design process for PT-SCWR fuel by limiting the future reliance on heuristic parameter optimization.

6.3.4 PT-SCWR Conceptual Design Features

The transient results presented in this work illustrate several features of the current PT-SCWR concept that deserve serious consideration from the designers. Since power excursions have been demonstrated in LOCA-like and LOFA transients, the requirements for a fast-acting shutdown system require additional analysis. It's not clear that the fuel channel concept could be modified in such a way that the power excursions are eliminated without reintroducing the possibility of BWR-like coupled power-flow oscillations. A comprehensive multivariable optimization of the fuel design that minimizes the magnitude of potential power excursions while still eliminating instabilities should be performed.

If the temporary positive reactivity insertion from flow transients is deemed acceptable, then heat transfer through the centre flow tube pipe wall should be considered in the PT-SCWR safety design for postulated accidents without reactor shutdown. For example, a thermal insulating layer on the flow tube would reduce heat flow to the centre coolant in certain transients, delaying the time at which negative reactivity is added from the coolant density decrease and potentially extending a power pulse.

6.4 Contributions to Knowledge

In this context, "contributions to knowledge" include the novel methods and results of this work as well as the additions to peer-reviewed scientific literature. This section summarized the various achievements over the course of this study.

6.4.1 Core-Level Coupled Modelling of the PT-SCWR Concept

This work represents the first attempt at core-level coupled transient (i.e. spatial kinetics and thermalhydraulics) modelling of the current PT-SCWR concept. The re-entrant channel design contains two quasi-independent coolant feedbacks that had to be incorporated in to the model, as opposed to typical core-level (CANDU or LWR) coupled transient models that contain only a single coolant density feedback. The model created for this work (achieved with some modification to the source code) is among the first to incorporate multiple coolant feedbacks in

core-level coupled spatial kinetics and thermalhydraulics transient analysis, and is the only model capable of modelling such transients in the PT-SCWR.

Regarding the coupling, this work was among the first to couple the DONJON and CATHENA computer codes for modelling core-level spatial kinetics and thermalhydraulics. This required creation of specialized scripts and programs that processed the input and output of each to facilitate passing information between two codes that were designed to be coupled together.

Using this newly created coupled model, this work was able to answer the question of the PT-SCWR concept's inherent coupled stability by executing several transient tests that attempted to instigate BWR-like coupled power and flow oscillations. It was demonstrated that the multiple flow paths in the channel design (specifically the positive coolant void reactivity in the outer/fuel region) make the concept immune to such oscillations and instability.

This work also demonstrated that certain flow transients in the PHTS, such as those that occur during a LOCA or LOFA, result in power pulses from the positive void reactivity in the outer/fuel region. It would not have been possible to simulate such transients without the unique coupled model (with two independent coolant feedbacks) created for the aforementioned stability study.

6.4.2 Peer-Reviewed Publications and Presentations

Contributions to the greater PT-SCWR conceptual development project were made steadily through the course of this work. This is best illustrated by listing the different peer-reviewed studies presented at international conferences and workshops on SCWR design and development.

6.4.2.1 Full Core Modelling and Code Coupling

These studies examined the steady-state and transient coupling of core-level models (using DONJON and CATHENA) for PT-SCWR conceptual design optimization and simulation of coupled transients:

1. **D. W. Hummel** and D. R. Novog, "Optimized Channel Inlet Orifice Sizing for the Pressure Tube type Supercritical Water-Cooled Reactor," in *The 19th Pacific Basin Nuclear Conference (PBNC-2014)*, Vancouver, Canada, 2014.

2. **D. W. Hummel** and D. R. Novog, "Coupled 3D Neutron Kinetics and Thermalhydraulic Characteristics of the Canadian SCWR," in *The 7th International Symposium on Supercritical Water-Cooled Reactors (ISSCWR-7)*, Helsinki, Finland, 2015.

3. **D. W. Hummel** and D. R. Novog, "Coupled 3D Neutron Kinetics and Thermalhydraulic Characteristics of the Canadian Supercritical Water Reactor", submitted to *Nuclear Engineering and Design*, June 2015.

4. **D. W. Hummel** and D. R. Novog, "Coupled Spatial Kinetics and Thermalhydraulics Analysis of Postulated Primary Heat Transport System Accidents in the Canadian Supercritial Water Reactor," to be submitted to *Nuclear Engineering and Design*, 2015.

6.4.2.2   Lattice Physics Modelling Methodology

These studies focused on establishing the correct procedures for modelling the PT-SCWR lattice cell, as well as determining the capabilities and limitations of the available simulation tools:

5. M. G. Scriven, **D. W. Hummel**, D. R. Novog, and J. C. Luxat, "Analysis of the Impact of Coolant Density Variations in the High Efficiency Channel of a Pressure Tube Super Critical Water Reactor," in *The 3rd China-Canada Joint Workshop on Supercritical-Water-Cooled Reactors (CCSC-2012)*, Xi'an, China, 2012.

6. **D. W. Hummel**, S. E. Langton, M. R. Ball, D. R. Novog, and A. Buijs, "Description and Preliminary Results of a Two-Dimensional Lattice Physics Code Benchmark for the Canadian Pressure Tube Supercritical Water-cooled Reactor (PT-SCWR)," in *The 6th International Symposium on Supercritical Water-Cooled Reactors (ISSCWR-6)*, Shenzhen, China, 2013.

    a. Also presented in *The 33rd Annual Conference of the Canadian Nuclear Society*, Toronto, Canada, 2013.

7. F. Salaun, **D. W. Hummel**, and D. R. Novog, "The Impact of the Radial Reflector on the 8-Group Cell-Averaged Cross-Sections for the SCWR 62-element Lattice Cell" in *2014 Canada-China Conference on Advanced Reactor Development (CCCARD-2014)*, Niagara Falls, Canada, 2014.

8. J. Sharpe, F. Salaun, **D. W. Hummel**, A. Moghrabi, M. Nowak, J. Pencer, D. R. Novog, and A. Buijs, "A Benchmark Comparison of the Canadian Supercritical Water-cooled Reactor (SCWR) 64-element Fuel Lattice Cell

Parameters using Various Computer Codes" in *The 35th Annual Conference of the Canadian Nuclear Society*, Saint John, Canada, 2015.

6.4.2.3   Supercritical Fluid Flow Instabilities

This study examined the purely thermalhydraulic instabilities of supercritical flows in heated channels to determine the similarities and differences to boiling channels in numerical models:

9. K. H. Leung, S. E. Langton, **D. W. Hummel**, and D. R. Novog, "Modelling of Flow Instabilities Under Supercritical Conditions," in *The 5th International Symposium on Supercritical Water-Cooled Reactors (ISSCWR-5)*, Vancouver, Canada, 2011.

6.4.2.4   PT-SCWR Design Optimization

These studies applied non-parametric analysis and heuristic optimization algorithms to the PT-SCWR fuel (both the fuel isotopic composition and geometry) and control system design:

10. **D. W. Hummel** and D. R. Novog, "Non-Parametric Study on the Optimization of Thorium Content in a 54-element Fuel Bundle for use in a CANDU-SCWR," in *The 32nd Annual Conference of the Canadian Nuclear Society*, Niagara Falls, Canada, 2011.
11. **D. W. Hummel** and D. R. Novog, "Optimization of Thorium-Uranium Content in a 54-element Fuel Bundle for use in a CANDU-SCWR," in *International Conference on Future of Heavy Water Reactors (HWR-Future)*, Ottawa, Canada, 2011.
12. **D. W. Hummel** and D. R. Novog, "Fuel Composition Optimization in a 78-Element Fuel Bundle for use in a Pressure Tube type Supercritical Water-Cooled Reactor," in *The 3rd China-Canada Joint Workshop on Supercritical-Water-Cooled Reactors (CCSC-2012)*, Xi'an, China, 2012.
13. F. Salaun, J. R. Sharpe, **D. W. Hummel**, A. Buijs, and D. R. Novog, "Optimization of the PT-SCWR Control Blade Sequence using PARCS and DAKOTA", in *The 7th International Symposium on Supercritical Water-Cooled Reactors (ISSCWR-7)*, Helsinki, Finland, 2015.

References

[1] J. F. Ahearne, "Prospects for nuclear energy," *Energy Economics,* vol. 33, pp. 572-580, 2011.

[2] World Nucear Association, "Number of nuclear reactors," 2014. [Online]. Available: www.world-nuclear.org/Nuclear-Basics/Global-number-of-nuclear-reactors/. [Accessed 12 September 2014].

[3] World Nuclear Association, "Electricity supplied by nuclear energy," 2014. [Online]. Available: www.world-nuclear.org/Nuclear-Basics/Electricty-supplied-by-nuclear-energy/. [Accessed 12 September 2014].

[4] J. A. Lake, "The Fourth Generation of Nuclear Power," *Progress in Nuclear Energy,* vol. 40, no. 3-4, pp. 301-307, 2002.

[5] U.S. DOE Nuclear Energy Research Advisory Committee and the Generation IV International Forum, "A Technology Roadmap for Generation IV Nuclear Energy Systems," 2002. [Online]. Available: https://www.gen-4.org/gif/jcms/c_40481/technology-roadmap. [Accessed June 2014].

[6] National Sciences and Engineering Research Council of Canada, "NSERC/NRCan/AECL Generation IV Energy Technology Grants," July 2012. [Online]. Available: http://www.nserc-crsng.gc.ca/professors-professeurs/rpp-pp/geniv-geniv_eng.asp. [Accessed May 2014].

[7] T. Abram and S. Ion, "Generation-IV nuclear power: A review of the state of the science," *Energy Policy,* vol. 36, pp. 4323-4330, 2008.

[8] Nuclear Energy Agency, "GIF Symposium Proceedings," Organization for Economic Co-operation and Development, San Diego, USA, 2012.

[9] D. F. Torgerson, B. A. Shalaby and S. Pang, "CANDU technology for Generation III+ and IV reactors," *Nuclear Engineering and Design,* vol. 236, pp. 1565-1572, 2006.

[10] P. G. Boczar, W. Shen, J. Pencer, B. Hyland, P. S. W. Chan and R. G. Dworshak, "Reactor Physics Studies for a Pressure Tube Supercritical Water Reactor (PT-SCWR)," in *The 2nd Canada-China Joint Workshop on Supercritical Water-Cooled Reactors (CCSC-2010)*, Toronto, 2010.

[11] J. Pencer and A. Colton, "Progression of the Lattice Physics Concept for the Canadian Supercritical Water Reactor," in *34th Annual Conference of the Canadian Nuclear Society*, Toronto, 2013.

[12] M. Yetisir, M. Gaudet and D. Rhodes, "Development and Integrationn of Canadian SCWR Concept With Counter-Flow Fuel Assembly," in *The 6th International Symposium on Supercritical Water-Cooled Reactors (ISSCWR-6)*, Shenzhen, Guangdong, China, 2013.

[13] L. K. H. Leung, "Developing the Canadian SCWR Concept for Addressing GIF Design Goals," in *The 3rd China-Canada Joint Workshop on Supercritical-Water-Cooled Reactors (CCSC-2012)*, Xi'an, China, 2012.

[14] D. Brady, T. Anderson, D. Guzonas, H. Khartabil, L. Leung, S. Quinn and W. Zheng, "Canada's NSERC/NRCan/AECL Generation IV Energy Technologies Program," in *30th Annual Conference of the Canadian Nuclear Society*, Calgary, 2009.

[15] J. Licht, M. Anderson and M. Corradini, "Heat transfer to water at supercritical pressures in a circular and square annular flow geometry," *International Journal of Heat and Fluid Flow,* vol. 29, no. 1, pp. 156-166, 2008.

[16] G. Harrison and G. Marleau, "Simulation Strategy for the Evaluation of Neutronic Properties of a Canadian SCWR Fuel Channel," *Science and Technology of Nuclear Installations,* 2013.

[17] P. Yang, L. Cao, H. Wu and C. Wang, "Core design study on CANDU-SCWR with 3D neutronics/thermal-hydraulics coupling," *Nuclear Engineering and Design,* vol. 241, no. 12, pp. 4714-4719, 2011.

[18] L. Monti, J. Starflinger and T. Schulenberg, "Development of a coupled neutronic/thermal-hydraulic tool with multi-scale capabilities and applications to HPLWR core analysis," *Nuclear Engineering and Design,* vol. 241, pp. 1579-1591, 2011.

[19] W. Ambrosini, "On the analogies in the dynamic behaviour of heated channels with boiling and supercritical fluids," *Nuclear Engineering and Design,* vol. 227, pp. 1164-1174, 2007.

[20] W. Ambrosini, "Discussion of the stability of heated channels with different fluids at supercritical pressures," *Nuclear Engineering and Design,* vol. 239, pp. 2952-2963, 2009.

[21] J. March-Leuba and T. L. Huang, "A Review of the Physical Phenomena that Impact the Stability of BWRs, invited," *Transactions of the American Nuclear Society,* vol. 99, pp. 732-733, 2008.

[22] W. Yang, "SCWR Stability Analysis," in *2nd SCWR Information Exchange Meeting,* University of Wisconsin - Madison, 2003.

[23] F. D'Auria, A. L. Costa and A. Bousbia-Salah, "The Boiling Water Reactor Stability," in *IAEA Course on Natural Circulation in Water-Cooled Nuclear Power Plants*, International Centre for Theoretical Physics (ICTP), Trieste, 2004.

[24] Y. Xu, T. Downar, R. Walls, K. Ivanov, J. Staudenmeier and J. March-Leuba, "Application of TRACE/PARCS to BWR stability analysis," *Annals of Nuclear Energy,* vol. 36, pp. 317-323, 2009.

[25] T. Kozlowski, T. Downar, Y. Xu, A. Wysocki, K. Ivanov, J. Magedanz, M. Hardgrove, I. Gajev, J. March-Leuba and N. Hudson, "Analysis of the OECD/NRC Oskarshamn-2 BWR Stability Benchmark," in *The 15th International Topica Meeting on Nuclear Reactor Thermal-Hydraulics (NURETH-15)*, Pisa, Italy, 2013.

[26] G. Marleau, A. Hébert and R. Roy, "A User Guide for DRAGON 3.06," Institut de génie nucléaire, Départment de génie physique, École Polytechnique de Montréal, Montréal, 2008.

[27] E. Varin, A. Hébert, R. Roy and J. Koclas, "A User Guide for DONJON Version 3.01," Institut de génie nucléaire, Départment de génie physique, École Polytechnique de Montréal, Montréal, 2005.

[28] B. N. Hanna, "CATHENA: a thermalhydraulics code for CANDU analysis," *Nuclear Engineering and Design,* vol. 180, pp. 113-131, 1998.

[29] K. Ehrlich, J. Konys and L. Heikinheimo, "Materials for high performance light water reactors," *Journal of Nuclear Materials,* vol. 327, pp. 140-147, 2004.

[30] S. Liu and J. Cai, "Neutronics assessment of thorium-based fuel assembly in SCWR," *Nuclear Engineering and Design,* vol. 260, pp. 1-10, 2013.

[31] K. Fischer, T. Schulenberg and E. Laurien, "Design of a supercritical water-

cooled reactor with a three-pass core arrangements," *Nuclear Engineering and Design*, vol. 239, pp. 800-812, 2009.

[32] T. Schulenberg, A. Vojacek, T. Zeiger and M. Raqué, "Risks and Safety Analyses of an SCWR Fuel Qualification Test Loop," in *The 6th International Symposium on Supercritical Water-Cooled Reactors (ISSCWR-6)*, Shenzhen, China, 2013.

[33] Y. Oka and S. Koshizuka, "Supercritical-pressure, Once-through Cycle Light Water Cooled Reactor Concept," *Nuclear Science and Technology,* vol. 38, no. 12, pp. 1081-1089, 2001.

[34] A. Yamaji, K. Kamei, Y. Oka and S. Koshizuka, "Improved core design of the high temperature supercritical-pressure light water reactor," *Annals of Nuclear Energy,* vol. 32, pp. 651-670, 2005.

[35] M. H. McDonald, B. Hyland, H. Hamilton, L. K. H. Leung, N. Onder, J. Pencer and R. Xu, "Pre-Conceptual Fuel Design Concepts for the Canadian Super Critical Water-Cooled Reactor," in *The 5th International Symposium on Supercritical Water-Cooled Reactors (ISSCWR-5)*, Vancouver, 2011.

[36] J. Pencer and B. Hyland, "Physics Aspects of the Pressure Tube Type SCWR Preconceptual Design," in *International Conference on Future of Heavy Water Reactors*, Ottawa, 2011.

[37] J. Pencer, M. Edwards and N. Onder, "Axial and Radial Graded Enrichment Options for the Canadian SCWR," in *The 3rd China-Canada Joint Workshop on Supercritical-Water-Cooled Reactors (CCSC-2012)*, Xi'an, China, 2012.

[38] J. Licht and R. Xu, "Prelinary No-Core Melt Assussment for the High Efficiency Channal Preconceptual Design," in *The 3rd China-Canada Joint Workshop on Supercritical-Water-Cooled Reactors (CCSC-2012)*, Xi'an, China, 2012.

[39] W. Liu, Y. Zhu, N. Bai, J. Shan and B. Zhang, "Coupled neutronics/thermal-hydraulics analysis of PT-SCWR fuel channel," in *The 6th International Symposium on Supercritical Water-Cooled Reactors (ISSCWR-6)*, Shenzhen, China, 2013.

[40] P. Adouki and G. Marleau, "Neutronics/Thermalhydraulics Coupling in a CANDU SCWR," in *The 3rd China-Canada Joint Workshop on Supercritical-Water-Cooled Reactors (CCSC-2012)*, Xi'an, China, 2012.

[41] P. Hu and P. P. H. Wilson, "Supercritical Water Reactor Steady-State,

Burnup, and Transient Analyses with Extended PARCS/RELAP5," *Nuclear Technology*, vol. 172, pp. 143-156, 2010.

[42] D. Grgic, "Basis for Coupling 3D Neutron-Kinetics/Thermal-Hydraulics Codes," in *Seminar and Training on Scaling, UNcertainty, and 3D COuPled calculations in nuclear technology (3D S.UN.COP 2008)*, Amsterdam, The Netherlands, 2008.

[43] J. A. Boure, A. E. Bergles and L. S. Tong, "Review of two-phase flow instability," *Nuclear Engineering and Design*, vol. 25, pp. 165-192, 1973.

[44] J. March-Leuba and J. M. Rey, "Coupled thermohydraulic-neutronic instabilities in boiling water reactors: a review of the state of the art," *Nuclear Engineering and Design*, vol. 145, pp. 97-111, 1993.

[45] H. Mochizuki, "Flow instabilities in boiling channels of pressure-tube-type reactor," *Nuclear Engineering and Design*, vol. 149, pp. 269-277, 1994.

[46] A. K. Nayak, P. K. Vijayan, D. Saha, V. Venkat Raj and M. Aritomi, "Analytical study of nuclear-coupled density-wave instability in a natural circulation pressure tube type boiling water reactor," *Nuclear Engineering and Design*, vol. 195, pp. 27-44, 2000.

[47] T. L. Huang and J. March-Leuba, "Boiling Water Reactor Stabiluity, a Regulatory Perspective, invited," *Transactions of the American Nuclear Society*, vol. 99, pp. 727-728, 2008.

[48] H. Ikeda, T. Fukahori, Y. Kubo, H. Soneda and S. Mizokami, "BWR Stability Issues in Japan," *Science and Technology of Nuclear Installations*, vol. 2008, 2008.

[49] G. M. Grandi, "Effect of the Discretization and Neutronic Thermal Hydraulic Coupling on LWR Transients," in *The 13th Internationl Topical Meeting on Nuclear Reactor Thermalhydraulics (NURETH-13)*, Kanazawa, Japan, 2009.

[50] T. Downar, "Coupled Neutronics and Thermal-Hyraulics Codes for Reactor Safety Analysis," in *Modeling-Experimentation-Validation, MeV Summer School*, Chicago, USA, 2011.

[51] B. Rouben, "CANDU Physics-Thermalhydraulics Code Coupling," in *Seminar and Training on Scaling, UNcertainty, and 3D COuPled calculations in nuclear technology (3D S.UN.COP 2007)*, Niagra Falls, Canada, 2007.

[52] D. Grgic, "Applications of 3D NK-TH Coupled Codes," in *Seminar and Traning on Scaling, UNcertainty and 3D COuPled calculations in nuclear technology (3D S.UN. COP 2008)*, Amsterdam, The Netherlands, 2008.

[53] T. Lefvert, "Ringhals 1 Stability Benchmark - Final Report," Nuclear Energy Agency - Organisation for Economic Co-operation and Development, 1996.

[54] United States Nuclear Regulatory Commission, "NRC: Computer Codes," 09 July 2014. [Online]. Available: http://www.nrc.gov/about-nrc/regulatory/research/safetycodes.html#th. [Accessed 28 July 2014].

[55] I. Gajev, W. Ma and T. Kozlowski, "Space-time convergence analysis on BWR stability using TRACE/PARCS," *Annals of Nuclear Energy*, vol. 51, pp. 295-306, 2013.

[56] T. van der Hagen, R. Zboray and W. de Kruijf, "Questioning the use of the decay ratio in BWR stability monitoring," *Annals of Nuclear Energy*, vol. 27, pp. 727-732, 2000.

[57] I. Gajev, W. Ma and T. Kozlowski, "Sensitivity analysis of input uncertain parameters on BWR stability using TRACE/PARCS," *Annals of Nuclear Energy*, vol. 67, pp. 49-58, 2014.

[58] I. Gajev, T. Kozlowski, Y. Xu and T. Downar, "Sensitivity and Uncertainty of the Neutronic Parameters of BWR Ringhals-1 TRACE/PARCS Stability Prediction," in *PHYSOS 2010 - Advances in Reactor Physics to Power the Nuclear Renaissance* , Pittsburgh, USA, 2010.

[59] W. Ambrosini and M. B. Sharabi, "Assessment of stability maps for heated channels with supercritical fluids versus the predictions of a system code," *Nuclear Engineering and Technology*, vol. 39, no. 5, pp. 627-636, October 2007.

[60] V. Chatoorgoon, "Stability of supercritical fluid flow in a single-channel natural-convection loop," *International Journal of Heat and Mass Transfer*, vol. 44, pp. 1963-1972, 2001.

[61] T. T. Yi, S. Koshizuka and Y. Oka, "A Linear Stability Analysis of Supercritical Water Reactors (I) Thermal-Hydraulic Stability," *Journal of Nuclear Science and Technology*, vol. 41, no. 12, pp. 1166-1175, 2004.

[62] J. Zhao, P. Saha and M. S. Kazimi, "Core-wide (in-phase) stability of supercritical water-cooled reactors-I: sensitivity to design and operating conditions," *Nuclear Technology*, vol. 161, pp. 108-123, 2008.

[63] T. T. Yi, S. Koshizuka and Y. Oka, "A Linear Stability Analysis of Supercritical Water Reactors (II) Coupled Neutronic Thermal-Hydraulic Stability," *Journal of Nuclear Science and Technology,* vol. 41, no. 12, pp. 1176-1186, 2004.

[64] J. Zhao, P. Saha and M. S. Kazimi, "Core-wide (in-phase) stability of supercritical water-cooled reactors-II: comparison with boiling water reactors," *Nuclear Technology,* vol. 161, pp. 124-139, 2008.

[65] J. Pan and J. Shan, "Stability Analysis of Supercritical Water Cooled Reactor," in *The 3rd China-Canada Joint Workshop on Supercritical-Water-Cooled Reactors (CCSC-2012),* Xi'an, China, 2012.

[66] C. T'Joen and M. Rohde, "Experimental study of the coupled thermo-hydraulic-neutronic stability of a natural circulation HPLWR," *Nuclear Engineering and Design,* vol. 242, pp. 221-232, 2012.

[67] D. Rozon, Introduction to Nuclear Reactor Kinetics, Montreal: École Polytechnique de Montréal International Press, 2000.

[68] J. J. Duderstadt and L. J. Hamilton, Nuclear Reactor Analysis, Ann Arbor: John Wiley & Sons, Inc., 1976.

[69] Brookhaven National Laboratory, "Evaluated Nuclear Data File(ENDF)," November 2011. [Online]. Available: http://www.nndc.bnl.gov/exfor/endf00.jsp.

[70] B. Rouben, "Fundamental Reactor-Physics Concepts," in *CANDU Reactor Physics Course,* Toronto, 2011.

[71] G. Marleau, "Lattice Physics - General," in *CANDU Reactor Physics Course,* Toronto, 2011.

[72] D. Altiparmakov, "New Capabilities of the Lattice Code WIMS-AECL," in *PHYSOR 2008 - International Conference on the Physics of Nuclear Reactors; Nuclear Power: A Sustainable Resource,* Interlaken, Switzerland, 2008.

[73] S. M. Bowman, "SCALE 6: Comprehensive Nuclear Safety Analysis Code System," *Nuclear Technology,* vol. 174, no. 2, pp. 126-148, 2011.

[74] X-5 Monte Carlo Team, "MCNP - A General Monte Carlo N-Particle Transport Code, Version 5," Los Alamos National Laboratory (LANL), Los Alamos USA, 2003.

[75] VTT Technical Research Centre of Finland, "Serpent - A Monte Carlo

Reactor Physics Burnup Calculation Code," 2014. [Online]. Available: montecarlo.vtt.fi. [Accessed 8 August 2014].

[76] B. Rouben, "RFSP-IST, the Industry Standard Tool Computer Program for CANDU Reactor Core Design and Analysis," in *The 13th Pacific Basin Nuclear Conference (PBNC-2002)*, Shenzhen China, 2002.

[77] T. Downar, Y. Xu, V. Seker and A. Ward, "PARCS: Purdue Advanced Reactor Core Simulator," in *ANS Reactor Physics Topical Meeting (PHYSOR 6)*, Vancouver Canada, 2006.

[78] E. Varin, "Reactor Core-Design Analysis," in *CANDU Reactor Physics Course*, Toronto, 2011.

[79] A. Hébert, Applied Reactor Physics, Montréal: Presses Internationales Polytechnique, 2009.

[80] A. Petruzzi and F. D'Auria, "Thermal-Hydraulic System Codes in Nuclear Reactor Safety and Qualification Procedures," *Science and Technology of Nuclear Installations*, vol. 2008, 2008.

[81] N. E. Todreas and M. S. Kazimi, Nuclear Systems Volume 1: Thermal Hydraulic Fundamentals, Boca Raton, FL: CRC Press, Taylor & Francis Group, 2012.

[82] C. T. Crowe, D. F. Elger and J. A. Roberson, Engineering Fluid Mechanics - Eigth Edition, Hoboken, NJ: John Wiley & Sons Inc., 2005.

[83] J. C. Chen, "Correlation for Boiling Heat Transfer to Saturated Fluids in Convective Flow," *Industrial & Engineering Chemistry Process Design & Development*, vol. 5, no. 3, pp. 322-329, 1966.

[84] F. P. Incropera, D. P. DeWitt, T. L. Bergman and A. S. Lavine, Fundamentals of Heat and Mass Transfer - Sixth Edition, Hoboken, NJ: John Wiley & Sons Inc., 2007.

[85] L. K. H. Leung and T. Beuthe, "Interaction with Universities and CATHENA Water Properties," Presented at the CNC-IAPWS meeting, Toronto, Canada, 2003.

[86] W. Wagner and A. Pruss, "The IAPWS Formulation 1995 for the Thermodynamic Properties of Ordinary Water Substance for General and Scientific Use," *Journal of Physical and Chemical Reference Data*, vol. 31, no. 2, pp. 387-535, 2002.

[87] W. Wagner, J. R. Cooper, A. Dittman, J. Kijima, H.-J. Kretzschmarr, A. Krure, R. Mares, K. Oguchi, H. Sato, I. Stöcker, O. Sifner, Y. Takaishi, I. Tanishita, J. Trübenbach and T. Willkommen, "The IAPWS Industrial Formulation 1997 for the Thermodynamic Properties of Water and Steam," *Transactions of the American Society of Mechanical Engineers,* vol. 122, pp. 150-182, 2002.

[88] G. Marleau, "DRAGON Theory Manual Part 1: Collision Probability Calculations," Institut de génie nucléaire, Départment de génie mécanique, École Polytechnique de Montréal, Montréal, 2001.

[89] P. G. Boczar, "ACR Technology Base: Reactor Physics," Presentation to the US Nuclear Regulatory Commission, 2002.

[90] International Atomic Energy Agency, "WIMS Library Update Project," 28 January 2008. [Online]. Available: http://www-nds.iaea.org/wimsd. [Accessed 29 October 2012].

[91] D. W. Hummel, S. E. Langton, M. R. Ball, D. R. Novog and A. Buijs, "Description and Preliminary Results of a Two-Dimensional Lattice Physics Code Benchmark for the Canadian Pressure Tube Supercritical Water-cooled Reactor (PT-SCWR)," in *The 6th International Symposium on Supercritical Water-Cooled Reactors (ISSCWR-6)*, Shenzhen, Guangdong, China, 2013.

[92] F. Salaun, D. W. Hummel and D. R. Novog, "The Impact of the Radial Reflector on the 8-Group Cell-Averaged Cross-Sections for the SCWR 62-element Lattice Cell," in *2014 Canada-China Conference on Advanced Reactor Development (CCCARD-2014)*, Niagara Falls, Canada, 2014.

[93] J. Pencer, D. Watts, A. Colton, X. Wang, L. Blomely, V. Anghel and S. Yue, "Core Neutronics for the Canadian SCWR Conceptual Design," in *The 6th International Symposium on Supercritical Water-Cooled Reactors (ISSCWR-6)*, Shenzhen, Guangdong, China, 2013.

[94] A. Hébert, G. Marleau and R. Roy, "A Description of the Data Structures for DRAGON 3.06," Institut de génie nucléaire, Départment de génie physique, École Polytechnique de Montréal, Montréal, 2008.

[95] E. Varin and G. Marleau, "CANDU reactor core simulations using fully coupled DRAGON and DONJON calculations," *Annals of Nuclear Energy,* vol. 33, pp. 682-691, 2006.

[96] W. Shen, "Assessment of the traditional neutron-diffusion core-analysis method for the analysis of the Super Critical Water Reactor," *Annals of Nuclear Energy,* vol. 45, pp. 1-7, 2012.

[97] T. Kozlowski and T. J. Downar, "PWR MOX/UO2 Core Transient Benchmark," Nuclear Energy Agency, Organisation for Economic Co-Operation and Development, US Nuclear Regulatory Commission, 2007.

[98] J. Koclas, M. Sissaoui and A. Hébert, "Solution of the Improved and Generalized Quasistatic Methods Using an Analytic Calculation or a Semi-Implicit Scheme to Compute the Precursor Equations," *Annals of Nuclear Energy,* vol. 23, no. 11, pp. 901-907, 1996.

[99] P. Schwanke and E. Nichita, "Preliminary Space-Time Kinetics Simulation of a Coolant Voiding-Induced Transient for a Supercritical Water Cooled Reactor with Re-entrant Fuel Channels," in *The 19th Pacific Basin Nuclear Conference (PBNC 2014)*, Vancouver, Canada, 2014.

[100] D. F. Wang and S. Wang, "A CATHENA Model of the Canadian SCWR Concept for Safety Analysis," in *The 6th International Symposium on Supercritical Water-Cooled Reactors (ISSCWR-6)*, Shenzhen, China, 2013.

[101] I. E. Idelchik, Handbook of Hydraulic Resistance, 2nd ed., E. Fried, Ed., Washinton DC: Hemisphere Publishing Corporation, 1979.

[102] D. W. Hummel, "Study of the Applicability of the TRACE Code to CANDU Safety Analysis by Modeling the RD-14M Experimental Facility," 2010.

[103] J. B. Ainscough, "Gap Conductance in Zircaloy-Clad LWR Fuel Rods," Committee on the Safety of Nuclear Installations - OECD Nuclear Energy Agency, Paris, France, 1982.

[104] K. W. Schlicting, N. P. Padture and P. G. Klemens, "Thermal conductivity of dense and porours yttria-stabilized zirconia," *Journal of Materials Science,* vol. 36, pp. 3003-3010, 2001.

[105] S. Rahgavan, H. Wang, W. D. Porter, R. B. Dinwiddie and M. J. Mayo, "Thermal Properties of Zirconia Co-Doped with Trivalent and Pentavalent Oxides," *Acta Materialia,* vol. 49, pp. 169-179, 2001.

[106] J. S. Nathwani, B. L. Kee, C. S. Kim and M. J. Kozluk, "Ontario Hydro's Leak Before Break Approach: Application to the Darlington (CANDU) Nuclear Generating Station," *Nuclear Engineering and Design,* no. 111, pp. 85-107, 1989.

[107] D. W. Hummel and D. R. Novog, "Optimized Channel Inlet Orifice Sizing for the Pressure Tube type Supercritical Water-Cooled Reactor," in *The 19th Pacific Basin Nuclear Conference (PBNC 2014)*, Vancouver, Canada, 2014.

[108] J. Shapre, F. Salaun, D. Hummel, A. Moghrabi, M. Nowak, J. Pencer, D. Novog and A. Buijs, "A Benchmark Comparison of the Canadian Supercritical Water-cooled Reactor (SCWR) 64-element Fuel Lattice Cell Parameters using Various Computer Codes," in *35th Annual Conference of the Canadian Nuclear Society*, Saint John, Canada, 2015.

[109] F. Salaun, J. R. Sharpe, D. W. Hummel, A. Buijs and D. R. Novog, "Optimization of the PT-SCWR Control Blade Sequence using PARCS and DAKOTA," in *The 7th International Symposium on Supercritical Water-Cooled Reactors (ISSCWR-7)*, Helsinki, Finland, 2015.

[110] J. J. Chang, W. R. Bo, Y. J. Jong and C. S. Ho, "LOCA Power Pulse Characteristics in a CANDU-6 with CANFLEX-RU Fuel," in *Proceedings of the Korean Nuclear Society Autumn Meeting*, Yongpyong, South Korea, 2003.

[111] J. Pencer, M. McDonald and V. Anghel, "Parameters for Transient Response Modeling for the Canadian SCWR," in *The 19th Pacific Basin Nuclear Conference (PBNC 2014)*, Vancouver, Canada, 2014.

[112] International Atomic Energy Agency, "Heat Transfer Behaviour and Thermalhydraulics Code Testing for Supercritical Water Cooled Reactors (SCWRs) (IAEA TECDOC 1746)," International Atomic Energy Agency (IAEA), Vienna, Austria, 2014.

Appendix A

PT-SCWR Model Input

This appendix contains excerpts of input to the DRAGON, DONJON, and CATHENA modelling codes. It would have been grossly impractical to print all inputs created within this thesis (requiring thousands of pages). These examples, including the author's comments, are meant to convey the general modelling principles employed in this work.

A.1 DRAGON Input (Lattice Neutronics)

The DRAGON models include an infinite lattice cell, a near-reflector multicell, and procedures for constructing the feedback database at each of the 20 axial locations. Since the geometry of the multicell is simply a repetition of the infinite lattice cell it has been omitted from this appendix for brevity.

A.1.1 Reference Lattice Cell

The temperatures and densities defined as 'REAL' variables in this input file indicate that this lattice cell is at the first axial position (0.125 m). The inputs for the other positions are identical except for the values of these variables.

```
*-----
*  Model of 64-element fuel bundle in a PT-SCWR lattice cell within HERC
*  Based on ptscwr_v7.x2m
*  David Hummel
*  June 2014
*-----
*
*-----
*  Define STRUCTURES and MODULES
*-----
LINKED_LIST
  LIBRARY PTSCWRS PTSCWRF TRACKS TRACKF CPMAT ;
XSM_FILE
  FLUX BURNUP EDITION HOMCELL REFLECT FTUBE FULLCELL ;
SEQ_BINARY
  TRKFILS TRKFILF ;
SEQ_ASCII
  fulledit.exp fullburn.exp celldata.exp tubedata.exp refldata.exp
  fullcell.exp ;
```

```
MODULE
  LIB: GEO: EXCELT: SHI: ASM: FLU: EDI: EVO: DELETE:
  CPO: UTL: BACKUP: END: ;
*-----
*  Define VARIABLES for local conditions
*-----
REAL
  cooldens cooltemp cladtemp linrtemp instemp  pttemp :=
  0.53583  644.19   684.35   637.83   535.83   409.77 ;
REAL
  cntrtemp cntrdens fueltemp :=
  635.73   0.57941  1136.85  ;
REAL tubetemp := cntrtemp 4.65 4.65 * * cooltemp 4.70 4.70 * * + ;
EVALUATE tubetemp := tubetemp 4.65 4.65 * 4.70 4.70 * + / ;
*-----
*  Define VARIABLES for burnup loop
*-----
REAL
  power    delta    timec    timei    timef :=
  47.2791  0.1      1.5      0.0      0.0 ;
REAL countdn := timec timef - ;
EVALUATE countdn := countdn delta / ;
INTEGER icountdn := countdn R_TO_I ;
INTEGER countup := 1 ;
STRING celldir refldir tubedir ;
*
*************************
*  Material Properties  *
*************************
*
*-----
* Unperturbed library
*-----
LIBRARY := LIB: ::
  EDIT 1
  NMIX 11 CTRA WIMS
*-----
*  Cross-sections and depletion data from "iaeagx" in WIMSD4 format
*-----
  DEPL LIB: WIMSD4 FIL: iaeagx
  MIXS LIB: WIMSD4 FIL: iaeagx
*-----
*  central flow tube coolant (light water)
*-----
  MIX 1  <<cntrtemp>>  <<cntrdens>>
    tH1H2O = '3001'   1.1190E+01
    tD2D2O = '3002'   1.0000E-10
    tOnat  = '6016'   8.8810E+01
    B10    = '1010'   1.0000E-10
*-----
*  flow tube (Zr-modified 310 stainless steel)
*-----
  MIX 2  <<tubetemp>>  7.90
    Cnat   = '2012'   3.4000E-02
    Sinat  = '29'     5.1000E-01
    Mnnat  = '55'     7.4000E-01
    Pnat   = '31'     1.6000E-02
    Snat   = '32'     2.0000E-03
    Ninat  = '58'     2.0820E+01
    Crnat  = '52'     2.5040E+01
    Fenat  = '2056'   5.1738E+01
    Monat  = '96'     5.1000E-01
    Zrnat  = '91'     5.9000E-01
*-----
*  inner pins (15 wt% reactor grade PuO2 in ThO2)
*-----
  MIX 3  <<fueltemp>>  9.91
```

```
    Pu238   = '948'    3.6383E-01 1
    Pu239   = '6239'   6.8743E+00 1
    Pu240   = '1240'   3.0376E+00 1
    Pu241   = '1241'   2.0149E+00 1
    Pu242   = '1242'   9.3933E-01 1
    Th232   = '2232'   7.4700E+01 1
    Pa233   = '1233'   0.0000E+00 1
    U233    = '9233'   0.0000E+00 1
    Onat    = '6016'   1.2070E+01
    Xe135   = '4135'   1.0000E-10
    Sm149   = '4149'   1.0000E-10
    Np239   = '1939'   1.0000E-10
*-----
*  outer pins (12 wt% reactor grade PuO2 in ThO2)
*-----
  MIX 4  <<fueltemp>> 9.87
    Pu238   = '948'    2.9123E-01 1
    Pu239   = '6239'   5.5026E+00 1
    Pu240   = '1240'   2.4315E+00 1
    Pu241   = '1241'   1.6129E+00 1
    Pu242   = '1242'   7.5189E-01 1
    Th232   = '2232'   7.7340E+01 1
    Pa233   = '1233'   0.0000E+00 1
    U233    = '9233'   0.0000E+00 1
    Onat    = '6016'   1.2080E+01
    Xe135   = '4135'   1.0000E-10
    Sm149   = '4149'   1.0000E-10
    Np239   = '1939'   1.0000E-10
*-----
*  cladding (Zr-modified 310 stainless steel)
*-----
  MIX 5  <<cladtemp>>  7.90
    Cnat    = '2012'   3.4000E-02
    Sinat   = '29'     5.1000E-01
    Mnnat   = '55'     7.4000E-01
    Pnat    = '31'     1.6000E-02
    Snat    = '32'     2.0000E-03
    Ninat   = '58'     2.0820E+01
    Crnat   = '52'     2.5040E+01
    Fenat   = '2056'   5.1738E+01
    Monat   = '96'     5.1000E-01
    Zrnat   = '91'     5.9000E-01
*-----
*  coolant (light water)
*-----
  MIX 6  <<cooltemp>>  <<cooldens>>
    cH1H2O  = '3001'   1.1190E+01
    cD2D2O  = '3002'   0.0000E+00
    cOnat   = '6016'   8.8810E+01
*-----
*  liner tube (Zr-modified 310 stainless steel)
*-----
  MIX 7  <<linrtemp>>  7.90
    Cnat    = '2012'   3.4000E-02
    Sinat   = '29'     5.1000E-01
    Mnnat   = '55'     7.4000E-01
    Pnat    = '31'     1.6000E-02
    Snat    = '32'     2.0000E-03
    Ninat   = '58'     2.0820E+01
    Crnat   = '52'     2.5040E+01
    Fenat   = '2056'   5.1738E+01
    Monat   = '96'     5.1000E-01
    Zrnat   = '91'     5.9000E-01
*-----
*  insulator (yttria-stabilized zirconia, without yttrium)
*-----
  MIX 8   <<instemp>>  5.37
```

```
    Zrnat  = '91'     7.2322E+01
    Onat   = '6016'   2.7678E+01
*-----
*  outer liner (Excel alloy)
*-----
  MIX 9   <<pttemp>>   6.52
    Monat  = '96'      8.0000E-01
    Nbnat  = '93'      8.0000E-01
    Snnat  = '118'     3.5000E+00
    Zrnat  = '91'      9.4900E+01
*-----
*  pressure tube (Excel alloy)
*-----
  MIX 10  <<pttemp>>   6.52
    Monat  = '96'      8.0000E-01
    Nbnat  = '93'      8.0000E-01
    Snnat  = '118'     3.5000E+00
    Zrnat  = '91'      9.4900E+01
*-----
*  moderator (D2O at 99.833% purity)
*-----
  MIX 11        342.16  1.0851
    H1H2O  = '3001'   1.7112E-02
    D2D2O  = '3002'   2.0082E+01
    Onat   = '6016'   7.9900E+01
;
*
*************************
*      Geometry         *
*************************
*
*-----
* PT-SCWR cell geometry
*-----
PTSCWRS := GEO: :: CARCEL 14
  X- REFL X+ REFL Y- REFL Y+ REFL
  MESHX -12.5000 12.5000
  MESHY -12.5000 12.5000
  RADIUS 0.0000 1.1500 2.3000 3.4500 4.6000 4.7000 5.9500 7.2000
         7.2500 7.8000 7.8500 9.0500 10.200 11.350 12.500
  MIX 1 1 1 1 2 6 6 7 8 9 10 11 11 11 11
  CLUSTER RING1 RING2
*-----
*  inner ring of fuel elements
*-----
  ::: RING1 := GEO: TUBE 2
    RADIUS 0.0000 0.4150 0.4750
    MIX 3 5
    NPIN 32 RPIN 5.4000 APIN 0.0000 ;
*-----
*  outer ring of fuel elements
*-----
  ::: RING2 := GEO: TUBE 2
    RADIUS 0.0000 0.4400 0.5000
    MIX 4 5
    NPIN 32 RPIN 6.5750 APIN 0.0000 ;
  ;
*-----
* PT-SCWR geometry for flux solution
*-----
PTSCWRF := GEO: PTSCWRS :: SPLITR 12 12 12 12 1 13 13 1 6 1 6 6 6 6
  ::: RING1 := GEO: RING1 SPLITR 4 1 ;
  ::: RING2 := GEO: RING2 SPLITR 4 1 ;
  ;
*
*************************
*  Tracking for SS Calc *
```

```
*************************
*
TRACKS TRKFILS := EXCELT: PTSCWRS ::
  EDIT 1
  TITL 'PT-SCWR Cell Self-Sheilding Tracking (EXCELT)'
  MAXR 300 TRAK TISO 14 25.0 ;
*
*************************
*    Self Sheilding     *
*************************
*
LIBRARY := SHI: LIBRARY TRACKS TRKFILS ::
  EDIT 1 LEVE 0 NOLJ ;
*
*************************
*Tracking for Flux Calc *
*************************
*
TRACKF TRKFILF := EXCELT: PTSCWRF ::
  EDIT 1
  TITL 'PT-SCWR Cell Flux Tracking (EXCELT)'
  MAXR 300 TRAK TISO 14 25.0 ;
*
*************************
* Collision Probability *
*************************
*
CPMAT := ASM: LIBRARY TRACKF TRKFILF ::
  EDIT 1 ;
*
*************************
*    Flux Calculation   *
*************************
*
FLUX := FLU: CPMAT LIBRARY TRACKF ::
  TYPE B B1 PNL EDIT 1 ;
*
*************************
*       Edition         *
*************************
*
*-----
* Save homogenized cell data
*-----
EVALUATE celldir := "HomCell    " countup I_TO_S + ;
EDITION := EDI: FLUX LIBRARY TRACKF ::
  MERG COMP MICR ALL EDIT 1
  COND 2.23130E+06 8.20850E+05 9.11882E+03 1.36742E+02 4.00000E+00
       6.25000E-01 1.40000E-01
  SAVE ON <<celldir>> ;
*-----
* Save centre flow tube data only
*-----
EVALUATE tubedir := "FlowTube   " countup I_TO_S + ;
EDITION := EDI: EDITION FLUX LIBRARY TRACKF ::
  MERG MIX 1 0 0 0 0 0 0 0 0 0 0 MICR ALL EDIT 1
  COND 2.23130E+06 8.20850E+05 9.11882E+03 1.36742E+02 4.00000E+00
       6.25000E-01 1.40000E-01
  SAVE ON <<tubedir>> ;
*-----
* Save reflector data only
*-----
EVALUATE refldir := "Reflect    " countup I_TO_S + ;
EDITION := EDI: EDITION FLUX LIBRARY TRACKF ::
  MERG MIX 0 0 0 0 0 0 0 0 0 0 1 MICR ALL EDIT 1
  COND 2.23130E+06 8.20850E+05 9.11882E+03 1.36742E+02 4.00000E+00
       6.25000E-01 1.40000E-01
```

```
  SAVE ON <<refldir>> ;
*-----
* Save Multigroup Flux
*-----
EDITION := UTL: EDITION ::
  STEP UP <<celldir>> STEP UP MULTIGRPFLUX ;
EDITION := BACKUP: EDITION FLUX ;
EDITION := UTL: EDITION ::
  STEP DOWN STEP DOWN ;
*
************************
*     Burnup Loop      *
************************
*
WHILE timei timec < DO
*-----
* Evolve isotopic concentrations
*-----
  EVALUATE timef := timei delta + ;
  EVALUATE icountdn := icountdn 1 - ;
  EVALUATE countup := countup 1 + ;
  IF timei 0.0 = THEN
    BURNUP LIBRARY := EVO: LIBRARY FLUX TRACKF ::
      DEPL <<timei>> <<timef>> DAY POWR <<power>>
      EDIT 1 ;
  ELSE
    BURNUP LIBRARY := EVO: BURNUP LIBRARY FLUX TRACKF ::
      DEPL <<timei>> <<timef>> DAY POWR <<power>>
      EDIT 1 ;
  ENDIF ;
*-----
* Recalculate flux
*-----
  LIBRARY := SHI: LIBRARY TRACKS TRKFILS ::
    EDIT 0 LEVE 0 NOLJ ;
  CPMAT := DELETE: CPMAT ;
  CPMAT := ASM: LIBRARY TRACKF TRKFILF ::
    EDIT 0 ;
  FLUX := FLU: FLUX CPMAT LIBRARY TRACKF ::
    TYPE B B1 PNL EDIT 1 ;
*-----
* Condense and homogenize cross-sections
*-----
  IF countup 10 < THEN
    EVALUATE celldir := "HomCell    " countup I_TO_S + ;
    EVALUATE tubedir := "FlowTube   " countup I_TO_S + ;
  ELSEIF countup 100 < THEN
    EVALUATE celldir := "HomCell   " countup I_TO_S + ;
    EVALUATE tubedir := "FlowTube  " countup I_TO_S + ;
  ELSE
    EVALUATE celldir := "HomCell  " countup I_TO_S + ;
    EVALUATE tubedir := "FlowTube " countup I_TO_S + ;
  ENDIF ;
  EDITION := EDI: EDITION FLUX LIBRARY TRACKF ::
    MERGE COMP MICR ALL EDIT 0
    COND 2.23130E+06 8.20850E+05 9.11882E+03 1.36742E+02 4.00000E+00
         6.25000E-01 1.40000E-01
    SAVE ON <<celldir>> ;
  EDITION := EDI: EDITION FLUX LIBRARY TRACKF ::
    MERGE MIX 1 0 0 0 0 0 0 0 0 0 0 MICR ALL EDIT 0
    COND 2.23130E+06 8.20850E+05 9.11882E+03 1.36742E+02 4.00000E+00
         6.25000E-01 1.40000E-01
    SAVE ON <<tubedir>> ;
  EDITION := UTL: EDITION ::
    STEP UP <<celldir>> STEP UP MULTIGRPFLUX ;
  EDITION := BACKUP: EDITION FLUX ;
  EDITION := UTL: EDITION ::
```

```
     STEP DOWN STEP DOWN ;
*-----
* adjust burnup timestep size
*-----
  IF icountdn 0 = THEN
    IF timec 1.5 = THEN
      EVALUATE delta timec := 0.5 4.0 ;
    ELSEIF timec 4.0 = THEN
      EVALUATE delta timec := 2.0 10.0 ;
    ELSEIF timec 10.0 = THEN
      EVALUATE delta timec := 15.0 100.0 ;
    ELSEIF timec 100.0 = THEN
      EVALUATE delta timec := 50.0 2000.0 ;
    ENDIF ;
    EVALUATE countdn := timec timef - 0.1 + ;
    EVALUATE countdn := countdn delta / ;
    EVALUATE icountdn := countdn R_TO_I ;
  ENDIF ;
  EVALUATE timei := timef ;
ENDWHILE ;
*
*************************
*     Save Results      *
*************************
*
fulledit.exp := EDITION ;
fullburn.exp := BURNUP ;
*-----
* few group CPO format for DONJON import
*-----
HOMCELL := CPO: EDITION BURNUP ::
  EDIT 1 BURNUP HomCell
  EXTRACT BMOD B10
  EXTRACT CWAT cOnat cD2D2O cH1H2O
  EXTRACT MWAT tOnat tD2D2O tH1H2O
  EXTRACT XE135 Xe135
  EXTRACT SM149 Sm149
  EXTRACT NP239 Pa233 Np239
  EXTRACT FPC U233 Pu239 Pu240 Pu241
  NAME REF ;
celldata.exp := HOMCELL ;
FULLCELL := CPO: EDITION BURNUP ::
  EDIT 1 BURNUP HomCell
  NAME REF ;
fullcell.exp := FULLCELL ;
FTUBE := CPO: EDITION BURNUP ::
  EDIT 1 STEP 'FlowTube  1'
  EXTRACT BMOD B10
  EXTRACT MWAT tOnat tD2D2O tH1H2O
  NAME MODREF ;
tubedata.exp := FTUBE ;
REFLECT := CPO: EDITION BURNUP ::
  STEP 'Reflect   1'
  NAME REFLECT ;
refldata.exp := REFLECT ;
*
*************************
*  Temp. file cleanup   *
*************************
*
BURNUP EDITION FLUX FTUBE HOMCELL REFLECT TRKFILF TRKFILS FULLCELL
:= DELETE:
BURNUP EDITION FLUX FTUBE HOMCELL REFLECT TRKFILF TRKFILS FULLCELL ;
*
END: ;
QUIT .
```

A.1.2   Perturbation Calculation

This example is a coolant density reduction at the first axial location, as indicated by the local thermalhydraulic parameters. The other perturbation calculations are performed similarly.

```
*-----
*  Model of 64-element fuel bundle for perturbation calculation
*  Based on reference model ptscwr64_v7.x2m
*  David Hummel
*  June 2014
*-----
*
*-----
*  Define STRUCTURES and MODULES
*-----
LINKED_LIST
  LIBRARY PTSCWRS PTSCWRF TRACKS TRACKF CPMAT ;
XSM_FILE
  FLUX REFBURN REFEDIT EDITION HOMCELL ;
SEQ_BINARY
  TRKFILS TRKFILF ;
SEQ_ASCII
  celldata.exp ;
MODULE
  LIB: GEO: EXCELT: SHI: ASM: FLU: EDI: EVO: DELETE:
  CPO: UTL: RECOVER: GREP: END: ;
*-----
* Load information from previous reference cell calculation
*-----
SEQ_ASCII fulledit.exp :: FILE 'fuel_0125.x2m+fulledit.exp' ;
SEQ_ASCII fullburn.exp :: FILE 'fuel_0125.x2m+fullburn.exp' ;
REFEDIT := fulledit.exp ;
REFBURN := fullburn.exp ;
*-----
*  Define VARIABLES for local conditions
*-----
REAL
  cooldens cooltemp cladtemp linrtemp instemp  pttemp :=
  0.02000  644.19   684.35   637.83   535.83   409.77  ;
REAL
  cntrtemp cntrdens fueltemp :=
  635.73   0.57941  1136.85  ;
REAL tubetemp := cntrtemp 4.65 4.65 * * cooltemp 4.70 4.70 * * + ;
EVALUATE tubetemp := tubetemp 4.65 4.65 * 4.70 4.70 * + / ;
STRING
  cposig := "CDEN-D" ;
*-----
*  Define VARIABLES for burnup loop
*-----
INTEGER numsteps ;
GREP: REFBURN ::
  GETVAL 'STATE-VECTOR' 3 >>numsteps<< ;
INTEGER countup := 1 ;
STRING celldir ;
*
************************
*  Material Properties  *
************************
*
*-----
* Perturbed library
*-----
LIBRARY := LIB: ::
```

```
  EDIT 1
  NMIX 11 CTRA WIMS
*-----
*  Cross-sections and depletion data from "iaeagx" in WIMSD4 format
*-----
  DEPL LIB: WIMSD4 FIL: iaeagx
  MIXS LIB: WIMSD4 FIL: iaeagx
*-----
*  central flow tube coolant (light water)
*-----
  MIX 1  <<cntrtemp>>  <<cntrdens>>
    tH1H2O  = '3001'   1.1190E+01
    tD2D2O  = '3002'   1.0000E-10
    tOnat   = '6016'   8.8810E+01
    B10     = '1010'   1.0000E-10
*-----
*  flow tube (Zr-modified 310 stainless steel)
*-----
  MIX 2  <<tubetemp>>  7.90
    Cnat    = '2012'   3.4000E-02
    Sinat   = '29'     5.1000E-01
    Mnnat   = '55'     7.4000E-01
    Pnat    = '31'     1.6000E-02
    Snat    = '32'     2.0000E-03
    Ninat   = '58'     2.0820E+01
    Crnat   = '52'     2.5040E+01
    Fenat   = '2056'   5.1738E+01
    Monat   = '96'     5.1000E-01
    Zrnat   = '91'     5.9000E-01
*-----
*  inner pins (15 wt% reactor grade PuO2 in ThO2)
*-----
  MIX 3  <<fueltemp>>  9.91
    Pu238   = '948'    3.6383E-01 1
    Pu239   = '6239'   6.8743E+00 1
    Pu240   = '1240'   3.0376E+00 1
    Pu241   = '1241'   2.0149E+00 1
    Pu242   = '1242'   9.3933E-01 1
    Th232   = '2232'   7.4700E+01 1
    Pa233   = '1233'   0.0000E+00 1
    U233    = '9233'   0.0000E+00 1
    Onat    = '6016'   1.2070E+01
    Xe135   = '4135'   1.0000E-10
    Sm149   = '4149'   1.0000E-10
    Np239   = '1939'   1.0000E-10
*-----
*  outer pins (12 wt% reactor grade PuO2 in ThO2)
*-----
  MIX 4  <<fueltemp>>  9.87
    Pu238   = '948'    2.9123E-01 1
    Pu239   = '6239'   5.5026E+00 1
    Pu240   = '1240'   2.4315E+00 1
    Pu241   = '1241'   1.6129E+00 1
    Pu242   = '1242'   7.5189E-01 1
    Th232   = '2232'   7.7340E+01 1
    Pa233   = '1233'   0.0000E+00 1
    U233    = '9233'   0.0000E+00 1
    Onat    = '6016'   1.2080E+01
    Xe135   = '4135'   1.0000E-10
    Sm149   = '4149'   1.0000E-10
    Np239   = '1939'   1.0000E-10
*-----
*  cladding (Zr-modified 310 stainless steel)
*-----
  MIX 5  <<cladtemp>>  7.90
    Cnat    = '2012'   3.4000E-02
    Sinat   = '29'     5.1000E-01
```

```
    Mnnat   = '55'    7.4000E-01
    Pnat    = '31'    1.6000E-02
    Snat    = '32'    2.0000E-03
    Ninat   = '58'    2.0820E+01
    Crnat   = '52'    2.5040E+01
    Fenat   = '2056'  5.1738E+01
    Monat   = '96'    5.1000E-01
    Zrnat   = '91'    5.9000E-01
*-----
*  coolant (light water)
*-----
  MIX 6  <<cooltemp>>  <<cooldens>>
    cH1H2O  = '3001'  1.1190E+01
    cD2D2O  = '3002'  0.0000E+00
    cOnat   = '6016'  8.8810E+01
*-----
*  liner tube (Zr-modified 310 stainless steel)
*-----
  MIX 7  <<linrtemp>>  7.90
    Cnat    = '2012'  3.4000E-02
    Sinat   = '29'    5.1000E-01
    Mnnat   = '55'    7.4000E-01
    Pnat    = '31'    1.6000E-02
    Snat    = '32'    2.0000E-03
    Ninat   = '58'    2.0820E+01
    Crnat   = '52'    2.5040E+01
    Fenat   = '2056'  5.1738E+01
    Monat   = '96'    5.1000E-01
    Zrnat   = '91'    5.9000E-01
*-----
*  insulator (yttria-stabilized zirconia, without yttrium)
*-----
  MIX 8   <<instemp>>  5.37
    Zrnat   = '91'    7.2322E+01
    Onat    = '6016'  2.7678E+01
*-----
*  outer liner (Excel alloy)
*-----
  MIX 9   <<pttemp>>   6.52
    Monat   = '96'    8.0000E-01
    Nbnat   = '93'    8.0000E-01
    Snnat   = '118'   3.5000E+00
    Zrnat   = '91'    9.4900E+01
*-----
*  pressure tube (Excel alloy)
*-----
  MIX 10  <<pttemp>>   6.52
    Monat   = '96'    8.0000E-01
    Nbnat   = '93'    8.0000E-01
    Snnat   = '118'   3.5000E+00
    Zrnat   = '91'    9.4900E+01
*-----
*  moderator (D2O at 99.833% purity)
*-----
  MIX 11       342.16 1.0851
    H1H2O   = '3001'  1.7112E-02
    D2D2O   = '3002'  2.0082E+01
    Onat    = '6016'  7.9900E+01
;
*
************************
*      Geometry        *
************************
*
*-----
* PT-SCWR cell geometry
*-----
```

```
PTSCWRS := GEO: :: CARCEL 14
  X- REFL X+ REFL Y- REFL Y+ REFL
  MESHX -12.5000 12.5000
  MESHY -12.5000 12.5000
  RADIUS 0.0000 1.1500 2.3000 3.4500 4.6000 4.7000 5.9500 7.2000
         7.2500 7.8000 7.8500 9.0500 10.200 11.350 12.500
  MIX 1 1 1 1 2 6 6 7 8 9 10 11 11 11 11
  CLUSTER RING1 RING2
*-----
*  inner ring of fuel elements
*-----
  ::: RING1 := GEO: TUBE 2
    RADIUS 0.0000 0.4150 0.4750
    MIX 3 5
    NPIN 32 RPIN 5.4000 APIN 0.0000 ;
*-----
*  outer ring of fuel elements
*-----
  ::: RING2 := GEO: TUBE 2
    RADIUS 0.0000 0.4400 0.5000
    MIX 4 5
    NPIN 32 RPIN 6.5750 APIN 0.0000 ;
  ;
*-----
* PT-SCWR geometry for flux solution
*-----
PTSCWRF := GEO: PTSCWRS :: SPLITR 12 12 12 12 1 13 13 1 6 1 6 6 6 6
  ::: RING1 := GEO: RING1 SPLITR 4 1 ;
  ::: RING2 := GEO: RING2 SPLITR 4 1 ;
  ;
*
************************
*  Tracking for SS Calc *
************************
*
TRACKS TRKFILS := EXCELT: PTSCWRS ::
  EDIT 1
  TITL 'PT-SCWR Cell Self-Sheilding Tracking (EXCELT)'
  MAXR 300 TRAK TISO 14 25.0 ;
*
************************
*    Self Sheilding     *
************************
*
LIBRARY := SHI: LIBRARY TRACKS TRKFILS ::
  EDIT 1 LEVE 0 NOLJ ;
*
************************
*Tracking for Flux Calc *
************************
*
TRACKF TRKFILF := EXCELT: PTSCWRF ::
  EDIT 1
  TITL 'PT-SCWR Cell Flux Tracking (EXCELT)'
  MAXR 300 TRAK TISO 14 25.0 ;
*
************************
*     Burnup Loop       *
************************
*
WHILE countup numsteps <= DO
  IF countup 10 < THEN
    EVALUATE celldir := "HomCell    " countup I_TO_S + ;
  ELSEIF countup 100 < THEN
    EVALUATE celldir := "HomCell   " countup I_TO_S + ;
  ELSE
    EVALUATE celldir := "HomCell  " countup I_TO_S + ;
```

```
    ENDIF ;
*-----
* Load fuel isotopic concentrations from reference
* calculation and update library for this burnup step
*-----
  LIBRARY := LIB: LIBRARY REFBURN ::
    EDIT 0 BURN <<countup>> MIX 3 MIX 4 ;
*-----
* Load reference flux for this burnup step
*-----
  REFEDIT := UTL: REFEDIT ::
    STEP UP <<celldir>> STEP UP MULTIGRPFLUX ;
  FLUX := RECOVER: REFEDIT ;
  REFEDIT := UTL: REFEDIT ::
    STEP DOWN STEP DOWN ;
*-----
* Calculate new perturbed flux
*-----
  LIBRARY := SHI: LIBRARY TRACKS TRKFILS ::
    EDIT 0 LEVE 0 NOLJ ;
  CPMAT := ASM: LIBRARY TRACKF TRKFILF ::
    EDIT 0 ;
  FLUX := FLU: FLUX CPMAT LIBRARY TRACKF ::
    TYPE B B1 PNL EDIT 1 ;
*-----
* Condense and homogenize cross-sections
*-----
  IF countup 1 = THEN
    EDITION := EDI: FLUX LIBRARY TRACKF ::
      MERGE COMP MICR ALL EDIT 0
      COND 2.23130E+06 8.20850E+05 9.11882E+03 1.36742E+02 4.00000E+00
           6.25000E-01 1.40000E-01
      SAVE ON <<celldir>> ;
  ELSE
    EDITION := EDI: EDITION FLUX LIBRARY TRACKF ::
      MERGE COMP MICR ALL EDIT 0
      COND 2.23130E+06 8.20850E+05 9.11882E+03 1.36742E+02 4.00000E+00
           6.25000E-01 1.40000E-01
      SAVE ON <<celldir>> ;
  ENDIF ;
*-----
* Perform cleanup of data strucutres
*-----
  FLUX CPMAT := DELETE: FLUX CPMAT ;
*
  EVALUATE countup := countup 1 + ;
ENDWHILE ;
*
*************************
*    Save Results       *
*************************
*
*-----
* few group CPO format for DONJON import
*-----
HOMCELL := CPO: EDITION REFBURN ::
  EDIT 1 BURNUP HomCell
  EXTRACT BMOD B10
  EXTRACT CWAT cOnat cD2D2O cH1H2O
  EXTRACT MWAT tOnat tD2D2O tH1H2O
  EXTRACT XE135 Xe135
  EXTRACT SM149 Sm149
  EXTRACT NP239 Pa233 Np239
  EXTRACT FPC U233 Pu239 Pu240 Pu241
  NAME <<cposig>> ;
celldata.exp := HOMCELL ;
*
```

```
*************************
*  Temp. file cleanup   *
*************************
*
REFBURN REFEDIT EDITION HOMCELL TRKFILF TRKFILS := DELETE:
REFBURN REFEDIT EDITION HOMCELL TRKFILF TRKFILS ;
*
END: ;
QUIT .
```

A.1.3   Feedback Database Creation Main Input

This is the main input file for the creation of the thermalhydraulic feedback database. Each axial location is processed in a separate procedure.

```
*-----
*  Input file creates FBM for transient DONJON calculations
*  David Hummel
*  July 2013
*-----
*
*-----
* Define PROCEDURES, STRUCTURES, and MODULES
*-----
PROCEDURE
  proc0125 proc0375 proc0625 proc0875
  proc1125 proc1375 proc1625 proc1875
  proc2125 proc2375 proc2625 proc2875
  proc3125 proc3375 proc3625 proc3875
  proc4125 proc4375 proc4625 proc4875 ;
XSM_FILE
  FBMDATA ;
MODULE
  END: DELETE: ;
SEQ_ASCII
  reffbm.exp ;
*-----
* Create a directory in the FBM for each fuel type
*-----
FBMDATA := proc0125 ;
FBMDATA := proc0375 ;
FBMDATA := proc0625 ;
FBMDATA := proc0875 ;
FBMDATA := proc1125 ;
FBMDATA := proc1375 ;
FBMDATA := proc1625 ;
FBMDATA := proc1875 ;
FBMDATA := proc2125 ;
FBMDATA := proc2375 ;
FBMDATA := proc2625 ;
FBMDATA := proc2875 ;
FBMDATA := proc3125 ;
FBMDATA := proc3375 ;
FBMDATA := proc3625 ;
FBMDATA := proc3875 ;
FBMDATA := proc4125 ;
FBMDATA := proc4375 ;
FBMDATA := proc4625 ;
FBMDATA := proc4875 ;
*-----
* Save results to file
*-----
reffbm.exp := FBMDATA ;
*-----
* Clean up temporary files
```

```
*-----
FBMDATA := DELETE: FBMDATA ;
*
END: ;
QUIT .
```

A.1.4 Feedback Database Creation Procedure

This procedure processes the output of all perturbation calculations at the first
axial location to create the feedback entries.

```
******************************************************************
*
* Procedure creates FBM database for a single PT-SCWR fuel
* type
*
* David Hummel
* August 2013
*
******************************************************************
*-----
* Declare PROCEDURE input and output
*-----
PARAMETER FBMDATA ::
  ::: XSM_FILE FBMDATA ; ;
*-----
* Declare STRUCTURES and MODULES
*-----
MODULE
  CFC: DELETE: END: ;
LINKED_LIST
  REF       FTEMPUP  FTEMPD  CTEMPUP  CTEMPD  MTEMPUP  MTEMPD
  CDENUP    CDEND    MDENUP  MDEND    BORON    PURITY   XENON
  SM149     NP239    MIXFD   MIXMD    POWERUP  POWERIN  POWERD
  MODREF    MODTPUP  MODTPD  MODDENU  MODDEND  MODBOR   MODPUR ;
*-----
* Load files containing cross-section data into CPOs
*-----
SEQ_ASCII ref.exp :: FILE 'fuel_0125.x2m+celldata.exp' ;
REF := ref.exp ;
*
SEQ_ASCII ftempup.exp :: FILE '0125fueltempup.x2m+celldata.exp' ;
FTEMPUP := ftempup.exp ;
*
SEQ_ASCII ftempd.exp :: FILE '0125fueltempdn.x2m+celldata.exp' ;
FTEMPD := ftempd.exp ;
*
SEQ_ASCII ctempup.exp :: FILE '0125cooltempup.x2m+celldata.exp' ;
CTEMPUP := ctempup.exp ;
*
SEQ_ASCII ctempd.exp :: FILE '0125cooltempdn.x2m+celldata.exp' ;
CTEMPD := ctempd.exp ;
*
SEQ_ASCII mtempup.exp :: FILE '0125tubetempup.x2m+celldata.exp' ;
MTEMPUP := mtempup.exp ;
*
SEQ_ASCII mtempd.exp :: FILE '0125tubetempdn.x2m+celldata.exp' ;
MTEMPD := mtempd.exp ;
*
SEQ_ASCII cdenup.exp :: FILE '0125cooldensup.x2m+celldata.exp' ;
CDENUP := cdenup.exp ;
*
SEQ_ASCII cdend.exp :: FILE '0125cooldensdn.x2m+celldata.exp' ;
CDEND := cdend.exp ;
*
```

```
SEQ_ASCII mdenup.exp :: FILE '0125tubedensup.x2m+celldata.exp' ;
MDENUP := mdenup.exp ;
*
SEQ_ASCII mdend.exp :: FILE '0125tubedensdn.x2m+celldata.exp' ;
MDEND := mdend.exp ;
*
SEQ_ASCII boron.exp :: FILE '0125tubeboron.x2m+celldata.exp' ;
BORON := boron.exp ;
*
SEQ_ASCII purity.exp :: FILE '0125tubeprty.x2m+celldata.exp' ;
PURITY := purity.exp ;
*
SEQ_ASCII xenon.exp :: FILE '0125xenonpert.x2m+celldata.exp' ;
XENON := xenon.exp ;
*
SEQ_ASCII sm149.exp :: FILE '0125sm149pert.x2m+celldata.exp' ;
SM149 := sm149.exp ;
*
SEQ_ASCII np239.exp :: FILE '0125np239pert.x2m+celldata.exp' ;
NP239 := np239.exp ;
*
SEQ_ASCII mixfd.exp :: FILE '0125mixdftcd.x2m+celldata.exp' ;
MIXFD := mixfd.exp ;
*
SEQ_ASCII mixmd.exp :: FILE '0125mixdctcd.x2m+celldata.exp' ;
MIXMD := mixmd.exp ;
*
SEQ_ASCII powerup.exp :: FILE '0125powerhi.x2m+celldata.exp' ;
POWERUP := powerup.exp ;
*
SEQ_ASCII powerin.exp :: FILE '0125powermed.x2m+celldata.exp' ;
POWERIN := powerin.exp ;
*
SEQ_ASCII powerd.exp :: FILE '0125powerlow.x2m+celldata.exp' ;
POWERD := powerd.exp ;
*
SEQ_ASCII modref.exp :: FILE 'fuel_0125.x2m+tubedata.exp' ;
MODREF := modref.exp ;
*
SEQ_ASCII modtpup.exp :: FILE '0125tubetempup.x2m+tubedata.exp' ;
MODTPUP := modtpup.exp ;
*
SEQ_ASCII modtpd.exp :: FILE '0125tubetempdn.x2m+tubedata.exp' ;
MODTPD := modtpd.exp ;
*
SEQ_ASCII moddenu.exp :: FILE '0125tubedensup.x2m+tubedata.exp' ;
MODDENU := moddenu.exp ;
*
SEQ_ASCII moddend.exp :: FILE '0125tubedensdn.x2m+tubedata.exp' ;
MODDEND := moddend.exp ;
*
SEQ_ASCII modbor.exp :: FILE '0125tubeboron.x2m+tubedata.exp' ;
MODBOR := modbor.exp ;
*
SEQ_ASCII modpur.exp :: FILE '0125tubeprty.x2m+tubedata.exp' ;
MODPUR := modpur.exp ;
*
*-----
* Define VARIABLES for reference conditions
*-----
REAL
  cooldens cooltemp cladtemp linrtemp instemp  pttemp :=
  0.53583  644.19   684.35   637.83   535.83   409.77  ;
REAL
  cntrtemp cntrdens fueltemp :=
  635.73   0.57941  1136.85  ;
REAL
```

```
  power :=
  377.9762 ;
*-----
* Define VARIABLES for perturbed conditions
*-----
REAL
    cooltu   cooltd   cntrtu   cntrtd :=
  1200.00   300.00  1200.00   300.00 ;
REAL
    fueltu   fueltd :=
  2100.00   600.00 ;
REAL
    cooldu   cooldd   cntrdu   cntrdd :=
  0.75000  0.02000  0.75000  0.02000 ;
REAL
  powerhi  powermed powerlow :=
  755.9254 188.9881 94.49405 ;
*-----
* Create FBM Database
*-----
FBMDATA := CFC:
  REF       FTEMPUP  FTEMPD   CTEMPUP  CTEMPD   MTEMPUP  MTEMPD
  CDENUP    CDEND    MDENUP   MDEND    BORON    PURITY   XENON
  SM149     NP239    MIXFD    MIXMD    POWERUP  POWERIN  POWERD
  MODREF    MODTPUP  MODTPD   MODDENU  MODDEND  MODBOR   MODPUR ::
  EDIT 1
  INFOR PTSCWR_FBM
  DNAME 0125REF
  PWR <<power>> <<powerhi>> <<powermed>> <<powerlow>>
  TCOOL <<cooltemp>> <<cooltu>> <<cooltd>>
  TMODE <<cntrtemp>> <<cntrtu>> <<cntrtd>>
  TFUEL <<fueltemp>> <<fueltu>> <<fueltd>>
  RHOC <<cooldens>>
  RHOM <<cntrdens>> ;
```

A.2 DONJON Input (Core Neutronics)

There were two separate DONJON models created for this work: the steady-state
model and the transient model, although some procedures are common between
the two (e.g. geometry definition and initialization).

A.2.1 Steady-State (Fuel Cycle Iteration) Main Input

The steady-state DONJON model is used to generate the equilibrium burnup
distributions at each initial core state (i.e. BOC, MOC, EOC). The methodolgy
was described graphically in Figure 4.6.

```
****************************************************************
*
* DONJON 3.02g Model of PT-SCWR (quarter-core)
*
* Creates BOC/EOC/MOC snapshot of equillibrium core with cross-sections
* imported from DRAGON 3.06K
*
* David Hummel
* October 2012
*
* Modified January 2013, March 2013, September 2013, November 2013
* January 2014, July 2014
*
```

```
* Note included procedures contained within accompanying .c2m
* files
*
*********************************************************************
*
*-----
* Declare PROCEDURES, STRUCTURES and MODULES
*-----
*
PROCEDURE
  ProcGeom ProcFixd ProcFMap ProcFTab ProcMacx ProcShuff
  ProcSTab ProcCTab ;
LINKED_LIST
  GEOMETRY FUELMAP FIXMACXS INDEX MACROLIB TRACK SYSTEM FLUX
  FULMACXS OLDBMAP OLDEMAP ;
XSM_FILE
  FUELTABS SIDETABS CRNRTABS ;
MODULE
  REFRES: TRIVAT: FLXAXC: REFUEL: INIMAC: TRIVAA: FLUD:
  DELETE: GREP: POWER: END: CRE: ;
SEQ_ASCII
  boc_coremap boc_coreprev eoc_coremap eoc_coreprev moc_coremap ;
*
*-----
* Declare and initialize VARIABLES
*-----
*
REAL totpower := 635.0 ;      ! reactor total power (MW)
REAL cyclen := 1.0 ;          ! cycle length (days), auto adjusts
REAL tstep := 1.0 ;           ! time step size (days)
REAL time := 0.0 ;            ! current time (days)
REAL keff ;                   ! value of keff at current time
REAL keffeoc := 1.01 ;        ! value of keff at end of cycle
*
INTEGER fiter := 0 ;          ! flux iteration number
REAL maxfeps := 1.0E-04 ;     ! flux convergence criterion
INTEGER nadi := 5 ;           ! number of inner flux iterations
INTEGER maxout := 200 ;       ! max number of outer flux iterations
*
INTEGER maxcycle := 100 ;     ! max number of refuelling cycles to run
INTEGER cycle := 1 ;          ! current cycle
REAL moctup moctdn ;          ! boundaries for middle-of-cycle
*
*************************************************************************
*                    Define core geometry                            *
*************************************************************************
*
GEOMETRY INDEX := ProcGeom ;
*
*
*************************************************************************
* Define mixtures for fixed materials  (i.e. not burnup dependent)   *
*************************************************************************
*
FIXMACXS := ProcFixd ;
*
*************************************************************************
*             Create fuel map and cross-reference index             *
*************************************************************************
*
FUELMAP := ProcFMap :: <<totpower>> ;
INDEX FUELMAP := REFRES: INDEX FUELMAP GEOMETRY ;
*
*************************************************************************
*                Create burnup dependent fuel tables                 *
*************************************************************************
*
```

```
FUELTABS := ProcFTab ;
SIDETABS := ProcSTab ;
CRNRTABS := ProcCTab ;
*
*************************************************************************
*                  Create 3D tracking information                      *
*************************************************************************
*
TRACK := TRIVAT: GEOMETRY ::
  EDIT 1
  TITL 'Tracking for 3D quarter-core PT-SCWR'
  MAXR 40000 MCFD 1 ;
*
*************************************************************************
*                Iterate through refueling cycles                      *
*************************************************************************
*
*
*-----
* Save first map files
*-----
*
OLDBMAP := FUELMAP ;
OLDEMAP := FUELMAP ;
boc_coreprev := OLDBMAP ;
boc_coremap := FUELMAP ;
eoc_coreprev := OLDEMAP ;
eoc_coremap := OLDEMAP ;
*
*-----
* Begin refuelling cycle loop
*-----
*
WHILE cycle maxcycle <= DO
  ECHO " " ;
  ECHO "BEGINNING BATCH REFUELLING CYCLE " cycle " OF " maxcycle ;
  ECHO " " ;
  WHILE time cyclen <= DO
    ECHO " " ;
    ECHO "CURRENT TIME IS " time " DAYS" ;
    ECHO " " ;
*
*-----
* Create new library of fuel cross-sections with the new burnups
*-----
*
  FULMACXS := ProcMacx FUELMAP FUELTABS SIDETABS CRNRTABS ;
*
*-----
* Combine fixed and burnup-dependent cross-sections to form
* complete library of macroscopic cross-sections
*-----
*
    MACROLIB := INIMAC: INDEX FIXMACXS FULMACXS ;
*
*-----
* Construct finite-element system matrix for flux calculation
*-----
*
    SYSTEM := TRIVAA: MACROLIB TRACK ::
      EDIT 0 ;
*
    EVALUATE fiter := fiter 1 + ;
*
*-----
* Calculate (or update) flux
*-----
```

```
*
    IF fiter 1 = THEN
      FLUX := FLUD: SYSTEM TRACK ::
        EDIT 5 ADI <<nadi>> EXTE <<maxout>> <<maxfeps>> THER ;
    ELSE
      FLUX := FLUD: FLUX SYSTEM TRACK ::
        EDIT 1 ADI <<nadi>> EXTE <<maxout>> <<maxfeps>> THER ;
    ENDIF ;
*
*-----
* Update axial flux distribution in fuel map (node fluxes)
*-----
*
    FUELMAP := FLXAXC: FUELMAP FLUX TRACK INDEX ::
      EDIT 0 AXIAL COMP ;
*
*-----
* Update node powers (normalized to reactor power)
*-----
*
    FUELMAP := POWER: FUELMAP FULMACXS ::
      EDIT 0 POWER <<totpower>> ;
*
*-----
* Output BOC core map to file
*-----
*
    IF time 0.0 = THEN
      ECHO " " ;
      ECHO "WRITING BOC FUELMAP TO FILE AT TIME " time " DAYS" ;
      ECHO " " ;
      boc_coreprev := DELETE: boc_coreprev ;
      boc_coreprev := OLDBMAP ;
      boc_coremap := DELETE: boc_coremap ;
      boc_coremap := FUELMAP ;
      OLDBMAP := DELETE: OLDBMAP ;
      OLDBMAP := FUELMAP ;
    ENDIF ;
*
*-----
* Output MOC core map to file
*-----
*
    IF cycle maxcycle = THEN
      EVALUATE moctup := cyclen 2.0 / ;
      EVALUATE moctup := tstep 2.0 / moctup + ;
      EVALUATE moctdn := cyclen 2.0 / ;
      EVALUATE moctdn := moctdn tstep 2.0 / - ;
      IF time moctdn > time moctup <=  * THEN
        ECHO " " ;
        ECHO "WRITING MOC FUELMAP TO FILE AT TIME " time " DAYS" ;
        ECHO " " ;
        moc_coremap := FUELMAP ;
      ENDIF ;
    ENDIF ;
*
*-----
* Clean up data structures
*-----
*
    MACROLIB SYSTEM FULMACXS := DELETE: MACROLIB SYSTEM FULMACXS ;
*
*-----
* Extract value of keff from FLUX structure
*-----
*
    GREP: FLUX :: GETVAL K-EFFECTIVE 1 >>keff<< ;
```

```
*
    IF keff keffeoc < THEN
      EVALUATE cyclen := time ;
      ECHO " " ;
      ECHO "EOC REACHED AT TIME " time " DAYS" ;
      ECHO " " ;
*
*-----
* Output EOC core map to file
*-----
*
      ECHO " " ;
      ECHO "WRITING EOC FUELMAP TO FILE AT TIME " time " DAYS" ;
      ECHO " " ;
      eoc_coreprev := DELETE: eoc_coreprev ;
      eoc_coreprev := OLDEMAP ;
      eoc_coremap := DELETE: eoc_coremap ;
      eoc_coremap := FUELMAP ;
      OLDEMAP := DELETE: OLDEMAP ;
      OLDEMAP := FUELMAP ;
    ELSE
*
*-----
* Age fuel according to power and time step length
*-----
*
      FUELMAP := REFUEL: FUELMAP ::
        EDIT 0
        FOLLOW TIME <<tstep>> DAY ;
      IF time cyclen = THEN
        EVALUATE cyclen := cyclen tstep + ;
      ENDIF ;
    ENDIF ;
*
    EVALUATE time := time tstep + ;
  ENDWHILE ;
*
*-----
* Perform batch refuelling
*-----
*
  FUELMAP := ProcShuff FUELMAP ;
*
  EVALUATE cycle := cycle 1 + ;
  EVALUATE time := 0.0 ;
ENDWHILE ;
*
*************************************************************************
*               Perform final cleanup of data files                   *
*************************************************************************
*
FUELTABS SIDETABS CRNRTABS := DELETE: FUELTABS SIDETABS CRNRTABS ;
*
END: ;
QUIT .
```

A.2.2   Core Geometry Definition Procedure

```
****************************************************************
*
* Procedure creates geometry definition for PT-SCWR core
*
* David Hummel
* October 2012
*
* Modified March 2013, November 2013, January 2014
*
```

```
****************************************************************
*
*-----
* Declare PROCEDURE input and output
*-----
*
PARAMETER GEOMETRY INDEX ::
  ::: LINKED_LIST GEOMETRY INDEX ; ;
*
*-----
* Declare STRUCTURES and MODULES
*-----
*
LINKED_LIST
  PREGEOM ;
MODULE
  GEOD: USPLIT: END: ;
*
************************************************************************
*                         Build core geometry                         *
************************************************************************
*
PREGEOM := GEOD: :: CAR3D 14 14 26
  EDIT 1
*
*-----
* Define boundary conditions
*-----
*
  X- VOID          X+ REFL
  Y- VOID          Y+ REFL
  Z- VOID          Z+ VOID
*
*-----
* Define mixture locations by axial plane
*-----
*
  MIX
*
    PLANE  1
*
       0  0  0  0  0  0  0  0  0  0 62 62 62 62
       0  0  0  0  0  0  0  0 62 62 62 62 62 62
       0  0  0  0  0  0 62 62 62 62 62 62 62 62
       0  0  0  0  0 62 62 62 62 62 62 62 62 62
       0  0  0  0 62 62 62 62 62 62 62 62 62 62
       0  0  0 62 62 62 62 62 62 62 62 62 62 62
       0  0 62 62 62 62 62 62 62 62 62 62 62 62
       0  0 62 62 62 62 62 62 62 62 62 62 62 62
       0 62 62 62 62 62 62 62 62 62 62 62 62 62
       0 62 62 62 62 62 62 62 62 62 62 62 62 62
      62 62 62 62 62 62 62 62 62 62 62 62 62 62
      62 62 62 62 62 62 62 62 62 62 62 62 62 62
      62 62 62 62 62 62 62 62 62 62 62 62 62 62
      62 62 62 62 62 62 62 62 62 62 62 62 62 62
*
    PLANE  2
*
       0  0  0  0  0  0  0  0  0  0 62 62 62 62
       0  0  0  0  0  0  0  0 62 62 62 62 62 62
       0  0  0  0  0  0 62 62 62 62 62 62 62 62
       0  0  0  0  0 62 62 62 62 62 62 62 62 62
       0  0  0  0 62 62 62 62 62 62 62 62 62 62
       0  0  0 62 62 62 62 62 62 62 62 62 62 62
       0  0 62 62 62 62 62 62 62 62 62 62 62 62
       0  0 62 62 62 62 62 62 62 62 62 62 62 62
       0 62 62 62 62 62 62 62 62 62 62 62 62 62
```

```
       0 62 62 62 62 62 62 62 62 62 62 62 62 62
      62 62 62 62 62 62 62 62 62 62 62 62 62 62
      62 62 62 62 62 62 62 62 62 62 62 62 62 62
      62 62 62 62 62 62 62 62 62 62 62 62 62 62
      62 62 62 62 62 62 62 62 62 62 62 62 62 62
*
    PLANE  3
*
       0  0  0  0  0  0  0  0  0  0 62 62 62 62
       0  0  0  0  0  0  0  0 62 62 62 62 62 62
       0  0  0  0  0  0 62 62 62 62 62 62 62 62
       0  0  0  0  0 62 62 62 62 61 61 61 61 61
       0  0  0  0 62 62 62 61 61 61 61 61 61 61
       0  0  0 62 62 61 61 61 61 61 61 61 61 61
       0  0 62 62 62 61 61 61 61 61 61 61 61 61
       0  0 62 62 61 61 61 61 61 61 61 61 61 61
       0 62 62 62 61 61 61 61 61 61 61 61 61 61
       0 62 62 61 61 61 61 61 61 61 61 61 61 61
      62 62 62 61 61 61 61 61 61 61 61 61 61 61
      62 62 62 61 61 61 61 61 61 61 61 61 61 61
      62 62 62 61 61 61 61 61 61 61 61 61 61 61
      62 62 62 61 61 61 61 61 61 61 61 61 61 61
*
    PLANE  4
*
       0  0  0  0  0  0  0  0  0  0 62 62 62 62
       0  0  0  0  0  0  0  0 62 62 62 62 62 62
       0  0  0  0  0  0 62 62 62 62 62 62 62 62
       0  0  0  0  0 62 62 62 62 61 61 61 61 61
       0  0  0  0 62 62 62 61 61 61 41 21 21 21
       0  0  0 62 62 61 61 61 41 21  1  1  1  1
       0  0 62 62 62 61 41 21  1  1  1  1  1  1
       0  0 62 62 61 61 21  1  1  1  1  1  1  1
       0 62 62 62 61 41  1  1  1  1  1  1  1  1
       0 62 62 61 61 21  1  1  1  1  1  1  1  1
      62 62 62 61 41  1  1  1  1  1  1  1  1  1
      62 62 62 61 21  1  1  1  1  1  1  1  1  1
      62 62 62 61 21  1  1  1  1  1  1  1  1  1
      62 62 62 61 21  1  1  1  1  1  1  1  1  1
*
    PLANE  5
*
       0  0  0  0  0  0  0  0  0  0 62 62 62 62
       0  0  0  0  0  0  0  0 62 62 62 62 62 62
       0  0  0  0  0  0 62 62 62 62 62 62 62 62
       0  0  0  0  0 62 62 62 62 61 61 61 61 61
       0  0  0  0 62 62 62 61 61 61 42 22 22 22
       0  0  0 62 62 61 61 61 42 22  2  2  2  2
       0  0 62 62 62 61 42 22  2  2  2  2  2  2
       0  0 62 62 61 61 22  2  2  2  2  2  2  2
       0 62 62 62 61 42  2  2  2  2  2  2  2  2
       0 62 62 61 61 22  2  2  2  2  2  2  2  2
      62 62 62 61 42  2  2  2  2  2  2  2  2  2
      62 62 62 61 22  2  2  2  2  2  2  2  2  2
      62 62 62 61 22  2  2  2  2  2  2  2  2  2
      62 62 62 61 22  2  2  2  2  2  2  2  2  2
*
    PLANE  6
*
       0  0  0  0  0  0  0  0  0  0 62 62 62 62
       0  0  0  0  0  0  0  0 62 62 62 62 62 62
       0  0  0  0  0  0 62 62 62 62 62 62 62 62
       0  0  0  0  0 62 62 62 62 61 61 61 61 61
       0  0  0  0 62 62 62 61 61 61 43 23 23 23
       0  0  0 62 62 61 61 61 43 23  3  3  3  3
       0  0 62 62 62 61 43 23  3  3  3  3  3  3
       0  0 62 62 61 61 23  3  3  3  3  3  3  3
```

```
     0 62 62 62 61 43  3  3  3  3  3  3  3  3
     0 62 62 61 61 23  3  3  3  3  3  3  3  3
    62 62 62 61 43  3  3  3  3  3  3  3  3  3
    62 62 62 61 23  3  3  3  3  3  3  3  3  3
    62 62 62 61 23  3  3  3  3  3  3  3  3  3
    62 62 62 61 23  3  3  3  3  3  3  3  3  3
*
    PLANE  7
*
     0  0  0  0  0  0  0  0  0  0 62 62 62 62
     0  0  0  0  0  0  0  0 62 62 62 62 62 62
     0  0  0  0  0  0 62 62 62 62 62 62 62 62
     0  0  0  0  0 62 62 62 62 61 61 61 61 61
     0  0  0  0 62 62 62 61 61 61 44 24 24 24
     0  0  0 62 62 61 61 61 44 24  4  4  4  4
     0  0 62 62 62 61 44 24  4  4  4  4  4  4
     0  0 62 62 61 61 24  4  4  4  4  4  4  4
     0 62 62 62 61 44  4  4  4  4  4  4  4  4
     0 62 62 61 61 24  4  4  4  4  4  4  4  4
    62 62 62 61 44  4  4  4  4  4  4  4  4  4
    62 62 62 61 24  4  4  4  4  4  4  4  4  4
    62 62 62 61 24  4  4  4  4  4  4  4  4  4
    62 62 62 61 24  4  4  4  4  4  4  4  4  4
*
    PLANE  8
*
     0  0  0  0  0  0  0  0  0  0 62 62 62 62
     0  0  0  0  0  0  0  0 62 62 62 62 62 62
     0  0  0  0  0  0 62 62 62 62 62 62 62 62
     0  0  0  0  0 62 62 62 62 61 61 61 61 61
     0  0  0  0 62 62 62 61 61 61 45 25 25 25
     0  0  0 62 62 61 61 61 45 25  5  5  5  5
     0  0 62 62 62 61 45 25  5  5  5  5  5  5
     0  0 62 62 61 61 25  5  5  5  5  5  5  5
     0 62 62 62 61 45  5  5  5  5  5  5  5  5
     0 62 62 61 61 25  5  5  5  5  5  5  5  5
    62 62 62 61 45  5  5  5  5  5  5  5  5  5
    62 62 62 61 25  5  5  5  5  5  5  5  5  5
    62 62 62 61 25  5  5  5  5  5  5  5  5  5
    62 62 62 61 25  5  5  5  5  5  5  5  5  5
*
    PLANE  9
*
     0  0  0  0  0  0  0  0  0  0 62 62 62 62
     0  0  0  0  0  0  0  0 62 62 62 62 62 62
     0  0  0  0  0  0 62 62 62 62 62 62 62 62
     0  0  0  0  0 62 62 62 62 61 61 61 61 61
     0  0  0  0 62 62 62 61 61 61 46 26 26 26
     0  0  0 62 62 61 61 61 46 26  6  6  6  6
     0  0 62 62 62 61 46 26  6  6  6  6  6  6
     0  0 62 62 61 61 26  6  6  6  6  6  6  6
     0 62 62 62 61 46  6  6  6  6  6  6  6  6
     0 62 62 61 61 26  6  6  6  6  6  6  6  6
    62 62 62 61 46  6  6  6  6  6  6  6  6  6
    62 62 62 61 26  6  6  6  6  6  6  6  6  6
    62 62 62 61 26  6  6  6  6  6  6  6  6  6
    62 62 62 61 26  6  6  6  6  6  6  6  6  6
*
    PLANE 10
*
     0  0  0  0  0  0  0  0  0  0 62 62 62 62
     0  0  0  0  0  0  0  0 62 62 62 62 62 62
     0  0  0  0  0  0 62 62 62 62 62 62 62 62
     0  0  0  0  0 62 62 62 62 61 61 61 61 61
     0  0  0  0 62 62 62 61 61 61 47 27 27 27
     0  0  0 62 62 61 61 61 47 27  7  7  7  7
     0  0 62 62 62 61 47 27  7  7  7  7  7  7
```

D. W. Hummel
Ph.D. Thesis

Appendix A
PT-SCWR Model Input

McMaster University
Engineering Physics

```
    0    0  62  62  61  61  27   7   7   7   7   7   7   7
    0  62  62  62  61  47   7   7   7   7   7   7   7   7
    0  62  62  61  61  27   7   7   7   7   7   7   7   7
   62  62  62  61  47   7   7   7   7   7   7   7   7   7
   62  62  62  61  27   7   7   7   7   7   7   7   7   7
   62  62  62  61  27   7   7   7   7   7   7   7   7   7
   62  62  62  61  27   7   7   7   7   7   7   7   7   7
*
    PLANE 11
*
    0    0    0    0    0    0    0    0    0    0  62  62  62  62
    0    0    0    0    0    0    0    0  62  62  62  62  62  62
    0    0    0    0    0    0  62  62  62  62  62  62  62  62
    0    0    0    0    0  62  62  62  62  61  61  61  61  61
    0    0    0    0  62  62  62  61  61  61  48  28  28  28
    0    0    0  62  62  61  61  61  48  28   8   8   8   8
    0    0  62  62  62  61  48  28   8   8   8   8   8   8
    0    0  62  62  61  61  28   8   8   8   8   8   8   8
    0  62  62  62  61  48   8   8   8   8   8   8   8   8
    0  62  62  61  61  28   8   8   8   8   8   8   8   8
   62  62  62  61  48   8   8   8   8   8   8   8   8   8
   62  62  62  61  28   8   8   8   8   8   8   8   8   8
   62  62  62  61  28   8   8   8   8   8   8   8   8   8
   62  62  62  61  28   8   8   8   8   8   8   8   8   8
*
    PLANE 12
*
    0    0    0    0    0    0    0    0    0    0  62  62  62  62
    0    0    0    0    0    0    0    0  62  62  62  62  62  62
    0    0    0    0    0    0  62  62  62  62  62  62  62  62
    0    0    0    0    0  62  62  62  62  61  61  61  61  61
    0    0    0    0  62  62  62  61  61  61  49  29  29  29
    0    0    0  62  62  61  61  61  49  29   9   9   9   9
    0    0  62  62  62  61  49  29   9   9   9   9   9   9
    0    0  62  62  61  61  29   9   9   9   9   9   9   9
    0  62  62  62  61  49   9   9   9   9   9   9   9   9
    0  62  62  61  61  29   9   9   9   9   9   9   9   9
   62  62  62  61  49   9   9   9   9   9   9   9   9   9
   62  62  62  61  29   9   9   9   9   9   9   9   9   9
   62  62  62  61  29   9   9   9   9   9   9   9   9   9
   62  62  62  61  29   9   9   9   9   9   9   9   9   9
*
    PLANE 13
*
    0    0    0    0    0    0    0    0    0    0  62  62  62  62
    0    0    0    0    0    0    0    0  62  62  62  62  62  62
    0    0    0    0    0    0  62  62  62  62  62  62  62  62
    0    0    0    0    0  62  62  62  62  61  61  61  61  61
    0    0    0    0  62  62  62  61  61  61  50  30  30  30
    0    0    0  62  62  61  61  61  50  30  10  10  10  10
    0    0  62  62  62  61  50  30  10  10  10  10  10  10
    0    0  62  62  61  61  30  10  10  10  10  10  10  10
    0  62  62  62  61  50  10  10  10  10  10  10  10  10
    0  62  62  61  61  30  10  10  10  10  10  10  10  10
   62  62  62  61  50  10  10  10  10  10  10  10  10  10
   62  62  62  61  30  10  10  10  10  10  10  10  10  10
   62  62  62  61  30  10  10  10  10  10  10  10  10  10
   62  62  62  61  30  10  10  10  10  10  10  10  10  10
*
    PLANE 14
*
    0    0    0    0    0    0    0    0    0    0  62  62  62  62
    0    0    0    0    0    0    0    0  62  62  62  62  62  62
    0    0    0    0    0    0  62  62  62  62  62  62  62  62
    0    0    0    0    0  62  62  62  62  61  61  61  61  61
    0    0    0    0  62  62  62  61  61  61  51  31  31  31
    0    0    0  62  62  61  61  61  51  31  11  11  11  11
```

```
       0   0 62 62 62 61 51 31 11 11 11 11 11 11
       0   0 62 62 61 61 31 11 11 11 11 11 11 11
       0 62 62 62 61 51 11 11 11 11 11 11 11 11
       0 62 62 61 61 31 11 11 11 11 11 11 11 11
      62 62 62 61 51 11 11 11 11 11 11 11 11 11
      62 62 62 61 31 11 11 11 11 11 11 11 11 11
      62 62 62 61 31 11 11 11 11 11 11 11 11 11
      62 62 62 61 31 11 11 11 11 11 11 11 11 11
*
    PLANE 15
*
       0   0   0   0   0   0   0   0   0   0 62 62 62 62
       0   0   0   0   0   0   0   0 62 62 62 62 62 62
       0   0   0   0   0   0 62 62 62 62 62 62 62 62
       0   0   0   0   0 62 62 62 62 61 61 61 61 61
       0   0   0   0 62 62 62 61 61 61 52 32 32 32
       0   0   0 62 62 61 61 61 52 32 12 12 12 12
       0   0 62 62 62 61 52 32 12 12 12 12 12 12
       0   0 62 62 61 61 32 12 12 12 12 12 12 12
       0 62 62 62 61 52 12 12 12 12 12 12 12 12
       0 62 62 61 61 32 12 12 12 12 12 12 12 12
      62 62 62 61 52 12 12 12 12 12 12 12 12 12
      62 62 62 61 32 12 12 12 12 12 12 12 12 12
      62 62 62 61 32 12 12 12 12 12 12 12 12 12
      62 62 62 61 32 12 12 12 12 12 12 12 12 12
*
    PLANE 16
*
       0   0   0   0   0   0   0   0   0   0 62 62 62 62
       0   0   0   0   0   0   0   0 62 62 62 62 62 62
       0   0   0   0   0   0 62 62 62 62 62 62 62 62
       0   0   0   0   0 62 62 62 62 61 61 61 61 61
       0   0   0   0 62 62 62 61 61 61 53 33 33 33
       0   0   0 62 62 61 61 61 53 33 13 13 13 13
       0   0 62 62 62 61 53 33 13 13 13 13 13 13
       0   0 62 62 61 61 33 13 13 13 13 13 13 13
       0 62 62 62 61 53 13 13 13 13 13 13 13 13
       0 62 62 61 61 33 13 13 13 13 13 13 13 13
      62 62 62 61 53 13 13 13 13 13 13 13 13 13
      62 62 62 61 33 13 13 13 13 13 13 13 13 13
      62 62 62 61 33 13 13 13 13 13 13 13 13 13
      62 62 62 61 33 13 13 13 13 13 13 13 13 13
*
    PLANE 17
*
       0   0   0   0   0   0   0   0   0   0 62 62 62 62
       0   0   0   0   0   0   0   0 62 62 62 62 62 62
       0   0   0   0   0   0 62 62 62 62 62 62 62 62
       0   0   0   0   0 62 62 62 62 61 61 61 61 61
       0   0   0   0 62 62 62 61 61 61 54 34 34 34
       0   0   0 62 62 61 61 61 54 34 14 14 14 14
       0   0 62 62 62 61 54 34 14 14 14 14 14 14
       0   0 62 62 61 61 34 14 14 14 14 14 14 14
       0 62 62 62 61 54 14 14 14 14 14 14 14 14
       0 62 62 61 61 34 14 14 14 14 14 14 14 14
      62 62 62 61 54 14 14 14 14 14 14 14 14 14
      62 62 62 61 34 14 14 14 14 14 14 14 14 14
      62 62 62 61 34 14 14 14 14 14 14 14 14 14
      62 62 62 61 34 14 14 14 14 14 14 14 14 14
*
    PLANE 18
*
       0   0   0   0   0   0   0   0   0   0 62 62 62 62
       0   0   0   0   0   0   0   0 62 62 62 62 62 62
       0   0   0   0   0   0 62 62 62 62 62 62 62 62
       0   0   0   0   0 62 62 62 62 61 61 61 61 61
       0   0   0   0 62 62 62 61 61 61 55 35 35 35
```

223

```
    0    0    0 62 62 61 61 61 55 35 15 15 15 15
    0    0 62 62 62 61 55 35 15 15 15 15 15 15
    0    0 62 62 61 61 35 15 15 15 15 15 15 15
    0 62 62 62 61 55 15 15 15 15 15 15 15 15
    0 62 62 61 61 35 15 15 15 15 15 15 15 15
   62 62 62 61 55 15 15 15 15 15 15 15 15 15
   62 62 62 61 35 15 15 15 15 15 15 15 15 15
   62 62 62 61 35 15 15 15 15 15 15 15 15 15
   62 62 62 61 35 15 15 15 15 15 15 15 15 15
*
    PLANE 19
*
    0    0    0    0    0    0    0    0    0    0 62 62 62 62
    0    0    0    0    0    0    0    0 62 62 62 62 62 62
    0    0    0    0    0    0 62 62 62 62 62 62 62 62
    0    0    0    0    0 62 62 62 62 61 61 61 61 61
    0    0    0    0 62 62 62 61 61 61 56 36 36 36
    0    0    0 62 62 61 61 61 56 36 16 16 16 16
    0    0 62 62 62 61 56 36 16 16 16 16 16 16
    0    0 62 62 61 61 36 16 16 16 16 16 16 16
    0 62 62 62 61 56 16 16 16 16 16 16 16 16
    0 62 62 61 61 36 16 16 16 16 16 16 16 16
   62 62 62 61 56 16 16 16 16 16 16 16 16 16
   62 62 62 61 36 16 16 16 16 16 16 16 16 16
   62 62 62 61 36 16 16 16 16 16 16 16 16 16
   62 62 62 61 36 16 16 16 16 16 16 16 16 16
*
    PLANE 20
*
    0    0    0    0    0    0    0    0    0    0 62 62 62 62
    0    0    0    0    0    0    0    0 62 62 62 62 62 62
    0    0    0    0    0    0 62 62 62 62 62 62 62 62
    0    0    0    0    0 62 62 62 62 61 61 61 61 61
    0    0    0    0 62 62 62 61 61 61 57 37 37 37
    0    0    0 62 62 61 61 61 57 37 17 17 17 17
    0    0 62 62 62 61 57 37 17 17 17 17 17 17
    0    0 62 62 61 61 37 17 17 17 17 17 17 17
    0 62 62 62 61 57 17 17 17 17 17 17 17 17
    0 62 62 61 61 37 17 17 17 17 17 17 17 17
   62 62 62 61 57 17 17 17 17 17 17 17 17 17
   62 62 62 61 37 17 17 17 17 17 17 17 17 17
   62 62 62 61 37 17 17 17 17 17 17 17 17 17
   62 62 62 61 37 17 17 17 17 17 17 17 17 17
*
    PLANE 21
*
    0    0    0    0    0    0    0    0    0    0 62 62 62 62
    0    0    0    0    0    0    0    0 62 62 62 62 62 62
    0    0    0    0    0    0 62 62 62 62 62 62 62 62
    0    0    0    0    0 62 62 62 62 61 61 61 61 61
    0    0    0    0 62 62 62 61 61 61 58 38 38 38
    0    0    0 62 62 61 61 61 58 38 18 18 18 18
    0    0 62 62 62 61 58 38 18 18 18 18 18 18
    0    0 62 62 61 61 38 18 18 18 18 18 18 18
    0 62 62 62 61 58 18 18 18 18 18 18 18 18
    0 62 62 61 61 38 18 18 18 18 18 18 18 18
   62 62 62 61 58 18 18 18 18 18 18 18 18 18
   62 62 62 61 38 18 18 18 18 18 18 18 18 18
   62 62 62 61 38 18 18 18 18 18 18 18 18 18
   62 62 62 61 38 18 18 18 18 18 18 18 18 18
*
    PLANE 22
*
    0    0    0    0    0    0    0    0    0    0 62 62 62 62
    0    0    0    0    0    0    0    0 62 62 62 62 62 62
    0    0    0    0    0    0 62 62 62 62 62 62 62 62
    0    0    0    0    0 62 62 62 62 61 61 61 61 61
```

```
        0    0    0    0  62  62  62  61  61  61  59  39  39  39
        0    0    0  62  62  61  61  61  59  39  19  19  19  19
        0    0  62  62  62  61  59  39  19  19  19  19  19  19
        0    0  62  62  61  61  39  19  19  19  19  19  19  19
        0  62  62  62  61  59  19  19  19  19  19  19  19  19
        0  62  62  61  61  39  19  19  19  19  19  19  19  19
       62  62  62  61  59  19  19  19  19  19  19  19  19  19
       62  62  62  61  39  19  19  19  19  19  19  19  19  19
       62  62  62  61  39  19  19  19  19  19  19  19  19  19
       62  62  62  61  39  19  19  19  19  19  19  19  19  19
*
     PLANE 23
*
        0    0    0    0    0    0    0    0    0    0  62  62  62  62
        0    0    0    0    0    0    0    0  62  62  62  62  62  62
        0    0    0    0    0    0  62  62  62  62  62  62  62  62
        0    0    0    0    0  62  62  62  62  61  61  61  61  61
        0    0    0    0  62  62  62  61  61  61  60  40  40  40
        0    0    0  62  62  61  61  61  60  40  20  20  20  20
        0    0  62  62  62  61  60  40  20  20  20  20  20  20
        0    0  62  62  61  61  40  20  20  20  20  20  20  20
        0  62  62  62  61  60  20  20  20  20  20  20  20  20
        0  62  62  61  61  40  20  20  20  20  20  20  20  20
       62  62  62  61  60  20  20  20  20  20  20  20  20  20
       62  62  62  61  40  20  20  20  20  20  20  20  20  20
       62  62  62  61  40  20  20  20  20  20  20  20  20  20
       62  62  62  61  40  20  20  20  20  20  20  20  20  20
*
     PLANE 24
*
        0    0    0    0    0    0    0    0    0    0  62  62  62  62
        0    0    0    0    0    0    0    0  62  62  62  62  62  62
        0    0    0    0    0    0  62  62  62  62  62  62  62  62
        0    0    0    0    0  62  62  62  62  61  61  61  61  61
        0    0    0    0  62  62  62  61  61  61  61  61  61  61
        0    0    0  62  62  61  61  61  61  61  61  61  61  61
        0    0  62  62  62  61  61  61  61  61  61  61  61  61
        0    0  62  62  61  61  61  61  61  61  61  61  61  61
        0  62  62  62  61  61  61  61  61  61  61  61  61  61
        0  62  62  61  61  61  61  61  61  61  61  61  61  61
       62  62  62  61  61  61  61  61  61  61  61  61  61  61
       62  62  62  61  61  61  61  61  61  61  61  61  61  61
       62  62  62  61  61  61  61  61  61  61  61  61  61  61
       62  62  62  61  61  61  61  61  61  61  61  61  61  61
*
     PLANE 25
*
        0    0    0    0    0    0    0    0    0    0  62  62  62  62
        0    0    0    0    0    0    0    0  62  62  62  62  62  62
        0    0    0    0    0    0  62  62  62  62  62  62  62  62
        0    0    0    0    0  62  62  62  62  62  62  62  62  62
        0    0    0    0  62  62  62  62  62  62  62  62  62  62
        0    0    0  62  62  62  62  62  62  62  62  62  62  62
        0    0  62  62  62  62  62  62  62  62  62  62  62  62
        0    0  62  62  62  62  62  62  62  62  62  62  62  62
        0  62  62  62  62  62  62  62  62  62  62  62  62  62
        0  62  62  62  62  62  62  62  62  62  62  62  62  62
       62  62  62  62  62  62  62  62  62  62  62  62  62  62
       62  62  62  62  62  62  62  62  62  62  62  62  62  62
       62  62  62  62  62  62  62  62  62  62  62  62  62  62
       62  62  62  62  62  62  62  62  62  62  62  62  62  62
*
     PLANE 26
*
        0    0    0    0    0    0    0    0    0    0  62  62  62  62
        0    0    0    0    0    0    0    0  62  62  62  62  62  62
        0    0    0    0    0    0  62  62  62  62  62  62  62  62
```

```
      0   0   0   0   0 62 62 62 62 62 62 62 62 62
       0   0   0   0 62 62 62 62 62 62 62 62 62 62
       0   0   0 62 62 62 62 62 62 62 62 62 62 62
       0   0 62 62 62 62 62 62 62 62 62 62 62 62
       0   0 62 62 62 62 62 62 62 62 62 62 62 62
       0 62 62 62 62 62 62 62 62 62 62 62 62 62
       0 62 62 62 62 62 62 62 62 62 62 62 62 62
      62 62 62 62 62 62 62 62 62 62 62 62 62 62
      62 62 62 62 62 62 62 62 62 62 62 62 62 62
      62 62 62 62 62 62 62 62 62 62 62 62 62 62
      62 62 62 62 62 62 62 62 62 62 62 62 62 62
*
*-----
* Create spatial mesh
*-----
*
  MESHX   0.00  25.00  50.00  75.00 100.00 125.00 150.00 175.00
        200.00 225.00 250.00 275.00 300.00 325.00 350.00
  MESHY   0.00  25.00  50.00  75.00 100.00 125.00 150.00 175.00
        200.00 225.00 250.00 275.00 300.00 325.00 350.00
  MESHZ   0.00  25.00  50.00  75.00 100.00 125.00 150.00 175.00
        200.00 225.00 250.00 275.00 300.00 325.00 350.00 375.00
        400.00 425.00 450.00 475.00 500.00 525.00 550.00 575.00
        600.00 625.00 650.00 ;
*
************************************************************************
*                  Finalize and create INDEX                          *
************************************************************************
*
GEOMETRY INDEX := USPLIT: PREGEOM :: MAXR 20000 ;
*
END: ;
```

A.2.3 Fixed Cross-Section Recovery Procedure

```
*****************************************************************
*
* Procedure creates library of fixed material cross-sections
* (i.e. not burnup dependent)
*
* David Hummel
* October 2012
*
* Modified March 2013, September 2013, November 2013, January 2014
*
*****************************************************************
*
*-----
* Declare PROCEDURE input and output
*-----
*
PARAMETER FIXMACXS ::
  ::: LINKED_LIST FIXMACXS ; ;
*
*-----
* Declare STRUCTURES and MODULES
*-----
*
LINKED_LIST
  REFL1 REFL2 ;
MODULE
  CRE: END: ;
SEQ_ASCII REFL1FIL :: FILE 'corn_2375.x2m+refl1dat.exp' ;
SEQ_ASCII REFL2FIL :: FILE 'corn_2375.x2m+refl2dat.exp' ;
*
*****************************************************************
*                    Load data from file                       *
```

```
**********************************************************************
*
REFL1 := REFL1FIL ;
REFL2 := REFL2FIL ;
*
**********************************************************************
*                       Create library from file                    *
**********************************************************************
*
FIXMACXS := CRE: REFL1 REFL2 ::
  EDIT 1
  NMIX 62 READ
   COMPO REFL1 MIX 61 'REFLECT    1' ENDMIX
   COMPO REFL2 MIX 62 'REFLECT    1' ENDMIX  ;
*
END: ;
```

A.2.4   FUELMAP Creation Procedure

```
****************************************************************
*
* Procedure creates map of local fuel properties, including
* burnups and powers for beginning of batch cycle
*
* David Hummel
* October 2012
*
* Modified March 2013, September 2013, November 2013, January 2014
*
****************************************************************
*
*-----
* Declare PROCEDURE input and output
*-----
*
PARAMETER FUELMAP ::
  ::: LINKED_LIST FUELMAP ; ;
*
*-----
* Declare STRUCTURES and MODULES
*-----
*
MODULE
  INIRES: END: ;
*
*-----
* Declare VARIABLES
*-----
*
REAL AVGNP
     n01p n02p n03p n04p n05p n06p n07p n08p n09p n10p
     n11p n12p n13p n14p n15p n16p n17p n18p n19p n20p
     b201 b202 b203 b204 b205 b206 b207 b208 b209 b210
     b211 b212 b213 b214 b215 b216 b217 b218 b219 b220
     b301 b302 b303 b304 b305 b306 b307 b308 b309 b310
     b311 b312 b313 b314 b315 b316 b317 b318 b319 b320 ;
REAL totpower ;
*
*-----
* Read input parameters
*-----
*
:: >>totpower<< ;
*
*-----
* Initialize variable values
*-----
```

```
*
EVALUATE AVGNP := totpower 1000.0 * ;
EVALUATE AVGNP := AVGNP 84.0 / ;
EVALUATE AVGNP := AVGNP 20.0 / ;        ! average node power (kw)
*
EVALUATE n01p := AVGNP 0.48381 * ;    ! initial power distribution (kW)
EVALUATE n02p := AVGNP 0.60802 * ;
EVALUATE n03p := AVGNP 0.70281 * ;
EVALUATE n04p := AVGNP 0.78322 * ;
EVALUATE n05p := AVGNP 0.85578 * ;
EVALUATE n06p := AVGNP 0.92326 * ;
EVALUATE n07p := AVGNP 0.98657 * ;
EVALUATE n08p := AVGNP 1.04710 * ;
EVALUATE n09p := AVGNP 1.10292 * ;
EVALUATE n10p := AVGNP 1.15391 * ;
EVALUATE n11p := AVGNP 1.19648 * ;
EVALUATE n12p := AVGNP 1.22874 * ;
EVALUATE n13p := AVGNP 1.24770 * ;
EVALUATE n14p := AVGNP 1.25182 * ;
EVALUATE n15p := AVGNP 1.23957 * ;
EVALUATE n16p := AVGNP 1.20909 * ;
EVALUATE n17p := AVGNP 1.15728 * ;
EVALUATE n18p := AVGNP 1.07862 * ;
EVALUATE n19p := AVGNP 0.96179 * ;
EVALUATE n20p := AVGNP 0.78151 * ;
*
EVALUATE b301 := 3.1693E+04 ;
EVALUATE b302 := 3.7203E+04 ;
EVALUATE b303 := 3.9660E+04 ;
EVALUATE b304 := 4.0711E+04 ;
EVALUATE b305 := 4.1144E+04 ;
EVALUATE b306 := 4.1329E+04 ;
EVALUATE b307 := 4.1434E+04 ;
EVALUATE b308 := 4.1567E+04 ;
EVALUATE b309 := 4.1716E+04 ;
EVALUATE b310 := 4.1918E+04 ;
EVALUATE b311 := 4.2121E+04 ;
EVALUATE b312 := 4.2328E+04 ;
EVALUATE b313 := 4.2509E+04 ;
EVALUATE b314 := 4.2654E+04 ;
EVALUATE b315 := 4.2733E+04 ;
EVALUATE b316 := 4.2661E+04 ;
EVALUATE b317 := 4.2256E+04 ;
EVALUATE b318 := 4.1138E+04 ;
EVALUATE b319 := 3.8524E+04 ;
EVALUATE b320 := 3.2764E+04 ;
*
EVALUATE b201 := b301 0.66667 * ;
EVALUATE b202 := b302 0.66667 * ;
EVALUATE b203 := b303 0.66667 * ;
EVALUATE b204 := b304 0.66667 * ;
EVALUATE b205 := b305 0.66667 * ;
EVALUATE b206 := b306 0.66667 * ;
EVALUATE b207 := b307 0.66667 * ;
EVALUATE b208 := b308 0.66667 * ;
EVALUATE b209 := b309 0.66667 * ;
EVALUATE b210 := b310 0.66667 * ;
EVALUATE b211 := b311 0.66667 * ;
EVALUATE b212 := b312 0.66667 * ;
EVALUATE b213 := b313 0.66667 * ;
EVALUATE b214 := b314 0.66667 * ;
EVALUATE b215 := b315 0.66667 * ;
EVALUATE b216 := b316 0.66667 * ;
EVALUATE b217 := b317 0.66667 * ;
EVALUATE b218 := b318 0.66667 * ;
EVALUATE b219 := b319 0.66667 * ;
EVALUATE b220 := b320 0.66667 * ;
```

```
*
*
*************************************************************************
*                         Create map geometry                         *
*************************************************************************
*
FUELMAP := INIRES: ::
*
*-----
* Define number of divisions and weight of fuel per division
*-----
*
  NBUND 20 NCHAN 84 NZONE 1 NGRP 8 WEIGHT 7.99457 IMOD 4
   ::: GEOD: CAR3D 14 14 26
     EDIT 1
*
*-----
* Define boundary conditions
*-----
*
    X- VOID         X+ REFL
    Y- VOID         Y+ REFL
    Z- VOID         Z+ VOID
*
*-----
* Define fuel mixture locations by axial plane
*-----
*
    MIX
*
    PLANE  1
*
      0  0  0  0  0  0  0  0  0  0  0  0  0  0
      0  0  0  0  0  0  0  0  0  0  0  0  0  0
      0  0  0  0  0  0  0  0  0  0  0  0  0  0
      0  0  0  0  0  0  0  0  0  0  0  0  0  0
      0  0  0  0  0  0  0  0  0  0  0  0  0  0
      0  0  0  0  0  0  0  0  0  0  0  0  0  0
      0  0  0  0  0  0  0  0  0  0  0  0  0  0
      0  0  0  0  0  0  0  0  0  0  0  0  0  0
      0  0  0  0  0  0  0  0  0  0  0  0  0  0
      0  0  0  0  0  0  0  0  0  0  0  0  0  0
      0  0  0  0  0  0  0  0  0  0  0  0  0  0
      0  0  0  0  0  0  0  0  0  0  0  0  0  0
      0  0  0  0  0  0  0  0  0  0  0  0  0  0
      0  0  0  0  0  0  0  0  0  0  0  0  0  0
*
    PLANE  2
*
      0  0  0  0  0  0  0  0  0  0  0  0  0  0
      0  0  0  0  0  0  0  0  0  0  0  0  0  0
      0  0  0  0  0  0  0  0  0  0  0  0  0  0
      0  0  0  0  0  0  0  0  0  0  0  0  0  0
      0  0  0  0  0  0  0  0  0  0  0  0  0  0
      0  0  0  0  0  0  0  0  0  0  0  0  0  0
      0  0  0  0  0  0  0  0  0  0  0  0  0  0
      0  0  0  0  0  0  0  0  0  0  0  0  0  0
      0  0  0  0  0  0  0  0  0  0  0  0  0  0
      0  0  0  0  0  0  0  0  0  0  0  0  0  0
      0  0  0  0  0  0  0  0  0  0  0  0  0  0
      0  0  0  0  0  0  0  0  0  0  0  0  0  0
      0  0  0  0  0  0  0  0  0  0  0  0  0  0
      0  0  0  0  0  0  0  0  0  0  0  0  0  0
*
    PLANE  3
*
      0  0  0  0  0  0  0  0  0  0  0  0  0  0
```

229

```
        0   0   0   0   0   0   0   0   0   0   0   0   0   0
        0   0   0   0   0   0   0   0   0   0   0   0   0   0
        0   0   0   0   0   0   0   0   0   0   0   0   0   0
        0   0   0   0   0   0   0   0   0   0   0   0   0   0
        0   0   0   0   0   0   0   0   0   0   0   0   0   0
        0   0   0   0   0   0   0   0   0   0   0   0   0   0
        0   0   0   0   0   0   0   0   0   0   0   0   0   0
        0   0   0   0   0   0   0   0   0   0   0   0   0   0
        0   0   0   0   0   0   0   0   0   0   0   0   0   0
        0   0   0   0   0   0   0   0   0   0   0   0   0   0
        0   0   0   0   0   0   0   0   0   0   0   0   0   0
        0   0   0   0   0   0   0   0   0   0   0   0   0   0
        0   0   0   0   0   0   0   0   0   0   0   0   0   0
*
    PLANE   4
*
        0   0   0   0   0   0   0   0   0   0   0   0   0   0
        0   0   0   0   0   0   0   0   0   0   0   0   0   0
        0   0   0   0   0   0   0   0   0   0   0   0   0   0
        0   0   0   0   0   0   0   0   0   0   0   0   0   0
        0   0   0   0   0   0   0   0   0   0  41  21  21  21
        0   0   0   0   0   0   0   0  41  21   1   1   1   1
        0   0   0   0   0   0  41  21   1   1   1   1   1   1
        0   0   0   0   0   0  21   1   1   1   1   1   1   1
        0   0   0   0   0  41   1   1   1   1   1   1   1   1
        0   0   0   0   0  21   1   1   1   1   1   1   1   1
        0   0   0   0  41   1   1   1   1   1   1   1   1   1
        0   0   0   0  21   1   1   1   1   1   1   1   1   1
        0   0   0   0  21   1   1   1   1   1   1   1   1   1
        0   0   0   0  21   1   1   1   1   1   1   1   1   1
*
    PLANE   5
*
        0   0   0   0   0   0   0   0   0   0   0   0   0   0
        0   0   0   0   0   0   0   0   0   0   0   0   0   0
        0   0   0   0   0   0   0   0   0   0   0   0   0   0
        0   0   0   0   0   0   0   0   0   0   0   0   0   0
        0   0   0   0   0   0   0   0   0   0  42  22  22  22
        0   0   0   0   0   0   0   0  42  22   2   2   2   2
        0   0   0   0   0   0  42  22   2   2   2   2   2   2
        0   0   0   0   0   0  22   2   2   2   2   2   2   2
        0   0   0   0   0  42   2   2   2   2   2   2   2   2
        0   0   0   0   0  22   2   2   2   2   2   2   2   2
        0   0   0   0  42   2   2   2   2   2   2   2   2   2
        0   0   0   0  22   2   2   2   2   2   2   2   2   2
        0   0   0   0  22   2   2   2   2   2   2   2   2   2
        0   0   0   0  22   2   2   2   2   2   2   2   2   2
*
    PLANE   6
*
        0   0   0   0   0   0   0   0   0   0   0   0   0   0
        0   0   0   0   0   0   0   0   0   0   0   0   0   0
        0   0   0   0   0   0   0   0   0   0   0   0   0   0
        0   0   0   0   0   0   0   0   0   0   0   0   0   0
        0   0   0   0   0   0   0   0   0   0  43  23  23  23
        0   0   0   0   0   0   0   0  43  23   3   3   3   3
        0   0   0   0   0   0  43  23   3   3   3   3   3   3
        0   0   0   0   0   0  23   3   3   3   3   3   3   3
        0   0   0   0   0  43   3   3   3   3   3   3   3   3
        0   0   0   0   0  23   3   3   3   3   3   3   3   3
        0   0   0   0  43   3   3   3   3   3   3   3   3   3
        0   0   0   0  23   3   3   3   3   3   3   3   3   3
        0   0   0   0  23   3   3   3   3   3   3   3   3   3
        0   0   0   0  23   3   3   3   3   3   3   3   3   3
*
    PLANE   7
*
```

```
        0   0   0   0   0   0   0   0   0   0   0   0   0   0
        0   0   0   0   0   0   0   0   0   0   0   0   0   0
        0   0   0   0   0   0   0   0   0   0   0   0   0   0
        0   0   0   0   0   0   0   0   0   0   0   0   0   0
        0   0   0   0   0   0   0   0   0   0  44  24  24  24
        0   0   0   0   0   0   0   0  44  24   4   4   4   4
        0   0   0   0   0   0  44  24   4   4   4   4   4   4
        0   0   0   0   0   0  24   4   4   4   4   4   4   4
        0   0   0   0   0  44   4   4   4   4   4   4   4   4
        0   0   0   0   0  24   4   4   4   4   4   4   4   4
        0   0   0   0  44   4   4   4   4   4   4   4   4   4
        0   0   0   0  24   4   4   4   4   4   4   4   4   4
        0   0   0   0  24   4   4   4   4   4   4   4   4   4
        0   0   0   0  24   4   4   4   4   4   4   4   4   4
*
    PLANE   8
*
        0   0   0   0   0   0   0   0   0   0   0   0   0   0
        0   0   0   0   0   0   0   0   0   0   0   0   0   0
        0   0   0   0   0   0   0   0   0   0   0   0   0   0
        0   0   0   0   0   0   0   0   0   0   0   0   0   0
        0   0   0   0   0   0   0   0   0   0  45  25  25  25
        0   0   0   0   0   0   0   0  45  25   5   5   5   5
        0   0   0   0   0   0  45  25   5   5   5   5   5   5
        0   0   0   0   0   0  25   5   5   5   5   5   5   5
        0   0   0   0   0  45   5   5   5   5   5   5   5   5
        0   0   0   0   0  25   5   5   5   5   5   5   5   5
        0   0   0   0  45   5   5   5   5   5   5   5   5   5
        0   0   0   0  25   5   5   5   5   5   5   5   5   5
        0   0   0   0  25   5   5   5   5   5   5   5   5   5
        0   0   0   0  25   5   5   5   5   5   5   5   5   5
*
    PLANE   9
*
        0   0   0   0   0   0   0   0   0   0   0   0   0   0
        0   0   0   0   0   0   0   0   0   0   0   0   0   0
        0   0   0   0   0   0   0   0   0   0   0   0   0   0
        0   0   0   0   0   0   0   0   0   0   0   0   0   0
        0   0   0   0   0   0   0   0   0   0  46  26  26  26
        0   0   0   0   0   0   0   0  46  26   6   6   6   6
        0   0   0   0   0   0  46  26   6   6   6   6   6   6
        0   0   0   0   0   0  26   6   6   6   6   6   6   6
        0   0   0   0   0  46   6   6   6   6   6   6   6   6
        0   0   0   0   0  26   6   6   6   6   6   6   6   6
        0   0   0   0  46   6   6   6   6   6   6   6   6   6
        0   0   0   0  26   6   6   6   6   6   6   6   6   6
        0   0   0   0  26   6   6   6   6   6   6   6   6   6
        0   0   0   0  26   6   6   6   6   6   6   6   6   6
*
    PLANE 10
*
        0   0   0   0   0   0   0   0   0   0   0   0   0   0
        0   0   0   0   0   0   0   0   0   0   0   0   0   0
        0   0   0   0   0   0   0   0   0   0   0   0   0   0
        0   0   0   0   0   0   0   0   0   0   0   0   0   0
        0   0   0   0   0   0   0   0   0   0  47  27  27  27
        0   0   0   0   0   0   0   0  47  27   7   7   7   7
        0   0   0   0   0   0  47  27   7   7   7   7   7   7
        0   0   0   0   0   0  27   7   7   7   7   7   7   7
        0   0   0   0   0  47   7   7   7   7   7   7   7   7
        0   0   0   0   0  27   7   7   7   7   7   7   7   7
        0   0   0   0  47   7   7   7   7   7   7   7   7   7
        0   0   0   0  27   7   7   7   7   7   7   7   7   7
        0   0   0   0  27   7   7   7   7   7   7   7   7   7
        0   0   0   0  27   7   7   7   7   7   7   7   7   7
*
    PLANE 11
```

```
*
      0  0  0  0  0  0  0  0  0  0  0  0  0  0
      0  0  0  0  0  0  0  0  0  0  0  0  0  0
      0  0  0  0  0  0  0  0  0  0  0  0  0  0
      0  0  0  0  0  0  0  0  0  0  0  0  0  0
      0  0  0  0  0  0  0  0  0  0 48 28 28 28
      0  0  0  0  0  0  0  0 48 28  8  8  8  8
      0  0  0  0  0  0 48 28  8  8  8  8  8  8
      0  0  0  0  0  0 28  8  8  8  8  8  8  8
      0  0  0  0  0 48  8  8  8  8  8  8  8  8
      0  0  0  0  0 28  8  8  8  8  8  8  8  8
      0  0  0  0 48  8  8  8  8  8  8  8  8  8
      0  0  0  0 28  8  8  8  8  8  8  8  8  8
      0  0  0  0 28  8  8  8  8  8  8  8  8  8
      0  0  0  0 28  8  8  8  8  8  8  8  8  8
*
    PLANE 12
*
      0  0  0  0  0  0  0  0  0  0  0  0  0  0
      0  0  0  0  0  0  0  0  0  0  0  0  0  0
      0  0  0  0  0  0  0  0  0  0  0  0  0  0
      0  0  0  0  0  0  0  0  0  0  0  0  0  0
      0  0  0  0  0  0  0  0  0  0 49 29 29 29
      0  0  0  0  0  0  0  0 49 29  9  9  9  9
      0  0  0  0  0  0 49 29  9  9  9  9  9  9
      0  0  0  0  0  0 29  9  9  9  9  9  9  9
      0  0  0  0  0 49  9  9  9  9  9  9  9  9
      0  0  0  0  0 29  9  9  9  9  9  9  9  9
      0  0  0  0 49  9  9  9  9  9  9  9  9  9
      0  0  0  0 29  9  9  9  9  9  9  9  9  9
      0  0  0  0 29  9  9  9  9  9  9  9  9  9
      0  0  0  0 29  9  9  9  9  9  9  9  9  9
*
    PLANE 13
*
      0  0  0  0  0  0  0  0  0  0  0  0  0  0
      0  0  0  0  0  0  0  0  0  0  0  0  0  0
      0  0  0  0  0  0  0  0  0  0  0  0  0  0
      0  0  0  0  0  0  0  0  0  0  0  0  0  0
      0  0  0  0  0  0  0  0  0  0 50 30 30 30
      0  0  0  0  0  0  0  0 50 30 10 10 10 10
      0  0  0  0  0  0 50 30 10 10 10 10 10 10
      0  0  0  0  0  0 30 10 10 10 10 10 10 10
      0  0  0  0  0 50 10 10 10 10 10 10 10 10
      0  0  0  0  0 30 10 10 10 10 10 10 10 10
      0  0  0  0 50 10 10 10 10 10 10 10 10 10
      0  0  0  0 30 10 10 10 10 10 10 10 10 10
      0  0  0  0 30 10 10 10 10 10 10 10 10 10
      0  0  0  0 30 10 10 10 10 10 10 10 10 10
*
    PLANE 14
*
      0  0  0  0  0  0  0  0  0  0  0  0  0  0
      0  0  0  0  0  0  0  0  0  0  0  0  0  0
      0  0  0  0  0  0  0  0  0  0  0  0  0  0
      0  0  0  0  0  0  0  0  0  0  0  0  0  0
      0  0  0  0  0  0  0  0  0  0 51 31 31 31
      0  0  0  0  0  0  0  0 51 31 11 11 11 11
      0  0  0  0  0  0 51 31 11 11 11 11 11 11
      0  0  0  0  0  0 31 11 11 11 11 11 11 11
      0  0  0  0  0 51 11 11 11 11 11 11 11 11
      0  0  0  0  0 31 11 11 11 11 11 11 11 11
      0  0  0  0 51 11 11 11 11 11 11 11 11 11
      0  0  0  0 31 11 11 11 11 11 11 11 11 11
      0  0  0  0 31 11 11 11 11 11 11 11 11 11
      0  0  0  0 31 11 11 11 11 11 11 11 11 11
*
```

```
    PLANE 15
*
     0   0   0   0   0   0   0   0   0   0   0   0   0   0
     0   0   0   0   0   0   0   0   0   0   0   0   0   0
     0   0   0   0   0   0   0   0   0   0   0   0   0   0
     0   0   0   0   0   0   0   0   0   0   0   0   0   0
     0   0   0   0   0   0   0   0   0   0  52  32  32  32
     0   0   0   0   0   0   0   0  52  32  12  12  12  12
     0   0   0   0   0   0  52  32  12  12  12  12  12  12
     0   0   0   0   0   0  32  12  12  12  12  12  12  12
     0   0   0   0   0  52  12  12  12  12  12  12  12  12
     0   0   0   0   0  32  12  12  12  12  12  12  12  12
     0   0   0   0  52  12  12  12  12  12  12  12  12  12
     0   0   0   0  32  12  12  12  12  12  12  12  12  12
     0   0   0   0  32  12  12  12  12  12  12  12  12  12
     0   0   0   0  32  12  12  12  12  12  12  12  12  12
*
    PLANE 16
*
     0   0   0   0   0   0   0   0   0   0   0   0   0   0
     0   0   0   0   0   0   0   0   0   0   0   0   0   0
     0   0   0   0   0   0   0   0   0   0   0   0   0   0
     0   0   0   0   0   0   0   0   0   0   0   0   0   0
     0   0   0   0   0   0   0   0   0   0  53  33  33  33
     0   0   0   0   0   0   0   0  53  33  13  13  13  13
     0   0   0   0   0   0  53  33  13  13  13  13  13  13
     0   0   0   0   0   0  33  13  13  13  13  13  13  13
     0   0   0   0   0  53  13  13  13  13  13  13  13  13
     0   0   0   0   0  33  13  13  13  13  13  13  13  13
     0   0   0   0  53  13  13  13  13  13  13  13  13  13
     0   0   0   0  33  13  13  13  13  13  13  13  13  13
     0   0   0   0  33  13  13  13  13  13  13  13  13  13
     0   0   0   0  33  13  13  13  13  13  13  13  13  13
*
    PLANE 17
*
     0   0   0   0   0   0   0   0   0   0   0   0   0   0
     0   0   0   0   0   0   0   0   0   0   0   0   0   0
     0   0   0   0   0   0   0   0   0   0   0   0   0   0
     0   0   0   0   0   0   0   0   0   0   0   0   0   0
     0   0   0   0   0   0   0   0   0   0  54  34  34  34
     0   0   0   0   0   0   0   0  54  34  14  14  14  14
     0   0   0   0   0   0  54  34  14  14  14  14  14  14
     0   0   0   0   0   0  34  14  14  14  14  14  14  14
     0   0   0   0   0  54  14  14  14  14  14  14  14  14
     0   0   0   0   0  34  14  14  14  14  14  14  14  14
     0   0   0   0  54  14  14  14  14  14  14  14  14  14
     0   0   0   0  34  14  14  14  14  14  14  14  14  14
     0   0   0   0  34  14  14  14  14  14  14  14  14  14
     0   0   0   0  34  14  14  14  14  14  14  14  14  14
*
    PLANE 18
*
     0   0   0   0   0   0   0   0   0   0   0   0   0   0
     0   0   0   0   0   0   0   0   0   0   0   0   0   0
     0   0   0   0   0   0   0   0   0   0   0   0   0   0
     0   0   0   0   0   0   0   0   0   0   0   0   0   0
     0   0   0   0   0   0   0   0   0   0  55  35  35  35
     0   0   0   0   0   0   0   0  55  35  15  15  15  15
     0   0   0   0   0   0  55  35  15  15  15  15  15  15
     0   0   0   0   0   0  35  15  15  15  15  15  15  15
     0   0   0   0   0  55  15  15  15  15  15  15  15  15
     0   0   0   0   0  35  15  15  15  15  15  15  15  15
     0   0   0   0  55  15  15  15  15  15  15  15  15  15
     0   0   0   0  35  15  15  15  15  15  15  15  15  15
     0   0   0   0  35  15  15  15  15  15  15  15  15  15
     0   0   0   0  35  15  15  15  15  15  15  15  15  15
```

```
*
    PLANE 19
*
     0   0   0   0   0   0   0   0   0   0   0   0   0   0
     0   0   0   0   0   0   0   0   0   0   0   0   0   0
     0   0   0   0   0   0   0   0   0   0   0   0   0   0
     0   0   0   0   0   0   0   0   0   0   0   0   0   0
     0   0   0   0   0   0   0   0   0   0  56  36  36  36
     0   0   0   0   0   0   0   0  56  36  16  16  16  16
     0   0   0   0   0   0  56  36  16  16  16  16  16  16
     0   0   0   0   0   0   0  36  16  16  16  16  16  16
     0   0   0   0   0  56  16  16  16  16  16  16  16  16
     0   0   0   0   0  36  16  16  16  16  16  16  16  16
     0   0   0   0  56  16  16  16  16  16  16  16  16  16
     0   0   0   0  36  16  16  16  16  16  16  16  16  16
     0   0   0   0  36  16  16  16  16  16  16  16  16  16
     0   0   0   0  36  16  16  16  16  16  16  16  16  16
*
    PLANE 20
*
     0   0   0   0   0   0   0   0   0   0   0   0   0   0
     0   0   0   0   0   0   0   0   0   0   0   0   0   0
     0   0   0   0   0   0   0   0   0   0   0   0   0   0
     0   0   0   0   0   0   0   0   0   0   0   0   0   0
     0   0   0   0   0   0   0   0   0   0  57  37  37  37
     0   0   0   0   0   0   0   0  57  37  17  17  17  17
     0   0   0   0   0   0  57  37  17  17  17  17  17  17
     0   0   0   0   0   0  37  17  17  17  17  17  17  17
     0   0   0   0   0  57  17  17  17  17  17  17  17  17
     0   0   0   0   0  37  17  17  17  17  17  17  17  17
     0   0   0   0  57  17  17  17  17  17  17  17  17  17
     0   0   0   0  37  17  17  17  17  17  17  17  17  17
     0   0   0   0  37  17  17  17  17  17  17  17  17  17
     0   0   0   0  37  17  17  17  17  17  17  17  17  17
*
    PLANE 21
*
     0   0   0   0   0   0   0   0   0   0   0   0   0   0
     0   0   0   0   0   0   0   0   0   0   0   0   0   0
     0   0   0   0   0   0   0   0   0   0   0   0   0   0
     0   0   0   0   0   0   0   0   0   0   0   0   0   0
     0   0   0   0   0   0   0   0   0   0  58  38  38  38
     0   0   0   0   0   0   0   0  58  38  18  18  18  18
     0   0   0   0   0   0  58  38  18  18  18  18  18  18
     0   0   0   0   0   0  38  18  18  18  18  18  18  18
     0   0   0   0   0  58  18  18  18  18  18  18  18  18
     0   0   0   0   0  38  18  18  18  18  18  18  18  18
     0   0   0   0  58  18  18  18  18  18  18  18  18  18
     0   0   0   0  38  18  18  18  18  18  18  18  18  18
     0   0   0   0  38  18  18  18  18  18  18  18  18  18
     0   0   0   0  38  18  18  18  18  18  18  18  18  18
*
    PLANE 22
*
     0   0   0   0   0   0   0   0   0   0   0   0   0   0
     0   0   0   0   0   0   0   0   0   0   0   0   0   0
     0   0   0   0   0   0   0   0   0   0   0   0   0   0
     0   0   0   0   0   0   0   0   0   0   0   0   0   0
     0   0   0   0   0   0   0   0   0   0  59  39  39  39
     0   0   0   0   0   0   0   0  59  39  19  19  19  19
     0   0   0   0   0   0  59  39  19  19  19  19  19  19
     0   0   0   0   0   0  39  19  19  19  19  19  19  19
     0   0   0   0   0  59  19  19  19  19  19  19  19  19
     0   0   0   0   0  39  19  19  19  19  19  19  19  19
     0   0   0   0  59  19  19  19  19  19  19  19  19  19
     0   0   0   0  39  19  19  19  19  19  19  19  19  19
     0   0   0   0  39  19  19  19  19  19  19  19  19  19
```

```
        0   0   0   0 39 19 19 19 19 19 19 19 19 19
*
    PLANE 23
*
        0   0   0   0   0   0   0   0   0   0   0   0   0   0
        0   0   0   0   0   0   0   0   0   0   0   0   0   0
        0   0   0   0   0   0   0   0   0   0   0   0   0   0
        0   0   0   0   0   0   0   0   0   0   0   0   0   0
        0   0   0   0   0   0   0   0   0   0 60 40 40 40
        0   0   0   0   0   0   0   0 60 40 20 20 20 20
        0   0   0   0   0   0 60 40 20 20 20 20 20 20
        0   0   0   0   0   0 40 20 20 20 20 20 20 20
        0   0   0   0   0 60 20 20 20 20 20 20 20 20
        0   0   0   0   0 40 20 20 20 20 20 20 20 20
        0   0   0   0 60 20 20 20 20 20 20 20 20 20
        0   0   0   0 40 20 20 20 20 20 20 20 20 20
        0   0   0   0 40 20 20 20 20 20 20 20 20 20
        0   0   0   0 40 20 20 20 20 20 20 20 20 20
*
    PLANE 24
*
        0   0   0   0   0   0   0   0   0   0   0   0   0   0
        0   0   0   0   0   0   0   0   0   0   0   0   0   0
        0   0   0   0   0   0   0   0   0   0   0   0   0   0
        0   0   0   0   0   0   0   0   0   0   0   0   0   0
        0   0   0   0   0   0   0   0   0   0   0   0   0   0
        0   0   0   0   0   0   0   0   0   0   0   0   0   0
        0   0   0   0   0   0   0   0   0   0   0   0   0   0
        0   0   0   0   0   0   0   0   0   0   0   0   0   0
        0   0   0   0   0   0   0   0   0   0   0   0   0   0
        0   0   0   0   0   0   0   0   0   0   0   0   0   0
        0   0   0   0   0   0   0   0   0   0   0   0   0   0
        0   0   0   0   0   0   0   0   0   0   0   0   0   0
        0   0   0   0   0   0   0   0   0   0   0   0   0   0
        0   0   0   0   0   0   0   0   0   0   0   0   0   0
*
    PLANE 25
*
        0   0   0   0   0   0   0   0   0   0   0   0   0   0
        0   0   0   0   0   0   0   0   0   0   0   0   0   0
        0   0   0   0   0   0   0   0   0   0   0   0   0   0
        0   0   0   0   0   0   0   0   0   0   0   0   0   0
        0   0   0   0   0   0   0   0   0   0   0   0   0   0
        0   0   0   0   0   0   0   0   0   0   0   0   0   0
        0   0   0   0   0   0   0   0   0   0   0   0   0   0
        0   0   0   0   0   0   0   0   0   0   0   0   0   0
        0   0   0   0   0   0   0   0   0   0   0   0   0   0
        0   0   0   0   0   0   0   0   0   0   0   0   0   0
        0   0   0   0   0   0   0   0   0   0   0   0   0   0
        0   0   0   0   0   0   0   0   0   0   0   0   0   0
        0   0   0   0   0   0   0   0   0   0   0   0   0   0
        0   0   0   0   0   0   0   0   0   0   0   0   0   0
*
    PLANE 26
*
        0   0   0   0   0   0   0   0   0   0   0   0   0   0
        0   0   0   0   0   0   0   0   0   0   0   0   0   0
        0   0   0   0   0   0   0   0   0   0   0   0   0   0
        0   0   0   0   0   0   0   0   0   0   0   0   0   0
        0   0   0   0   0 60   0   0   0   0   0   0   0   0
        0   0   0   0   0 40   0   0   0   0   0   0   0   0
        0   0   0   0   0   0   0   0   0   0   0   0   0   0
        0   0   0   0   0   0   0   0   0   0   0   0   0   0
        0   0   0   0   0   0   0   0   0   0   0   0   0   0
        0   0   0   0   0   0   0   0   0   0   0   0   0   0
        0   0   0   0   0   0   0   0   0   0   0   0   0   0
        0   0   0   0   0   0   0   0   0   0   0   0   0   0
        0   0   0   0   0   0   0   0   0   0   0   0   0   0
```

```
       0  0  0  0  0  0  0  0  0  0  0  0  0  0  0
       0  0  0  0  0  0  0  0  0  0  0  0  0  0  0
*
*-----
* Create spatial mesh
*-----
*
   MESHX   0.00  25.00  50.00  75.00 100.00 125.00 150.00 175.00
          200.00 225.00 250.00 275.00 300.00 325.00 350.00
   MESHY   0.00  25.00  50.00  75.00 100.00 125.00 150.00 175.00
          200.00 225.00 250.00 275.00 300.00 325.00 350.00
   MESHZ   0.00  25.00  50.00  75.00 100.00 125.00 150.00 175.00
          200.00 225.00 250.00 275.00 300.00 325.00 350.00 375.00
          400.00 425.00 450.00 475.00 500.00 525.00 550.00 575.00
          600.00 625.00 650.00 ;
*
*-----
* Create channel identifiers (2D array names)
*-----
*
  NXNAME 'Z1' 'Z2' 'Z3' 'Z4'  '1'  '2'  '3'  '4'  '5'  '6'  '7'  '8'
         '9' '10'
  NYNAME 'ZA' 'ZB' 'ZC' 'ZD'  'A'  'B'  'C'  'D'  'E'  'F'  'G'  'H'
         'J'  'K'
*
*-----
* Define burnrup "zone" (limited meaning for batch fuel)
*-----
*
  BURN-ZONE


                                    1  1  1  1
                                 1  1  1  1  1  1
                              1  1  1  1  1  1  1  1
                              1  1  1  1  1  1  1  1
                           1  1  1  1  1  1  1  1  1
                           1  1  1  1  1  1  1  1  1
                        1  1  1  1  1  1  1  1  1  1
                        1  1  1  1  1  1  1  1  1  1
                        1  1  1  1  1  1  1  1  1  1
                        1  1  1  1  1  1  1  1  1  1
  BURNUP-ZC 41500.0
*
************************************************************************
*              Specify initial powers (by node)                       *
************************************************************************
*
BUNDLE-PW
*
*    PLANE 4    *
*
   <<n01p>> <<n01p>> <<n01p>> <<n01p>> <<n01p>> <<n01p>> <<n01p>>
   <<n01p>> <<n01p>> <<n01p>> <<n01p>> <<n01p>> <<n01p>> <<n01p>>
   <<n01p>> <<n01p>> <<n01p>> <<n01p>> <<n01p>> <<n01p>> <<n01p>>
   <<n01p>> <<n01p>> <<n01p>> <<n01p>> <<n01p>> <<n01p>> <<n01p>>
   <<n01p>> <<n01p>> <<n01p>> <<n01p>> <<n01p>> <<n01p>> <<n01p>>
   <<n01p>> <<n01p>> <<n01p>> <<n01p>> <<n01p>> <<n01p>> <<n01p>>
   <<n01p>> <<n01p>> <<n01p>> <<n01p>> <<n01p>> <<n01p>> <<n01p>>
   <<n01p>> <<n01p>> <<n01p>> <<n01p>> <<n01p>> <<n01p>> <<n01p>>
   <<n01p>> <<n01p>> <<n01p>> <<n01p>> <<n01p>> <<n01p>> <<n01p>>
   <<n01p>> <<n01p>> <<n01p>> <<n01p>> <<n01p>> <<n01p>> <<n01p>>
   <<n01p>> <<n01p>> <<n01p>> <<n01p>> <<n01p>> <<n01p>> <<n01p>>
   <<n01p>> <<n01p>> <<n01p>> <<n01p>> <<n01p>> <<n01p>> <<n01p>>
*
```

```
*     PLANE 5    *
*
    <<n02p>> <<n02p>> <<n02p>> <<n02p>> <<n02p>> <<n02p>> <<n02p>>
    <<n02p>> <<n02p>> <<n02p>> <<n02p>> <<n02p>> <<n02p>> <<n02p>>
    <<n02p>> <<n02p>> <<n02p>> <<n02p>> <<n02p>> <<n02p>> <<n02p>>
    <<n02p>> <<n02p>> <<n02p>> <<n02p>> <<n02p>> <<n02p>> <<n02p>>
    <<n02p>> <<n02p>> <<n02p>> <<n02p>> <<n02p>> <<n02p>> <<n02p>>
    <<n02p>> <<n02p>> <<n02p>> <<n02p>> <<n02p>> <<n02p>> <<n02p>>
    <<n02p>> <<n02p>> <<n02p>> <<n02p>> <<n02p>> <<n02p>> <<n02p>>
    <<n02p>> <<n02p>> <<n02p>> <<n02p>> <<n02p>> <<n02p>> <<n02p>>
    <<n02p>> <<n02p>> <<n02p>> <<n02p>> <<n02p>> <<n02p>> <<n02p>>
    <<n02p>> <<n02p>> <<n02p>> <<n02p>> <<n02p>> <<n02p>> <<n02p>>
    <<n02p>> <<n02p>> <<n02p>> <<n02p>> <<n02p>> <<n02p>> <<n02p>>
    <<n02p>> <<n02p>> <<n02p>> <<n02p>> <<n02p>> <<n02p>> <<n02p>>
```

Author's note: The initial powers in planes 6 through 21 are defined similarly and have been omitted from this description for brevity.

```
*
*     PLANE 22   *
*
    <<n19p>> <<n19p>> <<n19p>> <<n19p>> <<n19p>> <<n19p>> <<n19p>>
    <<n19p>> <<n19p>> <<n19p>> <<n19p>> <<n19p>> <<n19p>> <<n19p>>
    <<n19p>> <<n19p>> <<n19p>> <<n19p>> <<n19p>> <<n19p>> <<n19p>>
    <<n19p>> <<n19p>> <<n19p>> <<n19p>> <<n19p>> <<n19p>> <<n19p>>
    <<n19p>> <<n19p>> <<n19p>> <<n19p>> <<n19p>> <<n19p>> <<n19p>>
    <<n19p>> <<n19p>> <<n19p>> <<n19p>> <<n19p>> <<n19p>> <<n19p>>
    <<n19p>> <<n19p>> <<n19p>> <<n19p>> <<n19p>> <<n19p>> <<n19p>>
    <<n19p>> <<n19p>> <<n19p>> <<n19p>> <<n19p>> <<n19p>> <<n19p>>
    <<n19p>> <<n19p>> <<n19p>> <<n19p>> <<n19p>> <<n19p>> <<n19p>>
    <<n19p>> <<n19p>> <<n19p>> <<n19p>> <<n19p>> <<n19p>> <<n19p>>
    <<n19p>> <<n19p>> <<n19p>> <<n19p>> <<n19p>> <<n19p>> <<n19p>>
    <<n19p>> <<n19p>> <<n19p>> <<n19p>> <<n19p>> <<n19p>> <<n19p>>
*
*     PLANE 23   *
*
    <<n20p>> <<n20p>> <<n20p>> <<n20p>> <<n20p>> <<n20p>> <<n20p>>
    <<n20p>> <<n20p>> <<n20p>> <<n20p>> <<n20p>> <<n20p>> <<n20p>>
    <<n20p>> <<n20p>> <<n20p>> <<n20p>> <<n20p>> <<n20p>> <<n20p>>
    <<n20p>> <<n20p>> <<n20p>> <<n20p>> <<n20p>> <<n20p>> <<n20p>>
    <<n20p>> <<n20p>> <<n20p>> <<n20p>> <<n20p>> <<n20p>> <<n20p>>
    <<n20p>> <<n20p>> <<n20p>> <<n20p>> <<n20p>> <<n20p>> <<n20p>>
    <<n20p>> <<n20p>> <<n20p>> <<n20p>> <<n20p>> <<n20p>> <<n20p>>
    <<n20p>> <<n20p>> <<n20p>> <<n20p>> <<n20p>> <<n20p>> <<n20p>>
    <<n20p>> <<n20p>> <<n20p>> <<n20p>> <<n20p>> <<n20p>> <<n20p>>
    <<n20p>> <<n20p>> <<n20p>> <<n20p>> <<n20p>> <<n20p>> <<n20p>>
    <<n20p>> <<n20p>> <<n20p>> <<n20p>> <<n20p>> <<n20p>> <<n20p>>
    <<n20p>> <<n20p>> <<n20p>> <<n20p>> <<n20p>> <<n20p>> <<n20p>>
*
************************************************************************
*              Specify initial burnups (by node)                      *
************************************************************************
*
  BURN-FUEL
*
*     PLANE 4    *
*
    <<b201>> 0.000000 <<b301>> 0.000000 0.000000 <<b201>> 0.000000
    <<b301>> 0.000000 <<b301>> 0.000000 <<b301>> <<b301>> 0.000000
    <<b301>> 0.000000 <<b301>> 0.000000 <<b301>> 0.000000 <<b201>>
    <<b201>> <<b201>> <<b301>> <<b201>> <<b201>> 0.000000 <<b301>>
    <<b201>> <<b301>> 0.000000 <<b201>> 0.000000 <<b201>> <<b301>>
    <<b201>> 0.000000 <<b201>> 0.000000 <<b301>> 0.000000 <<b301>>
    <<b301>> 0.000000 <<b201>> 0.000000 <<b301>> <<b201>> <<b201>>
    0.000000 <<b301>> <<b201>> 0.000000 <<b301>> 0.000000 <<b301>>
```

```
     0.000000 <<b301>> 0.000000 <<b301>> <<b201>> <<b201>> <<b201>>
     <<b201>> <<b301>> 0.000000 <<b301>> <<b201>> <<b201>> <<b301>>
     0.000000 <<b201>> <<b301>> <<b201>> 0.000000 <<b301>> 0.000000
     <<b201>> <<b301>> 0.000000 <<b301>> <<b201>> <<b201>> <<b201>>
*
*    PLANE 5    *
*
     <<b202>> 0.000000 <<b302>> 0.000000 0.000000 <<b202>> 0.000000
     <<b302>> 0.000000 <<b302>> 0.000000 <<b302>> <<b302>> 0.000000
     <<b302>> 0.000000 <<b302>> 0.000000 <<b302>> 0.000000 <<b202>>
     <<b202>> <<b202>> <<b302>> <<b202>> <<b202>> 0.000000 <<b302>>
     <<b202>> <<b302>> 0.000000 <<b202>> 0.000000 <<b202>> <<b302>>
     <<b202>> 0.000000 <<b202>> 0.000000 <<b302>> 0.000000 <<b302>>
     <<b302>> 0.000000 <<b202>> 0.000000 <<b302>> <<b202>> <<b202>>
     0.000000 <<b302>> <<b202>> 0.000000 <<b302>> 0.000000 <<b302>>
     0.000000 <<b302>> 0.000000 <<b302>> <<b202>> <<b202>> <<b202>>
     <<b202>> <<b302>> 0.000000 <<b302>> <<b202>> <<b202>> <<b302>>
     0.000000 <<b202>> <<b302>> <<b202>> 0.000000 <<b302>> 0.000000
     <<b202>> <<b302>> 0.000000 <<b302>> <<b202>> <<b202>> <<b202>>
```

Author's note: The initial burnups in planes 6 through 21 are defined similarly
and have been omitted from this description for brevity.

```
*
*    PLANE 22   *
*
     <<b219>> 0.000000 <<b319>> 0.000000 0.000000 <<b219>> 0.000000
     <<b319>> 0.000000 <<b319>> 0.000000 <<b319>> <<b319>> 0.000000
     <<b319>> 0.000000 <<b319>> 0.000000 <<b319>> 0.000000 <<b219>>
     <<b219>> <<b219>> <<b319>> <<b219>> <<b219>> 0.000000 <<b319>>
     <<b219>> <<b319>> 0.000000 <<b219>> 0.000000 <<b219>> <<b319>>
     <<b219>> 0.000000 <<b219>> 0.000000 <<b319>> 0.000000 <<b319>>
     <<b319>> 0.000000 <<b219>> 0.000000 <<b319>> <<b219>> <<b219>>
     0.000000 <<b319>> <<b219>> 0.000000 <<b319>> 0.000000 <<b319>>
     0.000000 <<b319>> 0.000000 <<b319>> <<b219>> <<b219>> <<b219>>
     <<b219>> <<b319>> 0.000000 <<b319>> <<b219>> <<b219>> <<b319>>
     0.000000 <<b219>> <<b319>> <<b219>> 0.000000 <<b319>> 0.000000
     <<b219>> <<b319>> 0.000000 <<b319>> <<b219>> <<b219>> <<b219>>
*
*    PLANE 23   *
*
     <<b220>> 0.000000 <<b320>> 0.000000 0.000000 <<b220>> 0.000000
     <<b320>> 0.000000 <<b320>> 0.000000 <<b320>> <<b320>> 0.000000
     <<b320>> 0.000000 <<b320>> 0.000000 <<b320>> 0.000000 <<b220>>
     <<b220>> <<b220>> <<b320>> <<b220>> <<b220>> 0.000000 <<b320>>
     <<b220>> <<b320>> 0.000000 <<b220>> 0.000000 <<b220>> <<b320>>
     <<b220>> 0.000000 <<b220>> 0.000000 <<b320>> 0.000000 <<b320>>
     <<b320>> 0.000000 <<b220>> 0.000000 <<b320>> <<b220>> <<b220>>
     0.000000 <<b320>> <<b220>> 0.000000 <<b320>> 0.000000 <<b320>>
     0.000000 <<b320>> 0.000000 <<b320>> <<b220>> <<b220>> <<b220>>
     <<b220>> <<b320>> 0.000000 <<b320>> <<b220>> <<b220>> <<b320>>
     0.000000 <<b220>> <<b320>> <<b220>> 0.000000 <<b320>> 0.000000
     <<b220>> <<b320>> 0.000000 <<b320>> <<b220>> <<b220>> <<b220>>
;
END: ;
```

A.2.5 Fuel Cross-Section Recovery Procedure

This procedure is specifically for recovering homogenized and condensed cross-
sections from the infinite lattice cell calculations. The procedures for the side and
corner cells are nearly identical and have thus been omitted for brevity.

```
******************************************************************
*
* Procedure creates tables of burnup dependent fuel properties
* by loading DRAGON data from files
*
* David Hummel
* October 2012
*
* Modified March 2013, September 2013
*
******************************************************************
*
*-----
* Declare PROCEDURE input and output
*-----
*
PARAMETER FUELTABS ::
  ::: XSM_FILE FUELTABS ; ;
*
*-----
* Declare STRUCTURES and MODULES
*-----
*
LINKED_LIST
  FUEL0125 FUEL0375 FUEL0625 FUEL0875 FUEL1125 FUEL1375 FUEL1625
  FUEL1875 FUEL2125 FUEL2375 FUEL2625 FUEL2875 FUEL3125 FUEL3375
  FUEL3625 FUEL3875 FUEL4125 FUEL4375 FUEL4625 FUEL4875 ;
MODULE
    XSCONS: END: ;
*
*-----
* State file names for CPO data and load
*-----
*
SEQ_ASCII ffil0125 :: FILE 'fuel_0125.x2m+fullcell.exp' ;
SEQ_ASCII ffil0375 :: FILE 'fuel_0375.x2m+fullcell.exp' ;
SEQ_ASCII ffil0625 :: FILE 'fuel_0625.x2m+fullcell.exp' ;
SEQ_ASCII ffil0875 :: FILE 'fuel_0875.x2m+fullcell.exp' ;
SEQ_ASCII ffil1125 :: FILE 'fuel_1125.x2m+fullcell.exp' ;
SEQ_ASCII ffil1375 :: FILE 'fuel_1375.x2m+fullcell.exp' ;
SEQ_ASCII ffil1625 :: FILE 'fuel_1625.x2m+fullcell.exp' ;
SEQ_ASCII ffil1875 :: FILE 'fuel_1875.x2m+fullcell.exp' ;
SEQ_ASCII ffil2125 :: FILE 'fuel_2125.x2m+fullcell.exp' ;
SEQ_ASCII ffil2375 :: FILE 'fuel_2375.x2m+fullcell.exp' ;
SEQ_ASCII ffil2625 :: FILE 'fuel_2625.x2m+fullcell.exp' ;
SEQ_ASCII ffil2875 :: FILE 'fuel_2875.x2m+fullcell.exp' ;
SEQ_ASCII ffil3125 :: FILE 'fuel_3125.x2m+fullcell.exp' ;
SEQ_ASCII ffil3375 :: FILE 'fuel_3375.x2m+fullcell.exp' ;
SEQ_ASCII ffil3625 :: FILE 'fuel_3625.x2m+fullcell.exp' ;
SEQ_ASCII ffil3875 :: FILE 'fuel_3875.x2m+fullcell.exp' ;
SEQ_ASCII ffil4125 :: FILE 'fuel_4125.x2m+fullcell.exp' ;
SEQ_ASCII ffil4375 :: FILE 'fuel_4375.x2m+fullcell.exp' ;
SEQ_ASCII ffil4625 :: FILE 'fuel_4625.x2m+fullcell.exp' ;
SEQ_ASCII ffil4875 :: FILE 'fuel_4875.x2m+fullcell.exp' ;
*
*-----
* Declare and initialize VARIABLES
*-----
*
REAL delta := 50.0 ; ! burnup step interpolation width
*
**********************************************************************
*      Read cross-section data from file and create fuel tables      *
**********************************************************************
*
FUEL0125 := ffil0125 ;
FUEL0375 := ffil0375 ;
```

```
FUEL0625 := ffil0625 ;
FUEL0875 := ffil0875 ;
FUEL1125 := ffil1125 ;
FUEL1375 := ffil1375 ;
FUEL1625 := ffil1625 ;
FUEL1875 := ffil1875 ;
FUEL2125 := ffil2125 ;
FUEL2375 := ffil2375 ;
FUEL2625 := ffil2625 ;
FUEL2875 := ffil2875 ;
FUEL3125 := ffil3125 ;
FUEL3375 := ffil3375 ;
FUEL3625 := ffil3625 ;
FUEL3875 := ffil3875 ;
FUEL4125 := ffil4125 ;
FUEL4375 := ffil4375 ;
FUEL4625 := ffil4625 ;
FUEL4875 := ffil4875 ;
*
FUELTABS := XSCONS: FUEL0125 FUEL0375 FUEL0625 FUEL0875 FUEL1125
                    FUEL1375 FUEL1625 FUEL1875 FUEL2125 FUEL2375
                    FUEL2625 FUEL2875 FUEL3125 FUEL3375 FUEL3625
                    FUEL3875 FUEL4125 FUEL4375 FUEL4625 FUEL4875 ::
  EDIT 1 READ
  COMPO FUEL0125 TYPE FUEL0125 'REF        1' BURNUP INTRPL <<delta>>
    ENDTYP
  COMPO FUEL0375 TYPE FUEL0375 'REF        1' BURNUP INTRPL <<delta>>
    ENDTYP
  COMPO FUEL0625 TYPE FUEL0625 'REF        1' BURNUP INTRPL <<delta>>
    ENDTYP
  COMPO FUEL0875 TYPE FUEL0875 'REF        1' BURNUP INTRPL <<delta>>
    ENDTYP
  COMPO FUEL1125 TYPE FUEL1125 'REF        1' BURNUP INTRPL <<delta>>
    ENDTYP
  COMPO FUEL1375 TYPE FUEL1375 'REF        1' BURNUP INTRPL <<delta>>
    ENDTYP
  COMPO FUEL1625 TYPE FUEL1625 'REF        1' BURNUP INTRPL <<delta>>
    ENDTYP
  COMPO FUEL1875 TYPE FUEL1875 'REF        1' BURNUP INTRPL <<delta>>
    ENDTYP
  COMPO FUEL2125 TYPE FUEL2125 'REF        1' BURNUP INTRPL <<delta>>
    ENDTYP
  COMPO FUEL2375 TYPE FUEL2375 'REF        1' BURNUP INTRPL <<delta>>
    ENDTYP
  COMPO FUEL2625 TYPE FUEL2625 'REF        1' BURNUP INTRPL <<delta>>
    ENDTYP
  COMPO FUEL2875 TYPE FUEL2875 'REF        1' BURNUP INTRPL <<delta>>
    ENDTYP
  COMPO FUEL3125 TYPE FUEL3125 'REF        1' BURNUP INTRPL <<delta>>
    ENDTYP
  COMPO FUEL3375 TYPE FUEL3375 'REF        1' BURNUP INTRPL <<delta>>
    ENDTYP
  COMPO FUEL3625 TYPE FUEL3625 'REF        1' BURNUP INTRPL <<delta>>
    ENDTYP
  COMPO FUEL3875 TYPE FUEL3875 'REF        1' BURNUP INTRPL <<delta>>
    ENDTYP
  COMPO FUEL4125 TYPE FUEL4125 'REF        1' BURNUP INTRPL <<delta>>
    ENDTYP
  COMPO FUEL4375 TYPE FUEL4375 'REF        1' BURNUP INTRPL <<delta>>
    ENDTYP
  COMPO FUEL4625 TYPE FUEL4625 'REF        1' BURNUP INTRPL <<delta>>
    ENDTYP
  COMPO FUEL4875 TYPE FUEL4875 'REF        1' BURNUP INTRPL <<delta>>
    ENDTYP
  ;
*
END: ;
```

A.2.6 Macroscopic Library Creation Procedure

```
******************************************************************
*
* Procedure creates macroscopic cross-section library
* from burnup fuel tables
*
* David Hummel
* March 2013
*
* Modified September 2013, November 2013
*
******************************************************************
*
*-----
* Declare PROCEDURE input and output
*-----
*
PARAMETER FULMACXS FUELMAP FUELTABS SIDETABS CRNRTABS ::
  ::: LINKED_LIST FULMACXS FUELMAP ;
  ::: XSM_FILE FUELTABS SIDETABS CRNRTABS ; ;
*
*-----
* Declare STRUCTURES and MODULES
*-----
*
MODULE
    CRE: END: ;
*
*
*************************************************************************
*           Create macroscopic library from burnup tables           *
*************************************************************************
*
*-----
* Interior fuel cells
*-----
*
FULMACXS := CRE: FUELTABS FUELMAP ::
  EDIT 0
  READ TABLE FUELTABS
    MIX  1 FUEL0125 BURNUP DIRECTC ENDMIX
    MIX  2 FUEL0375 BURNUP DIRECTC ENDMIX
    MIX  3 FUEL0625 BURNUP DIRECTC ENDMIX
    MIX  4 FUEL0875 BURNUP DIRECTC ENDMIX
    MIX  5 FUEL1125 BURNUP DIRECTC ENDMIX
    MIX  6 FUEL1375 BURNUP DIRECTC ENDMIX
    MIX  7 FUEL1625 BURNUP DIRECTC ENDMIX
    MIX  8 FUEL1875 BURNUP DIRECTC ENDMIX
    MIX  9 FUEL2125 BURNUP DIRECTC ENDMIX
    MIX 10 FUEL2375 BURNUP DIRECTC ENDMIX
    MIX 11 FUEL2625 BURNUP DIRECTC ENDMIX
    MIX 12 FUEL2875 BURNUP DIRECTC ENDMIX
    MIX 13 FUEL3125 BURNUP DIRECTC ENDMIX
    MIX 14 FUEL3375 BURNUP DIRECTC ENDMIX
    MIX 15 FUEL3625 BURNUP DIRECTC ENDMIX
    MIX 16 FUEL3875 BURNUP DIRECTC ENDMIX
    MIX 17 FUEL4125 BURNUP DIRECTC ENDMIX
    MIX 18 FUEL4375 BURNUP DIRECTC ENDMIX
    MIX 19 FUEL4625 BURNUP DIRECTC ENDMIX
    MIX 20 FUEL4875 BURNUP DIRECTC ENDMIX
  ;
*
*-----
* Side fuel cells
*-----
```

```
*
FULMACXS := CRE: FULMACXS SIDETABS FUELMAP ::
  EDIT 0
  READ TABLE SIDETABS
    MIX 21 SIDE0125 BURNUP DIRECTC ENDMIX
    MIX 22 SIDE0375 BURNUP DIRECTC ENDMIX
    MIX 23 SIDE0625 BURNUP DIRECTC ENDMIX
    MIX 24 SIDE0875 BURNUP DIRECTC ENDMIX
    MIX 25 SIDE1125 BURNUP DIRECTC ENDMIX
    MIX 26 SIDE1375 BURNUP DIRECTC ENDMIX
    MIX 27 SIDE1625 BURNUP DIRECTC ENDMIX
    MIX 28 SIDE1875 BURNUP DIRECTC ENDMIX
    MIX 29 SIDE2125 BURNUP DIRECTC ENDMIX
    MIX 30 SIDE2375 BURNUP DIRECTC ENDMIX
    MIX 31 SIDE2625 BURNUP DIRECTC ENDMIX
    MIX 32 SIDE2875 BURNUP DIRECTC ENDMIX
    MIX 33 SIDE3125 BURNUP DIRECTC ENDMIX
    MIX 34 SIDE3375 BURNUP DIRECTC ENDMIX
    MIX 35 SIDE3625 BURNUP DIRECTC ENDMIX
    MIX 36 SIDE3875 BURNUP DIRECTC ENDMIX
    MIX 37 SIDE4125 BURNUP DIRECTC ENDMIX
    MIX 38 SIDE4375 BURNUP DIRECTC ENDMIX
    MIX 39 SIDE4625 BURNUP DIRECTC ENDMIX
    MIX 40 SIDE4875 BURNUP DIRECTC ENDMIX
  ;
*
*-----
* Corner fuel cells
*-----
*
FULMACXS := CRE: FULMACXS CRNRTABS FUELMAP ::
  EDIT 0
  READ TABLE CRNRTABS
    MIX 41 CRNR0125 BURNUP DIRECTC ENDMIX
    MIX 42 CRNR0375 BURNUP DIRECTC ENDMIX
    MIX 43 CRNR0625 BURNUP DIRECTC ENDMIX
    MIX 44 CRNR0875 BURNUP DIRECTC ENDMIX
    MIX 45 CRNR1125 BURNUP DIRECTC ENDMIX
    MIX 46 CRNR1375 BURNUP DIRECTC ENDMIX
    MIX 47 CRNR1625 BURNUP DIRECTC ENDMIX
    MIX 48 CRNR1875 BURNUP DIRECTC ENDMIX
    MIX 49 CRNR2125 BURNUP DIRECTC ENDMIX
    MIX 50 CRNR2375 BURNUP DIRECTC ENDMIX
    MIX 51 CRNR2625 BURNUP DIRECTC ENDMIX
    MIX 52 CRNR2875 BURNUP DIRECTC ENDMIX
    MIX 53 CRNR3125 BURNUP DIRECTC ENDMIX
    MIX 54 CRNR3375 BURNUP DIRECTC ENDMIX
    MIX 55 CRNR3625 BURNUP DIRECTC ENDMIX
    MIX 56 CRNR3875 BURNUP DIRECTC ENDMIX
    MIX 57 CRNR4125 BURNUP DIRECTC ENDMIX
    MIX 58 CRNR4375 BURNUP DIRECTC ENDMIX
    MIX 59 CRNR4625 BURNUP DIRECTC ENDMIX
    MIX 60 CRNR4875 BURNUP DIRECTC ENDMIX
  ;
*
END: ;
```

A.2.7   Fuel Shuffling Procedure

```
****************************************************************
*
* Procedure refuels core according to batch refueling scheme
*
* David Hummel
* October 2012
*
* Modified November 2013
```

```
*
****************************************************************
*
*-----
* Declare PROCEDURE input and output
*-----
*
PARAMETER FUELMAP ::
  ::: LINKED_LIST FUELMAP ; ;
*
*-----
* Declare STRUCTURES and MODULES
*-----
*
MODULE
    REFUEL: END: ;
*
************************************************************************
*               Perform 3-cycle batch refueling                      *
************************************************************************
*
FUELMAP := REFUEL: FUELMAP ::
  EDIT 1
*
*-----
* Move thrice burnt fuel to spent fuel pool
*-----
*
  SHUFF CHAN A9  TO POOL
  SHUFF CHAN B8  TO POOL
  SHUFF CHAN B10 TO POOL
  SHUFF CHAN C4  TO POOL
  SHUFF CHAN C5  TO POOL
  SHUFF CHAN C7  TO POOL
  SHUFF CHAN C9  TO POOL
  SHUFF CHAN D3  TO POOL
  SHUFF CHAN D8  TO POOL
  SHUFF CHAN E3  TO POOL
  SHUFF CHAN E5  TO POOL
  SHUFF CHAN E10 TO POOL
  SHUFF CHAN F6  TO POOL
  SHUFF CHAN F8  TO POOL
  SHUFF CHAN F9  TO POOL
  SHUFF CHAN G3  TO POOL
  SHUFF CHAN G7  TO POOL
  SHUFF CHAN G10 TO POOL
  SHUFF CHAN H2  TO POOL
  SHUFF CHAN H4  TO POOL
  SHUFF CHAN H6  TO POOL
  SHUFF CHAN J1  TO POOL
  SHUFF CHAN J3  TO POOL
  SHUFF CHAN J6  TO POOL
  SHUFF CHAN J9  TO POOL
  SHUFF CHAN K2  TO POOL
  SHUFF CHAN K5  TO POOL
  SHUFF CHAN K7  TO POOL
*
*-----
* Move twice burnt fuel to new locations
*-----
*
  SHUFF CHAN A7  TO C7
  SHUFF CHAN B6  TO F6
  SHUFF CHAN D5  TO D8
  SHUFF CHAN D6  TO C9
  SHUFF CHAN D7  TO F8
  SHUFF CHAN D9  TO E10
```

```
  SHUFF CHAN D10 TO B10
  SHUFF CHAN E4  TO H4
  SHUFF CHAN E7  TO F9
  SHUFF CHAN E9  TO G10
  SHUFF CHAN F2  TO G7
  SHUFF CHAN F4  TO J3
  SHUFF CHAN G1  TO G3
  SHUFF CHAN G4  TO H6
  SHUFF CHAN G5  TO J6
  SHUFF CHAN G8  TO C5
  SHUFF CHAN H7  TO E3
  SHUFF CHAN H8  TO J9
  SHUFF CHAN H9  TO C4
  SHUFF CHAN H10 TO J1
  SHUFF CHAN J4  TO K5
  SHUFF CHAN J5  TO K7
  SHUFF CHAN J8  TO D3
  SHUFF CHAN J10 TO B8
  SHUFF CHAN K4  TO K2
  SHUFF CHAN K8  TO A9
  SHUFF CHAN K9  TO H2
  SHUFF CHAN K10 TO E5
*
*-----
* Move once burnt fuel to new locations
*-----
*
  SHUFF CHAN A8  TO H10
  SHUFF CHAN A10 TO D6
  SHUFF CHAN B5  TO J10
  SHUFF CHAN B7  TO H9
  SHUFF CHAN B9  TO D5
  SHUFF CHAN C3  TO H8
  SHUFF CHAN C6  TO E9
  SHUFF CHAN C8  TO D10
  SHUFF CHAN C10 TO B6
  SHUFF CHAN D4  TO K10
  SHUFF CHAN E2  TO K9
  SHUFF CHAN E6  TO G8
  SHUFF CHAN E8  TO D9
  SHUFF CHAN F3  TO J5
  SHUFF CHAN F5  TO H7
  SHUFF CHAN F7  TO E7
  SHUFF CHAN F10 TO D7
  SHUFF CHAN G2  TO J8
  SHUFF CHAN G6  TO G5
  SHUFF CHAN G9  TO A7
  SHUFF CHAN H1  TO K8
  SHUFF CHAN H3  TO K4
  SHUFF CHAN H5  TO J4
  SHUFF CHAN J2  TO E4
  SHUFF CHAN J7  TO G1
  SHUFF CHAN K1  TO F4
  SHUFF CHAN K3  TO F2
  SHUFF CHAN K6  TO G4
*
*-----
* Place fresh fuel in newly vacated channels
*-----
*
  REFUEL CHAN A8  20
  REFUEL CHAN A10 20
  REFUEL CHAN B5  20
  REFUEL CHAN B7  20
  REFUEL CHAN B9  20
  REFUEL CHAN C3  20
  REFUEL CHAN C6  20
```

```
 REFUEL CHAN C8  20
 REFUEL CHAN C10 20
 REFUEL CHAN D4  20
 REFUEL CHAN E2  20
 REFUEL CHAN E6  20
 REFUEL CHAN E8  20
 REFUEL CHAN F3  20
 REFUEL CHAN F5  20
 REFUEL CHAN F7  20
 REFUEL CHAN F10 20
 REFUEL CHAN G2  20
 REFUEL CHAN G6  20
 REFUEL CHAN G9  20
 REFUEL CHAN H1  20
 REFUEL CHAN H3  20
 REFUEL CHAN H5  20
 REFUEL CHAN J2  20
 REFUEL CHAN J7  20
 REFUEL CHAN K1  20
 REFUEL CHAN K3  20
 REFUEL CHAN K6  20
 ;
*
END: ;
```

A.2.8   Transient Core Model Main Input

The methodology for transient modelling was presented graphically in Figure 4.7.

```
****************************************************************
*
* DONJON 3.02g Model of PT-SCWR (quarter-core)
*
* Steps forward in time during spatial kinetics calculation
*
* David Hummel
* June 2014
*
* Based on ptscwr_v13.x2m
*
* Note included procedures contained within accompanying .c2m
* files
*
****************************************************************
*
*-----
* Declare PROCEDURES, STRUCTURES and MODULES
*-----
*
PROCEDURE
  ProcGeom ProcFixd ;
LINKED_LIST
  GEOMETRY FUELMAP INDEX MACROLIB TRACK SYSTEM FLUX FIXMACXS FULMACXS
  DELTAMAC FLUXP OLDMLIB PSYSTEM ;
XSM_FILE
  FBMDATA ;
MODULE
  REFRES: AFM: TRIVAT: FLXAXC: INIMAC: TRIVAA: FLUD: POWER: END: DMAC:
  IQS: GREP: DELETE: ;
SEQ_ASCII
  tempmap.exp fullfbm.exp newmap.exp oldflux.exp oldlib.exp oldfluxp.exp
  newfluxp.exp newlib.exp ;
*
*-----
```

```
* Declare and initialize VARIABLES
*-----
*
REAL totpower := 635.0 ;      ! reactor total power (MW)
*
INTEGER fiter := 0 ;          ! flux iteration number
REAL maxfeps := 1.0E-04 ;     ! flux convergence criterion
INTEGER nadi := 5 ;           ! number of inner flux iterations
INTEGER maxout := 200 ;       ! max number of outer flux iterations
*
*-----
* Load reactivity feedback database from file
*-----
FBMDATA := fullfbm.exp ;
*-----
* Load data from previous time step
*-----
OLDMLIB := oldlib.exp ;
FLUX := oldflux.exp ;
FLUXP := oldfluxp.exp ;
FUELMAP := tempmap.exp ;
*
*************************************************************************
*                     Define core geometry                           *
*************************************************************************
*
GEOMETRY INDEX := ProcGeom ;
*
*************************************************************************
* Define mixtures for fixed materials  (i.e. not burnup dependent)   *
*************************************************************************
*
FIXMACXS := ProcFixd ;
*
*************************************************************************
*             Cross-reference index with fuelmap                     *
*************************************************************************
*
INDEX FUELMAP := REFRES: INDEX FUELMAP GEOMETRY ;
*
*************************************************************************
*         Create 3D tracking information and system matrix           *
*************************************************************************
*
TRACK := TRIVAT: GEOMETRY ::
  EDIT 1
  TITL 'Tracking for 3D quarter-core PT-SCWR'
  MAXR 40000 MCFD 1 ;
SYSTEM := TRIVAA: OLDMLIB TRACK ::
  EDIT 0 ;
*
*************************************************************************
*         Simulate this snapshot and advance one timestep            *
*************************************************************************
*
*-----
* Create new library based on perturbed operating conditions
*-----
FULMACXS := AFM: FBMDATA FUELMAP ::
  MAP
  INFOR 'PTSCWR_FBM'
  DNAME 60
    'FUL0125REF' 'FUL0375REF' 'FUL0625REF' 'FUL0875REF'
    'FUL1125REF' 'FUL1375REF' 'FUL1625REF' 'FUL1875REF'
    'FUL2125REF' 'FUL2375REF' 'FUL2625REF' 'FUL2875REF'
    'FUL3125REF' 'FUL3375REF' 'FUL3625REF' 'FUL3875REF'
    'FUL4125REF' 'FUL4375REF' 'FUL4625REF' 'FUL4875REF'
```

```
      'FUL0125SID' 'FUL0375SID' 'FUL0625SID' 'FUL0875SID'
      'FUL1125SID' 'FUL1375SID' 'FUL1625SID' 'FUL1875SID'
      'FUL2125SID' 'FUL2375SID' 'FUL2625SID' 'FUL2875SID'
      'FUL3125SID' 'FUL3375SID' 'FUL3625SID' 'FUL3875SID'
      'FUL4125SID' 'FUL4375SID' 'FUL4625SID' 'FUL4875SID'
      'FUL0125COR' 'FUL0375COR' 'FUL0625COR' 'FUL0875COR'
      'FUL1125COR' 'FUL1375COR' 'FUL1625COR' 'FUL1875COR'
      'FUL2125COR' 'FUL2375COR' 'FUL2625COR' 'FUL2875COR'
      'FUL3125COR' 'FUL3375COR' 'FUL3625COR' 'FUL3875COR'
      'FUL4125COR' 'FUL4375COR' 'FUL4625COR' 'FUL4875COR'
    REFT
       1 'FUL0125REF'  2 'FUL0375REF'  3 'FUL0625REF'  4 'FUL0875REF'
       5 'FUL1125REF'  6 'FUL1375REF'  7 'FUL1625REF'  8 'FUL1875REF'
       9 'FUL2125REF' 10 'FUL2375REF' 11 'FUL2625REF' 12 'FUL2875REF'
      13 'FUL3125REF' 14 'FUL3375REF' 15 'FUL3625REF' 16 'FUL3875REF'
      17 'FUL4125REF' 18 'FUL4375REF' 19 'FUL4625REF' 20 'FUL4875REF'
      21 'FUL0125SID' 22 'FUL0375SID' 23 'FUL0625SID' 24 'FUL0875SID'
      25 'FUL1125SID' 26 'FUL1375SID' 27 'FUL1625SID' 28 'FUL1875SID'
      29 'FUL2125SID' 30 'FUL2375SID' 31 'FUL2625SID' 32 'FUL2875SID'
      33 'FUL3125SID' 34 'FUL3375SID' 35 'FUL3625SID' 36 'FUL3875SID'
      37 'FUL4125SID' 38 'FUL4375SID' 39 'FUL4625SID' 40 'FUL4875SID'
      41 'FUL0125COR' 42 'FUL0375COR' 43 'FUL0625COR' 44 'FUL0875COR'
      45 'FUL1125COR' 46 'FUL1375COR' 47 'FUL1625COR' 48 'FUL1875COR'
      49 'FUL2125COR' 50 'FUL2375COR' 51 'FUL2625COR' 52 'FUL2875COR'
      53 'FUL3125COR' 54 'FUL3375COR' 55 'FUL3625COR' 56 'FUL3875COR'
      57 'FUL4125COR' 58 'FUL4375COR' 59 'FUL4625COR' 60 'FUL4875COR'
    EDIT 1
 *   BORON 0.9282
    ;
 MACROLIB := INIMAC: INDEX FIXMACXS FULMACXS ;
 *-----
 * Calculate delta in cross-sections between reference and perturbed
 *-----
 DELTAMAC := DMAC: OLDMLIB MACROLIB ::
   EDIT 0 STEP 1 ;
 *-----
 * Create perturbation system matrix
 *-----
 PSYSTEM := TRIVAA: OLDMLIB TRACK DELTAMAC ::
   EDIT 0 PERT UNIT OVEL ;
 *-----
 * Solve for IQS flux
 *-----
 FLUXP := IQS: FLUXP
              FLUX PSYSTEM SYSTEM TRACK DELTAMAC OLDMLIB GEOMETRY ::
   EDIT 1
   TETA
   BETA 0.0000718 0.0007410 0.0005467 0.0010020 0.0003615 0.0000907
   DECR 0.0117727 0.0277209 0.1151299 0.2993739 1.0469525 2.5418856
   CONV 1.0000E-02 1.0000E-04 5
   KAPS DEL 1.0000E-06 HI 1.0000E-05 METHOD GRKA END
   CON2 1.0000E-04 1.0000E-04 1.0
   TMAC
   BEGIN
   PERT 1 STEP 1.000 END ;
 *-----
 * Calculate axial (node) fluxes from 3D flux and update node powers
 *-----
 GREP: FLUXP :: GETVAL POWER 1 >>totpower<< ;
 FUELMAP := FLXAXC: FUELMAP FLUXP TRACK INDEX ::
   EDIT 0 AXIAL COMP ;
 FUELMAP := POWER: FUELMAP FULMACXS ::
   EDIT 0 POWER <<totpower>> ;
 *
 ************************************************************************
 *                     Save data to files                              *
 ************************************************************************
```

```
*
newmap.exp := FUELMAP ;
newfluxp.exp := FLUXP ;
newlib.exp := MACROLIB ;
*
FBMDATA := DELETE: FBMDATA ;
*
END: ;
QUIT .
```

A.3 Single-Channel CATHENA Input (Core Thermalhydraulics)

This is the CATHENA input for the single-channel model described in Section
4.2.1. The quarter-core (84-channel) model is conceptually similar and the
component definitions are nearly identical except for the number of parallel
components and total volumes. The large number of components in the 84-
channel model means the input is over 50,000 lines long, making it impractical to
include in this thesis.

```
'PT-SCWR SINGLE CHANNEL MODEL',
'DAVID HUMMEL, OCTOBER 2013'/

'CONTROL PARAMETERS'/
'**----------------------------------------------------------------------'/
'*                         PROGRAM CONTROL                               '/
'*-----------------------------------------------------------------------'/
'SOLUTION CONTROL'/
0.00,1000.00, , 1.00E-03, 1.00E-04, 1.00E-01/
'*-----------------------------------------------------------------------'/
'PRINT CONTROL'/
10.00, 10.00, 10.00, , , , .TRUE., /
'*-----------------------------------------------------------------------'/
'RESTART CONTROL'/
 , 'ptscwr64_v1.rst', 10.00, , , , /
'*-----------------------------------------------------------------------'/
'PROCESSING OPTION'/
'RUN'/
'*-----------------------------------------------------------------------'/
'NUMERIC OPTIONS'/
'HLWP-VERSION(1)'/
'*-----------------------------------------------------------------------'/
'END'/

'COMPONENTS'/
'**----------------------------------------------------------------------'/
'*                 HYDRAULIC COMPONENT DEFINITION                        '/
'*-----------------------------------------------------------------------'/
'INBOUND', , , , , , , , , 'H2O', , , /
'*-----------------------------------------------------------------------'/
'PUMPDIS', 0.500, 0.000, 2.731E-01, 0.593, 4.500E-05, 0.000, 'CIRC',
 3, 'H2O', , , /
'*-----------------------------------------------------------------------'/
'INPLEN', , , , , , , 'VOLMC', , 'H2O', , 68.7190, /
'*-----------------------------------------------------------------------'/
'INNOZZLE', 1.697, -1.697, 1.614E-02, 0.100, 4.500E-05, 1.200, 'CIRC',
 3, 'H2O', 336, 9.20498, /
'*-----------------------------------------------------------------------'/
'FLOWTUBE', 5.000, -5.000, 6.648E-03, 0.092, 4.500E-05, 0.000, 'CIRC',
 20, 'H2O', 336, 11.16798, /
'*-----------------------------------------------------------------------'/
'RVRSEVOL', 0.250, 0.000, 1.629E-02, 0.144, 4.50E-05, 1.200, 'CIRC',
```

```
 1, 'H2O', 336, 1.36803, /
'*----------------------------------------------------------------'/
'FUELCHAN', 5.000, 5.000, 4.565E-03, 0.007, 4.50E-05, 20.000,
'CANFLEX', 20, 'H2O', 336, 7.66875, /
'*----------------------------------------------------------------'/
'OUTNOZLE', 1.697, 1.697, 3.136E-03, 0.063, 4.500E-05, 1.150, 'CIRC',
 3, 'H2O', 336, 1.78825, /
'*----------------------------------------------------------------'/
'RISER', 0.927, 0.927, 2.992E-03, 0.062, 4.500E-05, 0.000, 'CIRC',
 3, 'H2O', 336, 0.93192, /
'*----------------------------------------------------------------'/
'OUTPLEN', , , , , , , 'VOLMC', , 'H2O', , 14.23217, /
'*----------------------------------------------------------------'/
'DEADVOL', 0.927, -0.927, 2.274E-02, 0.141, 4.500E-05, 0.000, 'CIRC',
 3, 'H2O', 336, 7.08238, /
'*----------------------------------------------------------------'/
'TRBPIPE', 0.990, 0.000, 1.257E-01, 0.400, 4.500E-05, 0.000, 'CIRC',
 3, 'H2O', 336, 0.49760, /
'*----------------------------------------------------------------'/
'OUTBOUND', , , , , , , , , 'H2O', , , /
'*----------------------------------------------------------------'/
'END'/

'CONNECTIONS'/
'**---------------------------------------------------------------'/
'*                 HYDRAULIC CONNECTIONS DEFINITION               '/
'*----------------------------------------------------------------'/
'INBOUND', 'L-PUMPDIS'/
'R-PUMPDIS', 'INPLEN'/
'INPLEN', 'L-INNOZZLE'/
'R-INNOZZLE','L-FLOWTUBE'/
'R-FLOWTUBE', 'L-RVRSEVOL'/
'R-RVRSEVOL', 'L-FUELCHAN'/
'R-FUELCHAN', 'L-OUTNOZLE'/
'R-OUTNOZLE', 'L-RISER'/
'R-RISER', 'OUTPLEN'/
'L-DEADVOL'/
'R-DEADVOL','OUTPLEN'/
'OUTPLEN','L-TRBPIPE'/
'R-TRBPIPE', 'OUTBOUND'/
'*----------------------------------------------------------------'/
'END'/

'BOUNDARY CONDITIONS'/
'**---------------------------------------------------------------'/
'*            HYDRAULIC BOUNDARY CONDITIONS DEFINITION            '/
'*----------------------------------------------------------------'/
'RESERVOIR B.C.', 'INLETBC'/
'INBOUND'/
2.58E+07, , 350.00, 0.00, 'HG-BY-SAT', 'HF-BY-TEMP'/
'*----------------------------------------------------------------'/
'RESERVOIR B.C.', 'OUTLETBC'/
'OUTBOUND'/
2.50E+07, , 625.00, 0.00, 'HG-BY-SAT', 'HF-BY-TEMP'/
'*----------------------------------------------------------------'/
'END'/

'SYSTEM MODELS'/
'**---------------------------------------------------------------'/
'*                    SYSTEM MODELS (VALVES)                      '/
'*----------------------------------------------------------------'/
'VALVE', 'INLTORIF'/
'R-INNOZZLE','L-FLOWTUBE'/
4.072E-03, 0.61, 1.0, , , , , , , 'ASME', 'CHISHOLM'/
'*----------------------------------------------------------------'/
'END'/
```

```
'SYSTEM CONTROL'/
'**------------------------------------------------------------------'/
'*               SYSTEM CONTROLS (INCLUDING OUTPUTS)            '/
'*------------------------------------------------------------------'/
```

Author's note: Output controls have been omitted from this printing in order to save space.

```
/
'*------------------------------------------------------------------'/
'CONTROL DEVICE', 'ORIFCTRL', .TRUE./
'PI', 5.643E-04, 3.00, , 0.0, , 0.00/
0.01, 1.00/
  'TEMPF:OUTNOZLE(1)'/
  'CONSTANT(625.00)',-1.0/
  /
    'INLTORIF', 'OPENFR', .FALSE./
  /
'*------------------------------------------------------------------'/
'END'/

'INITIAL CONDITIONS'/
'**------------------------------------------------------------------'/
'*                 HYDRAULIC INITIAL CONDITIONS                 '/
'*------------------------------------------------------------------'/
'PUMPDIS', 'BY-ENDS', 'HG-BY-SAT', 'HF-BY-TEMP'/
2.580E+07, , 350.00, 0.00, 1512.00/
2.580E+07, , 350.00, 0.00, 1512.00/
'*------------------------------------------------------------------'/
'INPLEN', 'BY-NODE', 'HG-BY-SAT', 'HF-BY-TEMP'/
2.580E+07, , 350.00, 0.00, 1512.00/
'*------------------------------------------------------------------'/
'INNOZZLE', 'BY-ENDS', 'HG-BY-SAT', 'HF-BY-TEMP'/
2.580E+07, , 350.00, 0.00, 1512.00/
2.580E+07, , 350.00, 0.00, 1512.00/
'*------------------------------------------------------------------'/
'FLOWTUBE', 'BY-ENDS', 'HG-BY-SAT', 'HF-BY-TEMP'/
2.580E+07, , 350.00, 0.00, 1512.00/
2.580E+07, , 350.00, 0.00, 1512.00/
'*------------------------------------------------------------------'/
'RVRSEVOL', 'BY-ENDS', 'HG-BY-SAT', 'HF-BY-TEMP'/
2.580E+07, , 350.00, 0.00, 1512.00/
2.580E+07, , 350.00, 0.00, 1512.00/
'*------------------------------------------------------------------'/
'FUELCHAN', 'BY-NODES', 'HG-BY-SAT', 'HF-BY-TEMP'/
2.580E+07, , 354.85, 0.00, 1512.00/
2.576E+07, , 357.99, 0.00, 1512.00/
2.572E+07, , 363.10, 0.00, 1512.00/
2.567E+07, , 368.77, 0.00, 1512.00/
2.563E+07, , 376.50, 0.00, 1512.00/
2.559E+07, , 381.20, 0.00, 1512.00/
2.555E+07, , 384.79, 0.00, 1512.00/
2.551E+07, , 386.15, 0.00, 1512.00/
2.546E+07, , 388.33, 0.00, 1512.00/
2.542E+07, , 392.32, 0.00, 1512.00/
2.538E+07, , 399.68, 0.00, 1512.00/
2.534E+07, , 412.76, 0.00, 1512.00/
2.529E+07, , 431.12, 0.00, 1512.00/
2.525E+07, , 454.56, 0.00, 1512.00/
2.521E+07, , 482.85, 0.00, 1512.00/
2.517E+07, , 511.85, 0.00, 1512.00/
2.513E+07, , 540.05, 0.00, 1512.00/
2.508E+07, , 570.05, 0.00, 1512.00/
2.504E+07, , 589.85, 0.00, 1512.00/
2.500E+07, , 609.10, 0.00, 1512.00/
```

```
'*-------------------------------------------------------------------'/
'OUTNOZLE', 'BY-ENDS', 'HG-BY-SAT', 'HF-BY-TEMP'/
2.500E+07, , 625.00, 0.00, 1512.00/
2.500E+07, , 625.00, 0.00, 1512.00/
'*-------------------------------------------------------------------'/
'RISER', 'BY-ENDS', 'HG-BY-SAT', 'HF-BY-TEMP'/
2.500E+07, , 625.00, 0.00, 1512.00/
2.500E+07, , 625.00, 0.00, 1512.00/
'*-------------------------------------------------------------------'/
'OUTPLEN', 'BY-NODE', 'HG-BY-SAT', 'HF-BY-TEMP'/
2.500E+07, , 625.00, 0.00, 1512.00/
'*-------------------------------------------------------------------'/
'DEADVOL', 'BY-ENDS', 'HG-BY-SAT', 'HF-BY-TEMP'/
2.500E+07, , 625.00, 0.00, 0.00/
2.500E+07, , 625.00, 0.00, 0.00/
'*-------------------------------------------------------------------'/
'TRBPIPE', 'BY-ENDS', 'HG-BY-SAT', 'HF-BY-TEMP'/
2.500E+07, , 625.00, 0.00, 1512.00/
2.500E+07, , 625.00, 0.00, 1512.00/
'*-------------------------------------------------------------------'/
'INBOUND', 'L-PUMPDIS'/
1512.00/
'*-------------------------------------------------------------------'/
'R-PUMPDIS', 'INPLEN'/
1512.00/
'*-------------------------------------------------------------------'/
'INPLEN', 'L-INNOZZLE'/
1512.00/
'*-------------------------------------------------------------------'/
'R-INNOZZLE','L-FLOWTUBE'/
1512.00/
'*-------------------------------------------------------------------'/
'R-FLOWTUBE', 'L-RVRSEVOL'/
1512.00/
'*-------------------------------------------------------------------'/
'R-RVRSEVOL', 'L-FUELCHAN'/
1512.00/
'*-------------------------------------------------------------------'/
'R-FUELCHAN', 'L-OUTNOZLE'/
1512.00/
'*-------------------------------------------------------------------'/
'R-OUTNOZLE', 'L-RISER'/
1512.00/
'*-------------------------------------------------------------------'/
'R-RISER', 'OUTPLEN'/
1512.00/
'*-------------------------------------------------------------------'/
'R-DEADVOL','OUTPLEN'/
0.00/
'*-------------------------------------------------------------------'/
'OUTPLEN','L-TRBPIPE'/
1512.00/
'*-------------------------------------------------------------------'/
'R-TRBPIPE', 'OUTBOUND'/
1512.00/
'*-------------------------------------------------------------------'/
'END'/

'HEAT TRANSFER PACKAGE'/
'**------------------------------------------------------------------'/
'*             HEAT GENERATION AND TRANSFER DEFINITIONS              '/
'*-------------------------------------------------------------------'/
'MODEL:(TUBEWALL)', 'RADIAL CONDUCTION', , /
'RADIAL:(1,0.046,3,0.047)', 'AXIAL:(5.0,20)', , 'CYLINDER:(1,336)'/
'BOUNDARY CONDITIONS:(1,1)'/
'INSIDE HYDRAULIC:(FLOWTUBE)', 'BRANCH NODE:(1,20)',
 'MODEL NODE:(1,20)', , , , /
```

251

```
'TUBE-CIR', , , , , , , , , , , , , /
'OUTSIDE HYDRAULIC:(FUELCHAN)', 'BRANCH NODE:(20,1)',
 'MODEL NODE:(1,20)', , , , /
'TUBE-CIR', , , , , , , , , , , , , /
'STAINLESS STEEL'/
'HQ-NIL'/
'TEMP-2D-RAD-AXI'/
350.00, 479.55,       609.10/
350.00, 469.93, 589.85/
350.00, 460.43, 570.85/
350.00, 445.03, 540.05/
350.00, 430.93, 511.85/
350.00, 416.43, 482.85/
350.00, 402.28, 454.56/
350.00, 390.56, 431.12/
350.00, 381.38, 412.76/
350.00, 374.84, 399.68/
350.00, 371.16, 392.32/
350.00, 369.16, 388.33/
350.00, 368.08, 386.15/
350.00, 367.39, 384.79/
350.00, 365.60, 381.20/
350.00, 363.25, 376.50/
350.00, 359.39, 368.77/
350.00, 356.55, 363.10/
350.00, 353.99, 357.99/
350.00, 352.43, 354.85/
'NO-PRINT-OUT'/
'*----------------------------------------------------------------'/
'MODEL:(INFUEL)', 'RADIAL CONDUCTION', , /
'RADIAL:(3)','AXIAL:(5.0,20)', , 'CYLINDER:(1,10752)'/
0.0,4,0.004150,2,0.004232,2,0.004750/
'BOUNDARY CONDITIONS:(0,1)'/
'OUTSIDE HYDRAULIC:(FUELCHAN)', 'BRANCH NODE:(1,20)',
 'MODEL NODE:(1,20)', , , , /
'ALPHA-DEFAULT', 'HT-CRIT-(0,0,6,6,2,2)',
 'HT-CORR-(43,43,43,43,2,2,75,75,2)', , ,
 'WALL-INTERFACE-HEAT-TRANSFER(5,5,5,5,5,5,1)', , , , , , , , /
'MPF-TEMP:(28)'/
  27.0, 3.80, 2.18E+06,
 127.0, 3.42, 2.39E+06,
 227.0, 3.11, 2.51E+06,
 327.0, 2.86, 2.60E+06,
 427.0, 2.64, 2.66E+06,
 527.0, 2.45, 2.70E+06,
 627.0, 2.29, 2.72E+06,
 727.0, 2.15, 2.74E+06,
 827.0, 2.02, 2.75E+06,
 927.0, 1.91, 2.75E+06,
1027.0, 1.81, 2.75E+06,
1127.0, 1.72, 2.75E+06,
1227.0, 1.64, 2.75E+06,
1327.0, 1.57, 2.76E+06,
1427.0, 1.50, 2.76E+06,
1527.0, 1.44, 2.78E+06,
1627.0, 1.38, 2.79E+06,
1727.0, 1.33, 2.82E+06,
1827.0, 1.28, 2.86E+06,
1927.0, 1.23, 2.91E+06,
2027.0, 1.19, 2.98E+06,
2127.0, 1.15, 3.06E+06,
2227.0, 1.11, 3.15E+06,
2327.0, 1.08, 3.26E+06,
2427.0, 1.05, 3.40E+06,
2527.0, 1.01, 3.55E+06,
2627.0, 0.99, 3.73E+06,
2727.0, 0.96, 3.93E+06/
```

```
'GAP:(50000.0,0.5,0.8)'/
'STAINLESS STEEL'/
'HQ-SPACE:(1229.9E6)'/
'R-USER:(0.1111 0.3333 0.5556))', , 'A-USER', , /
0.0414,0.0454,0.0480,0.0494,0.0504,0.0512,0.0518,0.0524,0.0528,0.0530,
0.0532,0.0531,0.0529,0.0526,0.0521,0.0515,0.0506,0.0491,0.0464,0.0427/
'HQ-NIL'/
'HQ-NIL'/
'TEMP-2D-RAD-AXI'/
687.0, 687.0, 687.0, 687.0, 687.0, 687.0/
687.0, 687.0, 687.0, 687.0, 687.0, 687.0/
687.0, 687.0, 687.0, 687.0, 687.0, 687.0/
687.0, 687.0, 687.0, 687.0, 687.0, 687.0/
687.0, 687.0, 687.0, 687.0, 687.0, 687.0/
687.0, 687.0, 687.0, 687.0, 687.0, 687.0/
687.0, 687.0, 687.0, 687.0, 687.0, 687.0/
687.0, 687.0, 687.0, 687.0, 687.0, 687.0/
687.0, 687.0, 687.0, 687.0, 687.0, 687.0/
687.0, 687.0, 687.0, 687.0, 687.0, 687.0/
687.0, 687.0, 687.0, 687.0, 687.0, 687.0/
687.0, 687.0, 687.0, 687.0, 687.0, 687.0/
687.0, 687.0, 687.0, 687.0, 687.0, 687.0/
687.0, 687.0, 687.0, 687.0, 687.0, 687.0/
687.0, 687.0, 687.0, 687.0, 687.0, 687.0/
687.0, 687.0, 687.0, 687.0, 687.0, 687.0/
687.0, 687.0, 687.0, 687.0, 687.0, 687.0/
687.0, 687.0, 687.0, 687.0, 687.0, 687.0/
687.0, 687.0, 687.0, 687.0, 687.0, 687.0/
687.0, 687.0, 687.0, 687.0, 687.0, 687.0/
'NO-PRINT-OUT'/
'*----------------------------------------------------------------'/
'MODEL:(OUTFUEL)', 'RADIAL CONDUCTION', , /
'RADIAL:(3)', 'AXIAL:(5.0,20)', , 'CYLINDER:(1,10752)' /
0.0,4,0.004400,2,0.004482,2,0.005000/
'BOUNDARY CONDITIONS:(0,1)'/
'OUTSIDE HYDRAULIC:(FUELCHAN)', 'BRANCH NODE:(1,20)',
 'MODEL NODE:(1,20)', , , , /
'ALPHA-DEFAULT', 'HT-CRIT-(0,0,6,6,2,2)',
 'HT-CORR-(43,43,43,43,2,2,75,75,2)', , ,
 'WALL-INTERFACE-HEAT-TRANSFER(5,5,5,5,5,5,1)', , , , , , , , /
'MPF-TEMP:(28)'/
  27.0, 4.77, 2.17E+06,
 127.0, 4.20, 2.38E+06,
 227.0, 3.75, 2.50E+06,
 327.0, 3.39, 2.59E+06,
 427.0, 3.10, 2.64E+06,
 527.0, 2.85, 2.69E+06,
 627.0, 2.63, 2.71E+06,
 727.0, 2.45, 2.73E+06,
 827.0, 2.29, 2.74E+06,
 927.0, 2.15, 2.74E+06,
1027.0, 2.03, 2.74E+06,
1127.0, 1.92, 2.74E+06,
1227.0, 1.82, 2.74E+06,
1327.0, 1.73, 2.75E+06,
1427.0, 1.65, 2.75E+06,
1527.0, 1.58, 2.77E+06,
1627.0, 1.51, 2.79E+06,
1727.0, 1.45, 2.82E+06,
1827.0, 1.39, 2.86E+06,
1927.0, 1.34, 2.91E+06,
2027.0, 1.29, 2.98E+06,
2127.0, 1.24, 3.06E+06,
2227.0, 1.20, 3.16E+06,
2327.0, 1.16, 3.27E+06,
2427.0, 1.12, 3.41E+06,
2527.0, 1.09, 3.57E+06,
```

```
2627.0, 1.06, 3.75E+06,
2727.0, 1.03, 3.96E+06/
'GAP:(50000.0,0.5,0.8)'/
'STAINLESS STEEL'/
'HQ-SPACE:(1325.2E6)'/
'R-USER:(0.1111 0.3333 0.5556)', , 'A-USER', , /
0.0414,0.0454,0.0480,0.0494,0.0504,0.0512,0.0518,0.0524,0.0528,0.0530,
0.0532,0.0531,0.0529,0.0526,0.0521,0.0515,0.0506,0.0491,0.0464,0.0427/
'HQ-NIL'/
'HQ-NIL'/
'TEMP-2D-RAD-AXI'/
687.0, 687.0, 687.0, 687.0, 687.0/
687.0, 687.0, 687.0, 687.0, 687.0, 687.0/
687.0, 687.0, 687.0, 687.0, 687.0, 687.0/
687.0, 687.0, 687.0, 687.0, 687.0, 687.0/
687.0, 687.0, 687.0, 687.0, 687.0, 687.0/
687.0, 687.0, 687.0, 687.0, 687.0, 687.0/
687.0, 687.0, 687.0, 687.0, 687.0, 687.0/
687.0, 687.0, 687.0, 687.0, 687.0, 687.0/
687.0, 687.0, 687.0, 687.0, 687.0, 687.0/
687.0, 687.0, 687.0, 687.0, 687.0, 687.0/
687.0, 687.0, 687.0, 687.0, 687.0, 687.0/
687.0, 687.0, 687.0, 687.0, 687.0, 687.0/
687.0, 687.0, 687.0, 687.0, 687.0, 687.0/
687.0, 687.0, 687.0, 687.0, 687.0, 687.0/
687.0, 687.0, 687.0, 687.0, 687.0, 687.0/
687.0, 687.0, 687.0, 687.0, 687.0, 687.0/
687.0, 687.0, 687.0, 687.0, 687.0, 687.0/
687.0, 687.0, 687.0, 687.0, 687.0, 687.0/
687.0, 687.0, 687.0, 687.0, 687.0, 687.0/
687.0, 687.0, 687.0, 687.0, 687.0, 687.0/
'NO-PRINT-OUT'/
'*-------------------------------------------------------------'/
'MODEL:(PRESTUBE)', 'RADIAL CONDUCTION', , /
'RADIAL:(4,0.0720,2,0.0725,4,0.0780,2,0.0785,2,0.0905)',
 'AXIAL:(5.0,20)', ,'CYLINDER:(1,336)'/
'BOUNDARY CONDITIONS:(1,1)'/
'INSIDE HYDRAULIC:(FUELCHAN)', 'BRANCH NODE:(1,20)',
 'MODEL NODE:(1,20)', , , , /
'TUBE-CIR', , , , , , , , , , , , /
'OUTSIDE PRESCRIBED:(MODER)', , , , , 'SURFACE OPTION:(1)'/
'LIQUID-BATH'/
'P,H:(0.336E6,0.231E6)-VERTICAL', 'HT-CRIT-POOL', 'HT-CORR-POOL'/
'STAINLESS STEEL'/
'MPF-TEMP:(20)'/
  50.0, 2.51, 2.7497E+06,
 100.0, 2.52, 2.8991E+06,
 150.0, 2.47, 3.0545E+06,
 200.0, 2.39, 3.1783E+06,
 250.0, 2.31, 3.2834E+06,
 300.0, 2.22, 3.3458E+06,
 350.0, 2.15, 3.4292E+06,
 400.0, 2.09, 3.5075E+06,
 450.0, 2.03, 3.5493E+06,
 500.0, 1.99, 3.5649E+06,
 550.0, 1.96, 3.5828E+06,
 600.0, 1.93, 3.6379E+06,
 650.0, 1.91, 3.6738E+06,
 700.0, 1.90, 3.7045E+06,
 750.0, 1.90, 3.7208E+06,
 800.0, 1.92, 3.7659E+06,
 850.0, 1.94, 3.7630E+06,
 900.0, 1.97, 3.8086E+06,
 950.0, 2.00, 3.8377E+06,
1000.0, 2.06, 3.8632E+06/
'ZIRCALOY'/
'ZIRCALOY'/
```

```
'HQ-NIL'/
'HQ-NIL'/
'HQ-NIL'/
'HQ-NIL'/
'TEMP-2D-RAD-AXI'/
354.85, 304.88, 254.90, 204.93, 154.95, 104.98, 55.00/
357.99, 307.49, 256.99, 206.49, 156.00, 105.50, 55.00/
363.10, 311.75, 260.40, 209.05, 157.70, 106.35, 55.00/
368.77, 316.48, 264.18, 211.89, 159.59, 107.30, 55.00/
376.50, 322.92, 269.33, 215.75, 162.17, 108.58, 55.00/
381.20, 326.83, 272.47, 218.10, 163.73, 109.37, 55.00/
384.79, 329.82, 274.86, 219.89, 164.93, 109.96, 55.00/
386.15, 330.96, 275.77, 220.58, 165.38, 110.19, 55.00/
388.33, 332.77, 277.22, 221.66, 166.11, 110.55, 55.00/
392.32, 336.10, 279.88, 223.66, 167.44, 111.22, 55.00/
399.68, 342.24, 284.79, 227.34, 169.89, 112.45, 55.00/
412.76, 353.13, 293.51, 233.88, 174.25, 114.63, 55.00/
431.12, 368.44, 305.75, 243.06, 180.37, 117.69, 55.00/
454.56, 387.97, 321.38, 254.78, 188.19, 121.59, 55.00/
482.85, 411.54, 340.23, 268.93, 197.62, 126.31, 55.00/
511.85, 435.71, 359.57, 283.43, 207.28, 131.14, 55.00/
540.05, 459.21, 378.37, 297.53, 216.68, 135.84, 55.00/
570.85, 484.88, 398.90, 312.93, 226.95, 140.98, 55.00/
589.85, 500.71, 411.57, 322.43, 233.28, 144.14, 55.00/
609.10, 516.75, 424.40, 332.05, 239.70, 147.35, 55.00/
'NO-PRINT-OUT'/
'*----------------------------------------------------------------'/
'END'/
```

Appendix B

Coupling Scripts and Functions

The scripts and functions that facilitated the DONJON-CATHENA coupling in this work were written in the OCTAVE programming language. The OCTAVE interpreter is freely available and open-source under the GNU General Public License.

This work used multiple functions for processing DONJON and CATHENA input and output, which are dependencies of the main coupling scripts. The methodology for input and output parsing is fairly straightforward, so these functions have been omitted from this thesis for brevity.

B.1 Steady-State Coupling Script

This script implements the procedure presented in Figure 4.13.

```
% stdyscript.m
%
% DONJON/CATHENA steady-state iteration script
%
% David Hummel, August 2014
% Modified October 2014
%
% Dependencies: updatemap.m
%               mapgrab.m
%               catgrab.m
%               catingen2.m
%               orifgrab3.m
%
%%%%%%%%%%%%%%%%%%%
% Octave Commands %
%%%%%%%%%%%%%%%%%%%
%
more off
clc
warning('off','all')
%
%%%%%%%%%%%%%%%
% Definitions %
%%%%%%%%%%%%%%%
%
exec = 'testrundonjon'; % DONJON executable
stdyfile = 'steadyafm.x2m'; % steady-state iteration input file
```

```matlab
initfile = 'fluxinit.x2m' ; % 3D flux intitialization input file
catscript = 'catingen2.m'; % script that generates CATHENA input
firstmap = '../SteadyData/bocafmmod.exp'; % initial fuelmap
firstth  = '../SteadyData/boc_orif'; % initial TH distribution directory
orifdata = '../SteadyData/boc_orifices.dat'; % orifice distribution
procdir = '../PROCEDURES'; % directory that contains DONJON procedures
dbdir = '../DB8G'; % database directory
scratchdir = 'SCRATCH'; % scratch storage directory
resultsdir = 'Results'; % results directory
%
maxdiff = 0.01 ;  % maximum allowable relative power difference
%
maxiter = 50 ; % maximum number of iterations in calculation
relax = 0.2 ; % relaxation on node power variation
%
%%%%%%%%%%%%%%%%%%%%%
% Print Disclaimers %
%%%%%%%%%%%%%%%%%%%%%
%
printf('*-----\n* Full-core steady-state initialization script\n');
printf('* David Hummel\n* August 2014\n*-----\n');
printf('Uses the following inputs:\n');
printf('  DONJON steady-state input file:     ''%s''\n',stdyfile);
printf('  CATHENA input generation script:    ''%s''\n',catscript);
printf('  Initial power/burnup dist:          ''%s''\n',firstmap);
printf('  Initial flow/temperature dist:      ''%s''\n',firstth);
printf('  Flow limiting orifice data file:    ''%s''\n',orifdata);
%
%%%%%%%%%%%%%%%%%%%%%%%%%%%%
% Initial flux calculation %
%%%%%%%%%%%%%%%%%%%%%%%%%%%%
%
tic
%
iter = 0;
% Initialize flux calculation
command = horzcat('cp -f ',firstmap,' ',scratchdir,'/oldmap.exp');
[status cmdout] = system(command,'-echo');
printf('*\n*-----\n* Initializing flux calculation \n*-----\n*\n');
command = horzcat(exec,' ',initfile,' ',dbdir,' ',procdir,' ',...
    scratchdir,'/oldmap.exp');
printf('Executing ''%s'' ...',command);
[status cmdout] = system(command,'-echo');
printf(' Done\n');
command = horzcat('mv -f ',initfile,'+oldflux.exp ',...
    scratchdir,'/oldflux.exp');
[status cmdout] = system(command,'-echo');
% Load reference T/H properties and update DONJON fuelmap
printf('*\n*-----\n* Extract initial thermalhydraulic properties \n');
printf('*-----\n*\n');
printf('Parsing data from directory ''%s'' ...',firstth);
[chandens chantemp tubedens tubetemp fueltemp chanflow] = ...
    catgrab(firstth);
chandens = chandens/1000.0;
chantemp = chantemp + 273.15;
tubedens = tubedens/1000.0;
tubetemp = tubetemp + 273.15;
fueltemp = fueltemp + 273.15;
command = horzcat('cp ',orifdata,' ',scratchdir,'/orifdata.txt');
[status cmdout] = system(command,'-echo');
command = horzcat('cp ',firstmap,' ',scratchdir,'/oldmap.exp');
[status cmdout] = system(command,'-echo');
%
updatemap(firstmap,horzcat(scratchdir,'/oldmap.exp'),chandens,...
    chantemp,tubedens,tubetemp,fueltemp);
command = horzcat('cp ',scratchdir,'/oldmap.exp ',resultsdir,'/',...
    sprintf('stdyiter%03d',iter),'.exp');
```

```matlab
[status cmdout] = system(command,'-echo');
oldpower = mapgrab(horzcat(scratchdir,'/oldmap.exp'),...
    horzcat(resultsdir,'/',sprintf('stdyiter%03d',iter),'.png'));
printf(' Done\n');
plotiter(1) = iter;
plotpower(1) = 0;
%
% Loop iterates with steady-state flux calculation to find consistent
% distribution of flux and power
%
printf('*\n*-----\n* Steady-state initialization calculation\n');
printf('*-----\n*\n');
iter = iter + 1;
while iter <= maxiter
    printf('Iteration %03d of %03d\n----------------------------\n',...
        iter,maxiter);
    %
    % Run DONJON with the TH conditions
    %
    command = horzcat(exec,' ',stdyfile,' ',dbdir,' ',procdir,' ',...
        scratchdir,'/oldmap.exp ',scratchdir,'/oldflux.exp');
    printf('Executing ''%s'' ...',command);
    [status cmdout] = system(command,'-echo');
    printf(' Done\n');
    %
    % Grab power distribution from DONJON output
    %
    newpower = mapgrab(horzcat(stdyfile,'+newmap.exp'),...
        horzcat(resultsdir,'/',sprintf('stdyiter%03d',iter),'.png'));
    pause(0.1)
    command = horzcat('mv -f ',stdyfile,'+newmap.exp ',...
        scratchdir,'/oldmap.exp');
    [status cmdout] = system(command,'-echo');
    command = horzcat('cp ',scratchdir,'/oldmap.exp ',resultsdir,'/',...
        sprintf('stdyiter%03d',iter),'.exp');
    [status cmdout] = system(command,'-echo');
    % Show results on screen
    plotiter(iter + 1) = iter;
    plotpower(iter + 1) = max(oldpower./newpower) - 1.0;
    figure(2)
    plot(plotiter,plotpower)
    axis([0 maxiter -1 1])
    title('Core Power Change')
    xlabel('Iteration');
    ylabel('Max. Relative Power Difference');
    pause(0.1)
    %
    % Create CATHENA input to find orifice sizes
    %
    printf('\nCreating CATHENA input for valve controllers...');
    catingen2(((1-relax)*oldpower+relax*newpower),...
        horzcat(scratchdir,'/orifdata.txt'),1,1);
    printf(' Done\n')
    command = horzcat('cp -f ',scratchdir(1:3),'_valv.inp ',...
        scratchdir,'/');
    [status cmdout] = system(command,'-echo');
    % Run CATHENA
    chdir(horzcat(scratchdir,'/'))
    command = horzcat('runcathena ',scratchdir(1:3),'_valv.inp');
    printf('Executing ''%s'' ...',command);
    [status cmdout] = system(command,'-echo');
    printf(' Done\n\n');
    [status cmdout] = system('rm *.lis','-echo');
    [status cmdout] = system('rm *.rst','-echo');
    chdir('../');
    % Extract orifice sizes
    orifices = orifgrab3(scratchdir,horzcat(scratchdir,'/orifdata.txt'));
```

```matlab
    % Clean up
    command = horzcat('rm ',scratchdir,'/*.dat');
    [status cmdout] = system(command,'-echo');
    %
    % Create CATHENA input with static orifices
    %
    printf('\nCreating CATHENA input for static orifices...');
    catingen2(((1-relax)*oldpower+relax*newpower),...
        horzcat(scratchdir,'/orifdata.txt'),0,1);
    printf(' Done\n')
    command = horzcat('cp -f ',scratchdir(1:3),'_orif.inp ',...
        scratchdir,'/');
    [status cmdout] = system(command,'-echo');
    % Run CATHENA and cleanup
    chdir(horzcat(scratchdir,'/'))
    command = horzcat('runcathena ',scratchdir(1:3),'_orif.inp');
    printf('Executing ''%s'' ...',command);
    [status cmdout] = system(command,'-echo');
    printf(' Done\n\n');
    command = horzcat('mv ',scratchdir(1:3),'_orif.rst ../',...
        resultsdir,'/',sprintf('stdyiter%03d',iter),'.rst');
    [status cmdout] = system(command,'-echo');
    [status cmdout] = system('rm *.lis','-echo');
    chdir('../');
    %
    % Update T/H properties in fuel map
    %
    [newchandens newchantemp newtubedens newtubetemp newfueltemp ...
        newchanflow] = catgrab(horzcat(scratchdir));
    newchandens = newchandens/1000.0;
    newchantemp = newchantemp + 273.15;
    newtubedens = newtubedens/1000.0;
    newtubetemp = newtubetemp + 273.15;
    newfueltemp = newfueltemp + 273.15;
    updatemap(horzcat(scratchdir,'/oldmap.exp'),...
        horzcat(scratchdir,'/oldmap.exp'),newchandens,newchantemp,...
        newtubedens,newtubetemp,newfueltemp);
    % Clean up
    command = horzcat('mkdir ',resultsdir,'/',...
        sprintf('stdyiter%03d',iter));
    [status cmdout] = system(command,'-echo');
    command = horzcat('mv -f ',scratchdir,'/*.dat ',resultsdir,'/',...
        sprintf('stdyiter%03d',iter),'/');
    [status cmdout] = system(command,'-echo');
    % Advance iteration
    iter = iter + 1;
    oldpower = (1-relax)*oldpower+relax*newpower ;
end
printf('*-----\n* Execution complete\n*-----\n');
toc
```

B.2 Transient Coupling Script

The transient coupling procedure was summarized visually in Figure 4.15.

```matlab
% transcript.m
%
% DONJON transient script
%
% David Hummel, June 2014
% Modified August 2014
%
% Dependencies: updatemap.m
%               mapgrab.m
%               tstepchange.m
```

259

```octave
%              catrestarttrans.m
%              catgrab.m
%
%%%%%%%%%%%%%%%%%%%%
% Octave Commands %
%%%%%%%%%%%%%%%%%%%%
%
more off
clc
warning('off','all')
%
%%%%%%%%%%%%%%%
% Definitions %
%%%%%%%%%%%%%%%
%
exec = 'testrundonjon'; % DONJON executable
initinpfile = 'initialize.x2m'; % initial DONJON input file name
traninpfile = 'transstep.x2m'; % transient DONJON input file name
catscript = 'catrestarttrans.m'; % script that generates CATHENA input
firstmap = '../BOC_SteadyAFM/Results/stdyiter050.exp'; % initial fuelmap
firsttth = '../BOC_SteadyAFM/Results/stdyiter050.rst'; % restart file
orifdata = '../BOC_SteadyAFM/SCRATCH/orifdata.txt'; % orifice data
refthdir = '../BOC_SteadyAFM/Results/stdyiter050'; % initial T/H data
procdir = '../PROCEDURES'; % directory that contains DONJON procedures
dbdir = '../DB8G';  % database directory
scratchdir = 'SCRATCH'; % scratch storage directory
resultsdir = 'Results'; % results directory
%
time = 0.0 ;            % initial time (s)
tend = 100.0 ;          % transient end time (s)
%
maxtstep =  1.0E-00 ;   % maximum timestep size (s)
mintstep =  5.0E-04 ;   % minimum timestep size (s)
tstep =     5.0E-03 ;   % initial timestep size (s)
%
%
maxdiff = 0.005 ;   % maximum allowable relative power difference
%
pin = 2.58E7;
pout = 2.50E7;
tin = 350.00;
%
%
%%%%%%%%%%%%%%%%%%%%%%%
% Print Disclaimers %
%%%%%%%%%%%%%%%%%%%%%%%
%
printf('*-----\n* Coupled transient script\n* David Hummel\n*');
printf(' August 2014\n*-----\n');
printf('Uses the following inputs:\n');
printf('  DONJON initialization input file:  ''%s''\n',initinpfile);
printf('  DONJON transient input file:       ''%s''\n',traninpfile);
printf('  CATHENA input generation script:   ''%s''\n',catscript);
printf('  Initial power/burnup dist:         ''%s''\n',firstmap);
printf('  Initial flow/temperature dist:     ''%s''\n',firsttth);
printf('  Flow limiting orifice data file:   ''%s''\n\n',orifdata);
%
%%%%%%%%%%%%%%%%%%%%%%%%%%%%%%%
% Initialization Calculation %
%%%%%%%%%%%%%%%%%%%%%%%%%%%%%%%
%
tic
%
command = horzcat('cp ',firstmap,' ',scratchdir,'/tempmap.exp');
[status cmdout] = system(command,'-echo');
stdypower = mapgrab(firstmap,horzcat...
    (resultsdir,'/',sprintf('%2.4fs',time),'.png'));
```

```matlab
pause(0.1);
%
% Change timestep size in DONJON input file
tstepchange(initinpfile,tstep);
time = time + tstep;
%
% Run quasi-steady core for initial flux distribution
printf('*\n*-----\n* Transient initialization calculation\n');
printf('*-----\n*\n');
command = horzcat(exec,' ',initinpfile,' ',dbdir,' ',procdir,' ',...
    scratchdir,'/tempmap.exp');
printf('Executing ''%s'' ...',command);
[status cmdout] = system(command,'-echo');
printf(' Done');
command = horzcat('mv ',initinpfile,'+ ',resultsdir,'/',...
    sprintf('%2.4fs',time),'.x2m+');
[status cmdout] = system(command,'-echo');
%
% Show results on screen and save data
oldpower = mapgrab(horzcat(initinpfile,'+newmap.exp'),...
    horzcat(resultsdir,'/',sprintf('%2.4fs',time),'.png'));
i = 2;
plotpower(1) = sum(stdypower)/1E3;
plottime(1) = time - tstep;
plottime(i) = time;
plotpower(i) = sum(oldpower)/1E3;
figure(2)
plot(plottime,plotpower)
axis([0 tend 500 800])
title('Core Power History')
xlabel('Time (s)');
ylabel('Power (MW)');
pause(0.1)
% Copy initial results to scratch directory
command = horzcat('mv -f ',initinpfile,'+newflux.exp ',...
    scratchdir,'/oldflux.exp');
[status cmdout] = system(command,'-echo');
command = horzcat('mv -f ',initinpfile,'+newfluxp.exp ',...
    scratchdir,'/oldfluxp.exp');
[status cmdout] = system(command,'-echo');
command = horzcat('mv -f ',initinpfile,'+newmap.exp ',...
    scratchdir,'/oldmap.exp');
[status cmdout] = system(command,'-echo');
command = horzcat('mv -f ',initinpfile,'+newlib.exp ',...
    scratchdir,'/oldlib.exp');
[status cmdout] = system(command,'-echo');
% Initialize CATHENA restart file for this power distribution
[oldchandens oldchantemp oldtubedens oldtubetemp oldfueltemp ...
    oldchanflow] = catgrab(refthdir);
oldchandens = oldchandens/1000.0;
oldchantemp = oldchantemp + 273.15;
oldtubedens = oldtubedens/1000.0;
oldtubetemp = oldtubetemp + 273.15;
oldfueltemp = oldfueltemp + 273.15;
printf('Creating CATHENA input...');
catrestarttrans(horzcat...
    (scratchdir,'/oldmap.exp'),orifdata,tstep,tin,pin,pout);
printf(' Done\n')
command = horzcat('cp -f ','catstep.inp ',scratchdir,'/');
[status cmdout] = system(command,'-echo');
command = horzcat('cp -f ',firstth,' ',scratchdir,'/oldcatstep.rst');
[status cmdout] = system(command,'-echo');
chdir(horzcat(scratchdir,'/'))
command = 'runcathena catstep.inp';
printf('Executing ''%s'' ...',command);
[status cmdout] = system(command,'-echo');
printf(' Done\n');
```

```matlab
[status cmdout] = system('rm oldcatstep.rst','-echo');
[status cmdout] = system('mv newcatstep.rst oldcatstep.rst','-echo');
[status cmdout] = system('rm *.lis','-echo');
chdir('../');
% Move results to results directory
command = horzcat('mkdir ',resultsdir,'/',sprintf('%2.4fs',time));
[status cmdout] = system(command,'-echo');
command = horzcat('mv -f ',scratchdir,'/*.dat ',resultsdir,'/',...
    sprintf('%2.4fs',time),'/');
[status cmdout] = system(command,'-echo');
command = horzcat('cp ',scratchdir,'/oldmap.exp ',resultsdir,'/',...
    sprintf('%2.4fs',time),'.exp');
[status cmdout] = system(command,'-echo');
%
%%%%%%%%%%%%%%%%%%%%%%%%
% Transient Calcaultion %
%%%%%%%%%%%%%%%%%%%%%%%%%
%
consecutive = 0;
printf('*\n*-----\n* Transient flux calculation\n*-----\n*\n');
while(time < tend)
    time = time + tstep;
    consecutive = consecutive + 1 ;
    % Update T/H properties in fuel map
    [chandens chantemp tubedens tubetemp fueltemp chanflow] = ...
        catgrab(horzcat(resultsdir,'/',sprintf('%2.4fs',time-tstep)));
    chandens = chandens/1000.0;
    chantemp = chantemp + 273.15;
    tubedens = tubedens/1000.0;
    tubetemp = tubetemp + 273.15;
    fueltemp = fueltemp + 273.15;
    updatemap(horzcat(scratchdir,'/oldmap.exp'),horzcat(scratchdir,...
        '/tempmap.exp'),chandens,chantemp,tubedens,tubetemp,fueltemp);
    % Change timestep size in DONJON input file
    tstepchange(traninpfile,tstep);
    % Run IQS calculation
    command = horzcat(exec,' ',traninpfile,' ',procdir,' ',dbdir,' ',...
        scratchdir);
    printf('Step from %1.4f s to %1.4f s\n  Executing ''%s'' ...',...
        (time-tstep),time,command);
    [status cmdout] = system(command,'-echo');
    printf(' Done');
    % Show results on screen and save data
    newpower = mapgrab(horzcat(traninpfile,'+newmap.exp'),...
        horzcat(resultsdir,'/',sprintf('%2.4fs',time),'.png'));
    pause(0.1)
    % Check variation from previous time step
    difference = max(abs((newpower./oldpower)-1));
    if (difference > maxdiff) && (tstep > mintstep)
        % Reduce time step size and redo
        command = horzcat('rm ',resultsdir,'/',...
            sprintf('%2.4fs',time),'.png');
        [status cmdout] = system(command,'-echo');
        printf ('\n--> DECREASE timestep and redo\n\n');
        time = time - tstep ;
        tstep = max(tstep/2,mintstep);
        consecutive = 0;
    else
        % Advance time
        % Copy results to scratch directory
        command = horzcat('mv -f ',traninpfile,'+newfluxp.exp ',...
            scratchdir,'/oldfluxp.exp');
        [status cmdout] = system(command,'-echo');
        command = horzcat('mv -f ',traninpfile,'+newmap.exp ',...
            scratchdir,'/oldmap.exp');
        [status cmdout] = system(command,'-echo');
        command = horzcat('mv -f ',traninpfile,'+newlib.exp ',...
```

```matlab
            scratchdir,'/oldlib.exp');
        [status cmdout] = system(command,'-echo');
        command = horzcat('mv ',traninpfile,'+ ',resultsdir,'/',...
            sprintf('%2.4fs',time),'.x2m+');
        [status cmdout] = system(command,'-echo');
        % Show results on screen
        i = i + 1;
        plottime(i) = time;
        plotpower(i) = sum(newpower)/1E3;
        figure(4)
        plot(plottime,plotpower)
        axis([0 tend 500 800])
        title('Core Power History')
        xlabel('Time (s)');
        ylabel('Power (MW)');
        pause(0.1)
        % Execute CATHENA
        printf('  Creating CATHENA input...');
        catrestarttrans(horzcat(scratchdir,'/oldmap.exp'),orifdata,...
            tstep,tin,pin,pout);
        printf(' Done\n')
        command = horzcat('mv -f ','catstep.inp ',scratchdir,'/');
        [status cmdout] = system(command,'-echo');
        chdir(horzcat(scratchdir,'/'))
        command = 'runcathena catstep.inp';
        printf('  Executing ''%s'' ...',command);
        [status cmdout] = system(command,'-echo');
        printf(' Done\n');
        [status cmdout] = system('rm oldcatstep.rst','-echo');
        [status cmdout] = ...
            system('mv newcatstep.rst oldcatstep.rst','-echo');
        chdir('../');
        % Move results to results directory
        command = horzcat('mkdir ',resultsdir,'/',...
            sprintf('%2.4fs',time));
        [status cmdout] = system(command,'-echo');
        command = horzcat('mv -f ',scratchdir,'/*.dat ',...
            resultsdir,'/',sprintf('%2.4fs',time),'/');
        [status cmdout] = system(command,'-echo');
        command = horzcat('mv -f ',scratchdir,'/*.lis ',...
            resultsdir,'/',sprintf('%2.4fs',time),'/');
        [status cmdout] = system(command,'-echo');
        command = horzcat('cp ',scratchdir,'/oldmap.exp ',...
            resultsdir,'/',sprintf('%2.4fs',time),'.exp');
        [status cmdout] = system(command,'-echo');
        command = horzcat('cp ',scratchdir,'/oldfluxp.exp ',...
            resultsdir,'/',sprintf('%2.4fs',time),'oldfluxp.exp');
        [status cmdout] = system(command,'-echo');
        command = horzcat('cp ',scratchdir,'/oldcatstep.rst ',...
            resultsdir,'/',sprintf('%2.4fs',time),'oldcatstep.rst');
        [status cmdout] = system(command,'-echo');
        % Increase timestep size, if necessary
        if (difference < maxdiff*10) && (tstep < maxtstep) && ...
            (consecutive > 3)
            printf('\n--> INCREASE timestep\n\n')
            tstep = min(tstep*2,maxtstep);
            consecutive = 0;
        end
        oldpower = newpower;
    end
end
output = horzcat(plottime',plotpower');
save('-ascii',horzcat(resultsdir,'/powerhist.dat'),'output');
printf('*-----\n* Execution complete\n*-----\n');
toc
```

Appendix C

DONJON Modifications

The feedback module in DONJON 3.02g (AFM and its associated subroutines) required modification for this work. The list of changes includes:

1. Bug-fixes to the processing of the multigroup scattering matrix (performed by Professor Guy Marleau at École Polytechnique de Montréal with input from the author);

2. Extension of the "moderator" feedbacks to be by-node rather than global so that the centre flow tube could be included (performed by the author);

3. Disabling the saturating isotope concentration calculation (performed by the author).

Including the entire modified subroutines would require an impractical number of printed pages. The modifications made to the FORTAN functions can be isolated with *GNU diffutils,* a file comparison utility distributed under the GNU General Public License. This appendix highlights the changes to the FORTRAN source in context with the unified output format of the `diff` command.

C.1 AFM Main Function (AFM.F)

```
--- Original/AFM.f    2015-04-11 15:19:39.000000000 -0400
+++ Modified/AFM.f    2015-04-11 14:00:54.000000000 -0400
@@ -247,6 +247,7 @@
       CALL SETARA(BASE,MMIX*NGRP,IDIFZ)
       CALL SETARA(BASE,NGRP,IIJ)
       CALL SETARA(BASE,NGRP,INJ)
+      CALL SETARA(BASE,NGRP*NGRP,ISCTMP)
 *        L_MAP
       CALL SETARA(BASE,NCZO,IZONE)
       CALL SETARA(BASE,MMIX,IBRBG)
@@ -262,6 +263,9 @@
       CALL SETARA(BASE,MMIX,IDCOOL)
 C     FUEL TEMPERATURE PROFILES
       CALL SETARA(BASE,MMIX,ITFUEL)
+C     MODERATOR TEMPERATURE AND DENSITY PROFILES
+      CALL SETARA(BASE,MMIX,ITMOD)
+      CALL SETARA(BASE,MMIX,IDMOD)
 *
```

```
        CALL SETARA(BASE,NPS,IBRH)
        CALL SETARA(BASE,NPS,IPW)
@@ -314,6 +318,11 @@
        CALL SETARA(BASE,NUT,JTYP)
        CALL SETARA(IBASE,3*NUT,ITERB)
        CALL SETARA(IBASE,NISO,IJTAB)
+       CALL SETARA(BASE,NUT,ITCRG)
+       CALL SETARA(BASE,NUT,IDCRG)
+       CALL SETARA(BASE,NUT,ITMRG)
+       CALL SETARA(BASE,NUT,IDMRG)
+       CALL SETARA(BASE,NUT,ITFRG)
 *------------------------------------------------------------*
        CALL AFMDRV(HENTRY,KENTRY,ITYPE,NBURN,NGRP,NISO,ISC,NPS,
       1    NL,NTYP,NBCH,NCCO,NCZO,NUT,BASE(ISIGMA),BASE(IIJJ),
@@ -336,8 +345,15 @@
       1    LMCR,BASE(ISIGF),BASE(ISIGX),BASE(IFLR),
       1    BASE(IBSFT),BASE(IPSFT),IBASE(IVSFT),IBASE(IINDEX),
       1    IBASE(ITER),BASE(JTYP),IBASE(ITERB),IBASE(IJTAB),IXYZ,
-      1    BASE(IDCOOL),BASE(ITCOOL),BASE(ITFUEL))
+      1    BASE(IDCOOL),BASE(ITCOOL),BASE(ITFUEL),BASE(IDMOD),BASE(ITMOD),
+      1    BASE(ISCTMP),BASE(ITCRG),BASE(IDCRG),BASE(ITMRG),BASE(IDMRG),
+      1    BASE(ITFRG))
 *------------------------------------------------------------*
+       CALL RLSARA(BASE(ITFRG))
+       CALL RLSARA(BASE(IDMRG))
+       CALL RLSARA(BASE(ITMRG))
+       CALL RLSARA(BASE(IDCRG))
+       CALL RLSARA(BASE(ITCRG))
        CALL RLSARA(IBASE(IJTAB))
        CALL RLSARA(IBASE(ITERB))
        CALL RLSARA(BASE(JTYP))
@@ -393,6 +409,8 @@
        CALL RLSARA(BASE(ITFUEL))
        CALL RLSARA(BASE(IDCOOL))
        CALL RLSARA(BASE(ITCOOL))
+       CALL RLSARA(BASE(ITMOD))
+       CALL RLSARA(BASE(IDMOD))
        CALL RLSARA(IBASE(IINDEX))
        CALL RLSARA(BASE(IBFLUX))
        CALL RLSARA(IBASE(IVSFT))
@@ -403,6 +421,7 @@
        CALL RLSARA(BASE(IBRBG))
        CALL RLSARA(BASE(IZONE))
 *
+       CALL RLSARA(BASE(ISCTMP))
        CALL RLSARA(BASE(INJ))
        CALL RLSARA(BASE(IIJ))
        CALL RLSARA(BASE(IDIFZ))
```

C.2 AFM Driver (AFMDRV.F)

```
--- Original/AFMDRV.f 2015-04-11 15:19:39.000000000 -0400
+++ Modified/AFMDRV.f 2015-04-11 14:00:53.000000000 -0400
@@ -9,7 +9,8 @@
       1    DENSITB,HISO,CPW1B,CPW2B,HXEN1,HXEN2,HSAM1,HSAM2,HNEP1,
       1    HNEP2,FLUXB,OVERVB,
       1    CHIB,LTAB,LMCR,XSIGF,XSIGX,XFLUN,BSFT,PSFT,ISFT,
-      1    INDEX,ITEXTR,KTYP,ITXTAB,JTAB,IXYZ,PDCOOL,PTCOOL,PTFUEL)
+      1    INDEX,ITEXTR,KTYP,ITXTAB,JTAB,IXYZ,PDCOOL,PTCOOL,PDMOD,PTMOD,
+      1    PTFUEL,SCTCMP,TCRG,DCRG,TMRG,DMRG,TFRG)
 *
 *----------------------------------------------------------------------
 *
@@ -51,7 +52,7 @@
        REAL  STORE
        INTEGER ITEXTR(3*NUT),ITXTAB(3*NUT),ITYPE
```

```
        LOGICAL LNOMP,LTAV,LTAB,LXENON,LSAM,LNEP,LXEREF,LNEREF,LMCR,
-     1          LTFUEL,LDRAH,LTCOOL,LDCOOL
+     1          LTFUEL,LDRAH,LTCOOL,LDCOOL,LDMOD,LTMOD
      DIMENSION KENTRY(*),SIGMA(NBCH*NCCO,NGRP,NTYP),
     1 IJJ(NBCH*NCCO,NL,*),NJJ(NBCH*NCCO,NL,*),XBURN(NBURN,*),
     1 VOL(*),OVERV(NBCH*NCCO,*),FLUX(NBCH*NCCO,*),
@@ -93,7 +94,9 @@
     1 INDEX(*),KTYP(*),
     1 XSIGF(*),XSIGX(*),XFLUN(*),
     1 BSFT(NBCH*NCCO,*),PSFT(NBCH*NCCO,*),ISFT(*),RLOC(7),
-    1 PDCOOL(*),PTCOOL(*),PTFUEL(*),IBASE(1)
+    1 PDCOOL(*),PTCOOL(*),PTFUEL(*),PDMOD(*),PTMOD(*),IBASE(1)
+     REAL TCRG(NUT),DCRG(NUT),TMRG(NUT),DMRG(NUT),TFRG(NUT)
+     REAL SCTCMP(NGRP*NGRP)
      INTEGER LTST
      COMMON BASE(1)
      EQUIVALENCE(BASE(1),IBASE(1))
@@ -114,6 +117,8 @@
      LDRAH =.FALSE.
      LTCOOL=.FALSE.
      LDCOOL=.FALSE.
+     LDMOD =.FALSE.
+     LTMOD =.FALSE.
      ILBFLU=0
      IMPX=0
      IXENO=0
@@ -176,8 +181,6 @@
           DO 17 JGR=1,NGRP
             SCAT(IMX,IL,IGR,JGR)=0.0
  17       CONTINUE
-          IJJ(IMX,IL,IGR)=IGR
-          NJJ(IMX,IL,IGR)=1
  16       CONTINUE
          DO 11 ITYP=1,NTYP
            SIGMA(IMX,IGR,ITYP)=0.0
@@ -223,17 +226,11 @@
          IF(INDIC.NE.3)
     1       CALL XABORT('AFMDRV: CHARACTER DATA EXPECTED.')
          READ(TEXTR,'(3A4)') (ITEXTR((IN-1)*3+I),I=1,3)
- 111      CONTINUE
-          IF(LMCR .AND. KTYP(1).GT.MX)
-     +          CALL XABORT('AFMDRV: INVALID INDEX NUMBER.')
-C
-* CHECK THE NAME OF THE DIRECTORY
-          WRITE(TEXTR,'(3A4)') (ITEXTR(I1),I1=1,3)
-          CALL LCMLEN(IPFBM,TEXTR,ILENGT,ITYLCM)
-          IF(ILENGT.EQ.0) THEN
-            CALL XABORT('AFMDRV: UNABLE TO FIND '//TEXTR//' .')
-          ENDIF
-* RECOVER THE REFERENCE LOCAL PARAMETERS VALUES
+          CALL LCMLEN(IPFBM,TEXTR,ILENGT,ITYLCM)
+          IF(ILENGT.EQ.0) THEN
+            CALL XABORT('AFMDRV: UNABLE TO FIND '//TEXTR//' .')
+          ENDIF
+* RECOVER some THE REFERENCE LOCAL PARAMETERS VALUES
          CALL LCMSIX(IPFBM,TEXTR,1)
          CALL LCMSIX(IPFBM,'INFO-NOMINA',1)
          CALL LCMLEN(IPFBM,'NOMINALP',ILP,ITYLCM)
@@ -243,42 +240,94 @@
          DO 888 I=1,ILP
            WRITE(HMICRO,'(3A4)') (HISO((I-1)*3+IH),IH=1,3)
            IF(HMICRO.EQ.'PW') PWREF=RLOC(I)
-          IF(HMICRO.EQ.'TCOOL') TCR=RLOC(I)
-          IF(HMICRO.EQ.'TMOD') TMR=RLOC(I)
-          IF(HMICRO.EQ.'TFUEL') TFR=RLOC(I)
-          IF(HMICRO.EQ.'RHOC') DCR=RLOC(I)
-          IF(HMICRO.EQ.'RHOM') DMR=RLOC(I)
```

266

```
+              IF(HMICRO.EQ.'TCOOL') TCRG(IN)=RLOC(I)
+              IF(HMICRO.EQ.'TMOD') TMRG(IN)=RLOC(I)
+              IF(HMICRO.EQ.'TFUEL') TFRG(IN)=RLOC(I)
+              IF(HMICRO.EQ.'RHOC') DCRG(IN)=RLOC(I)
+              IF(HMICRO.EQ.'RHOM') DMRG(IN)=RLOC(I)
               IF(HMICRO.EQ.'PUR') XIR=RLOC(I)
  888      CONTINUE
          ENDIF
          CALL LCMSIX(IPFBM,' ',2)
          CALL LCMSIX(IPFBM,' ',2)
 * REFERENCE PARAMETER VALUES
+
+ 111     CONTINUE
+         IF(LMCR .AND. KTYP(1).GT.MX)
+     +          CALL XABORT('AFMDRV: INVALID INDEX NUMBER.')
+C
+* CHECK THE NAME OF THE DIRECTORY
+****      WRITE(TEXTR,'(3A4)') (ITEXTR(I1),I1=1,3)
+****      CALL LCMLEN(IPFBM,TEXTR,ILENGT,ITYLCM)
+****      IF(ILENGT.EQ.0) THEN
+****        CALL XABORT('AFMDRV: UNABLE TO FIND '//TEXTR//' .')
+****      ENDIF
+* RECOVER THE REFERENCE LOCAL PARAMETERS VALUES
+****      CALL LCMSIX(IPFBM,TEXTR,1)
+****      CALL LCMSIX(IPFBM,'INFO-NOMINA',1)
+****      CALL LCMLEN(IPFBM,'NOMINALP',ILP,ITYLCM)
+****      IF(ILP.GT.0) THEN
+****        CALL LCMGET(IPFBM,'NOMINALP',RLOC)
+****        CALL LCMGET(IPFBM,'NOMINALN',HISO)
+****        DO 888 I=1,ILP
+****          WRITE(HMICRO,'(3A4)') (HISO((I-1)*3+IH),IH=1,3)
+****          IF(HMICRO.EQ.'PW') PWREF=RLOC(I)
+****          IF(HMICRO.EQ.'TCOOL') TCR=RLOC(I)
+****          IF(HMICRO.EQ.'TMOD') TMR=RLOC(I)
+****          IF(HMICRO.EQ.'TFUEL') TFR=RLOC(I)
+****          IF(HMICRO.EQ.'RHOC') DCR=RLOC(I)
+****          IF(HMICRO.EQ.'RHOM') DMR=RLOC(I)
+****          IF(HMICRO.EQ.'PUR') XIR=RLOC(I)
+**** 888      CONTINUE
+****      ENDIF
+****      CALL LCMSIX(IPFBM,' ',2)
+****      CALL LCMSIX(IPFBM,' ',2)
+* REFERENCE PARAMETER VALUES
          PFIX=PWREF
          AW=15.9994 +2*(1-XIR)*1.0079 +2*XIR*2.014101
          PH=2*1.0079/AW
          PD=2*2.014101/AW
 * INITIALISATION OF PERTURBED PARAMETER
-         TF=TFR
-         TC=TCR
-         TM=TMR
-         DC=1.0
-         DM=1.0
+*        TF=TFR
+*        TC=TCR
+*        TM=TMR
+         IITM=0
+*        DC=1.0
+*        DM=1.0
+         IIDM=0
          XI=XIR
          BOR=0.0
          SM=0.0
          RNP9=0.0
          XEN=0.0
 C
+         IF(.NOT.(LTAB.OR.LMCR)) CALL LCMGET(IPMAP,'INDEX',INDEX)
```

```
              DO 15 IMX=1,MX
                POWER(IMX)=PWREF
                ISFT(IMX)=0
                BURBG(IMX)=0.0
                BURED(IMX)=0.0
                VOL(IMX)=0.0
-               PDCOOL(IMX)=DCR
-               PTCOOL(IMX)=TCR
-               PTFUEL(IMX)=TFR
+               IF(LTAB) THEN
+                 IDF=IMX
+               ELSE IF(LMCR) THEN
+                 NPS=2
+                 IDF=1
+               ELSE
+                 KDF=0
+                 DO IN=1,NUT
+                   IF(INDEX(IMX).EQ.KTYP(IN)) THEN
+                     IDF=IN
+                     KDF=1
+                   ENDIF
+                 ENDDO
+                 IF(KDF.EQ.0) CALL XABORT('AFMDRV: WRONG NUMBER OF INDEX')
+               ENDIF
+               PDCOOL(IMX)=DCRG(IDF)
+               PTCOOL(IMX)=TCRG(IDF)
+               PTFUEL(IMX)=TFRG(IDF)
+               PDMOD(IMX)= DMRG(IDF)
+               PTMOD(IMX)= TMRG(IDF)
   15         CONTINUE
 C          RECOVER THE TEMERATURE AND DENSITY PROFILES
            IF( .NOT.LTAB .AND. .NOT.LMCR ) THEN
@@ -290,6 +339,11 @@
              IF(IPROF2.GT.0) THEN
                CALL LCMGET(IPMAP,'B-TFUEL',PTFUEL)
              ENDIF
+            CALL LCMLEN(IPMAP,'B-TMOD',IPROF3,ITYLCM)
+            IF(IPROF3.GT.0) THEN
+              CALL LCMGET(IPMAP,'B-DMOD',PDMOD)
+              CALL LCMGET(IPMAP,'B-TMOD',PTMOD)
+            ENDIF
              WRITE(6,716)
            ENDIF
          ENDIF
@@ -329,21 +383,30 @@
   415        CONTINUE
 C
      ELSE IF(TEXT4.EQ.'TMOD') THEN
-        CALL REDGET (INDIC,NITMA,TM,TEXT4,DFLOTT)
+        CALL REDGET (INDIC,NITMA,TMI,TEXT4,DFLOTT)
        IF(INDIC.NE.2) CALL XABORT('AFMDRV: REAL DATA EXPECTED.')
+*       IITM=1
+        LTMOD = .TRUE.
+        DO 416 IMX=1,MX
+        PTMOD(IMX)=TMI
+  416    CONTINUE
 *
      ELSE IF(TEXT4.EQ.'RDCL') THEN
        CALL REDGET (INDIC,NITMA,DCU,TEXT4,DFLOTT)
        IF(INDIC.NE.2) CALL XABORT('AFMDRV: REAL DATA EXPECTED.')
        LDCOOL = .TRUE.
-        DO 416 IMX=1,MX
+        DO 417 IMX=1,MX
        PDCOOL(IMX)=DCU
-  416    CONTINUE
+  417    CONTINUE
 C
```

```
        ELSE IF(TEXT4.EQ.'RDMD') THEN
-         CALL REDGET (INDIC,NITMA,DM,TEXT4,DFLOTT)
+         CALL REDGET (INDIC,NITMA,DMI,TEXT4,DFLOTT)
          IF(INDIC.NE.2) CALL XABORT('AFMDRV: REAL DATA EXPECTED.')
-         DM=DM/DMR
+*        IIDM=1
+         LDMOD = .TRUE.
+         DO 418 IMX=1,MX
+         PDMOD(IMX)=DMI
+  418    CONTINUE
 *
        ELSE IF(TEXT4.EQ.'BORON') THEN
          CALL REDGET (INDIC,NITMA,BOR,TEXT4,DFLOTT)
@@ -557,33 +620,55 @@
                    CALL LCMGET(IPFBM,'IJJ',IJ)
                  ENDIF
                ENDIF
-              CALL LCMGET(IPFBM,'REF',SMACB(1,ITY,ISO,I,IN))
-              CALL LCMGET(IPFBM,'BOR',XBORB(1,ITY,ISO,I,IN))
-              CALL LCMGET(IPFBM,'PUR',XPURB(1,ITY,ISO,I,IN))
-              CALL LCMGET(IPFBM,'T1M',XT1MB(1,ITY,ISO,I,IN))
-              CALL LCMGET(IPFBM,'T2M',XT2MB(1,ITY,ISO,I,IN))
-              CALL LCMGET(IPFBM,'D1M',XD1MB(1,ITY,ISO,I,IN))
-              CALL LCMGET(IPFBM,'D2M',XD2MB(1,ITY,ISO,I,IN))
+              CALL AFMSCT(IPFBM,NGRP,NJ,IJ,'REF           ',SCTCMP,
+     >          SMACB(1,ITY,ISO,I,IN))
+              CALL AFMSCT(IPFBM,NGRP,NJ,IJ,'BOR           ',SCTCMP,
+     >          XBORB(1,ITY,ISO,I,IN))
+              CALL AFMSCT(IPFBM,NGRP,NJ,IJ,'PUR           ',SCTCMP,
+     >          XPURB(1,ITY,ISO,I,IN))
+              CALL AFMSCT(IPFBM,NGRP,NJ,IJ,'T1M           ',SCTCMP,
+     >          XT1MB(1,ITY,ISO,I,IN))
+              CALL AFMSCT(IPFBM,NGRP,NJ,IJ,'T2M           ',SCTCMP,
+     >          XT2MB(1,ITY,ISO,I,IN))
+              CALL AFMSCT(IPFBM,NGRP,NJ,IJ,'D1M           ',SCTCMP,
+     >          XD1MB(1,ITY,ISO,I,IN))
+              CALL AFMSCT(IPFBM,NGRP,NJ,IJ,'D2M           ',SCTCMP,
+     >          XD2MB(1,ITY,ISO,I,IN))
               IF(JTAB(1).EQ.1) THEN
-                CALL LCMLEN(IPFBM,'XEN',ILENG,ITYXSM)
+                CALL LCMLEN(IPFBM,'XEN           ',ILENG,ITYXSM)
                 IF(ILENG.GT.0) THEN
-                  CALL LCMGET(IPFBM,'XEN',XXENB(1,ITY,ISO,I,IN))
+                  CALL AFMSCT(IPFBM,NGRP,NJ,IJ,'XEN           ',SCTCMP,
+     >          XXENB(1,ITY,ISO,I,IN))
                 ENDIF
-              CALL LCMGET(IPFBM,'T1F',XT1FB(1,ITY,ISO,I,IN))
-              CALL LCMGET(IPFBM,'T2F',XT2FB(1,ITY,ISO,I,IN))
-              CALL LCMGET(IPFBM,'T1C',XT1CB(1,ITY,ISO,I,IN))
-              CALL LCMGET(IPFBM,'T2C',XT2CB(1,ITY,ISO,I,IN))
-              CALL LCMGET(IPFBM,'D1C',XD1CB(1,ITY,ISO,I,IN))
-              CALL LCMGET(IPFBM,'D2C',XD2CB(1,ITY,ISO,I,IN))
-*
-              CALL LCMGET(IPFBM,'SM149',XSMB(1,ITY,ISO,I,IN))
-              CALL LCMGET(IPFBM,'NP239',XNP9B(1,ITY,ISO,I,IN))
-              CALL LCMGET(IPFBM,'MIXFD',XMFDB(1,ITY,ISO,I,IN))
-              CALL LCMGET(IPFBM,'MIXMD',XMMDB(1,ITY,ISO,I,IN))
-              CALL LCMGET(IPFBM,'FPCH1',XPF1B(1,ITY,ISO,I,IN))
-              CALL LCMGET(IPFBM,'FPCL1',XPF1LB(1,ITY,ISO,I,IN))
-              CALL LCMGET(IPFBM,'FPCH2',XPF2B(1,ITY,ISO,I,IN))
-              CALL LCMGET(IPFBM,'FPCL2',XPF2LB(1,ITY,ISO,I,IN))
+              CALL AFMSCT(IPFBM,NGRP,NJ,IJ,'T1F           ',SCTCMP,
+     >          XT1FB(1,ITY,ISO,I,IN))
+              CALL AFMSCT(IPFBM,NGRP,NJ,IJ,'T2F           ',SCTCMP,
+     >          XT2FB(1,ITY,ISO,I,IN))
+              CALL AFMSCT(IPFBM,NGRP,NJ,IJ,'T1C           ',SCTCMP,
+     >          XT1CB(1,ITY,ISO,I,IN))
```

D. W. Hummel
Ph.D. Thesis

Appendix C
DONJON Modifications

McMaster University
Engineering Physics

```
+                    CALL AFMSCT(IPFBM,NGRP,NJ,IJ,'T2C          ',SCTCMP,
+        >          XT2CB(1,ITY,ISO,I,IN))
+                    CALL AFMSCT(IPFBM,NGRP,NJ,IJ,'D1C          ',SCTCMP,
+        >          XD1CB(1,ITY,ISO,I,IN))
+                    CALL AFMSCT(IPFBM,NGRP,NJ,IJ,'D2C          ',SCTCMP,
+        >          XD2CB(1,ITY,ISO,I,IN))
+*
+                    CALL AFMSCT(IPFBM,NGRP,NJ,IJ,'SM149        ',SCTCMP,
+        >          XSMB(1,ITY,ISO,I,IN))
+                    CALL AFMSCT(IPFBM,NGRP,NJ,IJ,'NP239        ',SCTCMP,
+        >          XNP9B(1,ITY,ISO,I,IN))
+                    CALL AFMSCT(IPFBM,NGRP,NJ,IJ,'MIXFD        ',SCTCMP,
+        >          XMFDB(1,ITY,ISO,I,IN))
+                    CALL AFMSCT(IPFBM,NGRP,NJ,IJ,'MIXMD        ',SCTCMP,
+        >          XMMDB(1,ITY,ISO,I,IN))
+                    CALL AFMSCT(IPFBM,NGRP,NJ,IJ,'FPCH1        ',SCTCMP,
+        >          XPF1B(1,ITY,ISO,I,IN))
+                    CALL AFMSCT(IPFBM,NGRP,NJ,IJ,'FPCL1        ',SCTCMP,
+        >          XPF1LB(1,ITY,ISO,I,IN))
+                    CALL AFMSCT(IPFBM,NGRP,NJ,IJ,'FPCH2        ',SCTCMP,
+        >          XPF2B(1,ITY,ISO,I,IN))
+                    CALL AFMSCT(IPFBM,NGRP,NJ,IJ,'FPCL2        ',SCTCMP,
+        >          XPF2LB(1,ITY,ISO,I,IN))
+                  ENDIF
 *
                    CALL LCMSIX(IPFBM,' ',2)
@@ -719,7 +804,6 @@
 *        LOOP OVER THE MIXTURES
        DO 302 NMIX=MXSH,MMIX
          TC=PTCOOL(NMIX)
-          DC=PDCOOL(NMIX)/DCR
          IF(LTAB) THEN
            VOL(NMIX)=VOL(1)
            NPS=2
@@ -737,8 +821,12 @@
              KDF=1
            ENDIF
  113     CONTINUE
-          IF(KDF.EQ.0) CALL XABORT('AFMDRV: WRONG NUMBER OF INDEX')
+          IF(KDF.EQ.0) CALL XABORT('AFMDRV: WRONG NUMBER OF INDEX')
          ENDIF
+          DC=PDCOOL(NMIX)/DCRG(IDF)
+          TM=PTMOD(NMIX)
+          DM=PDMOD(NMIX)/DMRG(IDF)
+
 * IF TIME AVERAGE CALCULATION:
 * EVALUATION OF THE BURNUPS STEPS EMBEDED IN THE INTEGRATION
          IF(LTAV) THEN
@@ -874,8 +962,8 @@
  290         CONTINUE
            ELSE IF(ILBFLU.NE.0.AND.XIFL.NE.0.0) THEN
 *        COMPUTE THE XENON AND NEPTUNIUM CONCENTRATIONS
-              CALL AFMXNC(NGRP,XSIGX,XSIGF,BFLUX(1,NMIX),
-     1                    XEN,RNP9,XFLUN)
+*              CALL AFMXNC(NGRP,XSIGX,XSIGF,BFLUX(1,NMIX),
+*     1                    XEN,RNP9,XFLUN)
            ENDIF
 * COMPUTE THE XENON AND NEPTUNIUM CONCENTRATIONS
          IF(LXENON) XEN=FXEN
@@ -888,9 +976,22 @@
              TF=TFU
 !        reference fuel temperature
            ELSEIF(LMCR) THEN
-              TF=TFR
+              TF=TFRG(IDF)
            ENDIF
          ENDIF
```

```
+            TCR=TCRG(IDF)
+            TFR=TFRG(IDF)
+            TMR=TMRG(IDF)
+*            IF(IITM .EQ. 1) THEN
+*              TM=TMI
+*            ELSE
+*              TM=TMR
+*            ENDIF
+*            IF(IIDM .EQ. 1) THEN
+*              DM=DMI/DMRG(IDF)
+*            ELSE
+*              DM=1.0
+*            ENDIF
 *----------------------------------------------------------------*
 * XSECTION CALCULATION
 *----------------------------------------------------------------*
@@ -981,6 +1082,8 @@
 * COMPUTE  TIME AVERAGED X-SECTIONS
            CALL SETARA(BASE,NBURN,IALFA)
            CALL SETARA(BASE,NBURN,IBETA)
+            WRITE(6,*) 'ALLOCATE ', (NBURN*4 + 8)
+            WRITE(6,*) 'ALLOCATE ', (NBURN*4 + 8)
            DO 101 IGR=1,NGRP
              DO 101 ITY=1,NTM+1
                CALL AFMTAV(NBURN,ITM,XBMAX,XBMIN,SIGAV(1,IGR,ITY),
@@ -1017,16 +1120,6 @@
          ENDIF
 *
          IL=1
-          DO 980 IGR=1,NGRP
-              NJJ(NMIX,IL,IGR)=NJ(IGR)
-              IJJ(NMIX,IL,IGR)=IJ(IGR)
-              IF(LMCR) THEN
-                DO 98 NI=1,MMIX
-                   NJJ(NI,IL,IGR)=NJ(IGR)
-                   IJJ(NI,IL,IGR)=IJ(IGR)
-  98             CONTINUE
-              ENDIF
- 980      CONTINUE
 * MIX LOOP
   302 CONTINUE
 *
@@ -1122,24 +1215,6 @@
   379          CONTINUE
   377          CONTINUE
 *
-          DO 384 IZ=1,NCZO
-             IWORK(IZ)=NJJ(IZ,IL,IGR)
- 384      CONTINUE
-          DO 385 IC=1,NCCO
-           DO 385 IB=1,NBCH
-             ICB=NBCH*(IC-1)+IB
-             NJJ(ICB,IL,IGR)=IWORK(IZONE(IC))
- 385      CONTINUE
-*
-          DO 394 IZ=1,NCZO
-             IWORK(IZ)=IJJ(IZ,IL,IGR)
- 394      CONTINUE
-          DO 395 IC=1,NCCO
-           DO 395 IB=1,NBCH
-             ICB=NBCH*(IC-1)+IB
-             IJJ(ICB,IL,IGR)=IWORK(IZONE(IC))
- 395      CONTINUE
-*
   303    CONTINUE
 *
          DO 344 IZ=1,NCZO
```

271

```
@@ -1249,6 +1324,7 @@
 *
            IL=1
            CALL SETARA(BASE,NGRP,ISSCAT)
+           WRITE(6,*) 'ALLOCATE ', (NGRP*4 + 8)
            DO 212 IGR=1,NGRP
              BASE(ISSCAT+IGR-1)= SCAT(MMIX,IL,IGR,JGR)
              SCAT(MMIX,IL,IGR,JGR) = 0.0
@@ -1315,15 +1391,18 @@
          IL=1
          WRITE (CM,'(I2.2)') IL-1
          IPOSDE=0
-         DO 190 IX=1,MMIX
+         DO IX=1,MMIX
            IPOS(IX)=IPOSDE+1
-          FLUX(IX,JGR)=0.0
-          DO 190 IGR=IJJ(IX,IL,JGR),IJJ(IX,IL,JGR)-NJJ(IX,IL,JGR)+1,
+          DO IGR=IJJ(IX,IL,JGR),IJJ(IX,IL,JGR)-NJJ(IX,IL,JGR)+1,
      1            -1
              IPOSDE=IPOSDE+1
              WORK(IPOSDE)=SCAT(IX,IL,IGR,JGR)
-            FLUX(IX,JGR)=FLUX(IX,JGR)+ SCAT(IX,IL,IGR,JGR)
- 190      CONTINUE
+          ENDDO
+          FLUX(IX,JGR)=0.0
+          DO IGR=1,NGRP
+            FLUX(IX,JGR)=FLUX(IX,JGR)+ SCAT(IX,IL,JGR,IGR)
+          ENDDO
+         ENDDO
 *
          CALL LCMPUT(IPMACX,'SCAT'//CM,IPOSDE,2,WORK)
          CALL LCMPUT(IPMACX,'IPOS'//CM,MMIX,1,IPOS)
```

C.3 Multigroup Scattering Matrix Decompression (AFMSCT.F)

This FORTRAN subroutine is not part of the of the original DONJON 3.02g release and was added by Professor Guy Marleau as part of a bug-fix for the processing of the multigroup scattering matrix.

```
*DECK AFMSCT
      SUBROUTINE AFMSCT(IPFBM,NGRP,NJ,IJ,NAME,SCTCMP,SCTUNF)
*
*----------------------------------------------------------------*
* Read and decompress scattering cross section
*  IPFBM  : ADDRESS OF THE FBM DATABASE.
*  NGRP   : NUMBER OF ENERGY GROUPS.
*  NJ     : NJ COMPRESSION INDEX.
*  IJ     : IJ COMPRESSION INDEX.
*  NAME   : RECORD NAME TO READ.
*  SCTCMP : COMPRESS SCATTERING MATRIX.
*  SCTUNF : UNFOLDED SCATTERING MATRIX
*----------------------------------------------------------------*
*
      INTEGER      IPFBM,NGRP
      INTEGER      NJ(NGRP),IJ(NGRP)
      CHARACTER*12 NAME
      REAL         SCTCMP(NGRP*NGRP),SCTUNF(NGRP,NGRP)
      INTEGER      IGR,JGR,IELE
*----
* Read compressed scattering matrix
*----
      CALL LCMGET(IPFBM,NAME,SCTCMP)
*----
```

```
*  Uncompress scattering matrix
*  SCAT(IGR,JGR) is scattering
*  from group IGR to group JRG
*----
      IELE=0
      DO JGR=1,NGRP
        DO IGR=IJ(JGR),IJ(JGR)-NJ(JGR)+1,-1
          IELE=IELE+1
          SCTUNF(IGR,JGR)=SCTCMP(IELE)
        ENDDO
      ENDDO
      RETURN
      END
```

C.4 AFM Cross-Section Processing (AFMCPT.F)

```
--- Original/AFMCPT.f 2015-04-11 15:19:39.000000000 -0400
+++ Modified/AFMCPT.f 2015-04-11 15:24:09.000000000 -0400
@@ -278,6 +278,8 @@
 *
 * RECOVER MACROSCOPIC X-SECTIONS
       II=0
+      CPF1 = 0.0
+      CPF2 = 0.0
      DO 901 I = IRMIN,IRMAX
        II=II+1
        DO 100 ISO=1,NISO
@@ -332,21 +334,19 @@
   1                    XPURB(IGR,ITY,ISO,I,IDF)
              WRITE(6,*) ' BORE ET PUR CONC ', CB,PUR,BOR,XIR
            ENDIF
-*
  100     CONTINUE
  901     CONTINUE
 * STORE SCATTERING
      IL= 1
      ITY=5+2*IXYZ+IL
      IGAR=0
-     DO 120 JGR=1,NGRP
-       DO 120 IGR=IJJ(JGR),IJJ(JGR)-NJJ(JGR)+1,-1
-         IGAR=IGAR+1
-         SCAT(NMIX,IL,IGR,JGR)=SMAC(IGAR,ITY,1)
-* TOTAL OR ABS
-         SMAC(IGR,2,1)=SMAC(IGR,2,1)+SCAT(NMIX,IL,IGR,JGR)
- 120     CONTINUE
- 130   CONTINUE
+     DO JGR=1,NGRP
+       DO IGR=1,NGRP
+         IGAR=IGAR+1
+         SCAT(NMIX,IL,IGR,JGR)=SMAC(IGAR,ITY,1)
+         SMAC(IGR,2,1)=SMAC(IGR,2,1)+SCAT(NMIX,IL,IGR,JGR)
+       ENDDO
+     ENDDO
 * STORE X-SECTIONS
      DO 260 ITY=1,NTYP
        DO 260 IGR=1,NGRP
```